



# **Neuroimaging of human motor control in real world scenarios: from lab to urban environment**

**Sara Pizzamiglio**

**Ph.D.**

**A thesis submitted in partial fulfilment of the requirements of the University of East London for the degree of Doctor of Philosophy**

**September 2017**

## **Abstract**

The main goal of this research programme was to explore the neurophysiological correlates of human motor control in real-world scenarios and define mechanism-specific markers that could eventually be employed as targets of novel neurorehabilitation practice. As a result of recent developments in mobile technologies it is now possible to observe subjects' behaviour and monitor neurophysiological activity whilst they perform natural activities freely. Investigations in real-world scenarios would shed new light on mechanisms of human motor control previously not observed in laboratory settings and how they could be exploited to improve rehabilitative interventions for the neurologically impaired. This research programme was focussed on identifying cortical mechanisms involved in both upper- (i.e. reaching) and lower-limb (i.e. locomotion) motor control. Complementary results were obtained by the simultaneous recordings of kinematic, electromyographic and electrocorticographic signals. To study motor control of the upper-limb, a lab-based setup was developed, and the reaching movement of healthy young individuals was observed in both stable and unstable (i.e. external perturbation) situations. Robot-mediated force-field adaptation has the potential to be employed in rehabilitation practice to promote new skills learning and motor recovery. The muscular (i.e. intermuscular couplings) and neural (i.e. spontaneous oscillations and cortico-muscular couplings) indicators of the undergoing adaptation process were all symbolic of adaptive strategies employed during early stages of adaptation. The medial frontal, premotor and supplementary motor regions appeared to be the principal cortical regions promoting adaptive control and force modulation. To study locomotion control, a mobile setup was developed and daily life human activities (i.e. walking while conversing, walking while texting with a smartphone) were investigated outside the lab. Walking in hazardous environments or when simultaneously performing a secondary task has been demonstrated to be challenging for the neurologically impaired. Healthy young adults showed a reduced motor performance when walking in multitasking conditions, during which whole-brain and task-specific neural correlates were observed. Interestingly, the activity of the left posterior parietal cortex was predictive of the level of gait stability across individuals, suggesting a crucial role of this area in gait control and determination of subject specific motor capabilities. In summary, this research programme provided evidence on different cortical mechanisms operative during two specific scenarios for "real-world" motor behaviour in and outside the laboratory-setting in healthy subjects. The results suggested that identification of neuro-muscular indicators of specific motor control mechanisms could be exploited in future "real-world" rehabilitative practice.

### **Declaration**

I declare that the work reported in this thesis was carried out in accordance with the regulations of the University of East London. The work is novel except where indicated by special reference in the text and no part of this thesis has been submitted for any other degrees. Any views expressed in the dissertation are those of the author and in no way represent those of the University of East London.

The thesis has not been presented to any other University for examination either in the United Kingdom either overseas.

Sara Pizzamiglio

01/ 09/ 2017

## Table of Contents

Abstract .....	ii
Declaration .....	iii
Table of Contents .....	iv
List of Figures .....	x
List of Tables.....	xii
List of Equations .....	xiii
List of Accompanying Material .....	xiv
Abbreviations .....	xv
Acknowledgements .....	xvii
1 Introduction .....	1
1.1 Overview .....	1
1.2 Goals and hypotheses .....	3
1.2.1 Motor control of the upper limb: the neurorehabilitation scenario .....	3
1.2.2 Motor control of the lower limb: the real-world scenario.....	6
1.3 Thesis outline .....	9
1.4 Research contributions and novelty .....	11
1.4.1 Neurorehabilitation scenario .....	11
1.4.2 Real-world scenario .....	12
2 Literature review .....	14
2.1 Human motor control .....	14
2.1.1 The neural motor system.....	14
2.1.2 The peripheral motor system.....	17
2.1.3 The role of attention .....	20
2.2 Motor control of the upper limb during reaching.....	20
2.2.1 Neural correlates of reaching .....	21
Neurophysiology of reaching – animal studies.....	21
Neurophysiology of reaching – human studies.....	24
Non-invasive neuroimaging studies .....	25
2.2.2 Reaching impairments and assistive technologies .....	27
2.2.3 Neurorehabilitation after stroke .....	30
Rehabilitative interventions .....	30
Motor skill learning.....	33
2.3 Motor control of the lower limb during locomotion .....	35
2.3.1 Neural correlates of locomotion.....	38
Neurophysiology of locomotion – animal studies .....	38
Neurophysiology of locomotion – human studies .....	40
Non-invasive neuroimaging studies .....	41

2.3.2	Assistive technologies and rehabilitation for gait impairments .....	44
2.3.3	Single- and dual-task walking.....	47
3	General framework and methodologies .....	51
3.1	Overview .....	51
3.2	Ethics .....	53
3.3	Subjects recruitment .....	53
3.4	Experimental protocols and setups.....	53
3.5	Physiological evidences .....	54
3.5.1	Electromyography .....	54
3.5.2	Electroencephalography.....	55
3.6	Signal processing.....	58
3.6.1	Measures of kinematics.....	58
	The reaching movement .....	58
	Gait monitoring .....	59
3.6.2	Pre-processing .....	59
	EMG.....	59
	EEG .....	60
3.6.3	Measures of basic muscle activity.....	61
3.6.4	Measures of neural Event-Related Potentials (ERPs).....	62
3.6.5	Measures of neural Power Spectral Density (PSD) .....	62
3.6.6	Measures of Event-Related Spectral Perturbations (ERSPs).....	63
3.6.7	Measures of Cortico-Muscular Coherence (CMC).....	65
3.6.8	Theory of source localization.....	65
3.7	Statistical analyses.....	67
3.7.1	Statistics for kinematics and EMG evidences .....	67
3.7.2	Non-parametric cluster-based permutation tests for EEG evidences.....	68
3.7.3	Assumptions for Multiple Linear Regressions (MLRs).....	69
	Study I: Neurorehabilitation Scenario.....	70
4	Kinematics and muscle activity during robot-mediated motor adaptation of reaching with the upper limb .....	70
4.1	Introduction .....	70
4.2	Materials and methods.....	72
4.2.1	Ethical approval .....	72
4.2.2	Robot equipment .....	73
4.2.3	The reaching task .....	74
4.2.4	The experimental protocol .....	74
4.2.5	Recording techniques .....	75

4.2.6	Data analyses.....	80
	Reaching kinematics .....	80
	EMG pre-processing and basic muscle activity .....	80
4.2.7	Statistics .....	81
4.3	Results .....	81
4.3.1	Kinematics measures of motor adaptation .....	82
4.3.2	Basic muscle activity measures of motor adaptation .....	82
4.4	Discussions .....	89
4.4.1	Novel findings .....	89
4.4.2	The motor adaptation process .....	89
	Kinematics and behaviour.....	89
	Muscle activations.....	90
4.4.3	Further insights into muscular correlates for rehabilitation .....	91
4.4.4	Limitations .....	93
5	Sensor-level neural correlates of robot-mediated motor adaptation during reaching with the upper-limb .....	94
5.1	Introduction .....	94
5.2	Materials and methods.....	96
5.2.1	Data collection and experimental protocol .....	96
5.2.2	Data analyses.....	96
	EEG pre-processing .....	96
	Event-Related Potentials (ERPs).....	97
	Event-Related Spectral Perturbations (ERSPs).....	98
5.2.3	Statistics .....	102
	ERPs.....	102
	ERSPs.....	102
5.3	Results .....	103
5.3.1	ERPs during natural undisturbed reaching.....	103
5.3.2	ERSPs during natural undisturbed reaching .....	107
5.3.3	ERPs changes during robot-mediated motor adaptation with respect to natural reaching.....	109
5.3.4	ERSPs changes during robot-mediated motor adaptation with respect to natural reaching.....	111
5.3.5	ERSPs during robot-mediated motor adaptation .....	111
5.4	Discussions .....	117
5.4.1	Novel findings .....	117
5.4.2	The natural reaching movement.....	117
5.4.3	The disturbed reaching movement and the motor adaptation process ....	119

5.4.4	Error-Related Negativity during motor adaptation .....	122
5.4.5	Limitations .....	123
6	Source-level neural correlates of robot-mediated motor adaptation during reaching with the upper-limb .....	125
6.1	Introduction .....	125
6.2	Materials and methods.....	127
6.2.1	Data collection and experimental setup .....	127
6.2.2	Data analyses.....	127
	Cortico-Muscular Coherence (CMC) at sensor-level .....	127
	Source localization .....	128
6.2.3	Statistics .....	129
	Cluster-based permutation tests .....	129
	Regions of Interest (ROIs) .....	129
6.3	Results .....	131
6.3.1	Sensor- and source-level CMC during reaching in different conditions.....	131
6.3.2	CMC correlates of robot-mediated motor adaptation .....	136
6.3.3	CMC changes during adaptation.....	136
6.4	Discussions .....	143
6.4.1	Novel findings.....	143
6.4.2	The natural reaching movement.....	143
6.4.3	The disturbed reaching movement and the adaptation process.....	145
6.4.4	Cortico-muscular and intermuscular coherence in rehabilitation .....	148
6.4.5	Limitations .....	150
	Study II: Real-world Scenario.....	151
7	Neural correlates of single- and dual-task walking in the real-world .....	151
7.1	Introduction .....	151
7.2	Materials and methods.....	153
7.2.1	Ethical approval .....	153
7.2.2	Experimental protocol.....	153
7.2.3	Recording techniques .....	154
7.2.4	Data analyses.....	160
	Gait measures .....	162
	EMG pre-processing and basic muscle activity .....	162
	EEG pre-processing .....	163
	Time-Frequency analyses.....	164
	Morlet-wavelet decomposition.....	164
	Power Spectral Density (PSD).....	165

7.2.5	Statistics .....	169
	Statistical analyses of gait measures .....	169
	Statistical analyses of EMG measures .....	169
	Non-parametric cluster-based permutation tests on PSD.....	169
7.3	Results .....	170
7.3.1	Gait measures .....	170
7.3.2	EMG RMS measures .....	171
7.3.3	Natural walking vs. resting-state EEG: non-parametric cluster-based tests on PSD	176
7.3.4	Dual-task vs. single-task walking EEG: non-parametric cluster-based permutation tests on PSD.....	176
7.4	Discussions .....	181
7.4.1	Novel findings.....	181
7.4.2	Gait and EMG measures .....	181
7.4.3	Neurophysiological evidence .....	183
	Natural walking in the real-world .....	183
	Walking while conversing.....	184
	Walking while texting with a smartphone .....	185
7.4.4	The role of the cortex in gait control.....	187
7.4.5	Limitations .....	189
8	Brain and behaviour: investigating the relationships between brain activations and gait patterns during single- and dual-task walking in the real world .....	191
8.1	Introduction .....	191
8.2	Materials and methods.....	192
8.2.1	Experimental setup and recording techniques .....	192
8.2.2	Data analyses.....	192
	Gait measures .....	192
	EEG pre-processing and ROI-based power spectrum.....	193
	Models of gait behaviour vs. EEG PSD activations .....	194
8.3	Results .....	194
8.3.1	Relationship between single-task walking acceleration and neurophysiological activity .....	194
8.3.2	Relationship between dual-task walking acceleration and neurophysiological activity: walking while conversing.....	195
8.3.3	Relationship between dual-task walking acceleration and neurophysiological activity: walking while texting with a smartphone .....	195
8.4	Discussions .....	200
8.4.1	Novel findings.....	200
8.4.2	Gait acceleration RMS as measure of gait stability and behaviour .....	200



8.4.3	Relationship between brain and behaviour .....	201
	Task-specific relationships between brain activation and gait behaviour.....	202
8.4.4	The potential role of the left posterior parietal cortex in gait rehabilitation 203	
8.4.5	Limitations .....	205
9	Final conclusions.....	207
9.1	The central role of the human brain in motor control of both upper- and lower- limb 207	
9.2	Novel indicators of human motor control of both upper- and lower-limb .....	209
9.3	Future considerations .....	212
9.4	Methodological considerations.....	215
10	Future perspectives: a case study .....	217
	References .....	224
	Appendix I Ethical Approval .....	257
	Appendix II Confidential volunteer medical questionnaire .....	259
	Appendix III Written volunteer consent form.....	260
	Appendix VI Peer-reviewed publications .....	263

## List of Figures

Figure 2-1: The motor cortical areas and descending neural pathways of the human motor control system. ....	16
Figure 2-2: Skeletal muscle anatomy. ....	19
Figure 2-3: Gait biomechanics. ....	37
Figure 3-1: System architecture thesis diagram. ....	52
Figure 3-2: 64-channel Waveguard cap (ANT Neuro, Enschede, Netherlands). ....	57
Figure 4-1: Experimental setup workflow and single components. ....	77
Figure 4-2: Experimental task environment and protocol. ....	78
Figure 4-3: Upper limb muscles. ....	79
Figure 4-4: The motor adaptation process. ....	84
Figure 4-5: Trial-by-trial kinematic measures of motor adaptation. ....	85
Figure 4-6: Block-by-block muscle specific activation profiles. ....	86
Figure 5-1: Stereotypical artefactual Independent Components topoplots. ....	100
Figure 5-2: Group grand average whole-brain Event-Related Spectral Perturbation changes during natural undisturbed reaching. ....	101
Figure 5-3: ERPs during natural reaching. ....	106
Figure 5-4: ERSPs during natural undisturbed reaching in each FOI. ....	108
Figure 5-5: ERPs activations and statistical comparisons for the N300 component. ...	110
Figure 5-6: ERSPs changes during early adaptation to the robot-mediated force field in each FOI. ....	112
Figure 5-7: Event-Related Spectral Perturbations changes during late adaptation to the robot-mediated force field in each FOI. ....	113
Figure 5-8: Event-Related Spectral Perturbations during late wash out of the adaptation effects in each FOI. ....	114
Figure 5-9: Event-Related Spectral Perturbations differences between late and early adaptation in each FOI. ....	115
Figure 6-1: Sensor-level plots of an exemplary single subject cortico-muscular coherence between all EEG electrodes and the Triceps Brachii (first row), the Biceps Brachii (second row) and the Extensor Carpi Radialis (third row) muscles in both $\beta$ and low $\gamma$ frequency bands during natural reaching. ....	132
Figure 6-2: Source-level plots of all subjects grand average of cortico-muscular coherence between all EEG electrodes and the Triceps Brachii muscle. ....	133
Figure 6-3: Source-level plots of all subjects grand average of cortico-muscular coherence between all EEG electrodes and the Biceps Brachii muscle. ....	134
Figure 6-4: Source-level plots of all subjects grand average of cortico-muscular coherence between all EEG electrodes and the Extensor Carpi Radialis muscle. ....	135
Figure 6-5: Source-level non-parametric permutation test on $\gamma$ CMC with Biceps Brachii muscle when comparing Early MA vs. Late Fam. ....	138
Figure 6-6: Source-level non-parametric permutation test on $\beta$ CMC with Extensor Carpi Radialis muscle when comparing Late MA vs. Late Fam. ....	139
Figure 6-7: Source-level non-parametric permutation test on $\beta$ CMC with Biceps Brachii (A) and Extensor Carpi Radialis (B) muscle when comparing Late MA vs. Early MA. ....	140
Figure 6-8: Changes in ECR-left SMA $\beta$ CMC average between late and early adaptation correlate with differences in maximum exerted force. ....	141
Figure 7-1: UEL Stratford Campus map and subjects walking path. ....	156
Figure 7-2: Mobile Setup for real-world experiments. ....	157

Figure 7-3: Offline analyses analytical pipeline. ....	161
Figure 7-4: Time-Frequency power spectrum for each single subject across conditions from P3 (A) and P4 electrode (B). ....	167
Figure 7-5: Condition specific topoplots of PSD grand-average across all subjects in each FOI. ....	168
Figure 7-6: Condition-by-condition gait speed. ....	172
Figure 7-7: Condition-by-condition acceleration RMS and RMSR profiles. ....	173
Figure 7-8: Lower limb muscles EMG profiles. ....	174
Figure 7-9: Non-parametric cluster-based permutation test comparing PSD in ST and Resting State. ....	178
Figure 7-10: Non-parametric cluster-based permutation test comparing PSD in DT1 vs. ST. ....	179
Figure 7-11: Non-parametric cluster-based permutation test comparing PSD in DT2 vs. and DT1. ....	180
Figure 8-1: ROIs of interest. ....	196
Figure 8-2: Observed vs. Predicted ver-RMSR values according to the multiple regression model during ST. ....	197
Figure 8-3: Observed vs. Predicted ver-RMSR values according to the multiple regression model during DT1. ....	198
Figure 8-4: Observed vs. Predicted ml-RMSR values according to the multiple regression model during DT2. ....	199
Figure 10-1: The direct and indirect basal ganglia pathways according to the Rate Model. ....	220
Figure 10-2: Pilot study with one Parkinson's disease patient. ....	221
Figure 10-3: Example of one Parkinson's disease patient's natural walking performance with respect to the healthy subjects sample recruited in Study II. ....	223

## **List of Tables**

Table 4-1: Kinematics results.....	87
Table 4-2: EMG results.....	88
Table 5-1: Non-parametric cluster-based permutation test on Event-Related Spectral Perturbations changes with respect to natural reaching. ....	116
Table 6-1: Non-parametric cluster-based permutation test on CMC changes with respect to natural reaching.....	142
Table 6-2: Non-parametric cluster-based permutation test on CMC changes during adaptation. ....	142
Table 7-1: Dual-task conditions. ....	158
Table 7-2: Summary of each single subject experiment. ....	159
Table 7-3: Single- and Dual-task conditions gait measures.....	175
Table 7-4: Single- and Dual-task conditions EMG measures.....	175
Table 10-1: Natural walking gait measures of one Parkinson's disease patient. ....	222

## **List of Equations**

Equation 3-1: FFT Algorithm formula.....	63
Equation 3-2: Gaussian taper formula. ....	64
Equation 3-3: Scaled and translated Gaussian taper formula.....	64
Equation 3-4: ERSP formula.....	64
Equation 3-5: Coherence formula. ....	65
Equation 3-6: DICS spatial filter formula. ....	66
Equation 4-1: Robot-mediated velocity dependent force field. ....	73
Equation 6-1: Confidence Interval formula. ....	128
Equation 6-2: Multiple regression models formula. ....	137
Equation 6-3: $\Delta$ Peak Force multiple regression model formula. ....	137
Equation 7-1: RMSR formula. ....	162
Equation 8-1: Multiple regression models for RMSR formula.....	194
Equation 8-2: Multiple regression model for verRMSR during ST formula. ....	195
Equation 8-3: Multiple regression model for verRMSR during DT1 formula. ....	195
Equation 8-4: Multiple regression model for mlRMSR during DT2 formula. ....	195
Equation 10-1: Multiple regression model for verRMSR with PD patient's data when simply walking. ....	219
Equation 10-2: Multiple regression model for mlRMSR with PD patient's data when simply walking. ....	219

### **List of Accompanying Material**

Accompanying this work are copies of the peer-reviewed publications published or accepted for publication during the period of PhD before thesis submission. Specifically:

- PIZZAMIGLIO, S., DE LILLO, M., NAEEM, U., ABDALLA, H. & TURNER, D. 2017. High-frequency intermuscular coherence between arm muscles during robot-mediated motor adaptation. *Frontiers in Physiology*. 7: 668. doi: 10.3389/fphys.
- PIZZAMIGLIO, S., DESOWSKA, A., SHOJAIL, P., TAGA, M. & TURNER, D. L. 2017. Muscle co-contraction patterns in robot-mediated force field learning to guide specific muscle group training. *NeuroRehabilitation*, 41(1), 17-29.
- PIZZAMIGLIO, S., NAEEM, U., UR REHMAN, S., SHARIF, M.S., ABDALLA, H. & TURNER, D.L. 2017. A multimodal approach to measure the levels of distraction of pedestrians using mobile sensing. *Procedia Computer Science*, 113, 89-96.

## Abbreviations

<b>AD</b> – Anterior Deltoid	<b>DV</b> - Dependent Variable
<b>Ag</b> – Silver	<b>Early MA</b> – Early Motor Adaptation
<b>AgCl</b> – Silver Chloride	<b>EC</b> – Eyes Closed
<b>Ap</b> – Antero-posterior direction	<b>ECG</b> - Electrocardiogram
<b>ASL</b> - Amyotrophic Lateral Sclerosis	<b>ECoG</b> – Electrocorticography
<b>ANOVA</b> – Analysis of Variance	<b>ECR</b> – Extensor Carpi Radialis
<b>BA</b> – Brodmann Area	<b>EEG</b> – Electroencephalography
<b>BB</b> – Biceps Brachii	<b>EMG</b> – Electromyography
<b>BCI</b> – Brain-Computer Interfaces	<b>ENG</b> – Electroneurography
<b>BG</b> – Basal Ganglia	<b>EO</b> – Eyes Open
<b>BMI</b> – Brain-Machin Interfaces	<b>EOG</b> - Electrooculogram
<b>BR</b> – Brachioradialis	<b>ERD</b> – Event-Related Desynchronization
<b>BWS</b> – Body Weight Support	<b>ERP</b> – Event-Related Potential
<b>CBT</b> – Corticobulbar Tract	<b>ERS</b> – Event-Related Synchronization
<b>CI</b> – Condition Index	<b>ERSP</b> – Event-Related Spectral Perturbation
<b>CIMT</b> – Constrained-Induced Therapy	<b>FC</b> – Frontal Cortex
<b>CLR</b> – Cerebellar Locomotor Region	<b>FCR</b> – Flexor Carpi Radialis
<b>CMC</b> – Cortico Muscular Coherence	<b>FES</b> – Functional Electrical Stimulation
<b>CMT</b> – Corticomesencephalic Tract	<b>FFT</b> – Fast Fourier Transform
<b>CNS</b> – Central Nervous System	<b>fMRI</b> – functional Magnetic Resonance Imaging
<b>CPG</b> – Central Pattern Generator	<b>fNIRS</b> – functional Near-Infrared Spectroscopy
<b>CSD</b> – Cross-Spectral Density	<b>FoG</b> – Freezing of Gait
<b>CST</b> – Cortispinal Tract	<b>FOI</b> – Frequency of Interest
<b>DBS</b> – Deep Brain Stimulation	<b>FSRs</b> – Force Sensing Resistor sensors
<b>DICS</b> – Dynamic Imaging of Coherent Sources	<b>FWER</b> – Family-Wise Error Rate
<b>DLPFC</b> – Dorso-Lateral Pre-Frontal Cortex	<b>GABA</b> – Gamma-Aminobutyric
<b>DT1</b> – Dual-Task 1	<b>GIF</b> – Gait Initiation Failure
<b>DT2</b> – Dual-Task 2	<b>IC</b> – Independent Component

**ICA** – Independent Component Analysis

**IMC** – Inter Muscular Coherence

**IPL** – Inferior parietal Lobule

**IV** – Independent Variable

**Late Fam** – Late Familiarization

**Late MA** – Late Motor Adaptation

**Late WO** – Late WO

**LR** – Loading Response

**M1** – Primary Motor Cortex

**MCP** – Multiple Comparisons Problem

**MEA** – Micro-Electrodes Array

**MI** – Motor Imagery

**MI** – Medio-lateral direction

**MLR** – Midbrain Locomotor Region

**MNI** – Montreal Neurological Institute

**MoBI** – Mobile Brain/Body Imaging

**MRF** – Medullary Reticular Formation

**MRI** – Magnetic Resonance Imaging

**MS** – Multiple Sclerosis

**PC** – Personal Computer

**PD** – Parkinson’s disease

**PD** – Posterior Deltoid

**PFC** – Pre-Frontal Cortex

**PS** – Pre-Swing

**PSD** – Power Spectral Density

**PET** – Positron Emission Tomography

**PLSR** – Partial-Least Square Regression

**PMBS** – Post-Movement Beta Synchronization

**PMC** – Pre-Motor Cortex

**PPC** – Posterior Parietal Cortex

**RAGT** – Robot-Assisted Gait Training

**rCBF** – regional Cerebral Blood Flow

**RMS** – Root Mean Square

**RMSR** – Root Mean Square Ratio

**ROI** – Region of Interest

**S1** – Primary Sensory Cortex

**SCI** – Spinal Cord Injury

**SD** - Standard Deviation

**SMA** – Supplementary Motor Area

**ST** – Single Task

**TB** – Triceps Brachii

**TFr** - Time-Frequency

**TTL** – Transistor-Transistor Logic

**VE** – Virtual Environment

**Ver** – Vertical direction

**VIF** – Variance Inflation Factor

**VNS** – Vagus Nerve Stimulation



## **Acknowledgements**

I would like to thank all my supervisors, Prof. Hassan Abdalla, Prof. Duncan Turner and Dr. Usman Naeem, for their valuable support, advice and guidance given me throughout the three years of research presented in this work of thesis. I am especially grateful to Prof. Duncan Turner for his-daily basis teaching and mentoring: to him I owe my newly acquired abilities to work strategically and independently, as well as my way of thinking ahead of times.

I wish also to sincerely thank Prof. Klaus Gramann for his extremely valuable mentoring throughout my research, for which I am very grateful.

I would like to thank all my beloved family whose support and love gave me the right motivation to never let go. Mum and Dad, I dedicate this thesis to you.

Lastly, my dearest thank goes to Gabriele, cause together everything is possible.

# 1 Introduction

## 1.1 Overview

The human brain is known to play a central role in motor control of the upper limb because invasive (Truccolo et al., 2008) as well as non-invasive (Fabbri et al., 2010; Toxopeus et al., 2011) neurophysiological investigations have demonstrated the direct encoding of final motor commands within the primary motor cortex and the programming of the movement within the posterior parietal regions. Non-invasive EEG studies reported the neural correlates of the reaching movement whereby the so called “dorso-visual stream” is recruited including occipital-parietal and frontal-premotor and motor areas contralateral to the moving limb (McDowell et al., 2002; Naranjo et al., 2007; Demandt et al., 2012; Dipietro et al., 2014; Storti et al., 2015). The central role of the human cortex and of deep brain structures in the control and adaptation of upper-limb movements have been also extensively demonstrated through studies of motor learning. Initial unskilled performance is mediated by a cortico-striatal network and more consolidated skilled performance is in contrast promoted by cortico-cerebellar interactions (Shadmehr and Holcomb, 1997; Krebs et al., 1998). The human brain is also believed to be important for coordinating and adapting gait behaviour even though the hierarchy behind gait control is far more complex. Both supra-spinal (cortex, basal ganglia, cerebellum, brainstem) and spinal (Central Pattern Generators, CPGs) structures are known to be involved in locomotion, but the specific role of each of these elements is still under debate (Takakusaki et al., 2013; Kim et al., 2016; Takakusaki et al., 2017). Evidence in favour of a central role of the human cortex in high level control and programming of gait were obtained by observing walking behaviour both invasively and non-invasively. By investigating neural changes to specific gait training paradigms with both healthy individuals and stroke survivors, increased activations in premotor, sensorimotor and supplementary motor areas were observed. This suggests that adaptive control of locomotion is taken over primarily by different cortical regions, which in turn modulate the activity of spinal structures for the generation of gait rhythm and muscle activation patterns (Miyai et al., 2002; Kim et al., 2016). Recent invasive studies with implanted epileptic patients demonstrated that the primary motor cortex activity is modulated in a gait specific manner and this is unrelated to lower limb muscles activity and/or trajectories, further strengthening the putative role of the cerebral cortex in gait control (McCrimmon et al., 2017). The neural correlates of gait control have been difficult to carefully explore because of the technical limitations of the available instrumentation (Dobkin et al., 2004; Bartels and Leenders, 2008; Jahn et al., 2008; Ikeda et al., 2016;

Bürki et al., 2017; Labriffe et al., 2017). Recent developments in mobile technologies currently allow wireless recordings of kinematic, muscular, hemodynamic and neural evidence of ambulatory activities real-world scenarios.

The development of mobile technologies has gained substantial interest in the fields of sports sciences (Park et al., 2015; Cheron et al., 2016), urban architecture (Aspinall et al., 2013; Tilley et al., 2017), and human neuroscience (Contreras-Vidal et al., 2017; Gramann et al., 2014). The study of human natural behaviour in real-world settings rather than controlled laboratory environment would shed some light on the neural correlates of daily-life activities (i.e. ecological validity). Moreover, current trends in rehabilitation and recovery also aim to provide assistive technologies and assessment tools that could reliably work within the patients' home environment. Indeed, performance of patients within laboratory settings does not resemble the real status of the disease or recovery as they strive to perform better whilst being observed in the lab (Del Din et al., 2016). Monitoring systems that could be used at home and register patients' performance during daily life activities have been developed as, for example, a home-based system for the evaluation of upper limb reaching recovery after stroke (van Meulen et al., 2014; van Meulen et al., 2016). The design of such systems is currently possible thanks to the new generation of wearable sensors able to record angular and linear kinematics and dynamics of the body segments on which they are placed. Moreover, the developments of wireless systems for the recording of neural and muscular activity has made monitoring of neural plasticity during recovery possible. Systems of support for movement or other human functions, such as brain-computer/machine interfaces, have explored many possible ways for patients to control the assistive devices (Millan et al., 2010; Tucker et al., 2016). So far, the most reliable and less invasive controllers that can be used in the home environment with a long-term perspective are based on the recording of electro-cortical activity from which to decode intentional motor (Choi et al., 2016; Presacco 2011; Georgopoulos and Carpenter, 2015; Ubeda et al., 2017) or functional commands (Birbaumer et al., 1999). BCI-training in the home environment was recently shown to promote optimal neural plasticity with no compensatory maladaptive mechanisms, as well as to engage and motivate patients (Zich et al., 2017).

Recovery after neural injuries such as stroke can be provided through many different types of paradigms specific to the upper or lower limb, as well as according to the level of showed impairment (Huang and Krakauer 2009; Beyaert et al., 2015). One of the latest frontiers in neurorehabilitation is the employment of neurofeedback signals in order to

train subjects on how to modulate the activity of a specific brain area or network (Linden and Turner, 2016). Real-time detected fMRI BOLD signals from one single brain region or network can be fed back to subjects through means of visual representations (i.e. thermometer bars) and eventually modulated by asking subjects to increase or decrease the height of the visualised bar. Neurofeedback training has been employed in preliminary investigations for emotional control (Zotev et al., 2014), pain control (Chapin et al., 2012) and motor control (Berman et al., 2012; Hui et al., 2014; Cevallos et al., 2015; Marins et al., 2015). Studies of motor control of the upper-limb with healthy individuals showed difficulties in self-regulating the M1 BOLD activity when targeted alone during motor imagery of hand movement (Yoo et al., 2008; Berman et al., 2012). On the other hand, positive effects were detected when modulating activity from ventral PMC (Marins et al., 2014) or both ipsilateral and contralateral M1 together (Auer et al., 2015). Despite most of the neurofeedback studies reported so far have been carried out using functional magnetic resonance, this technique has limits in terms of accessibility and costs (Linden and Turner, 2016). Early insights into neurofeedback paradigms provided through measures of surface electroencephalography have been reported in motor control of fingers through reference measures of neuro-muscular couplings (i.e. cortico-muscular coherence) (von Carlowitz-Ghori et al., 2015), as well as in the improvement of balance control in healthy adults and dual-task walking in stroke survivors through reference measures of region specific electrocortical activity (Lee et al., 2015; Azarpaikan and Torbati, 2017). Thus the need arises for the investigation and definition of reliable indicators of specific neurophysiological control mechanisms through more accessible alternative techniques, such as EEG, that could be eventually employed in real-life rehabilitation settings. As a first step, this research programme aimed to investigate the neurophysiological correlates of human motor control of both the upper and the lower limb in real-world scenarios and to propose different markers of specific motor activities which could be further exploited by novel neurorehabilitation paradigms such as neurofeedback training.

## **1.2 Goals and hypotheses**

### **1.2.1 Motor control of the upper limb: the neurorehabilitation scenario**

A lab-based experimental setup was designed to investigate upper-limb motor control and the neuro-muscular correlates of reaching movements in both stable (natural) and unstable (applied external perturbation) situations. Robot-mediated force-field adaptation is a motor learning paradigm potentially exploitable during rehabilitation after neural

injuries such as stroke. For example, it has been demonstrated that the manipulation of the external perturbation could induce training after-effects in stroke survivors resembling natural movement behaviours (Patton and Mussa-Ivaldi, 2004). Applying an external perturbation while reaching induces initial significant movement deviations which subjects learn to reduce exponentially with practice (Milner and Franklin, 2005; Trewartha et al., 2014). It has been suggested that both peripheral (muscular) and central (cerebral) mechanism work in tandem in this adaptive behaviour, although there is a paucity of evidence. Indeed, the specific responses of muscles and the brain during the adaptation practice are still not fully understood (Turner et al., 2013). This research programme was designed to test hypotheses involving both peripheral and central mechanisms in more detail than previously considered. The goal of the first scenario was therefore to define neural and muscular indicators specific of an adaptation protocol that could be feasible for patients in future neurorehabilitation practice (such as neurofeedback training).

When an external force-field is applied during reaching behaviour, initial muscular activations are thought to be of a feedback nature, that is, they are spontaneous reactions due to feedback drives triggering muscle activation to accomplish the final goal (i.e. reaching) (Milner and Franklin, 2005). With practice however, subjects develop predictive mechanisms which increase early muscle activity in anticipation of the externally applied force field – a so-called feedforward response to adapted reaching (Milner and Franklin, 2005; Huang and Ahmed 2014). It was hypothesised that muscle activation would be adapted during reaching in a force field in a specific pattern related to the direction of the force field (i.e. Posterior Deltoid, Triceps Brachii and Extensor Carpi Radialis would be most recruited to counteract the perturbation (Thoroughman and Shadmehr, 1999)). Furthermore, it was hypothesised that in the initial stage of adaptation, all the analysed muscles would show similar profiles of systematic increased activity. In contrast, in later stages of adaptation, those muscles not strictly required to compensate for the applied force-field were hypothesised to reduce their initial increased activations towards normal profiles, whereas selected muscles would develop a more robust activation pattern and suggest the development of a feedforward model of adaptation in the later stages. Several different methods of analysis were used to test these hypotheses such as measures of muscle co-activation (more likely in early adaptation) and cortico-muscular coherence (stronger cortical control over individual muscle activation developing in later adaptation). Source reconstructed neuro-muscular correlates (cortico-muscular coherence) in the period of reaching may demonstrate coupling in the medium

frequency spectrum ( $\beta$  band) between the contralateral primary motor cortex (Fang et al., 2009) and those muscles recruited during the reaching movement and subsequent adaptation to the applied counter-clockwise force-field (i.e. upper-limb extensors).

Reaching is underpinned by activation of parietal-occipital areas in parallel to frontal-premotor and motor areas (Naranjo et al., 2007; Demandt et al., 2012; Dipietro et al., 2014). Long-term force-field motor adaptation involves a shift from the cortical-striatal loop in early stages (i.e. frontal areas and striatum) to the cortical-cerebellar loop (i.e. parietal regions and cerebellum) in later stages of motor adaptation (Shadmehr and Holcomb, 1997; Krebs et al., 1998). Moreover, the primary motor cortex is believed to be involved in after-practice consolidation of the newly acquired motor memories (Della-Maggiore et al., 2017). It was hypothesised that spontaneous neural fluctuations (Event-Related Potentials) in response to the reaching movement would show a sequential activation of the occipital-parietal regions paralleled by the sequential activation of frontal-premotor regions. Reaching-related electrocortical spectral power (Event-Related Spectral Perturbations) was hypothesised to show correlates during reaching (Demandt et al., 2012). These correlates include a sustained low ( $\alpha$ ) and medium ( $\beta$ ) frequency decrease of activity (event-related desynchronization) during the reaching period with respect to the prior period of stillness that is spread over a broad area including supplementary motor, premotor and sensorimotor areas. In addition, it was hypothesised that there would be an increase (event-related synchronization) of high frequency ( $\gamma$ ) power in the beginning of reaching (around movement onset time) mostly focused in the contralateral sensorimotor cortex (Ball et al., 2008; Babiloni et al., 2016).

Different specific hypotheses were made on the neural correlates of reaching in the perturbed condition, mostly based on the previously reported findings on force-field motor adaptation (Shadmehr and Holcomb, 1997; Krebs et al., 1998). First, event-related spontaneous neural deflections related only to movement initiation and execution (i.e. around the time of movement onset) were hypothesised to show increased activity during adaptation, whereas no changes were expected in the earlier components mostly related to visual feedback and target selection. In line with the previous findings, the postulated changes were expected in frontal electrodes and in posterior parietal-occipital electrodes during early and later stages of adaptation, respectively. Secondly, changes in neural spectral power were hypothesised to encompass premotor, supplementary motor (early phase) and parietal regions (later phases), whereby a stronger  $\beta$  desynchronization was expected as an indicator of stronger sensorimotor integration (Engel and Fries, 2010).

Lastly, changes in cortico-muscular coherence during adaptation were expected to occur within the  $\beta$  and  $\gamma$  frequencies of oscillations in, once again, premotor, supplementary motor (early phase) and parietal regions (later phases).

The thorough investigation of the motor task through different techniques aimed to ultimately identify crucial cortical areas involved in the adaptation process whose activities could eventually be target of future modulation and self-regulation paradigms (for example through measures of event-related potentials, spectral power or cortico-muscular coherence) with the final goal of promoting restoration of impaired functions and facilitating recovery after neural injuries.

### **1.2.2 Motor control of the lower limb: the real-world scenario**

The second focus of this research programme was the study of gait control and, using novel mobile technologies, it was possible to move outside the lab into real-world contexts for more ecologically valid results. The goal was to observe how different real-life situations (i.e. walking naturally, walking while conversing and walking while texting with a smartphone) impacted on gait behaviour and how neural and muscular activity changed among the three situations.

Walking in hazardous environments has been demonstrated to reduce gait speed and increase trunk sway in both young and elderly individuals (Iosa et al., 2014; Menz et al., 2002; Menz et al., 2003). Most interestingly, it was postulated that walking while performing tasks preventing subjects from visual scanning the surroundings have the strongest negative effects on gait control (Beurskens and Bock, 2013), such as walking while texting over a smartphone (Plummer et al., 2015; Agostini et al., 2015). When walking while carrying out a secondary cognitive task (i.e. Verbal Fluency Test) without specific task prioritization gait speed decreased and gait dysrhythmicity increased, regardless of age (Yogev-Silgemann et al., 2010). Several other studies confirmed that the simultaneous performance of a secondary task, such as numerical subtractions (Mirelman et al., 2014; Al-Yaya et al., 2016), Verbal Fluency Test (Doi et al., 2013), reciting aloud alphabet letters (Holtzer et al., 2011; Holtzer et al., 2015), negatively influences gait performance. It was therefore hypothesised that conversing with the experimenter and texting over the smartphone while walking would induce reduced gait speed, increased trunk sway and gait variability (expressed through different measures, Yang et al., 2012) with respect to a natural walking task. Moreover, since vision is focussed on texting over the smartphone, constant visual scanning of the surroundings would likely be limited. It was therefore postulated that the greatest increase in gait

variability would be observed when subjects walked while texting over the smartphone (Caramia et al., 2017). In contrast, the effects of walking on the performance of the secondary task are contrasting. For example, no significant differences were reported in counting backwards while walking and while standing in both healthy young adults and stroke survivors (Mirelman et al., 2014; Al-Yaya et al., 2016). In another instance however, the rate of errors in reciting alternate alphabet letters aloud increased when healthy young adults walked in comparison to when seated still (Holtzer et al., 2015). In the current research programme, the secondary tasks were designed to resemble real-life situations and thus were complex in terms of assessing the related performance given the lack of a structured scheme (i.e. when conversing with the experimenter subjects were allowed to talk as much as they wanted without any guidelines). Moreover, intra-personal (i.e. character, previous experiences) and environmental (i.e. weather, surrounding people) might have also influenced the performance of the real-life secondary tasks. Therefore, it was decided not to investigate effects of walking on the secondary task performance and to instead simply focus on the neurophysiological correlates related to gait control during different real-world situations.

Neural hemodynamic activations during natural gait encompass the medial primary sensorimotor (Homunculus leg area), bilateral supplementary and anterior prefrontal regions (Miyay et al., 2001). Consistent findings were reported by electroencephalographic recordings whereby sustained reduced spectral power in low ( $\alpha$ ) and medium frequencies ( $\beta$ ) were observed in bilateral sensorimotor and dorsal anterior cingulate regions in parallel to modulated increased power in high ( $\gamma$ ) frequencies in bilateral posterior parietal, anterior cingulate and sensorimotor cortices (Gwin et al., 2011). The sustained desynchronization of low-medium frequencies was postulated to represent an active state promoting voluntary movement (Engel and Fries, 2010), whereas the modulated synchronization of high frequencies was believed to be symbolic of sensorimotor integration mechanisms (Seeber et al., 2014; Seeber et al., 2015). It was therefore hypothesised that walking naturally outside the laboratory would recruit the same neural mechanisms observed in treadmill-based experiments, that is a sustained power desynchronization within the low-medium frequency spectrum and a modulated power synchronization within the high-frequency spectrum in the medial and bilateral sensorimotor premotor and posterior parietal cortices.

The simultaneous performance of a secondary cognitive task has been shown to increase the oxygenation levels of the rostral prefrontal cortex (BA10) in correlation with the



difficulty of the secondary cognitive task (i.e. counting forward and subtracting 7 by a 3-digit number) (Mirelman et al., 2014). Increased oxygenation levels in bilateral anterior prefrontal cortex, dorsolateral prefrontal cortex and inferior frontal gyrus were reported in a cohort of elderly individuals with mild cognitive impairments (MCI) when walking and simultaneously performing a Verbal Fluency Test (Doi et al., 2013). Increased levels of hemodynamic activity in bilateral anterior and dorsolateral prefrontal cortex was also reported when walking while reciting aloud alternate alphabet letters in both young and elderly adults (Holtzer et al., 2011; Holtzer et al., 2015). Despite the emerging interest and focus of dual-task effects on the prefrontal cortex, other studies have demonstrated that other areas may be involved in dual task performance, depending also on the type of second task performed. In a cohort of young healthy individuals walking on a treadmill while performing a Verbal Fluency Test, increased oxygenation levels were observed in areas expanding from inferior frontal gyrus to middle temporal gyrus, eventually suggested to be related to both talking and recruiting executive functions, as pure language production would have resulted in the involvement of the Broca's area only (Metzger et al., 2017). Moreover, walking in hazardous situations such as on a balance beam (Sipp et al., 2013), uphill (Bradford et al., 2016) and while accelerating/decelerating (Wagner et al., 2016), showed stronger  $\beta$  desynchronization in bilateral sensorimotor and posterior parietal areas, likely symbolic of stronger sensorimotor integration mechanisms recruited to promote the more challenging voluntary movement (Engel and Fries, 2010). Therefore, in the current research it was postulated that, with respect to the single-task condition, walking while conversing would show increased spectral power in anterior prefrontal, dorsolateral prefrontal and inferior frontal gyrus, most likely in the left hemisphere (i.e. Broca's area) within the very low frequencies ( $\theta$ ) (i.e. recently shown to be involved in speech detection, understanding and creation, Giraud et al., 2017). On the contrary, walking while texting over the smartphone was considered to be quite uncommon and challenging even for healthy young adults, thus increased low-frequency prefrontal (anterior and dorsolateral) activations were expected in parallel to stronger  $\beta$  desynchronization in bilateral sensorimotor and posterior parietal areas.

Different studies reported significant relationships between the level of cortical activations and performance in dual-task conditions: for example, gait variability and cognitive performance were negatively correlated with prefrontal oxygenation levels in healthy young adults (Mirelman et al., 2014). The authors suggested that subjects requiring less cognitive effort were more predisposed to perform better in the cognitive task. In another study, prefrontal hemodynamic activity negatively correlated with the

level of executive functions of elderly individuals with MCI, suggesting that subjects that were more impaired required more cognitive effort to accomplish a dual-task situation (Doi et al., 2013). Prefrontal oxygenation levels were also positively related to the value of stride length and to the rate of correct letters generated during dual-task performance by a cohort of healthy elderly adults (Holtzer et al., 2015). However, as previously mentioned, other areas than the prefrontal cortex could be involved in the promotion of dual-task performance while walking. Since the goal of the current research was to define neural correlates of gait control under different real-life situations, it was postulated that the activity recorded from the prefrontal cortex (average of electrodes located over anterior and dorsolateral prefrontal cortex) as well as from the bilateral posterior parietal cortices (promoter of sensorimotor integration) would be potentially involved in locomotion control. Given the successful employment of measures of trunk acceleration in the study and classification of gait stability in neurological populations (Sekine et al., 2013; Sekine et al., 2014; Iosa et al., 2014), it was hypothesised that spectral power in the selected cortical regions would be significantly related to trunk acceleration during the three walking conditions.

The identification of preliminary significant relationships between a specific cortical activity and measures of gait stability could eventually be exploited in further research as predictors of gait behaviour as well as easy-to-follow targets of neurofeedback and/or BCI training paradigms aimed to promote recovery through self-regulation of gait stability (Ang et al., 2015; Lee et al., 2015). Moreover, the identification of a significant relationship between cortical activations and gait performance would further strengthen the theories on the central role of the brain in gait control (Miyai et al., 2002; Takakusaki et al., 2013; Kim et al., 2016; Takakusaki et al., 2017).

### **1.3 Thesis outline**

This work of research therefore focused on designing comprehensive setups, compiling a transferable analytical pipeline and defining different evaluation measures with which to examine in full details different aspects of motor control and recovery. Given the recent need for reliable mobile setups for ambulatory real-world investigations, the main technical challenge of the work was to define an optimal experimental pipeline that could be transferred in different real-world scenarios and that could successfully investigate either behavioural and neurophysiological aspects of upper and lower limb motor control. Therefore, two major studies were carried out and here presented, both employing the

same experimental structure but adapted to the scenario specificities. Specifically, the document is structured as follows:

- Study I describes the “Hospital Neurorehabilitation Unit scenario” whereby a robot for the rehabilitation of the upper limb has been employed during a force field motor adaptation protocol for the reaching movement. Chapter 4 describes the full experimental setup able to monitor the adaptation task from both a behavioural (i.e. kinematics) and neurophysiological (i.e. EMG, EEG) perspective. This chapter focuses on the kinematic and muscular evidence of the adaptation process. To this chapter belong two published works reported in Appendix IV (Pizzamiglio et al., 2017; Pizzamiglio et al., 2017), which further questioned the specificity of muscular activations during the adaptation process through more sophisticated measures of muscular co-contraction and intermuscular coherence. Chapter 5 argues on the effects of motor adaptation on the human brain through measures of cortical Event Related Potentials (ERPs) and Event Related Spectral Perturbations (ERSPs) extracted from the sensor level EEG data. Many motor learning and motor adaptation studies focused on the changes before and after practice (Shadmehr and Holcomb, 1997; Krebs et al., 1998), but little is known on the cortical correlates of these protocols while they are executed. Lastly, chapter 6 focuses on the neural correlates of the motor adaptation process by investigating the relationship between source-reconstructed cortical and muscular activations during both natural and disturbed reaching (Rossiter et al., 2013; Belardinelli et al., 2017);
- Study II describes the “Real-World Urban scenario”, whereby different walking conditions resembling real life situations have been investigated using behavioural, muscular and neural measures. The same experimental framework of Study I was employed but adapted to a mobile, real-world context. Chapter 7 describes the developed fully mobile setup able to monitor different walking situations (i.e. walking naturally, walking while conversing and walking while texting with a smartphone) through behavioural (i.e. kinematics) and neurophysiological evidence (i.e. EMG, EEG). This chapter focuses on the changes in gait performance across conditions (from single to dual task), and how muscular and neural correlates are modulated in each specific situation. It is known that walking while engaging in a secondary task impairs gait behaviour and that the nature of the secondary task influences the level of impairment in both healthy young adults, old adults and patients (Yogev-Silgmann et al., 2010; Iosa et al., 2014; Sekine et al., 2013; Sekine et al., 2014; Agostini et al., 2015; Beurskens et al., 2016). However, little is known on the specific neural changes

at the basis of these tasks. Lastly, chapter 8 reasons on measures of trunk movement magnitude (i.e. acceleration RMSR) and how these could be possibly related to neural activations during each specific walking condition. Acceleration RMSR have been extensively used as marker of gait disability and abnormalities in different types of patients (Latt et al., 2009; Van Crielinge et al., 2017; Sekine et al., 2013; Sekine et al., 2014), but no direct link with brain activity has been proposed so far.

#### **1.4 Research contributions and novelty**

As previously mentioned, in this work of research attention was drawn to the investigation of neurophysiological mechanisms of human motor control in real-world scenarios and to the identification of novel mechanism-specific markers that could be employed by future rehabilitative practice. In each study, analyses were carried out first to replicate previous findings and were then expanded to provide novel evidence of the neurophysiological mechanisms underlying the investigated motor activities. Overall, the findings reported in the current work of thesis further strengthen the theories on the central role of the brain in the control of both upper- and lower limb motor acts (see chapter 9, paragraph 9.1), following previous claims and hypothesis found in literature (Fabbri et al., 2010; Toxopeus et al. 2011, Takakusaki, 2013; Takakusaki, 2017). Two cortical areas have been here identified as potential major contributors during the analysed scenarios: activity of medial frontal, premotor and supplementary motor regions are likely reliable markers of early stages of adaptation during reaching, as previously suggested (Shadmehr and Holcomb, 1997; Krebs et al., 1998), whereas activations of the posterior parietal cortex could be a potential marker of motor variability and individual-specific motor capabilities for both upper- and lower limb (Bürki et al., 2017; Haar et al., 2017). The major contributions of each study of the current work of research are hereafter summarized.

##### **1.4.1 Neurorehabilitation scenario**

A comprehensive experimental setup for the simultaneous monitoring of behavioural, muscular (EMG) and neural (EEG) data was developed to study different mechanisms and strategies responsible for motor control and adaptation during reaching in unstable situations. The concurrent recording of three different types of evidences allowed the identification of complementary indicators of the adaptation process. Specifically:

- Kinematics and muscular evidences demonstrated that different perturbation directions induce direction-specific muscle co-contraction profiles (see Appendix IV; Pizzamiglio et al., 2017), and the analysis of muscular neural coupling in the

frequency domain highlighted the development of specific pattern of coherent muscle activity during the adaptation process (see Appendix IV; Pizzamiglio et al., 2017). Evidences of high-frequency IMC in parallel to task-specific patterns of muscle co-contraction could be crucial physiological markers in the assessment of functional recovery as well as potential target of biofeedback training where subjects could learn to self-modulate their intermuscular couplings. Moreover, these findings have a strong impact on the design of future rehabilitative strategies as they could influence how an external perturbation is shaped in order to induce required subject-specific muscle activations;

- Neural recordings during natural reaching revealed the engagement of the reaching-specific frontal-parietal network called “dorsal-visual stream” (Grafton et al., 1996), whereas during adaptation changes in cortical activity (both at sensor and at source level) occurred in the medial frontal, premotor and supplementary motor regions, areas likely involved in early stages of adaptation for planning necessary motor strategies to counteract the external perturbation and modulating exerted force. Measures of event-related potentials, event-related spectral perturbations and corticomuscular coherence all revealed a major contribution from the above-mentioned areas, consistently confirming their role in adaptive control of the upper-limb in unstable situations. These findings validate the employment of both sensor- and source-level measures of cortical activity as potential markers of motor performance and recovery as well as potential targets for future rehabilitative paradigms promoting plasticity (i.e. BCI training) and self-modulation of neural activity (i.e. neurofeedback training).

#### **1.4.2 Real-world scenario**

In the second study, a novel Mobile Brain/Body Imaging (MoBI) setup was developed in order to comprehensively study human motor control in real-life situations outside the lab environment. This represents the most innovative contribution of this work of thesis as it allowed the study of natural human behaviours in a non-over controlled environment and would be a useful experimental approach to comprehensively monitor performance in everyday life activities and in clinical settings with the neurologically impaired (see chapter 10 for a potential application of the mobile setup). The inspected daily-life activities are also a novel experimental approach, whereby subjects were not constrained by performing over-simplified and monotonous tasks, but actually engaged in real-life multitasking activities. Investigations led to very interesting findings, specifically:

- The setup reliably captured changes in behaviour due to the specific task requirements as walking performance showed good variability across conditions. At the same time, neural correlates of walking under different conditions showed whole-brain frequency-specific changes in areas most involved in processes of executive functions and multitasking (dorsolateral and anterior prefrontal cortex) as well as in sensorimotor integration (posterior-parietal cortex). In line with previous cautious claims (Bürki et al., 2017; Metzger et al, 2017), the current findings confirmed the need for a whole-brain approach when studying complex multitasking situations as broad networks are likely involved and worth investigating. The reported results successfully demonstrated the applicability of the implemented MoBI setup and shed some new lights on the neurophysiological correlates underlying real-life human activities;
- By investigating potential linear relationships between brain activations and gait behaviour, the left-PPC activity was found to always correlate with measures of gait variability and abnormality (i.e. trunk acceleration), which suggested a potential major contribution of the left-PPC in the control of walking in the real-world regardless of any secondary tasks simultaneously performed. These findings are in line with recent claims on the relationship between the posterior parietal cortex and motor variability and outcomes of both upper- and lower limb movements (Bürki et al., 2017; Haar et al., 2017). These results bring a strong contribution to the current methodologies of gait evaluation and pave the path for future rehabilitative interventions that could for example target the identified cortical areas to promote restoration of gait and/or self-modulation of the neural mechanisms required to promote stability and control of motor variability.

## **2 Literature review**

### **2.1 Human motor control**

#### **2.1.1 The neural motor system**

The principal player within the neural motor control system is the primary motor cortex (M1) together with adjacent motor areas, such as the premotor cortex (PMC) and the supplementary motor area (SMA), and deeper structures of basal ganglia and cerebellum. M1 is located bilaterally in both hemispheres anterior to the central sulcus (i.e. it is also called the precentral gyrus) and extends from the lateral side of the hemisphere to its medial surface. The primary motor cortex has a topographical representation of each body part according to the motor homunculus as represented in Figure 2-1, with the medial part contains the leg and foot representations and more lateral parts representing face, tongue and mouth (even if overlaps are typical). The neuronal fibres located within M1 are those entitled to mediate fine voluntary movements. Different neuron types coming from M1, and in small contribution also from PMC and SMA, converge together into a descending pathway called the pyramidal tract, which carries down motor commands and other related information for the control of voluntary movements from the related hemisphere through the spinal cord and is divided into three sub-pathways (see Figure 2-1) (Wise and Shadmehr, 2002). The Corticobulbar Tract (CBT) contains a small portion of fibres that partially cross and partially remain on the same side and all innervate motor cranial nerves nuclei for the bilateral control of neck muscles. Similarly, the Corticomesencephalic Tract (CMT) contains a very small number of fibres coming from the frontal cortex that innervate the nuclei of the cranial nerves that mediate eye movements. Most interestingly, the Corticospinal Tract (CST) contains the highest number of descending fibres of the pyramidal pathway, it travels down through the brainstem until the decussation of pyramids, where 80% of the fibres cross to the other side forming the lateral corticospinal tract and the rest further descend along the same side forming the anterior corticospinal tract, and eventually end at the spinal cord level where the fibres make synapses with interneurons connected to spinal motor neurons (Baehr and Frotscher, 1998). The anatomical characteristics of the CST shed light on the fact that muscles on the right side of the body are controlled by the brain left hemisphere and vice versa. Moreover, the CST is directly involved in the control of proprioceptive and sensory inputs generated by movements and the gating of such afferent drives to central centres: indeed, ascending sensory neurons innervating the peripheral muscles transmit information to the central motor system for a continuous simultaneous control (Lemon, 2008). Lesions of the cerebral cortex such as trauma, stroke or tumour cause weaknesses or even paresis of the

contralateral body side, mostly of face and upper limb muscles as those have the widest cortical representation according to the homunculus. Lesions of the pyramidal tract at cervical level below the decussation of pyramids cause ipsilateral hemiplegia as the fibres have already crossed at higher level, whereas lesions above the crossing level can cause quadri-paresis or quadriplegia. Lesions of the CST at different level of the spinal cord cause a complete paralysis and the loss of all sensations.

Deep brain structures are not directly involved in the generation of motor commands activating muscle contractions but do work in tandem with the motor cortex for optimizing planning, execution and online monitoring of the movement (Middleton and Strick, 2000). The basal ganglia are a group of bilateral subcortical nuclei (i.e. Thalamus, Globus Pallidus, Putamen, Caudate Nucleus and Amygdala) located within deep within the brain which contribute to the control of voluntary movements and work in parallel and in direct contact with the motor cortex and the pyramidal tract. They are specifically recruited in the modulation of excitatory and inhibitory mechanisms of the motor cortex and their major role is promoting the initiation and facilitation of voluntary movements as well as the suppression of unwanted influences that might prevent the smooth execution of the action (Baehr and Frotscher, 1998). Lesions of the basal ganglia (the best known is in Parkinson's disease, PD) cause complex movement disorders typically featured by deficiency or an excess of movement (hypo- or hyperkinesia and tremor) as well as by abnormalities in muscles tone (Peterson and Horak, 2016). The cerebellum is located in the posterior fossa, it is intensely connected to the motor cortex and other brain areas and plays a major role in motor learning and memory (Shadmehr and Holcomb 1997; Krebs et al., 1998). Specifically, it maintains balance and ensures that movement are precisely coordinated and executed through sensory feedback from the periphery, (Baehr and Frotscher, 1998). Cerebellar lesions do not cause paralysis but impair the ability to learn new motor skills and to adapt to changes in the external environment (Butcher et al., 2017).



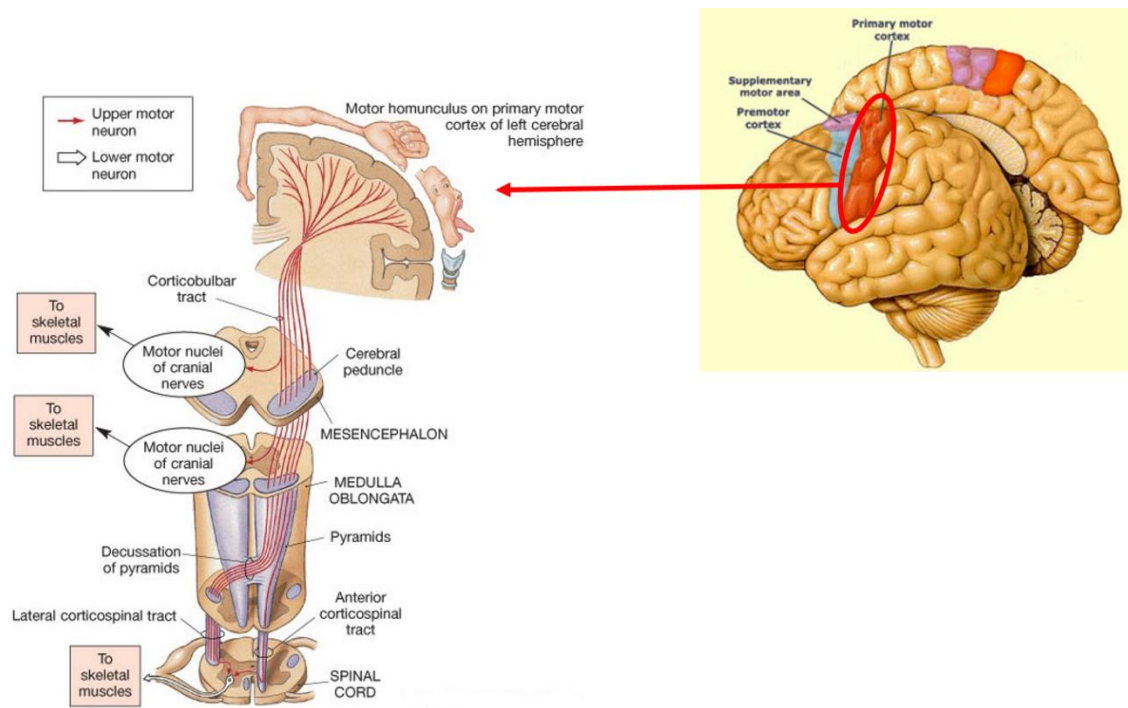


Figure 2-1: The motor cortical areas and descending neural pathways of the human motor control system.

The neural motor system: primary motor and premotor cortices (on the right) and the descending pyramidal tract with all its components (on the left).

### **2.1.2 The peripheral motor system**

Skeletal muscles are the effector organs of the motor system and are composed by two types of cells: extrafusal fibres, producing force and promoting movement, and intrafusal fibres, generating afferent sensory feedback to be sent to the central nuclei (Wise and Shadmehr, 2002). Extrafusal muscles fibres are excitable cells that promote contraction and force generation through specific chemical reactions happening within each muscle cell. Actin and myosin are filamentous proteins organized into highly ordered structures called sarcomeres (i.e. the contractile unit): each sarcomere forms between two Z structural proteins and is composed by thin filaments of helically coiled actin, projecting perpendicularly from the Z proteins towards the centre of the cell, alternated by thick bundles of myosin filaments located in the centre of the contractile unit (anchored to central vertical M proteins). Myosin filaments are composed by a long tail and a globular head whereas actin filaments dispose of specific binding sites (hidden at rest to the myosin head) which regulate the link between the two types of filament (Hopkins, 2006). When a peripheral nerve stimulates a muscle endplate (only area of possible neural stimulation) a motor action potential is generated which triggers a sequence of chemical reactions promoting the opening of calcium channels on the fibres membrane. When  $\text{Ca}^{2+}$  is reversed within the cytoplasm of a sarcomere it binds with the actin binding site, causing a change in the sub-unit's conformation and consequently exposing the whole binding site to the myosin globular head. As myosin binds with actin they slide relative to each other causing the shortening of the sarcomere, but plural actin-myosin bindings are needed to produce a contraction (Taggart and Podolsky, 1961; Hultman and Sjöholm, 1983; Greenhaf, 2003). The produced contraction generates a specific force and potential movement depending on the interaction between muscle, tendon and skeleton. The overall output force depends on the transmission properties (stiffness and elasticity) of the other muscle elements, specifically the endomysium (the connective tissue that holds together different muscle fibres), the perimysium (the connective tissue that holds groups of fibres together within a muscle fascicle) and the epimysium (the connective tissue that holds together muscle fascicles in a muscle bundle) (Hopkins, 2006; Wise and Shadmehr, 2002). Abnormalities or degeneration of the mechanisms connecting sarcomeres to the connective tissue have been linked to either hereditary or acquired diseases as muscular dystrophies (Baehr and Frotscher, 1998). The skeletal muscle anatomy is clearly represented in Figure 2-2. In order to regulate the generation of the contraction force subsequent fibres contractions can sum up if triggered relatively close to each other (i.e. summation) and/or more motor units can be recruited by the central nervous system (i.e.

recruitment) (Hopkins, 2006). A motor unit is the assembly of a lower motor neuron, originating from the spinal cord, and the muscle fibres it innervates. Muscles apt to fine movements (e.g. face, eye) have motor units in which only 3-10 fibres are innervated by one single motor unit, whereas muscles mediating more vigorous movements (e.g. gastrocnemius) dispose of larger motor units whereby one single motor neurons can innervate up to hundreds of muscle fibres.  $\alpha$ - and  $\gamma$ -motor neurons innervate respectively extrafusal and intrafusal muscular fibres, and at the same time several sensory neurons innervating the muscles provide the central neural system with information on muscle stretch and generated force (Wise and Shadmehr, 2002).

In summary, the central motor system sends motor commands through the descending pyramidal tract in the spinal cord to the motor neuronal pool apt to trigger electrical impulses to the target muscle fibres. At the same time, sensory neurons transmit information on the current contraction through ascending pathways in the spinal cord (parallel to the CST) allowing the central system to monitor the ongoing movement. Altogether, the central and the peripheral motor systems regulate intentional and automatic mechanisms that promote goal-directed movement and behaviours (Takakusaki, 2013).

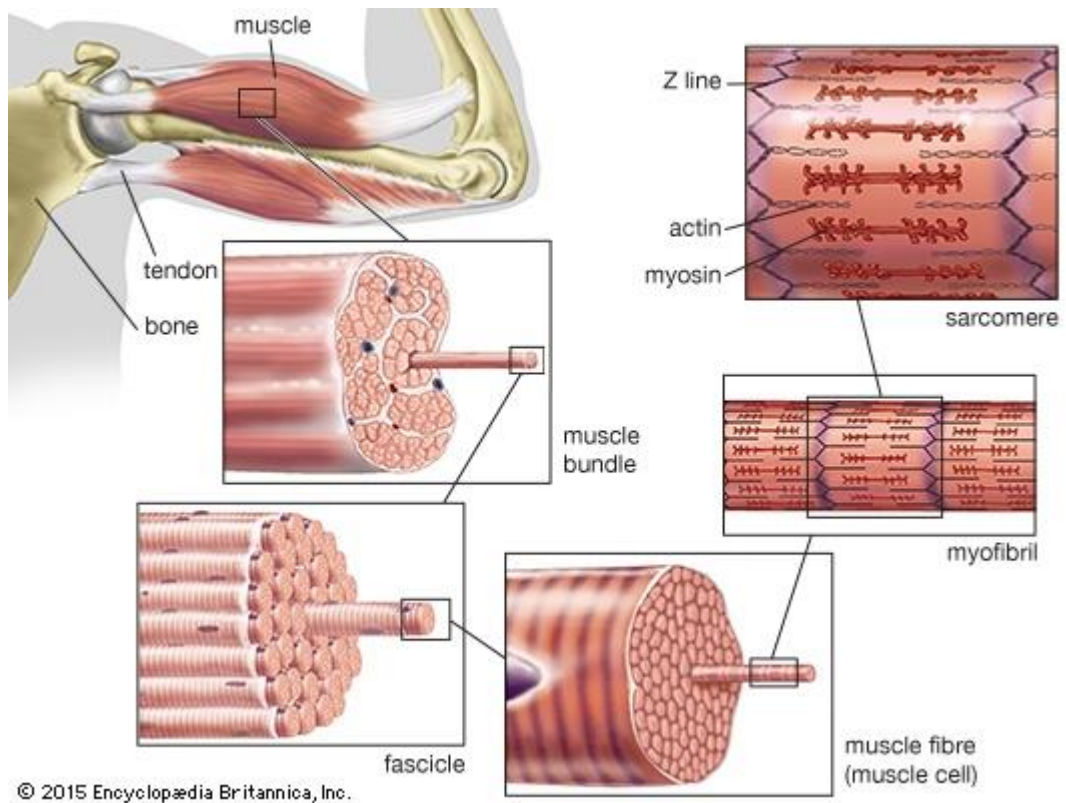


Figure 2-2: Skeletal muscle anatomy.

From macro- to microscopic view of skeletal muscles anatomy as adapted from (<https://www.britannica.com/science/skeletal-muscle>).

### **2.1.3 The role of attention**

Fine motor control can be undermined when multiple tasks are carried out simultaneously. It seems like humans can carry out multiple tasks at the same time until they are overwhelmed by the excessive amount of engagement required by both tasks simultaneously. The human ability to perform multiple tasks relies on attentional mechanisms that allow us to attend to certain stimuli and neglect others (Wahn and König, 2017). Low-difficulty tasks allow the simultaneous allocation of spared attentional resources to the secondary task, whereas high-difficulty tasks exhaust all of them. It is still debated if attentional resources are specific to a given sensory modality or if they are shared across sensory modalities differently according to the performed tasks. Investigations based on dual-task experimental designs demonstrated that, when the two simultaneously performed tasks share attentional resources, performance is reduced with respect to carrying them out separately; on the other hand, when attentional resources are not shared, performance is equal. Previous findings investigating the matter of dual-task interference showed, for example, that the visual and the tactile modalities share attentional resources (Soto-Faraco et al., 2002), whereas the visual and the auditory systems likely employ different attentional sources (Larsen et al., 2003; Alais et al., 2006). Indeed, attending to a visual and an auditory task together or separately leads to the same level of performance, both in case of a simple object-based and of a complex object- and spatial-based task (Arrighi et al., 2011). Neurophysiological evidence demonstrated that visual and auditory modalities partially involve overlapping frontal-parietal networks whose time of information processing however differed allowing good performance of either stimuli (Finoia et al., 2015; Haroush et al., 2011). Different sensory modalities could therefore recruit separate attentional resources as well as overlapping neural populations but in a different way.

## **2.2 Motor control of the upper limb during reaching**

Reaching is a movement of the upper limb that aims to a specific object/target in the surrounding space and is based on the motion of both the shoulder and elbow joints thanks to pre-calibrated torques generated by accurate muscle contractions. Reaching is an ability developed gradually in months after birth: at first it is based on a sequence of small intermitted movements, each one covering only a small portion of the total distance, but already at 36 weeks it is mostly composed by only few movements covering the full distance (i.e. reduced movement fragmentation) (von Hofsten, 1979). Forward reaching usually involves the Anterior Deltoid muscle first, to protract the shoulder, and the Triceps and Biceps Brachii to brake the action of the gravity force on the forearm and to

guide the extension of the elbow according to the target position (Georgopoulos 1986). The concomitant contraction of several muscles is needed to perform the movement and different level of activations are required for different types of reaching. Elements such as planned trajectory, velocity and magnitude of movement as well as the fixed or mobile position of the reaching target influence the movement itself and consequently also the required muscles contractions. Specifically, it can be described by:

- **Path & Trajectory:** the former is the sequence of positions the hand follows within the surrounding space, the latter is the time sequence of these positions within space. If the movement is not constraint, it is usually curvilinearly shaped (Hollerbach and Flash, 1982);
- **Velocity:** it is usually dome-shaped and single-peaked during a reach and can become asymmetric with practice (i.e. ascending trace steeper than the descending one). If the same time of movement is required, peak velocity increases with movement amplitude and the velocity profile changes according to the optimized parameter such as energy, stiffness, etc.;
- **Accuracy:** depends on target, velocity and lack of vision. Slow movements are usually more accurate and errors detected midway of the movement and eventually corrected by additional movements. Experiments requiring to move in the dark or with prevented vision demonstrated the importance of visual guidance to locate the target in space, monitor the hand/arm during the movement and eventually adjust the hand to grasp/touch the target (Brown et al., 1948).

The reaching movement is the result of a complex sensorimotor integration and planning processes, the latter happening within the reaction time in cued movements and taking longer time with increasing difficulty of movement choice (Georgopoulos, 1986). It has been extensively shown that both supra-spinal (motor and parietal cortices) and propriospinal (spinal cord at level of cervical vertebrae C3-C4) mechanisms work on the generation of and monitoring of the reaching movement.

### **2.2.1 Neural correlates of reaching**

#### **Neurophysiology of reaching – animal studies**

The motor cortex has been the main focus of researchers investigating the mechanisms through which the reaching movement is generated and controlled. Early studies recording single-neuron activity in behaving monkeys demonstrated the dependency of the activity of motor and parietal neuronal populations on specific reaching parameters, specifically the movement direction (Mountcastle et al., 1975; Georgopoulos et al., 1983).

Specifically, single-neuron intra-cortical recordings showed that each cell fires at its maximum when movements are executed in a preferred direction and the rate of firing changes gradually with other directions. To better understand how an evolving reaching movement is encoded in the motor cortices a novel technique called population code was developed, able to predict the movement direction in both the 2D and 3D space, as well as during free movements such as drawing (Georgopoulos et al., 1982; Schwartz et al., 1988; Schwartz and Moran, 1999). According to this analytical method the overall movement direction and amplitude can be predicted by, respectively, the angle and the length of the vector sum of each single cell firing contribution, the so-called population vector. A very similar principle was observed in the visual cortex whereby visual-cells are tuned towards the direction of a moving visual stimuli (Steinmetz, 1998). As in the visual cortex, preferred movement directions are orderly mapped within the motor cortex into micro-columns disposed tangentially along the cortex (Georgopoulos et al., 2007). To investigate how changes in the external environment could influence the central neural control of reaching, monkeys were taught to adapt to an external force field perturbation while intra-cortical recordings were obtained (Gandolfo et al., 2000). From the overall neuronal population recorded, nearly  $\frac{1}{4}$  showed changes in the cell tuning properties related to movement direction and maintained these properties also when the perturbation was removed. These adapting cells were called dynamic and they took on properties of the cells most involved in the control of the disturbed movement, a phenomenon called directional tuning (i.e. kinematic cells do not change their tuning properties as they are already tuned for the disturbed direction) (Overduin et al., 2009). Of note, these changes in tuning properties did not correlate with changes in muscle activity, therefore they were attributed to mechanisms of formation of internal models handling the applied perturbations. More recent investigations observed how different external perturbations (i.e. clockwise and counter-clockwise force fields) affected the tuning properties of the monitored motor neuronal population whereby, again, a percentage of the observed cells changed tuning properties according to the applied perturbation (Cherian et al., 2013). However, in this study no evidence of memory was observed once the force field was removed and no change in cell preferred direction was recorded as movement curvature shifted towards zero with practice (i.e. reduced movement error). This led to the conclusion that adaptation with practice was not due to changes in neuron tuning, since they maintained their changed properties throughout the whole experiment, but it could instead be the result of changes in external inputs to these cells. The same principle was deduced observing changes in tuning properties of cells firing during reaching

movements that differed only in terms of starting position and posture (Sergio and Kalaska, 2003; Ajemian et al., 2001). There are in fact many dense interactions between different cortical and deep brain structures which all influence the control of the reaching movement and its adaptation to changes in the external environment (Georgopoulos and Carpenter 2015). Directional tuning has been described for neuronal populations located in different part of the brain such as motor and premotor cortices, parietal cortices, cerebellum, basal ganglia and thalamus, a phenomenon called directional motor resonance (Mahan and Georgopoulos, 2013). According to this theory, both excitatory and inhibitory mechanisms are involved in shaping the required directional tuning based on local as well as external neurons whereby the overall output is then transmitted in a topographically ordered fashion to interconnected areas. Moreover, the directional tuning is thought to be shaped according to the required movement accuracy whereby the more accuracy that is needed, the narrower is the directional tuning profile, and an increase in the inhibitory drive (at both cortical and/or spinal level) would promote more accurate even if slower/weaker movements (speed-accuracy trade-off). In summary, early stages findings demonstrated that the motor cortex and other brain areas are directly involved in the description of reaching and that the observation of changes in firing rate of neuronal population can predict the planned movement direction. As no direct relationships between changes in neuronal firing rate and changes in muscle activity was detected, it was thought that muscle activations were modulated at the spinal level by local motoneurons (Gandolfo et al., 2000). Rhythmic neural oscillatory activity was subsequently observed in monkeys' brains when performing different types of reaching, (a non-rhythmic activity) which however were not tuned to movement velocity, complex kinematic parameters or even EMG activity, but were found to potentially decode plural oscillatory drives whose overall sum could fit muscle activity (Churchland et al., 2012). This hypothesis has been recently confirmed by further intra-cortical recordings of behaving monkeys which found a direct relationship between reaching movement direction, neuronal population vector and muscles recruited to promote the planned task (Heming et al., 2016). Specifically, when classifying neuronal populations according to their directional tuning, their activity well predicted not only the reaching movement direction but also the spatio-temporal dynamics of the muscles groups associated to each specific direction. Lastly, neuronal populations in premotor and primary motor cortices were also demonstrated to decode trial-by-trial reaching error information, specifically in a period after movement and with a causal link (Inoue et al., 2016). These findings suggest



the involvement of the motor cortices in both high- (movement planning and error detection) and low-level (muscle activity) motor programming processes.

### **Neurophysiology of reaching – human studies**

Due to ethical limitations, intra-cortical recordings in humans have always been limited to studies with consenting neurologically impaired populations such as paraplegic patients (Truccolo et al., 2008), whose neurons in the motor cortex were however very sensitive to reaching movement direction. Subsequent non-invasive functional Magnetic Resonance Imaging (fMRI) investigations confirmed that, also in humans, movement direction is indeed the parameter employed during sensorimotor integration to translate high level visual motor processing into low level motor commands (i.e. sensorimotor info translated into muscle activation patterns through directional tuning) (Toxopeus et al., 2011). The primary motor cortex was appointed as the potential candidate from which to decode intentional motion commands to be eventually used in assistive technologies, such as brain-computer interfaces (BCI). However, many studies have shown that severe neural injuries are likely to affect and degenerate the primary motor cortex (Wrigley et al., 2008), thus there was the need to identify alternative cortical areas from which to decode movement intentions. In a recent study (Fabbri et al., 2010), 14 healthy subjects were asked to adapt to reach towards a specific direction while fMRI of their behaving brain was recorded. Changes in movement direction and motor task at the end of reaching (i.e. grasp or press) were instructed to the participants in order to observe which brain areas were most sensitive to directional tuning (high level of movement programming) and type of motor act (low level of movement programming). This was the first study that employed a non-invasive neuroimaging technique instead of intra-cortical recordings to study directional tuning in the healthy human brain. Neuronal populations tuned to diverse movement directions in different brain areas such as the primary motor cortex, the dorsal premotor cortex, the parietal reach region, the anterior and medial inter-parietal sulcus and the cerebellum. Specifically, 1) the strongest sensitivity to the type of final motor act was observed in the primary motor cortex and was weakest in the parietal region, whereas 2) the strongest directional sensitivity was detected in the reach parietal region and was weakest in the motor cortex. These results suggested that the parietal region is most involved in the programming of reaching at the highest level of abstractness: it is likely to process information before the real motor command is specified in terms of muscle activations, torques and joint angles. On the contrary, final motor commands are likely to be decoded in the primary motor cortex, the place with the lowest level of abstractness.

It is therefore likely that the primary motor cortex is involved in both high (abstract processing) and low (motor commands) level of movement programming. In summary, upper-limb reaching is a complex movement promoted by abstract and low-level sensorimotor integration and planning processes involving many cortical areas and deep brain structures in an orderly synchronized fashion (Georgopoulos and Carpenter, 2015). Moreover, thanks to the relationship between intra-cortical and non-invasive neuroimaging techniques (Fabbri et al., 2010), it is now possible to reliably observe, study and draw conclusions about brain activations during natural and disturbed reaching in healthy and neurologically impaired populations.

### **Non-invasive neuroimaging studies**

Non-invasive recording techniques are indeed more easily employed than intra-cortical recordings for the study of neural activations in both healthy subjects and patients, especially from an ethical point of view. Early non-invasive investigations of the neural correlates of the natural reaching movement observed changes in regional cerebral blood flow (rCBF) through Positron Emission Tomography (PET), a nuclear imaging technique able to detect gamma rays emitted by a tracer injected into the body via a biologically active molecule and convert the captured energy into electrical signal then used to create images (Phelps et al., 1980). PET confirmed previous findings obtained via intra-cortical recordings in monkeys a multiple brain sites showed increased blood flow during the reaching movement: it was suggested that reaching activates a fronto-parietal network called the dorsal visual stream (Grafton et al., 1996, Battaglia-Mayer et al., 2003) contralateral to the moving arm. Specifically, neuronal activity in the parietal areas are thought to be most related to the visual location of the target within the external space (Andersen et al., 1997) as well as the hand movement during the action (Nakamura et al., 2001), whereas premotor and motor cortex neuronal populations seem to be involved in the encoding of requested movement direction and amplitude (Fu et al., 1995). Despite the positive results obtained with PET, this technique does not represent the actual activity of neuronal populations (expressed through electrical impulses), but simply the changes in blood amount received by a specific brain region. Instead, electroencephalography (EEG) is another non-invasive recording methodology that, through surface metal electrodes positioned in predefined specific locations on the human scalp, is able to detect electrical activity generated by neuronal potentials (Berger, 1931). EEG has been and is currently extensively used for several different applications from psychology and psychiatry, physiology and rehabilitation and is able to register neural electrical activity with a good temporal resolution (usually of milliseconds). The electrical signals

registered by the scalp electrodes are the sum of several single-neuron activations attenuated of a certain gain because of the transmission through scalp tissues (bone and skin). Electrical impulses travelling through the scalp are also likely to spread over a wider area because of the high conductivity of scalp tissue, a problem called volume conduction, which implies a poor spatial resolution. However, this problem can nowadays be overcome by advanced analytical methods able to localize the sources of the recorded surface signals. Moreover, recordings are very easy to setup and instrumentation is cheaper than functional neuroimaging scanners, which makes EEG one of the favourite non-invasive neural recording techniques. Through EEG recordings, the neural correlates of voluntary externally-cued reaching were non-invasively investigated and the involvement of several brain areas collaborating together for the planning and execution of the movement was further confirmed (Naranjo et al., 2007; Dipietro et al., 2014). Measures of time-locked spontaneous changes in the activity of neuronal populations as induced by specific external sensory events, called Event-Related Potentials (ERPs) were firstly employed (Pfurtscheller and da Silva 1999). Different brain areas activations were demonstrated to temporally act both sequentially and in parallel: in fact, when reaching with the right arm, a complex pattern of activation including premotor, prefrontal, paracentral and parietal areas occurred in healthy subjects between 140-170 ms after the cue, to which the left occipital cortex joined at around 210 ms together with the bilateral superior parietal lobules until 300 ms, after which ERPs decreased until movement onset (Naranjo et al., 2007). As previously mentioned, the reaching movement is usually composed by more than one sub-movements as online control mechanisms monitor and update the action correcting potential ongoing errors to achieve a smoother behaviour (von Hofsten 1979). This has had strong implications in rehabilitation strategies, for example for stroke survivors: hemiplegic patients that trained with a robot-mediated point-to-point reaching task improved their movement performance on a not-trained task (i.e. circle drawing) by performing smoother movements made of fewer, longer and faster sub-movements (Dipietro et al., 2009). The study of the neural correlates of sub-movements during externally-cued voluntary reaching further confirmed the involvement of a fronto-parietal network during planning and movement execution time periods, but also demonstrated that the occurrence of each sub-movement was accompanied by equal stereotyped ERP components and topographical scalp activations (Dipietro et al., 2014). Specifically, there was an increased negativity over parietal-occipital areas as well as an increased positivity over frontal and central areas within 200 ms after target presentation; polarity inverted at the onset of muscular activity and lasted till nearly 500 ms, in line

with previous findings (Naranjo et al., 2007). This pattern was observed at the advent of each sub-movement, suggesting that the neural control of sub-movements is stereotyped. Studies investigating changes of EEG power activity also shed some light on the neural correlates of externally-cued voluntary reaching movements, typically characterized by an increase of intensity of oscillatory waves at both low ( $< 8$  Hz) and high ( $> 35$  Hz) frequencies and by a decrease of amplitudes of oscillations at middle frequencies (between 10 Hz and 30 Hz) with respect to a resting period (Waldert et al., 2008; Demandt et al., 2012; Storti et al., 2015). Reaching movement intentional direction could be inferred on a trial-by-trial basis through the detection of low frequency oscillations ( $\theta$ ) increased power (i.e. Event-Related Synchronization, ERS) (Waldert et al., 2008; Ubeda et al., 2017). High-frequency oscillatory activity ( $\gamma$ ) usually show an increase (ERS) around movement onset and offset localized over contralateral primary motor cortex (Ball et al., 2008) and frontal areas (Babiloni et al., 2016), and are thought to be involved in fast processing of information mostly during movement execution. On the contrary, middle frequencies oscillations power ( $\alpha$  and  $\beta$ ) typically decreases (i.e. Event-Related Desynchronization, ERD), during voluntary (reaching) movement and is symbolic of ongoing sensorimotor integration processes (Pfurtscheller and da Silva, 1999; Engel and Fries, 2010). Moreover, the period after movement offset is usually characterized by a  $\beta$  ERS called Post-Movement  $\beta$  Synchronization (PMBS) or  $\beta$  rebound, thought to reflect neural processes related to trial-by-trial error detection and update of neural mechanisms of motor control (Tan et al., 2014; Torrecillos et al., 2015; Fry et al., 2016; Tan et al., 2016).

In summary, the neural correlates of voluntary reaching have been extensively studied and described with different techniques, both invasive and non-invasive; it usually recruits a group of brain areas (the fronto-parietal network) in order to achieve movement planning and execution; several stereotypical features of reaching have been identified through intra-cortical recordings (e.g. the population vector) and electroencephalography (e.g. frequency-specific ERD/ERS), which could be potential candidates as controlling signals for assistive technologies.

## **2.2.2 Reaching impairments and assistive technologies**

Reaching impairments can arise from many disorders of different nature and cause. For example, it is known that temporarily prevented vision of the reaching arm undermines reaching performance in healthy subjects, and severe disorders caused by lesions in the posterior parietal cortex such as optic ataxia (Balint, 1909) and visual disorientation

(Holmes, 1918) confirm the importance of visual guidance during reaching. Poor reaching performance can also be observed in parkinsonian patients when no online feedback is provided to them during unfamiliar tasks (Krebs et al., 2001), suggesting difficulties in operating in different sensory modalities where integration of proprioceptive information of the moving limb without visual aid is required. Upper-limb motor impairments can also originate from neurodegenerative disorders such as neuropathies, myopathies and Amyotrophic Lateral Sclerosis (ALS), whereby recovery is not an option and long-term functional assistive systems are required (Tsu et al., 2015). Acute stroke is a sudden neurological deficit, due to lack of blood flow (ischemic stroke) or the spread of blood within neural tissues (haemorrhagic stroke), which lasts for more than 24 hours and usually causes the hemiparesis of the limb(s) contralateral to the infarct brain hemisphere (Beyaert et al., 2015). Post-stroke recovery is usually slow and incomplete within the first year after the traumatic episode (Langhorne et al., 2011). Reduced upper-limb movement ability in stroke survivors can be due to paresis, loss of fractionated movement (i.e. abnormal synergies of the upper-limb), abnormal muscle tone (usually hypertonicity), and loss of somato-sensation (i.e. ability to monitor and correct movement online) (Nordin et al., 2014). In general, neurologically impaired patients can be classified into two categories: those with absolute no ability of muscular control remaining and those showing partial control of their muscle activations.

Patients with moderate to severe motor deficits are usually not able to consistently and actively engage in rehabilitation therapies. Examples are patients that have suffered from severe Spinal Cord Injuries (SCI), which are injuries of the spinal cord (that can happen at any level of the spine) caused by compulsion, incision or contusion. As a result, all or most of the functions performed by the spinal cord are interrupted at the distal level of the injury. According to the American Spinal Injury Association (ASIA) scale for spinal cord injury (Nas et al., 2015), SCI patients can be classified into five categories (ASIA-A/B/C/D/E) based on their level of sensory and motor functions as assessed by international standards (International Standards for Neurological Classification of Spinal Cord Injury, ISNCSCI) (Kirshblum et al., 2011). For patients with no/poor motor and sensory functions, brain-machine/computer interfaces (BMIs/BCIs) are strongly suggested as definitive means through which to substitute a lost control ability and augment human interactions with the external environment (assistive BMIs/BCIs) (Millan et al., 2010). All BCI/BMI systems are based on the same principle of decoding brain intentional signals through which an external device is then activated. Current technologies are able to record single-neuron activity (i.e. spikes) through implanted

micro-electrodes arrays (MEAs) or electrocorticography (ECoG) (Tsu et al., 2015) which allow reliable detection of intentional movement commands. This was for example the case of a tetraplegic 52-year old woman who learnt how to interact with a BCI robotic system that translated her intentional movement commands, recorded through a single-neuron intra-cortical implant placed on her motor cortex and expressed through neuronal population vector (Georgopoulos et al., 1982), into movements (Collinger 2012). This system showed the potential of recent developments in assistive technologies, but also highlighted some design weaknesses that still need to be overcome: these advanced systems are indeed so far only lab-based, and there is the need for implantable wireless and more robust/durable systems (Tsu et al., 2015). Other types of BMI/BCI systems have therefore been developed based on non-invasive recordings of movement intentions such as scalp electroencephalography electrodes: these applications have been used extensively in clinical rehabilitation purposes, are non-invasive thus easier to implement and allow the control of different devices even if less accurately than single-neuron recordings (Courtine et al., 2013; Millan et al., 2010). Several non-invasive BCIs/BMIs have been developed to tackle different human deficits from the impossibility to speak (Birbaumer et al., 1999), to promote mobility (Millan et al., 2009) and rehabilitate (Ang et al., 2015). When no motor ability is left, motor BCIs/BMIs can be controlled through brain signals generated through Motor Imagery (MI), a dynamic neural state during which the representation of the intentional movement is created within the brain without any external motor output (Millan et al., 2010). Motor BMIs based on MI have been recently used in extended clinical trials coupled with targeted physiotherapy and were shown to be promising in terms of long-term motor recovery (Simmons et al., 2008). Moreover, hybrid BCI systems are nowadays of great interest since, combining one brain channel with other bio-signals (e.g. electromyography, EMG) or special devices (e.g. switches), the control can be operated through different modalities and patients can switch between them according to the level of fatigue, preference or performance (Millan et al., 2010; Leeb et al., 2010b). In general, non-invasive brain interfaces are indeed preferred at the moment and optimization studies are currently investigating how to improve quality and reliability of these systems. For example, it is currently debated whether dry or gel-based EEG electrodes would be more appropriate for a home-based BCI application (Käthner et al., 2017). Contextualized BMIs/BCIs in the home environment is the current challenge and researchers are trying to create light and user-friendly systems that could be easily operated by patients or care-giver at home in the long-term.

When residual motor ability is available, BCI/BMI systems are usually used as potential long-term rehabilitative tools (rehabilitative BMIs/BCIs) whereby therapeutic interventions are programmed according to the patient-specific motor deficits status with the final goal to promote neural plasticity and facilitate motor re-learning (Soekadar et al., 2015). The basic principle at the basis of BMI/BCI-mediated rehabilitation comes from the Hebbian theory according to which neural plasticity is mostly promoted by the simultaneous activation of presynaptic (descending commands) and postsynaptic (ascending feedback) (Hebb, 1949). To strengthen the injured ipsilesional cortex and boost neural plasticity, rehabilitative BMIs/BCIs should therefore include a sensory-proprioceptive feedback channel to subjects (Oweiss and Baldreldin, 2015). One of the first non-invasive BMI based on these principles exploited EEG signals within the sensorimotor rhythms (SMR, 8-15 Hz) to enable severely affected stroke survivors to control an orthotic to open and close their paralyzed hand (Birbaumer and Cohen, 2007). BMI training of the ipsilesional limb paired with specifically targeted physiotherapy promoted notable motor improvements in stroke survivors that had no finger movement abilities (Ramos-Murguialday et al., 2013). The evolution of brain interfaces technologies saw the combination of an EEG-based MI BCI coupled with a rehabilitation robotics (MIT-Manus) for the recovery of the upper-limb mobility (both shoulder and elbow joints) tested on a group of hemiplegic chronic stroke survivors (Ang et al., 2015). The study showed that both the BCI + robot-based and the robot-based trained group improved the motor score of the paretic limb in a similar way despite the different number of arm exercise (BCI + robot training = 136 repetitions/session; robot training = 1040 repetitions/session). These findings confirm the crucial validity of sensorimotor feedback for the recovery of functional abilities after neural injuries. It is therefore important to plan a comprehensive rehabilitation path including more types of therapy when recovering stroke survivors as repetitive rehabilitative sessions based on different therapy types enhances the chance of recovery. Standard physiotherapy, repetitive active robot-mediated movement with sensory feedback, training in a virtual reality environment, functional electrical stimulation of muscles (FES) and constraint-induced therapy (CIMT) are all potential therapeutic interventions that could boost recovery in both the acute and the chronic stroke phases (Millan et al., 2010).

### **2.2.3 Neurorehabilitation after stroke**

#### **Rehabilitative interventions**

Stroke is one of the leading causes of long-term cognitive and motor disabilities worldwide and recovery times are patient-specific. Some patients recover spontaneously

during the acute phase but the majority remain permanently disabled with different forms of hemiparesis and gait abnormalities, and only few are able to recover during the chronic stage with long-term specific therapies (Huang and Krakauer, 2009). In order to accomplish motor tasks, if not properly trained, stroke survivors develop typical motor abnormalities such as pathological muscle synergies (Brunnstrom, 1970), trunk compensatory activations (Cirstea and Levin, 2000), and longer and more segmented movements (Dipietro et al., 2009). The goal of neurorehabilitation is to promote the development of healthy recovery strategies while removing pathological compensatory mechanisms. Targeted physiotherapy is the most common rehabilitative service offered to stroke survivors, it aims to improve paretic limb mobility, range of motion and muscle tone, but it is a passive therapy that does not boost the active regeneration of lost neural function and is therapist-dependent. Following the Hebbian theory, functional recovery is mostly boosted when the injured neural pathways are stimulated from both the centre (feedforward motor intentional commands) and the periphery (feedback sensory drives), thus the active engagement of the patients is strongly recommended despite the lack of any residual ability to move. A recent clinical investigation exploited the Hebbian principle and combined vagus nerve stimulation (VNS) with upper limb standard rehabilitation to promote the generation of novel neural pathways and reported preliminary improvements in movement abilities after training (Dawson et al., 2016). An example of active movement training is the Constraint-Induced Movement Therapy (CIMT), whereby the healthy limb is usually constrained and patients are forced to use the paretic limb. This type of intervention has been reported effective for rehabilitation of chronic stroke (Sirtori et al., 2009), but it requires remaining residual mobility (which many stroke survivors do not have) and is also thought to induce the creation of compensatory strategies instead of actual functional recovery. On the contrary, robot-mediated rehabilitation of the upper-limb (e.g. via exoskeleton or end-effector robots) offers the possibility of either assisted or active movements according to patients' capabilities and is currently one of the most recommended therapeutic interventions (Huang and Krakauer, 2009; Nordin et al., 2014). Rehabilitation robotics are currently programmed with adaptive rules that allow the active movement engagement (non-assistive modality) but can also detect if patients are not able to independently move, thus eventually assisting and allowing the patient to complete the action passively (assistive modality) (Krebs et al., 2003). Robotic systems overcome the problem of therapist-dependent physiotherapy as they never experience human fatigue and limits, thus permitting longer training sessions and more repeated movements within each session



(Lo et al., 2010). Moreover, they are able to record kinematic data of the performed movements through sensors embedded in the robotic arm (e.g. position, velocity and exerted force), thus allowing for more specific quantitative descriptions of the recovery status. End-effector robots usually mediate simple planar reaching movements (i.e. 2D only) and record kinematic data at the end-effector with no possibility to monitor joint-specific dynamics (e.g. of elbow and shoulder joints) (Turner et al., 2013); exoskeleton systems can potentially mediate more free movements within the three-dimensional space and record joint-specific parameters, which however need to be then transformed from the robotic frame to anatomical coordinates (Nordin et al., 2014). The possibility to record reaching-related kinematic parameters is a great advantage for the assessment of the effects of rehabilitation and the recovery status as less-subjective and more quantitative conclusions can be drawn in comparison to standard assessment scale measures such as the Fugl-Meyer score (Fugl-Meyer et al., 1974; Turner et al., 2013). Many clinical studies confirmed the usefulness of assessing recovery and movement quality through a combination of kinematic measures and clinical scores (Mazzoleni et al., 2014; Dipietro et al., 2007; Zollo et al., 2011; Turner et al., 2013), and other recording techniques could potentially be simultaneously employed to register the physiological activity of muscles (EMG) and brain (EEG), for a comprehensive multi-level analysis of recovery (Sale 2015). End-effector robotics has been proved very useful in the rehabilitation of stroke survivors as it promotes the re-acquisition of transferable motor skills: chronic stroke patients trained for 18 weeks with a simple point-out reaching protocol showed an overall improvement of upper-limb control, smoothness of movement and muscular synergies also when performing a not-trained task (i.e. drawing a circle) (Dipietro et al., 2007). It is indeed quite common that, with time, patients improve performance on the trained task but are not able to accomplish not-trained natural movements such as grasping a bottle of water or opening a door in the home environment. Moreover, each patient has his/her-specific impairments and recovery potentials, thus it is not possible to define a standard therapeutic path that could successfully rehabilitate every stroke survivors (Semrau et al., 2015). To summarise, there is the need for identifying personalized therapeutic interventions that could boost a generalized recovery, and rehabilitation robotics seems a valid candidate to promote it. Moreover, more specific and comprehensive assessment measures, both behavioural and physiological, would support the identification of the right therapeutic interventions and are therefore needed in order to describe different aspects of the recovery process from a multi-level perspective.

## **Motor skill learning**

As aforementioned, rehabilitation after a neural injury is crucial for a good recovery: as stroke survivors have lost their ability to move a specific limb as well as the knowledge of how to do that, thus the rehabilitation process need to promote the re-learning of the lost motor skills. New motor skill learning is a process that promotes changes at neural level needed for improving movement performance in terms of velocity and accuracy (i.e. speed-accuracy trade-off), and can be obtained by learning new motor execution strategies (i.e. movement known, improved speed and accuracy as in visuomotor tracking) or by improving selection skills (i.e. movement not known, improved prediction skills and reaction times as in serial reaction time tasks) (Diedrichsen and Kornysheva, 2015). Motor learning is a long-term process involving adaptation to a new task, user-dependent plasticity, retention across training sessions, consolidation over time, and awareness (Huberdeau et al., 2015; Krakauer and Mazzoni, 2011); it includes many different types of tasks such as serial reaction time, sequential force control, fast sequential finger tapping and visuomotor rotations. Motor adaptation alone is the basis of motor learning and is defined as the re-calibration of an already known movement as a reaction to specific changes in the interacting environment (Huang and Krakauer, 2009). It is usually characterized by an increase in movement error when the environmental change is first presented, followed by a trial-by-trial performance improvement based on the optimization of the sensory-prediction error and eventually characterized by temporarily persisting adapted behaviours (i.e. after effects) once the external alteration is removed. To understand the basis of motor learning several studies investigated how subjects adapt their motor output and computed potential internal (neural) models able to describe and predict behaviour. It is thought that motor learning involves multiple adapting processes working in parallel which have been so far described by linear time-invariant multiple-state models (Smith et al., 2006), Bayesian probabilistic models (Wei and Körding, 2010) or non-parametric regression algorithms (Lonini et al., 2009). Each model describes the rules by which each process updates its internal model on a trial basis at a process-specific rate and the sum of all processes outputs generates the required compensating motor command. To simplify, adaptation was shown to depend on two major memory processes, 1) a slow component that adapts slowly, is associated to implicit memory (i.e. learning without awareness), is modulated by prediction errors and can be expressed at low reaction times, and 2) a fast component that adapts rapidly, is associated to explicit memory (i.e. learning with awareness), is sensitive to performance error and requires a long time before it is expressed (Smith et al., 2006; Huberdeau et al., 2015).

Recent findings showed that older adults' decline in motor learning abilities is likely due to impaired retention (i.e. ability to maintain a fraction of the previously learnt task) of the slow process and that additional impairments of retention of the fast process is subject-dependent and would further influence the decline of motor learning capabilities (Trewartha et al., 2014). Robot-mediated adaptation to an external force-field (e.g. velocity- or position-dependent, curl or resistive forces) has been extensively studied in order to identify the different aspects of motor learning and to test it as a potential therapeutic intervention for stroke rehabilitation: it was indeed shown that stroke patients can adapt as healthy subjects even if over more trials (Scheidt and Stoeckmann, 2007), and that it is possible to manipulate the training environment so that the adaptation after-effects resemble a more natural behaviour (Patton and Mussa-Ivaldi, 2004). Investigating how motor learning can be facilitated and stabilized over time, it was recently demonstrated that providing punishment feedback enhanced memory retention in error-based protocols (probably triggering increased cerebellar sensitivity to sensory prediction error), whereas providing reward feedback enhanced memory retention regardless of the followed protocol (likely mediated by stronger memory traces in the primary motor cortex) (Galea 2015). These findings would have a strong impact for the definition of neurorehabilitation protocols as accelerated online performance improvements and stronger memory retention could be simply obtained by providing punishment and reward feedback (Quattrocchi et al., 2017). On the contrary, learning a secondary task straight after adaptation to a primary perturbation has been shown to prevent motor memory consolidation and undermine motor learning, a phenomenon called retrograde interference (Brashers-Krug et al., 1996). However, if the secondary task depends on a different kinematic parameter (e.g. adaptation to velocity-dependent force field and then to a position-dependent force field) both retrograde and anterograde interference (i.e. the disrupted performance of a secondary task due to adaptation to a previous perturbation) are not complete, suggesting that motor memory retention is likely not affected when consecutive tasks do not conflict in the working memory (Bays et al., 2005). Moreover, it has been recently shown that learning to adapt to two subsequent velocity-dependent force fields (in order: clockwise and counter-clockwise) is possible when specific limb orientations are chosen (Yeo et al., 2015). Internal (neural) models of adaptation have been linked to specific muscular activations during adaptation to novel environmental dynamics (Milner and Franklin, 2005). It was indeed observed that the initial stage of adaptation is usually characterized by feedback responses based on reflexes and voluntary corrections, whereas later stages of adaptation are featured by feedforward mechanisms

such as muscle co-contraction patterns able to produce the required counteracting force. This evidence supports the hypothesis that internal adaptation models adapt and generate responses in a feedback or feedforward fashion according to the adaptation stages. Functional neuroimaging studies have shown that, at early stages of adaptation, a cortico-striatal loop is involved in which the frontal cortex temporarily store the sensorimotor information for imminent use, whereas at later stages of adaptation a cortico-cerebellar loop is recruited in which the parietal cortex as well as the cerebellum act as long-term memory storages (Shadmehr and Holcomb, 1997; Krebs et al., 1998; Doyon et al., 2009). The passage from novice to skilled performer is therefore mediated by passing from the cortico-striatal to the cortico-cerebellar control of the performed motor action. The importance of either mechanisms has been confirmed by motor adaptation studies with cerebellar patients (Thach, 2007), who showed impaired performance and inability to adapt, and with patients with basal-ganglia dysfunctions (Smith and Shadmehr, 2005), who showed adaptation on a trial basis with however a poor compensation in the early part of the reaching movement. Moreover, consolidation is a crucial element of motor learning and it strongly depends on the type of learning paradigm: for example, motor sequence learning is sleep dependent and consolidation can be observed by increased functional connectivity of the striatum when the same task is repeated after sleep, whereas motor adaptation is simply time dependent and mostly relies on the cerebellum (Debas et al., 2010). Specifically, sensorimotor adaptation was shown to stabilize in a time window of 6 hours and to activate a network including motor, premotor, posterior parietal cortex, cerebellum and putamen whose activation positively correlated with long-term memory retention (Della-Maggiore et al., 2017), in line with previous findings. How permanent neural changes (i.e. neural plasticity) are obtained during motor skill learning is still under debate: large-scale brain networks were found more flexible during early stages of motor learning and the subject-specific degree of flexibility was then positively correlated with the observed learning rate and performance (Bassett et al., 2011). Motor adaptation paradigms, combined with real-time biofeedback, non-invasive brain stimulation or pharmacological treatments should target and modulate neural networks flexibility exploiting neural redundancy (i.e. ability to maintain a given behaviour despite the injury) and variability (i.e. ability to generate novel pathways) for a successful and functional recovery (Buch et al., 2016).

### **2.3 Motor control of the lower limb during locomotion**

Bipedal locomotion is the ambulatory characteristic typical of the human species and one of the most spontaneous activity humans do every day. It is orchestrated by a hierarchical

structure composed of different levels of neural, muscular and sensory control which together stabilize the body and generate the forward propelling force. Figure 2-3 describes the biomechanical sequence of the events of a complete stride (i.e. right-left-right foot sequence, or vice versa). At the time of heel strike/contact with the ground (initial loading response (LR) phase), the leg is completely extended thanks to knee and hip extensor muscles, while reaction forces with the ground decelerate the trunk forward movement. In the late LR phase, trunk deceleration is further supported by foot plantar-flexor muscles as the foot is completely flat on the ground, when the single-leg support phase begins (i.e. stance phase). Stance is mediated by knee extension and calf muscles contraction, while the ankle joint executes a dorsiflexion movement promoting the passage from mid- to late-stance (i.e. flat foot to heel rise). In the subsequent pre-swing (PS) phase, the plantar-flexor muscles contract first to promote body support and forward progression beyond the standing foot, and then to generate enough force to push-off the leg and begin the swing phase. Swing phase is obtained by ankle dorsiflexion, knee and hip extension, and the forward movement of the swinging leg is ultimately obtained by the contraction of the hip flexors. Gait is a rhythmic activity, the same sequence of events is repeated on the contralateral side of the body (Burnfield, 2010). Each stride event has been attributed to the synchronous activation of a group of muscles collaborating together to accomplish a specific task, namely synergies or modules (Neptune et al., 2009). Body weight is supported by hip extensors, knee extensors and hip abductors (Module 1) in early stance and by plantar-flexors in late stance (Module 2). Forward propulsion is promoted by hamstrings (Module 4) in early stance and Module 2 in late stance, whereas trunk deceleration is mediated by both Module 1 and Module 2. Ankle dorsi-flexors and rectus femoris (Module 3) contract together with hip flexors and adductors (Module 5) to accelerate the leg in early swing. Module 4 decelerates body weight before heel contact with the ground. By changing the duration and amplitude of any of the modules (i.e. synergies) it is possible to produce different biomechanics and consequently different walking patterns (Allen and Neptune, 2012).

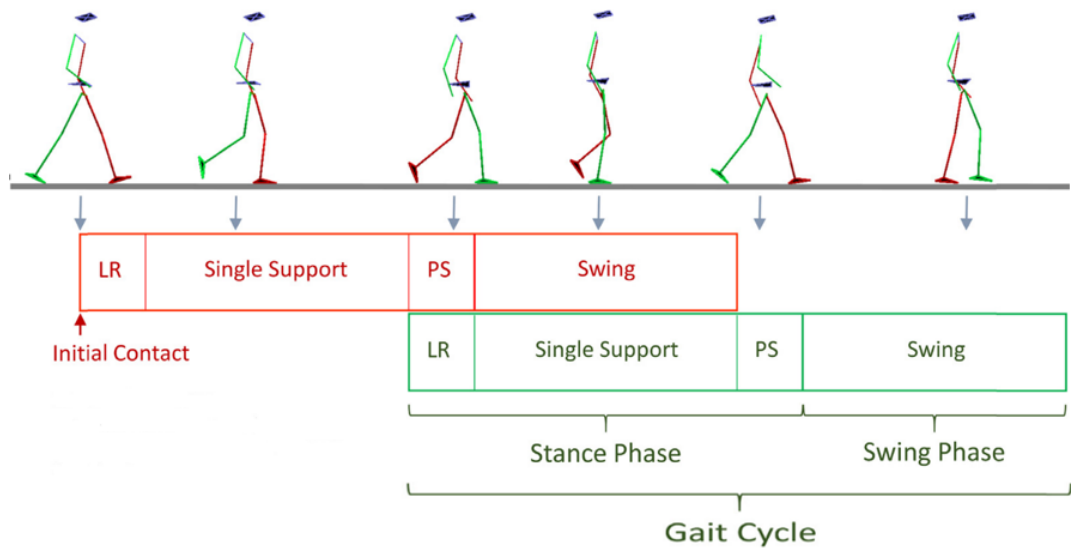


Figure 2-3: Gait biomechanics.

Temporal evolution of gait biomechanics over a complete gait stride (as adapted from Beyaert et al., 2015).

### **2.3.1 Neural correlates of locomotion**

#### **Neurophysiology of locomotion – animal studies**

A complex hierarchical neural structure controls each element of forward walking, monitoring and correcting potential errors through volitional and automatic processes (Bayert et al., 2015). The spinal cord contains specific inter-neuronal populations, the Central Pattern Generators (CPGs), composed by two half-centres (i.e. extensors' and flexors' centres), which reciprocally inhibit each other and generate the rhythmic neural activity needed to activate extensors and flexors in an alternate fashion. This activity is then transmitted through a second layer of interneurons (the pattern generators) to the target motor-neurons innervating the ipsilateral leg and induces the muscle contractions needed to promote gait (Takakusaki, 2013). To understand if the CPGs half-centres had comparable roles, fictive locomotion was induced in de-cerebrated cats by stimulating higher supra-spinal structures and registering the activity of peripheral nerves innervating flexors and extensors through invasive hook electrodes (i.e. electroneurography, ENG) at the transition between two consecutive phases of locomotion (Boothe et al., 2013). Interestingly, it was observed that stronger inhibition was exerted in the transition from extensors to flexors activation than vice versa. The CPGs are commanded by higher spinal structures: the brainstem is involved in the control of gait, namely the cerebellar locomotor region (CLR) and the midbrain locomotor region (MLR). The MLR directly activates the rhythm-generating system composed of reticulo-spinal neurons located within the medullary reticular formation (MRF), which indirectly excite or inhibit motoneurons via the spinal interneurons (Takakusaki, 2013). When stimulating the MRF of de-cerebrated cats while recording intra- and extra-cellular activity at the lumbar spine, mechanisms of inter-neural inhibition and of supra-spinal and peripheral interactions were revealed and linked to the control of postural muscle tone (Takakusaki et al., 2003). Subsequent studies demonstrated that the electrical stimulation of the MLR structure in de-cerebrated cats initiated locomotion and dictated the level of the force generated when stepping (Drew et al., 2004). Information on the generated rhythm and the muscular pattern are also simultaneously sent to supra-spinal centres for a continuous control of the movement through afferent pathways within the spinal cord. Muscles spindles, joint mechanoreceptors, proprioceptors and skin sensors generate all sensory afferent drives that travel to the spinal cord and eventually to supra-spinal centres and promote the control of movement phase alternation, the regulation of muscles activations and force, the monitoring of obstacles and the prevention of muscles fibres overstretch (Rossignol et al., 2006). Rhythmic motor systems usually convey motor patterns consisting of two

phases associated to the movement of distinct body segments and the transition from one phase to the next could be triggered by sensory feedback (e.g. the passage from stance to swing phase during walking is thought to be promoted by mechanoreceptors at hip joints signalling the loading of the leg) (Takakusaki, 2013). This is believed to be a control mechanism to ensure that the rhythm is properly coupled to the biomechanical state of the moving segment (Pearson, 2004). However, the generation of rhythmic activity cannot simply rely on afferent feedback as any damage to sensory pathways would deteriorate or even interrupt movement generation. Moreover, sensory feedback contains information on movement error further employed by supra-spinal mechanisms for adaptation and online modification of the motor pattern. The posterior parietal cortex (PPC), for example, was found to be involved in sensorimotor integration mechanisms (Buneo and Andersen, 2006) and subsequently appointed as the potential visuomotor integrator during gait. Indeed, intra-cortical recordings of visually-guided walking cats showed rhythmically discharging neurons in the PPC (Beloozerova and Sirota, 2003). It was then postulated that PPC neurons were involved in the regulation of inter-limb coordination during locomotion requiring visual guidance (Lajoie et al., 2010). Implanted electrodes recorded PPC neuronal activity in walking cats and showed a higher level of firing in the majority of neurons when both fore- and hind-limbs stepped over an obstacle; moreover, when the obstacles were shifted forwards delaying the overstep, a portion of those neurons maintained higher firing rate. These results suggested that PPC is involved in processes of sensorimotor integration (i.e. visuomotor integration) able to estimate the spatio-temporal dynamics of obstacles, as well as in mechanisms of working memory able to maintain the previously acquired info and motor program. To test if PPC neurons completely relied on visual info to promote visuomotor integration, cats were trained to walk on a treadmill with obstacles while their vision was temporarily interrupted (Marigold and Drew, 2011). Despite the increased level of difficulty due to prevented vision, cats managed to step over obstacles, as if able to memorize the projected obstacle position and their relative position for the whole duration of the prevented vision. Intra-cortical recordings showed that more than half of the recorded PPC neurons did not change their discharging rate when vision was obscured, suggesting that these cells were likely maintaining memory of the motor plan. However, when vision was restored, cats updated the ongoing step and, at the same time, some cells changed their firing pattern as if updating the built-in storage capacity of the parietal cortex. Central cortical control remains therefore necessary in order to update motor patterns and to generate volitional motor commands, such as initiation of gait and pre-gait postural adjustments. The primary



motor cortex (M1) is known to generate descending motor commands, the supplementary motor area (SMA) is believed to enable anticipatory postural control and the premotor cortex (PMC) is thought to be responsible for promoting sensory-guided gait initiation commands. Confirmation of these hypotheses was recently obtained as the injection of muscimol (a GABA<sub>A</sub> agonist that blocks spontaneous neurons firing) in the trunk/leg region of the SMA of Japanese monkeys disturbed their postural control during walking on a treadmill, whereas muscimol injection in the dorsal PMC prevented gait initiation when sensory guided but not when gait spontaneously started (Nakajima et al., 2003; Mori et al., 2003). In summary, a complex hierarchical structures controls locomotion in animal, whereby automatic motor programmers within the spinal cord are able to generate rhythmic bursts of activity in motoneurons activating extensors and flexors in an alternate fashion, and central neural mechanisms, together with sensory feedback from the periphery, play a role in movement generation, adaptation and correction.

### **Neurophysiology of locomotion – human studies**

Human studies also aimed to understand how human locomotion is managed and if a similar hierarchical structure to that of animals could be found. For instance, the presence of spinal cord inter-neuronal populations automatically generating gait patterns was observed in humans by electrically stimulating the lumbar spine of paraplegic patients suffering of long-standing spinal cord injury. Interestingly, muscular activations similar to those generated when walking were observed and rhythmic alternating stance-swing phases were successfully induced (Dimitrijevic et al., 1998). Moreover, evidence that the brainstem is also involved in the control of human locomotion were deduced from studies with a patient with lesions of the MLR structure who could not stand or walk (Masdeu et al., 1994), with patients with brainstem lesions showing gait difficulties (Hathout and Bhidayasiri, 2005), and with parkinsonian patients that, when implanted with DBS stimulating the MLR, improved their gait abilities (Plaha and Gill, 2005; Stefani et al., 2007). The role and collaboration of different supra-spinal structures were then observed through different investigations. In an fMRI study, whereby healthy subjects imagined walking, both cortical and midbrain structures involved in planning the execution of the gait movement (as they were performing motor imagery and not actually moving) were found (Jahn et al., 2008). First, an increase of activity occurred in the frontal and the parahippocampal gyri, known to send signals to the basal ganglia and through them to the rhythm generators; second, the cerebellum, the CLR and the vermis, known to integrate several sensory feedbacks (proprioceptive, visual and vestibular), were found more active; third, an increased activation occurred in the MLR, which is known to send

motor commands to the MRF and through it to the spinal cord CPGs. Subsequently, evidence of cortical activity related to locomotor control were mostly deduced observing patient behaviours and impairments (Bartels and Leenders, 2008). Studies of balance control improvements after stroke showed that SMA activity registered through functional near-infrared spectroscopy (fNIRS) was significantly increased after intensive gait rehabilitation, confirming its major role in postural adjustments and balance control already postulated in animal studies (Fujimoto et al., 2014). As the brainstem receives descending pathways from both SMA/PMC and M1, it is possible that either postural preparation information is received before actual motor commands either information of precise lower limb segments movement is first forwarded to M1 and subsequently transmitted downwards through the corticospinal tract (Takakusaki, 2013). Many investigations have focused on gait impairments in neurological patients such as Freezing of Gait (FoG), a complex gait condition in which patients cannot initiate a step, likely caused by the degeneration of essential gait control components such as frontal and (right-) parietal networks (Bartels et al., 2006). Frontal cortex involvement could explain the presence of FoG also in frontal lobe disorders and could also impair the ability to maintain focused attention on gait while in need to simultaneously process external stimuli (i.e. multi-tasking ability) (Gilaldi and Jeffrey, 2006). The PPC is instead believed to be involved in the integration of sensory info with motor plans, which is severely impaired in PD patients with FoG (Lee et al., 2005). Moreover, degeneration of the basal ganglia (BG) likely contributes to enhanced gait impairments: BG send facilitating drives to the PMC to promote gait initiation based on sensorimotor info received through efferent projections from sensorimotor and associative cortices (Huang et al., 2007). Any damage in this loop will most likely contribute to increase gait impairments and worsen FoG. In summary, a hierarchical structure similar to those of animals is therefore likely to underlie rhythmic (e.g. rhythm generation and muscle tone) and volitional (e.g. gait initiation and online correction) human gait control, whereby a stronger supra-spinal control is assumed to be in place (Takakusaki, 2013; Takakusaki, 2017).

### **Non-invasive neuroimaging studies**

The most challenging aspect of studying the neural correlates of human gait lays within the technical limitations of the current neuroimaging techniques. Brain activations registered during ankle dorsi-flexion movements were first employed to assess motor learning during gait rehabilitation (Dobkin et al., 2004). With this protocol, chronic stroke survivors exhibited walking kinematics improvements associated with practice-induced brain plasticity such as increased activity in M1, S1 and CMA during recovery. Motor

imagery has also been employed to evaluate brain activations during imagined gait through fMRI (Jahn et al., 2008, Labriffe et al., 2017), and recent MRI-compatible systems allow simulation of “walking sensations” while subjects are lying in an MRI scanner (Labriffe et al., 2017; Ikeda et al., 2016). However, all these protocols are far from representing real walking behaviours. To overcome these issues, studies have started to use alternative mobile techniques, such as fNIRS, able to record the brain hemodynamic responses in mobile paradigms. By observing changes in oxygenation levels through a whole-head fNIRS system, increased activity was observed in the medial primary sensorimotor cortex as well as in bilateral supplementary motor area during treadmill walking (Miyai et al., 2001). A recent study investigated through a whole-head fNIRS system the effects of different gait training paradigms, hypothesising that different cortical activations would be observed (Kim et al., 2016). Stepping walking, treadmill walking and robot-assisted walking paradigms at different speeds were employed, and regardless of the undertaken protocol an increased activity in a locomotor network including sensorimotor (SMC), premotor (PMC) and supplementary motor areas (SMA) was observed. Several investigations are also exploiting real-world contexts by employing mobile fNIRS systems to study brain activities during real-life situations (Fujimoto et al., 2014; Al-Yahya et al., 2016; Holtzer et al., 2011), although many of them focused only on a limited brain area (i.e. PFC) which limits a more comprehensive understanding of the underlying whole-brain cortical mechanisms (Metzger et al., 2017). EEG has very recently been optimized for mobile approaches and currently is widely used in studies investigating the neural correlates of gait and other natural behaviours (Cevallos et al., 2015; Ladouce et al., 2017). EEG evidence confirmed that gait control in healthy adults recruits a widely distributed cortical network involving primary somatosensory, somatosensory associative, primary motor and cingulate cortices (Knaepen et al., 2015), in line with previous indirect fMRI findings (Dobkin et al., 2004). The gait-cycle phase related cortical oscillations were first investigated as healthy subjects walked freely on a treadmill (Gwin et al., 2011). Specifically,  $\alpha$  and  $\beta$  frequency power increased during the late stance phase within the bilateral sensorimotor and dorsal anterior cingulate regions, and high  $\gamma$  frequency power modulations were also evident in the PPC, anterior cingulate and sensorimotor cortices. Given the complex hierarchical structure at the basis of locomotor control, it was subsequently questioned what was the role of the primary motor cortex. The relationship between the activities of the leg motor cortical area and that of the lower leg Tibialis Anterior muscle was assessed during treadmill walking through cortico-muscular coherence measures. Significant coherence was observed during the

swing phase in low  $\gamma$  frequency range (24-40 Hz), likely modulated by sensory feedback and demonstrating the direct involvement of the primary motor cortex in the regulation of muscle activity during walking (Petersen et al., 2012). The premotor cortex was found to be directly involved in maintaining gait stability, with higher  $\beta$  frequency power within the left PMC during stabilized (i.e. constrained medio-lateral movements) versus natural walking (Bruijn et al., 2015). The EEG recording technique was also employed to evaluate the effects of robot-assisted gait training (RAGT) on cortical activations. M1 and PMC  $\alpha$  and  $\beta$  activities were constantly suppressed during active RAGT (i.e. PMC was more active) than during standing or passive RAGT, whereas low  $\gamma$  was modulated so that ERD occurred in pre-swing phase and ERS occurred during stance phase. This is likely symbolic of undergoing sensorimotor processes monitoring motion of the lower limbs (Wagner et al., 2012). Further investigations confirmed the presence of a sustained  $\alpha$  and  $\beta$  power suppression during the whole gait-cycle duration, resembling an active state of the sensorimotor areas during walking with respect to standing (Engel and Fries, 2010). Furthermore, gait-cycle phase modulated low  $\gamma$  oscillations were observed, likely symbolic of sensorimotor processing and integration mechanisms (Seeber et al., 2014, Seeber et al., 2015; Bulea et al., 2015). RAGT training within a virtual reality (VE) environment showed increased parietal activations and VE-dependent gait-phase modulated low  $\gamma$  oscillations, promoting VE as a valid tool for active gait rehabilitation (Wagner et al., 2014).  $\gamma$  band cortical activity has also been recently suggested to convey information on the attentional level during gait as it was possible to decode the attentional mechanisms of both healthy subjects and SCI patients, thereby demonstrating different levels of selective attentional mechanisms (e.g. patients focused more on gait than on the environment and external stimuli) (Costa et al., 2016). This is an useful finding for the design of brain-computer interfaces able to decode the cognitive state of the patients and adapt the interface accordingly. Non-invasive EEG recordings are indeed used in BCI applications for the lower limb (Tucker et al., 2015), and recent analytical methods has demonstrated the possibility to infer both gait intentions (Choi et al., 2016) and joint kinematics (Presacco et al., 2011). Current and future investigations are exploiting novel fully-mobile setups able to register synchronized cortical EEG activity and behavioural performance which could be used outside the laboratory environment. This would shed some light on natural human behaviour, monitor patient performance in the home environment during recovery, and help design better assistive technologies.

### **2.3.2 Assistive technologies and rehabilitation for gait impairments**

During bipedal locomotion, the motor control system needs to support body weight, give forward and lateral stability as well as promoting forward progression. These processes can be damaged or even stopped in the advent for a neurological injury or disease. Lesions of any of the level of the neural control hierarchy impairs initiation and/or maintenance and/or modulation of posture and gait. In the advent of a stroke, cortical and descending neural pathways are damaged or disrupted, but spinal and musculoskeletal systems remains intact, as well as brainstem and cerebellum in the majority of cases (Beyaert et al., 2015). Gait abnormalities after stroke can be due to the pathology itself (i.e. disruption of descending neural pathways) or to subsequently developed compensatory strategies (i.e. abnormal neural adaptive processes). Stroke survivors typically exhibit reduced walking speed and asymmetrical walking behaviours, whereby the un-affected side is usually most involved in carrying the body weight and propelling the body forward. This abnormal behaviour gives way to spatio-temporal asymmetries (e.g. shorter stance and longer swing times of the affected limb, shorter step length of the un-affected limb) and is strongly correlated with risk of falls and balance impairments (Lewek et al., 2014). Muscular impaired control is another consequence of neural infarct: muscles often show spasticity (due to the hyper-excitability of spinal reflexes), atrophy (due to limb initial immobilisation), and abnormal co-activation patterns (i.e. synergies, modules). The latter may be an adaptive strategy adopted to generate joint stiffness and compensate for gait instability. A reduced number of activated muscular modules was observed in stroke survivors with respect to healthy subjects during gait, likely resulted from merging healthy synergetic patterns together (Clark et al., 2010). The number of recorded modules correlated with gait velocity and asymmetries and was believed to be the result of adaptive response of the central motor system for the automatic and simplified control of the affected limb (Routson et al., 2013). Arm swing and trunk movements are also characterised by asymmetries in gait-post stroke, with an increase of trunk rotation compensating reduced pelvis rotation (Hacmon et al., 2012) and increased trunk acceleration especially in the medio-lateral plane (Van Crielinge et al., 2017) with respect to healthy adults. Curiously, trunk abnormal movement magnitude has been recently demonstrated to be a reliable marker of movement stability and abnormality in healthy adults, stroke and even PD patients (Sekine et al., 2013; Sekine et al., 2014). Patients with cerebellar damage due to stroke are surprisingly able to react to movement changes during gait as well as to learn predictive locomotor adaptive strategies. On the contrary, patients with non-stroke cerebellar impairments are not able to learn predictive changes in any

adaptation context, especially when walking (e.g. split-belt treadmill protocols) (Morton et al., 2006). A completely different scenario concerns spinal cord injury (SCI) patients. SCI is a partial or complete lesion of the neural pathways embedded in the spinal cord which causes reduced or lost control of those body parts whose peripheral nerve starts below the injury location. Locomotor abilities are frequently affected in SCI patients, and only those with partial lesions are potentially able to restore gait control via specific rehabilitation therapies (Nam et al., 2017). Indeed, lower limb cortical representations are intact in SCI patients, which could be very useful for the design of assistive BCI systems (Koenraadt et al., 2014).

As previously mentioned, rehabilitation after a neural injury needs to 1) promote new motor skill acquisition and training in order to stimulate restorative neural plasticity and avoid interference of un-healthy compensatory mechanisms (recovery vs. compensation); 2) plan therapies that can induce the acquisition of transferable and not only task-specific motor skills; 3) focus on both repetition and intensity of training (Huang and Krakauer, 2009). Motor recovery in both stroke survivors and SCI patients can nowadays be conveyed through many different types of therapies, for example over-ground walking therapy (OWT, in which subjects try to walk with the simple aid of parallel bars on the side and the physiotherapist), muscle strength training (such as eccentric or concentric strength training), and transferable skill training (sit-to-stand, tilted-table-standing and fitness exercises). A recently developed therapy is body-weight supported treadmill training (BWS). BWS has gained a lot of attention for its advantage to allow patients to start gait training very early in the recovery process (as patients not able to stand are supported by a harness), to repeat stepping sequences with high intensity and for its potential to stimulate normal and symmetric gait patterns. However, it is an exhausting protocol for physiotherapists who are needed to control and assist with lower limbs movements (Beyaert et al., 2015). Subsequently, robotic systems were developed to permit BWS treadmill training without the need for excessive manpower and robot-assisted gait trainings (RAGT) were introduced. These have the advantage of allowing natural and symmetric walking patterns while however increasing the intensity and duration of a training sessions and can also record patient performance through embedded sensors. Robotic systems can be programmed so that they partially or completely guide the lower limb movements through adaptive controllers, thus allowing subjects to try to initiate the movement (efferent motor commands) and eventually assisting them to finish it (afferent feedback drives), inducing neural plasticity (Stevenson et al., 2015; Nam et al., 2017). RAGT approach to gait rehabilitation has much potential for improving time

and quality of motor recovery. It induced changes in spinal reflexes circuitries and the re-emergence of physiologically modulated H-reflex in the soleus muscles during walking in SCI patients (Knikou, 2013). RAGT induced additional improvements in comparison to standard physiotherapy in stroke patients (Chung, 2017, Hong Kong-based study), and combined with conventional gait training could lead to more effective results (Morone et al., 2011, Italy-based clinical trial; Schwartz et al., 2015 for a review). RAGT is also believed to be a good aerobic exercise for patients, thus having potential metabolic and cardiopulmonary benefits (Nam et al., 2017). An example of robotic exoskeleton for RAGT is the Lokomat system (Hocoma, Zurich, CH): it is essentially a treadmill equipped with an harness supporting the patients in an up-right position and with robotic arms that can be attached to the patient's legs able to move them in a natural and symmetrical pattern (Jezernik et al., 2003). Active RAGT was shown to activate sensorimotor regions more than during passive RAGT, and that the changes in cortical activity were related to gait-cycle phases (Wagner et al., 2012). A very recent study investigated the functional connectivity correlates of RAGT through EEG recordings highlighting the presence of a frontal-central-parietal network during and post-training whose strength correlated with step kinematic errors. The fronto-centroparietal network was therefore proposed as a potential neural marker of motor learning and adaptation for patients undergoing RAGT (Youssofzadeh et al., 2016). It also was recently shown that high-level of guide force (i.e. 100%, passive movement) minimizes the involvement of the sensorimotor cortex. As this brain region is known to be essential in visuo-motor integration and learning during walking, lower levels of guidance should be preferred in order to stimulate active participation and cortical activations (Knaepen et al., 2015). Indeed, passive movement of the impaired limb does not stimulate the patients to be engaged and self-directed into the movement. Accordingly, robotic systems for RAGT define a specific trajectory and sequence of movements and impose it to the patient, preventing variability of step length and timing. On the contrary, split-belt treadmills allow subjects to behave naturally and to explore different motor control strategies according to the provided protocol (Helm and Reisman, 2015). Split-belt treadmills have two independently controlled belts which permit different motor patterns on the two legs (e.g. one could walk two times faster than the other) and the exploration of gait adaptation paradigms specific to the patients' needs. With stroke survivors for example, treadmill walking speed was increased in order to augment step length asymmetry and this induced after effects of reduced step length asymmetry in over-ground walking, which were surprisingly maintained in the long term with repeated practice (Reisman et al., 2013). A

very recently developed system, the MIT-Skywalker (InMotion Technologies, Boston, US), exploits the principle of the split-belt treadmills and goes beyond the standard therapies (Bosecker and Krebs, 2009; Artemiadis and Krebs, 2010). Indeed, it can be programmed to train rhythmic movements (speed and symmetry training), discrete movements (heel strike practice) or balance, potentially stimulating different neural circuits according to the task (Susko et al., 2016). It can accommodate patients with different pathologies by modulating speed and task and it allows the patients to engage with the task while ensuring self-directed movements. The MIT-Skywalker was tested with stroke and cerebral palsy patients and shown to be able to accommodate each patient and successfully induce locomotor and balance improvements (Susko et al., 2016).

In summary, there exist many types of therapeutic approaches that can be used for neurorehabilitation of gait, and novel assistive technologies are currently under development. Future therapies should promote the acquisition of transferable skills that would permit patients to improve their motor abilities also on tasks not previously trained, as well as investigating both behavioural and neural changes due to practice and recovery.

### **2.3.3 Single- and dual-task walking**

Walking while inserted in contexts that require high concentration levels can result difficult for both neurologically impaired patients and healthy individuals. For example, walking on an irregular surface is difficult and can compromise gait performance as it requires a higher level of attention to decide where to place the feet on the ground, to maintain up-right gait stability and avoid risk of a fall (Iosa et al., 2014). Healthy young adults walking on irregular surfaces choose a lower gait speed, likely to optimize gait patterns and stability (Menz et al., 2003). Also, older adults walking on irregular surfaces choose to walk more slowly to maintain stability and reduce risk of falling. The lower gait speed in this case is believed to be a compensatory strategy for the decline of sensorimotor and cognitive functions that would prevent them to properly react to a potential risk of fall (Menz et al., 2003). In high-difficulty situations, more pronounced trunk movements occur, possibly due to the effort of maintaining balance control and stability. Therefore, measures of trunk accelerations have been extensively used as descriptors of the quality of gait and performance in both healthy young adults, older adults and neurologically impaired patients (Menz et al., 2002; Menz et al., 2003; Latt et al., 2009; Sekine et al., 2013; Sekine et al., 2014). It has also always been observed that, if left free to choose, healthy subjects and patients would always decide to walk at their preferred walking velocity as it maximises performance and stability (Iosa et al., 2014;



Sekine et al., 2013). Gait performance is particularly impaired in both healthy adults and neurological patients when they are asked to walk while simultaneously engaging in a secondary task (i.e. multitasking) of different nature. Walking while carrying out a secondary cognitive task (i.e. Verbal Fluency Test) without specific prioritization instructions decreased gait speed and increased dysrhythmicity in both young and elderly adults (Yogev-Silgeman et al., 2010). The authors demonstrated that the effects of task prioritization on gait variability are age dependent, as gait is more altered in young than in elderly adults, suggesting reduced ability to prioritize and flexibly allocate attention to different tasks in ageing. Walking while reciting aloud alternate letters of the alphabet induced higher hemodynamic activity in the bilateral pre-frontal cortex (mostly in anterior PFC, bilateral ventro-lateral PFC and left dorso-lateral PFC measured through fNIRS) of both healthy young and old adults case. It was suggested that the PFC would be more activated as it is involved in attention-demanding tasks (Holtzer et al., 2011). The sustained bilateral increase of PFC (recorded from all anterior, dorso-lateral and ventro-lateral PFC areas) oxygenation level of healthy elderly adults when walking while performing secondary tasks (e.g. reciting alphabet letters aloud) has been also correlated to bigger stride length and better cognitive performance (Holtzer et al., 2015). Walking on a treadmill while counting backward in sevens aloud reduced the cadence of steps in both healthy young adults and stroke survivors while their left and right PFC (i.e. FP1-F3-F7 and FP2-F4-F8 electrodes according to 10-20 international system, covering SMA, dorso-lateral PFC and inferior frontal gyrus) hemodynamic activity significantly and uniformly increased with respect to the levels registered during natural walking (i.e. single-task), especially in the patients (Al-Yahya et al., 2016). Therefore, high-cognitive demands undermine gait behaviour in both healthy adults and stroke survivors, with the latter having stronger limitations in walking in real-life situations because of the lack of effective adaptive mechanisms. On the contrary, middle-aged and old adults with multiple sclerosis (MS) showed comparable motor (i.e. gait) as well as dual-task (i.e. number of corrected utterances/sec) performance with respect to healthy controls when walking while reciting alternated alphabet letters aloud, accompanied however by higher oxygenation levels uniformly distributed across PFC optodes (covering anterior, dorso-lateral and ventro-lateral PFC, Ayaz et al., 2012; Carlen, 2017). The authors suggested that the increased uniform cortical activation could be the means by which MS patients could achieve motor behaviours similar to healthy adults (Hernandez et al., 2016). When faced with a dual-task situation, patients as well as old adults have to decide whether to prioritize gait stability and balance over cognitive performance or vice versa (Li et al.,

2001). When walking while simultaneously reciting alphabet letters aloud, healthy old adults and elderly with neurological gait abnormalities (NGA) both increased uniformly their PFC (from anterior, dorso-lateral and ventro-lateral PFC) hemodynamic activity. During the dual-task condition, healthy old adults showed a negative correlation between levels of HbO<sub>2</sub> and gait velocity and a positive correlation with rate of correct letter production; on the contrary, elderly adults with NGA showed a positive correlation between HbO<sub>2</sub> levels and gait velocity during and a negative correlation with rate of correct letter generation (Holtzer et al., 2016). This was thought to be a strategy of the elderly with NGA for reducing dual-task costs and preserve gait performance in contrast with the strategy employed by healthy participants whereby maintenance of good dual-task performance was chosen instead. It has also been recently argued that the nature of the secondary task might influence gait performance differently, with motor and combined motor-cognitive secondary tasks impairing gait performance more than simple cognitive tasks (Lin and Lin, 2016; Maidan et al., 2016). Secondary tasks requiring a constant visual processing are more likely to disturb the gait (Beurskens and Bock, 2013). For example, walking while texting over a smartphone (high-difficulty motor-cognitive secondary task with visual focus on the phone) has been shown to reduce gait velocity and worsen gait stability and could undermine subjects' safety if performed in risky environments (Shabrun et al., 2014; Plummer et al., 2015; Agostini et al., 2015). The neural EEG correlates of walking under different conditions have been only recently presented thanks to development of reliable mobile setups and the definition of more sophisticated analytical methods able to remove source of noise present in data acquired during ambulatory tasks (Oliveira 2017). In comparison to fNIRS measurements, EEG recordings describe the actual electrical neural activity underlying the performed tasks, have a better temporal resolution, and can record activity from the whole head (mobile fNIRS systems currently allow only PFC recordings). The neural correlates of loss of balance were studied while subjects walked on a balance beam: sustained  $\beta$  power desynchronization was registered for the whole walk duration over the bilateral sensorimotor cortex (stronger than when naturally walking) and the first sign of loss of balance could be observed in the left sensorimotor cortex as an increase of  $\theta$  power right before stepping off the beam (Sipp et al., 2013). Walking uphill also recruits a stronger  $\beta$  power desynchronization together with an increase of  $\theta$  power in the anterior cingulate, sensorimotor and posterior parietal cortices (Bradford et al., 2016). Walking while adapting speed following an external auditory cue (i.e. accelerating or decelerating) induced a stronger  $\beta$  power desynchronization in central midline and parietal cortices,

likely symbolic of a continuous sensorimotor integration process while movement is ongoing, but also a  $\beta$  power synchronization in frontal and premotor cortices, possibly resembling motor initiation processes (Wagner et al., 2016).  $\beta$  activity was found reduced in motor and premotor midline electrodes when walking while performing an attentional demanding task (i.e. pressing a button when hearing a low-pitch sound), whereas an increase of  $\beta$  activity in frontal midline electrodes was observed when walking while performing a motor interference task (i.e. holding two sticks and preventing them from touching each other) (Beurskens et al., 2016). Therefore, it seems like stronger  $\beta$  power desynchronization is needed in sensorimotor and parietal cortices during high-difficulty gait conditions as a stronger sensorimotor integration process is needed to better and faster integrate sensory feedback and motor commands (Engel and Fries, 2010), whereas the frontal lobe is differently recruited according to the task. Future studies should employ novel single- and dual-task walking protocols in order to study the neural correlates of locomotor control when challenged and to find reliable casual relationships between brain activations and gait performance that could be then transferred into clinical practice as well as used as assessment tools in neurorehabilitation therapies. Given the current developments in mobile technologies and recording techniques, real-world studies should also be performed in order to better understand human locomotion in its natural environment.

### **3 General framework and methodologies**

#### **3.1 Overview**

This chapter describes the general aspects of the common methodologies employed in this work of thesis. Study I and Study II are based on two different study designs and therefore employ different protocols, materials and technologies. Each section contains detailed descriptions of the methods employed to accomplish the specific hypothesis: the robotic equipment, the reaching task and the motor adaptation protocol are detailed in chapter 4 of section Study I, whereas the mobile setup, the single-task and dual-task walking protocol are described in chapter 7 of the second section Study II. To some degree, differences in the employed analytical measures and in the signal processing steps can also occur as customized to the specific hypothesis and task: for example, the segmentation of continuous EEG data into epochs was done before visual inspection in the first study but at the end of all the pre-processing steps in the second study. These differences were dictated by the different types of experimental design employed: triggered-based with a trial-by-trial structure in the first study, continuous with no external cues in the second study. Nevertheless, the study design and data analytics were based on the same framework and analysis pipeline, which provided a powerful tool to investigate complex situations and datasets. Specifically, both studies were based on one principle and goal, investigating neuro-muscular correlates of human motor control in a real-scenario, thus share the same physiological recording techniques, signal processing pipeline and statistical approaches. All recordings were non-invasive: muscular activities were measured via surface electrodes for electromyography from the upper- (Study I) or lower-limb (Study II) muscles; neural oscillations were recorded from the scalp through 64-channels caps in both studies; kinematics of the reaching task (Study I) and features of gait patterns (Study II) were both monitored and used as evidence of performance for the respective study. Both studies shared many features in the signal processing employed to analyse physiological data such as pre-processing steps, filter choices, rejection of artefactual data and measures employed. The statistical analyses used were the same for both studies: parametric analyses of variances for kinematics and electromyography evidence and non-parametric approaches for electroencephalography signals. The multiple-comparisons problem was also common in both studies and handled by specific methods as later described. Figure 3-1 shows the overall structure of this thesis, highlighting study-specific aspects as well as interactions and commonalities.

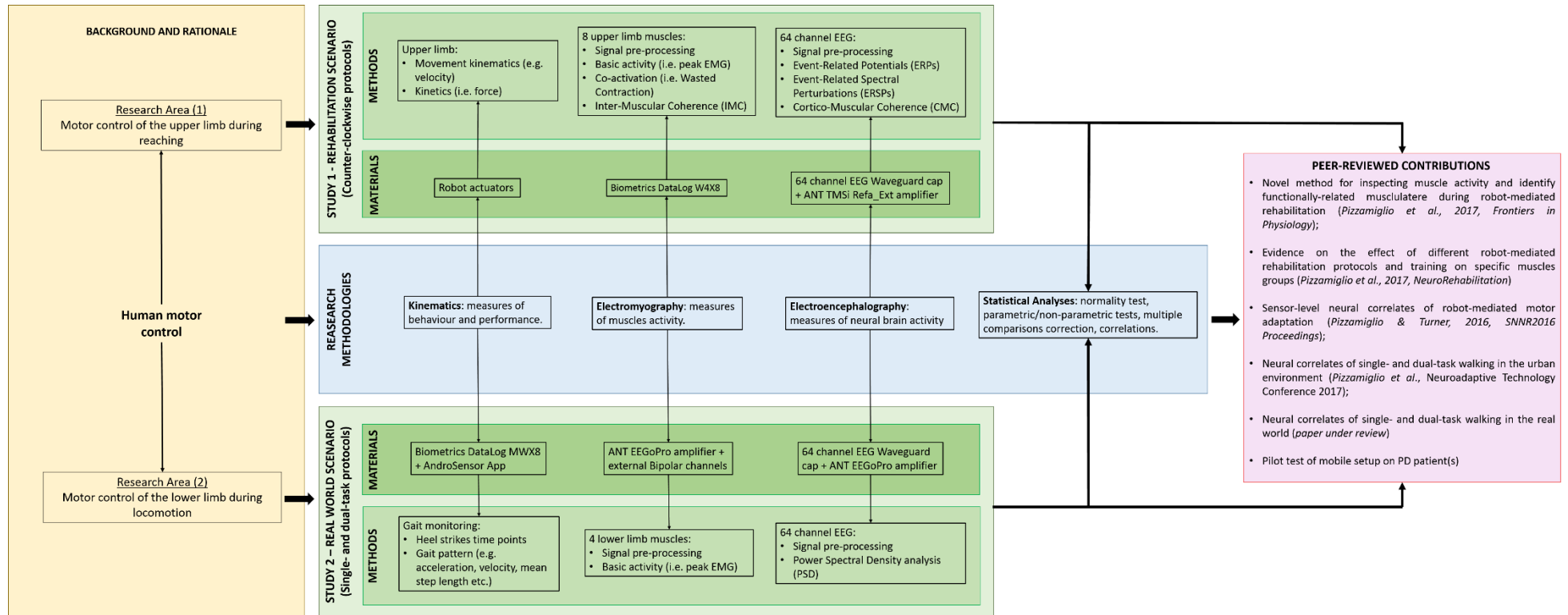


Figure 3-1: System architecture thesis diagram.

This work of thesis is based on a unique goal: identifying neuro-muscular correlates of human motor control in real-world scenarios. The work was based on two main studies investigating a neuro-rehabilitation scenario and real-world (i.e. outside the laboratory environment) situations, respectively. The two studies employed context-specific materials and technologies, but were based on the same recording techniques, analytical pipeline and statistical methods. Successful investigations led to the publication of several peer-reviewed articles and the presentation of the results to international conferences.

### **3.2 Ethics**

The studies were conducted in accordance with the Declaration of Helsinki for Human Experimentation (48th World Medical Association General Assembly, Somerset West, Republic of South Africa, October 1996) and were approved by the University of East London ethics committee (UREC\_1415\_29, see Appendix I). Each subject was first orally informed about the experiment upon recruitment and was given written detailed information on the day of the experiment. Before testing, subjects were required to complete a medical questionnaire to ensure that there were no contraindications to participate to the studies (e.g. history of neurological, psychiatric or muscular disorders, see Appendix II), and lastly gave their written informed consent (see Appendix III). Subjects could withdraw from the studies at any time without specifying the reason.

### **3.3 Subjects recruitment**

Subjects were recruited from personal contacts as well as from existing member of staff and students of the University of East London. The recruited subjects always resembled samples of the healthy young population, with ages ranging from 20 to 42 years old, and were all right handed. Handedness was determined through a questionnaire (reported in Appendix II) by asking the subject to identify the writing hand and the kicking foot. Subjects were tested approximately always at the same time on different days in order to control for changes in cortical excitability due to testing day time (Ridding and Rothwell, 2007). Subjects were asked to avoid alcohol for at least 24 hours before the experimental session, and were kindly asked to wash their hair before without conditioner as this optimizes EEG recordings. Experiments lasted between 2 and 3 hours in total (setup preparation + testing), and subjects were given regular resting periods to avoid fatigue and help maintaining attention to the task.

### **3.4 Experimental protocols and setups**

Two different experimental protocols have been used in this thesis:

- Study I is based on a robot-mediated motor adaptation protocol for the reaching movement and aimed to 1) investigate the neural and muscular correlates of different stages of adaptation, 2) validate the use of specific physiological measures as markers of changes in reaching performance and outcome optimization, as well as 3) pave the path for future studies of rehabilitation and recovery assessment with the neurologically impaired. Details of the experimental setup and protocol are described in section Study I, chapter 4, paragraph 4.2.2, 4.2.3 and 4.2.4;

- Study II is based on a Mobile Brain/Body Imaging (MoBI) design and a fully mobile setup. It aimed to 1) investigate the neural and muscular correlates of different walking conditions outside the laboratory in the urban environment, 2) validate the mobile setup and test its reliability as well as 3) identify preliminary relationships between neural activations and gait performance in order to plan potential future studies with clinical populations. Details of the experimental setup and protocol are described in section Study II, chapter 7, paragraph 7.2.2 and 7.2.3.

### **3.5 Physiological evidences**

#### **3.5.1 Electromyography**

Electromyography (EMG) is a neurophysiological technique able to record and describe the quality of muscular activity (i.e. myoelectric signals) as well as abnormal changes due to pathologies such as peripheral nerves diseases. Recordings can be done invasively with needle EMG electrodes in order to capture single-fibre activities, or non-invasively through surface EMG electrodes to register the sum of many single-fibre/motor-units activities (Basmajian et al., 1985). In this thesis, muscle activations were always assessed non-invasively through surface EMG electrodes: bipolar integral dry reusable EMG electrodes were used in Study I (single sensor area ~ 0.8 cm<sup>2</sup>, sensors fixed distance: 1.5 cm, material: silver chlorite, model SX230, Biometrics Ltd, Newport, UK), whereas monopolar disposable ECG/EMG electrodes were employed in Study II (sensor area: 0.8 cm<sup>2</sup>, sensor material: polymer Ag/AgCl coated, model Arbo<sup>TM</sup> H124SG, Kendall<sup>TM</sup> ECG Electrodes, Convidien Commercial Ltd, Gosport Hampshire, UK), with an inter-sensors distance of 1.5 – 2 cm circa. In both studies, surface EMG electrodes were positioned on the belly of the muscles of interest according to the belly-belly montage and along the muscle fibres direction following the SENIAM guidelines (Hermens et al., 2000). EMG activity was recorded at 1 kHz and amplified by a 14 bit analog-to-digital converter (DataLog WaX8 EMG system, Biometrics Ltd, Newport, UK) in Study I, and by an EEGoPro amplifier (ANT Neuro, Enschede, Netherlands) in Study II. The monitored muscles were:

- Study I: Anterior and Posterior Deltoid (flexion and extension of the shoulder joint respectively), Biceps and Triceps Brachii (flexion and extension of the elbow joint respectively), Extensor and Flexor Carpi Radialis (extension and flexion of the wrist joint respectively) and Brachioradialis (assists the Biceps Brachii in the flexion of the elbow joint and work on pronation and supination of the forearm). These muscles

were all recorded only from the right arm, except for the Biceps Brachii which was monitored bilaterally from both arms;

- Study II: Tibialis Anterior (dorsiflexion and inversion of the foot) and Soleus (plantarflexion of the foot). These muscles are both recorded bilaterally from both legs.

Study specific muscle locations are represented in section Study I, chapter 4, Figure 4-3, and in section Study II, chapter 7, Figure 7-2.

### **3.5.2 Electroencephalography**

Electroencephalography (EEG) is a neurophysiological technique able to measure the electrical activity of the human brain and to describe changes in voltage over time (Berger, 1929). Despite the existence of intra-cortical invasive recording techniques such as iEEG and ECoG, EEG is by definition only non-invasive and records electrical potentials on the scalp through surface electrodes. Using non-invasive electrodes positioned over the scalp the electrical potentials generated within the brain by the single neurons (i.e. both action and post-synaptic potentials) cannot be disentangled, instead the result of sum and cancellation of potentials from neighbour neurons is recorded (Luck, 2014). In this thesis, neural oscillations were assessed non-invasively through a 64-channel (i.e. electrodes) Waveguard cap (ANT Neuro, Enschede, Netherlands) disposed according to the 10-20 international system (Jasper, 1958). This is a method internationally recognized to describe the location of scalp electrodes with respect to the underlying areas of the cerebral cortex. According to this method, the scalp is divided into arcs starting from four reference points: the nasion (point between forehead and nose), the inion (lowest point of the skull from the back of the head), and the left/right pre-auricular points anterior to the ears. The intersection between the longitudinal and the lateral arcs is called vertex: from this point, all electrodes are located at 10% or 20% of the total longitudinal or lateral distances (Klem et al., 1999). Figure 3-2 shows the electrodes locations of the Waveguard caps used in both studies of this thesis. According to the participant's head size, the EEG cap size that suited the head best was chosen (i.e. small, medium and large). The electrode Cz was always located at the vertex and, maintaining it fixed, the cap was adjusted so that all the electrodes were in the right position; a chin strap could eventually be used to tight the cap. Wet electrodes were used, which required a quick-gel solution to be injected between the scalp and the electrodes themselves thus to amplify the signal recorded and maximize their impedance (i.e. quality of electrode-skin connection). To optimize the quality of the recorded data, impedances



were kept always below 5 k $\Omega$ . EEG signals were recorded continuously during each experiment in both studies with the ground electrode (i.e. earth electrode, connects the system to the earth) located always in AFz position and the reference electrode (ideally with a stable potential, used as reference for measurements by the other electrodes) in Fz (Study I) or FCz (Study II) positions. In Study I, EEG data were recorded at a sampling frequency of 1024 Hz and amplified by a TMSi Ref-Ext amplifier (ANT Neuro, Enschede, Netherlands); in Study II, neural oscillations were registered at 1 kHz by an EEGoPro amplifier (ANT Neuro, Enschede, Netherlands). In both studies, data were band-pass filtered during recordings between 0.1 and 500 Hz. No electrooculogram (EOG) was recorded as blink and saccades movements could be reliably identified and removed from the continuous data during offline pre-processing through ICA decomposition.

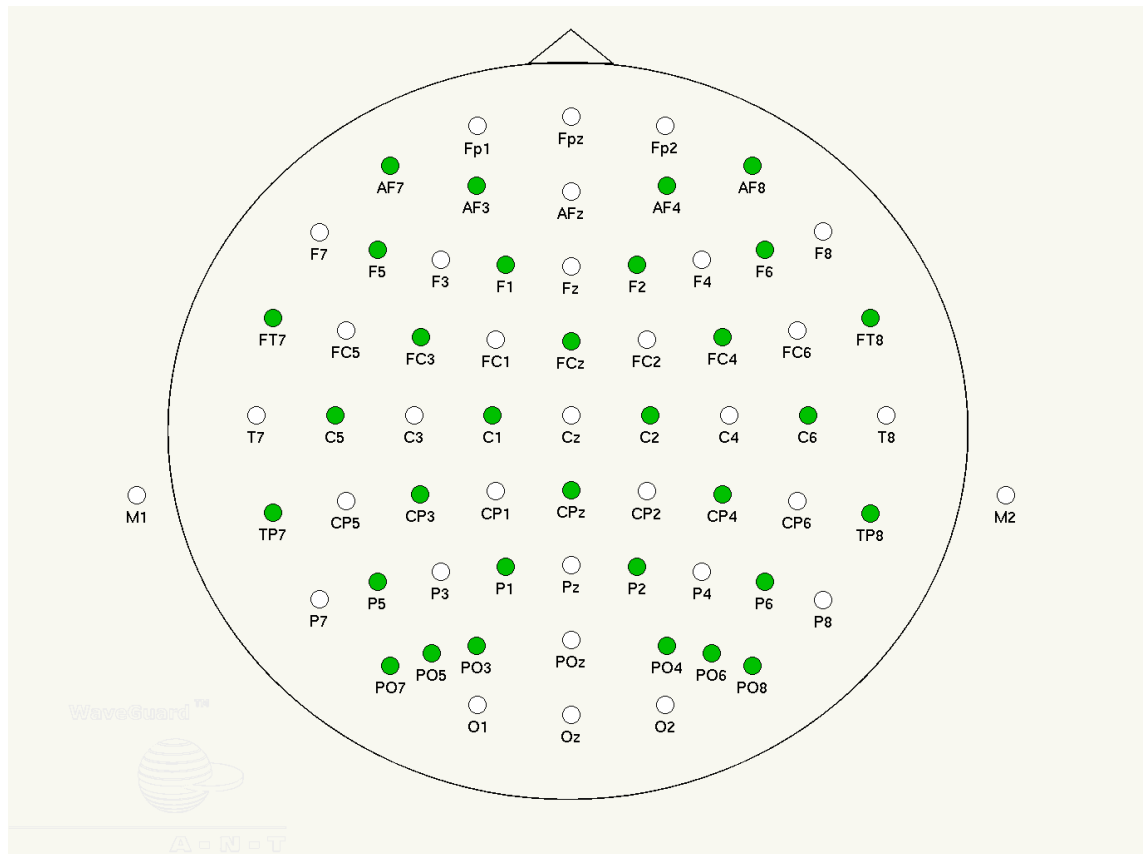


Figure 3-2: 64-channel Waveguard cap (ANT Neuro, Enschede, Netherlands).

This electrode scheme is an extension of the original 32-channel 10-20 international system and allows the positioning of 64 electrodes in total. Ground electrode: AFz. Reference Electrode: Fz (Study I), FCz (Study II). (Figure adapted from [www.ant-neuro.com](http://www.ant-neuro.com) official website).

### **3.6 Signal processing**

All the data analyses carried out in this thesis were performed with MatLab 2013b/2015b (The MathWorks Inc.). In order to properly analyse the data and obtain successful correlations between different evidences, two requirements needed to be met:

- A careful synchronization of all the devices within each setup was required in order to be able to align separately recorded evidences on the same time scale. Methods of synchronization are described in details for the two setups in section Study I, chapter 4, paragraph 4.2.5, and in section Study II, chapter 7, paragraph 7.2.3 and 7.2.4;
- All signals needed to have the same sampling frequency in order to have a good correspondence of time points. When not possible due to hardware specification, interpolation or down-sampling of the recorded signals were performed offline. The reference sampling frequency used in both studies for all evidences is 1 kHz.

#### **3.6.1 Measures of kinematics**

Kinematics describes objects and bodies movements without taking care of the causes of the movement itself. Acceleration, velocity and position are all measures employed in this work of thesis to describe the evolution of movements of both upper and lower limbs. Kinematics data of reaching were recorded by sensors embedded into the robotic equipment in section Study I (see chapter 4, paragraph 4.2.6, section Reaching kinematics), whereas gait kinematics was recorded by mobile sensors placed at level of the pelvis and of the feet during walking in section Study II (see chapter 7, paragraph 7.2.4, section Gait measures).

#### **The reaching movement**

First of all, reaching movements were described by a starting time point (Movement Onset, defined by a speed profile exceeding a threshold of 0.03 m/s) and by an end time point (Movement Offset, defined by a speed profile lower than the threshold of 0.03 m/s after Movement Onset). Changes in Movement Onset and Offset were monitored throughout the whole duration of the experiments in Study I as potentially symbolic of changes in reaction times and movement durations. Reaching could ideally evolve along a straight trajectory connecting the starting point and the end target, but even during practiced movements slight deviations from this ideal straight path occur. Applying an external perturbation, as in the robot-mediated motor adaptation protocol implemented in section Study I, induces even bigger deviations from the ideal straight line. To describe

movement deflections from the ideal straight line a measure of trajectory error called Summed Error was employed (Hunter et al., 2009): it consists of the sum of the perpendicular distance between the actual and the ideal trajectories at each time point between Movement Onset and Offset. The reduction of trajectory errors over the motor adaptation condition period is symbolic of an adaptation process undergoing, whereby subjects learn how to compensate for the external perturbation to improve their performance in the novel environment. Maximum velocity (m/s) and maximum force (N) were also evaluated and monitored during each reaching movement as likely to describe, respectively, changes in movement speed and exerted forces to counteract the applied perturbation and support the adaptation process.

### **Gait monitoring**

Linear acceleration data recorded during walking at the level of the pelvis (i.e. lower back) were further used to extract spatio-temporal features of the gait pattern via a MatLab based toolbox (Yang et al., 2012). Many measures were obtained (see Study II, chapter 7, paragraph 7.2.4, section Gait measures), but of major interest were gait Velocity (m/s), Steps Cadence (step/min) and entity of trunk movements as expressed through the measures of Acceleration RMS (a.u.). Changes in these parameters would demonstrate changes in the velocity and stability of the trunk during walking, and would be symbolic of changes in gait performance during different demanding conditions. Moreover, times of heel strikes were recorded through mobile sensors placed on both heels, which allowed the calculation of the measure of Step Latency employed for further analyses and as a control of the previously extracted gait parameters.

### **3.6.2 Pre-processing**

#### **EMG**

A pseudo-common pipeline for EMG data pre-processing was developed for both studies. EMG data were first de-trended (i.e. mean subtracted) in order to emphasize the oscillations around the trend and remove potential data shifts due to potential hardware issues (e.g. sensors drift). A band-pass filter was then applied to remove low-frequencies intrinsic noise and high-frequency content of no interest. In section Study I, data were band-pass filtered between 45 – 100 Hz in order to remove all possible noise and movement artefacts, whereas in section Study II EMG signals were band-pass filtered between 20 - 100 Hz as per guidelines (De Luca et al., 2010). In both studies, EMG activity from each muscle of each subject was then normalized to the maximum value registered in that same muscle across the whole experimental condition (i.e. activation

ratio, %), thus to minimize variability across subjects due to potential differences in electrode-skin impedances. Full-wave signal rectification was used in both studies to reverse the negative portions of the oscillating EMG profile making it entirely positive. Once performed all these steps, EMG data were ready to be further analysed.

## EEG

As EEG data are very sensitive to external (i.e. from the environment or movements) and internal (i.e. from the body such as heart beat and blinks) sources of noise, a careful and meticulous pre-processing pipeline was developed with EEGLab toolbox (Delorme and Makeig, 2004) to clean the data and remove artefactual components. This pipeline was employed in both studies:

1. Data were first band-pass filtered between 0.5 and 100 Hz, to remove the very slow drifts and higher contents of no interest (FIR filter, order automatically set by EEGLab), and notch-filtered at 50 Hz, to remove the power line noise (FIR notch filter, order = 3302);
  - 1.1. Only in section Study I an additional notch filter was applied at the frequency of 25 Hz to remove an electrical noise within the laboratory robotic-equipment. Again, only in Study I, data were here segmented into epochs (i.e. trials) and de-trended;
2. A careful visual inspection of the data was then carried out to remove trials (Study I) or periods of continuous data (Study II) characterized by prominent artefacts, as well as to identify channels affected by major sources of noise for the whole experiment duration;
3. After visual inspection, noisy channels were temporarily removed from the data, which were then re-referenced to the common average reference. As aforementioned, the neural activity recorded is the difference between the actual activity at any electrodes and the activity from the reference electrode, which shouldn't be related to any brain or muscle activity. This in practice is not possible, therefore, to minimize the effects of the reference electrodes on the results, EEG data are usually re-referenced to the common average across all electrodes signals. This method is the most commonly used in literature as it minimizes the effect of large or small signals at the edge of the EEG cap;
4. Data were then decomposed using the Independent Component Analysis (ICA) with the Infomax algorithm as implemented in EEGLab (Delorme et al., 2007). ICA is a statistical methodology able to transform a recorded complex (i.e. multidimensional)

random signal into a set of single components linearly independent (Independent Components, ICs) (Hyvärinen and Oja, 1997). The purpose of using ICA is to “reshuffle” the original EEG channels, where each channel carries a signal mixed from different brain sources, to new virtual channels (i.e. components, ICs), where each component is an estimate of the unmixed signal from a single source. ICA has been widely used to compare neural sources across different tasks, but in this thesis it is used only as a means for removing artefactual sources within the EEG signal. To identify and remove artefactual contributions the power spectral, the spatial and the temporal features of each IC were inspected and those representing stereotypical artefacts were eventually discarded. The remaining components were then projected back to recreate cleaned scalp channels;

5. Previously removed channels were then interpolated through the spherical spline method as implemented in EEGLab. This procedure consists in first defining the electrodes that need to be interpolated and calculating their location with respect to their neighbours (i.e. same approach as the 10-20 system for defining electrodes locations on the scalp). Secondly, the electrical potentials are interpolated through a spherical spline interpolation method as previously described (Perrin et al., 1989). All the data were then re-referenced to common average for a second time as new interpolated channels were added, thus a new common average reference was needed;
  - 5.1. Only in section Study II data were segmented into epochs and de-trended;
6. One final visual inspection was performed to check the quality of the pre-processed data and eventually remove still noisy trials/epochs.

At the end of the pre-processing pipeline, for both studies, there were 64 channels available for further analyses as the artefactual ones were interpolated from cleaned data. As a matter of fact, only 62 electrodes were then actually used as mastoids electrodes (M1 and M2, see Figure 3-2) were not further considered.

### **3.6.3 Measures of basic muscle activity**

In this thesis, muscle activity was quantified through basic (i.e. simple) measures such as maximum EMG activity (see Study I, chapter 4, paragraph 4.2.6, section EMG pre-processing and basic muscle activity) and Root-Mean-Square (see Study II, chapter 7, paragraph 7.2.4, section EMG processing and basic muscle activity). More complex measures investigating muscular activation in the time domain (i.e. Wasted Contraction) and synchrony in the frequency domain (i.e. Intermuscular Coherence) have also been

employed and reported elsewhere (see Appendix IV; Pizzamiglio et al., 2017; Pizzamiglio et al., 2017).

#### **3.6.4 Measures of neural Event-Related Potentials (ERPs)**

Event-Related Potentials represent spontaneous responses of the brain to external stimuli such as visual, auditory or mechanical cues, and have been extensively used in literature. Only in the first study were ERPs evaluated given the dependence of ERPs on an external stimulus and the type of study protocols designed in this thesis. Data were first low-pass filtered at 45 Hz to remove high-frequency content not typical of ERPs, and then a simple mathematical average of electrical potential across a set of trials was performed for each electrode, in each condition, for each subject. The analysis of ERPs then focused only on three windows of time of interest as these periods were shown to be mostly related to neural processes of sensory feedback, visuomotor planning and movement initiation (Naranjo et al., 2007; Dipietro et al., 2014).

#### **3.6.5 Measures of neural Power Spectral Density (PSD)**

The spectral content of an EEG trace describes the different typologies of neural oscillations (i.e. brain waves) that are contained in the signal. The EEG power represents the amplitude or intensity of a specific brain wave category of interest. Brain waves are classified according to their oscillatory frequency into different ranges:  $\delta$  waves are the slowest (oscillatory frequency between 1 Hz up to 3 Hz), they have the biggest amplitude and are typical of deep meditation and sleep states;  $\theta$  waves are slow (oscillatory frequency between 4 Hz up to 7 Hz), have a big amplitude and are seen in many memory and spatial-navigation tasks;  $\alpha$  waves are moderately slow (oscillatory frequency between 8 Hz up to 12 Hz), have moderately big amplitude and are typical of conscious thoughts and alertness;  $\beta$  waves are moderately fast (oscillatory frequencies from 15 Hz up to 30 Hz), have moderately small amplitude and are usually seen in cognitive and motor tasks;  $\gamma$  waves are the fastest (oscillatory frequency between 30 Hz up to 80 Hz), they have the smallest amplitude and typically represent simultaneous processing of information from different brain areas, such as sensorimotor integration. The analysis of the power spectral content of the EEG can be useful in clinical practice where brain waves could be symbolic of a specific disease (e.g. epileptic seizures are characterized by synchronous alpha wave discharges) (Gestaut, 1970).

The standard analysis of the EEG spectral power is embedded into the frequency domain only. The oldest technique employed to quantify the intensity of a particular brain wave in an EEG signal is the Fast Fourier Transform (FFT) (Fourier, 1822). Given an EEG time

series (i.e. signal), the FFT algorithm transforms it into a potential-by-frequency spectral graph (i.e. the power spectrum) according to the formula:

$$f(\xi) = \int_{-t}^t f(x) \cdot e^{-2\pi i x \xi} dx$$

*Equation 3-1: FFT Algorithm formula.*

where  $\xi$  is the frequency and  $[-t \ t]$  is the time interval of interest. The longer the time window of interest, the higher the frequency resolution of the FFT. The calculation consists in 1) evaluating the EEG magnitude, defined as the integral of the peak-to-peak amplitude of the EEG signal within a certain period of time of interest, and then in 2) squaring the obtained EEG magnitude, thus obtaining the EEG power spectrum. To avoid spectral leakages (i.e. the creation of new frequency components not-existent in the original signal but due to the mathematical algorithm), the data within the time period of interest can be selected by applying an a-priori window function (or taper) that minimizes the creation of artificial contents (Harris, 1978). An alternative to the FFT method is the Welch's periodogram (Welch, 1967), which consists of segmenting the original data into multiple overlapping segments, to which a taper is applied before the FFT algorithm. The individual periodograms are then averaged to reduce the individual power measurements. This more robust methodology has been employed only in the second study whereby the time domain was negligible (i.e. no external stimuli applied, conditions considered as continuous) and the overall power within an epoch was of major interest (see section Study II, chapter 7, paragraph 7.2.4, section Power Spectral Density (PSD)), in order to reduce the amount of variance within a subject-specific recording and across subjects due to the partially controlled walking paradigm.

### **3.6.6 Measures of Event-Related Spectral Perturbations (ERSPs)**

Recent developments in analytical methods allow the investigation of changes in EEG spectral power over time. To evaluate the time-frequency evolution of the power spectrum a time-frequency sliding window is usually used, whose dimensions could be fixed or mutable. The latter is a more proper approach when investigating the EEG spectral power at different frequencies: usually the sliding window gets shorter along the time axis and longer along the frequency axis with increasing frequencies, which emphasizes the content of higher frequencies, whose amplitudes are typically low, by smoothing over a bigger frequency range. Many techniques can be implemented to obtain an accurate time-frequency representation of the EEG spectral power such as single taper with changing length, multi-tapers, and wavelet decomposition. In this thesis, the Morlet wavelet



decomposition (Torrence and Compo 1998) was used, which, in line with what described above, evaluates the power over time and frequency domains by applying a specific Gaussian shaped taper according to the formula:

$$\psi_0(\eta) = \pi^{-\frac{1}{4}} \cdot e^{i\omega_0\eta} \cdot e^{-\frac{\eta^2}{2}}$$

Equation 3-2: Gaussian taper formula.

The continuous wavelet transform is obtained through the convolution of the EEG signal with a scaled and translated version of the Gaussian taper following the formula:

$$W_n(s) = \sum_{n'=0}^{N-1} x_{n'} \cdot \psi * \left[ \frac{(n' - n)\delta t}{s} \right]$$

Equation 3-3: Scaled and translated Gaussian taper formula.

where \* indicates the complex conjugate. By varying the scale  $s$  and translating along the time index  $n$ , it is possible to obtain information on the amplitude of any brain waves within the signal and how this amplitude changes over time. In order to observe changes in power spectrum during the task with respect to a period of baseline (i.e. when the subject is at rest, not engaged in anything) the Event-Related Spectral Perturbation changes were obtained by subtracting the baseline power ( $Pow_{base}$ ) from the task-related power ( $Pow_{task}$ ) according to the formula:

$$ERSP(i) = Pow_{task}(i) - Pow_{base}$$

Equation 3-4: ERSP formula.

where  $i$  is the current trial/epoch. This method was implemented throughout this thesis in both studies, whereby the baseline was defined as the average across trials of a period of 900 ms before the cue to reach (Study I) or as a resting-state EEG period recorded before the experiments (Study II). To assess if the changes in EEG power during the task were statistically significant from the spontaneous baseline oscillations, a bootstrap randomization technique was used as implemented in EEGLab (Grandchamp and Delorme, 2014). Specifically, a distribution of surrogate data trials was obtained and permutation statistics was then applied to identify non-significant features in the task-related power with respect to the baseline power. The level of significance for the bootstrap randomization technique was maintained at 99% ( $P < 0.01$ ) for both studies, and data not-statistically significant were zeroed out and plotted in green (see Study I, chapter 5, Figure 5-3, and Study II, chapter 7, Figure 7-4).

### 3.6.7 Measures of Cortico-Muscular Coherence (CMC)

Coherence is a normalized measure of the coupling between two signals at a given frequency (Rosenberg et al., 1989; Amjad et al., 1997). Specifically, Cortico-Muscular Coherence (CMC) reflects the functional direct- or indirect-synchrony between a given brain area and a contralateral muscle. EEG-EMG coherence can be assessed with the formula:

$$Coh(f) = \frac{|S_{xy}(f)|^2}{S_{xx} \cdot S_{yy}}$$

Equation 3-5: Coherence formula.

where  $S_{xx}$  and  $S_{yy}$  are the individual power spectra (i.e. of an EEG channel and an EMG muscle respectively), whereas  $S_{xy}$  is the cross-spectrum between the two signals. Coherence values are comprised between 0 (i.e. no coherence, no synchrony) and 1 (i.e. maximum coherence, maximum synchrony). In this thesis, CMC analysis was performed only in the first study to investigate changes in brain-to-muscle drives during the adaptation protocol; no CMC analyses were carried out in the second study given the priority of neural changes due to the performance of multiple tasks at the same time. Details of the CMC method employed are described in Study I, chapter 6, paragraph 7.2.2 (section Cortico-muscular coherence (CMC) at sensor level), but it is worth mentioning that the simple FFT algorithm (see paragraph 3.6.5) with Slepian sequences tapers (i.e. dpss taper as automatically implemented in FieldTrip) was applied to both EEG and EMG data to evaluate CMC over a fixed period of time capturing the full reaching movement (i.e. no time information).

### 3.6.8 Theory of source localization

Scalp EEG signals do not reflect the exact intensity and location of the activated neuronal populations: this is due to the fact that the real electrical signal is attenuated when travelling through the layers between cortex and head surface (i.e. brain, skull and skin), and to the high conductance of the scalp because of which it can spread over wide scalp areas (i.e. volume conduction problem). A large part of the current EEG literature has reported findings at scalp (sensor) level, which however need to be carefully considered due to the aforementioned problems. One way to overcome these issues is to reconstruct and localize the real neuronal sources from the sensor data. This problem however is an ill-posed inverse problem as an infinite number of solutions could explain the observed EEG data (Ramirez, 2008). In order to successfully estimate the neural activity at source

level, a priori information is needed to limit the number of potential solutions, specifically:

- The EEG data at sensor level;
- The spatial locations of the sensors (i.e. channel positions on the scalp);
- The geometrical and electro-magnetical properties of the head (i.e. the head model);
- The location of the sources (i.e. the source model).

Source localization consists of two main steps:

- Forward Modelling: estimating the source model, head model and the potentials at known sources;
- Inverse Modelling: estimating the unknown source activity from the corresponding scalp potential data.

First of all, a volume conduction model needs to be created to characterize the geometry of the head and the conductivity of each tissue. This model is used to evaluate how the electrical currents can flow and spread through the tissues of the head. The more accurate is the description of the geometry and conductivity of the head, the better the quality of the forward model. To create an accurate volume conduction model, the individual anatomical MRI of the subject should be used in order to calculate the subject-specific head dimensions and conductivity. Secondly, the source model needs to be calculated: here the brain volume is discretized into a 3D grid and a neural dipole is associated to each grid point. Once the channel locations, the volume conduction model and the source model are available, the forward model can be described through a lead-field matrix of coefficients that map current sources to potential differences at the scalp.

The inverse solution can then be obtained from the forward model output. There exist many different techniques able to approach the ill-posed inverse problem (Ramirez, 2008; Jatoi et al., 2014), among which Dynamic Imaging of Coherent Sources (DICS) is specific for data in the frequency domain such as power spectrum and coherence. It is a spatially adaptive filter able to evaluate the amount of activity at a given location in the brain according to the formula:

$$W_s^T(f) = (L_s^T \cdot C(f)^{-1} \cdot L_s)^{-1} \cdot L_s^T \cdot C(f)^{-1}$$

Equation 3-6: DICS spatial filter formula.

where  $C(f)$  is the cross-spectral-density matrix between two signals at a given frequency  $f$ ,  $L_s$  is the lead-field matrix at a given source  $s$ ,  $W_s(f)$  is the output spatial filtering matrix and the superscript  $T$  indicates the matrix transpose. This inverse adaptive filter aims to optimize the activity at a given source in a given frequency while minimizing the contribution from all the other sources (i.e. unit-gain constraint) (Gross et al., 2001). By applying the spatial filter  $W_s$  to the spectral data, the spectral measures of interest can be estimated at source level. Moreover, by overlying the newly estimated source potentials on an individual MRI it is possible to anatomically visualise the localized source activities.

In this thesis, localization of cortical sources has been applied only to CMC data in Study I. As later detailed (see Study I, chapter 6, paragraph 6.2.2, section Source localization), no one of the recruited participants had an individual anatomical MRI, therefore a template MRI was used as well as a pre-calculated forward model (both provided by FieldTrip). As CMC data is within the frequency domain only, the DICS algorithm has been employed.

### **3.7 Statistical analyses**

Both studies in this thesis are designed according to a within-subject format, whereby data from the same subject are recorded in multiple time points (i.e. conditions). Subjects are therefore going to be different observations in dependent-samples statistical approaches.

#### **3.7.1 Statistics for kinematics and EMG evidences**

In both studies, behavioural, kinematics and EMG data were supposed to be normally distributed and Kolmogorov-Smirnoff normality tests were employed to validate this hypothesis. Data were always normally distributed, thus parametric statistics was employed. Analysis of Variance (ANOVA) were first used, usually with a one-way fashion, as in both studies more than one experimental condition was included (within-subject factor: Condition). ANOVA significance values was always set at 95% ( $p < 0.05$ ). In case of a significant ANOVA, post hoc paired samples t-Tests were carried out to identify the differences within the dataset. T-Tests significance level was always set at 95% ( $p < 0.05$ ). When more than one comparison was performed, corrections for multiple comparisons was made in order to avoid false positive errors and control for the Family-Wise Error Rate (FWER). Bonferroni method for multiple comparison was always employed whereby the significance level was reduced according to the number  $N$  of repeated t-Tests performed ( $p_{adj} = 0.05/N$ ).

### 3.7.2 Non-parametric cluster-based permutation tests for EEG evidences

EEG data are multidimensional: they usually have a spatio-temporal or spatio-temporal-spectral structure as they are recorded from multiple locations (64 in this thesis), multiple time-points according to the sampling-frequency (1 kHz in this thesis), and multiple frequencies of interest in spectral analyses. The multidimensionality of the EEG data creates an enormous number of multiple comparisons in statistical analysis: changes across experimental conditions are indeed evaluated at a high number of (channel, time)-pairs or (channel, time, frequency)-triplets (i.e. samples). Therefore, there is the need to control for the FWER at a critical significance level.

To solve the multiple comparison problem, a specific non-parametric statistical analysis as implemented in FieldTrip (Maris and Oostenveld, 2007) has been used throughout the whole thesis when dealing with EEG data. First, a cluster-based test is run on the EEG data (ERPs, PSD or ERSs): for every sample in two conditions a paired-sample t-Test is performed and only the samples whose t-values are larger than a predefined threshold ( $\alpha_{\text{cluster}} = 95\%$ ,  $p_{\text{cluster}} < 0.05$  in Study I;  $\alpha_{\text{cluster}} = 99\%$ ,  $p_{\text{cluster}} < 0.01$  in Study II) are selected. The selected samples are clustered according to their temporal, spectral and spatial adjacency and the cluster-level statistics is calculated by taking the maximum sum of the t-values of each sample within the cluster. The result of this procedure is the cluster test statistics with which the effects of the experimental conditions are then evaluated through the Monte-Carlo method. According to this method, trials are randomly exchanged between the two considered datasets (i.e. random partition) and the cluster-level test statistics is evaluated for these surrogate sets. This step is repeated for a large number of times (that need to be specified) in order to obtain a histogram of the test statistics. Once the cluster-level test statistics is calculated for all the surrogate sets, the proportion of the surrogate test statistics whose values are larger than the one obtained from the real datasets is calculated. This proportion represent the Monte-Carlo significance probability and, if lower than the predefined significance level ( $\alpha = 95\%$ ,  $p < 0.05$  in both studies), the data in the two experimental conditions are statistically different.

This method has been used throughout the whole thesis when dealing spatio-temporal (ERPs), spatio-spectral (PSD, CMC at source level), and spatio-temporal-spectral (ERSs) EEG evidence.

### 3.7.3 Assumptions for Multiple Linear Regressions (MLRs)

Multiple linear regression is usually employed when trying to predict the value of a target variable, called Dependent Variable (DV), from the values of two or more explanatory variables, called Independent Variables, IVs. Multiple linear regression models have been generated in both studies of this thesis to find a relationship between brain activations and task behavioural performance (see Study I, chapter 6, paragraph 6.2.3, section Regions of Interest (ROIs); see Study II, chapter 8, paragraph 8.2.2, section Models of gait behaviour vs. EEG PSD activations). The multiple regression models created in this thesis were all based on the stepwise technique, where only the IVs that are significantly correlated with the DV are entered into the model. Several assumptions must be checked before reporting multiple regression models results, specifically:

- The presence of any outliers and the type of relationship between DV and IV must be verified through a scatterplot of the DV against the IVs. A linear relationship should be visible by the scatterplots;
- The adherence of the regression model residuals to a normal distribution must be checked through the residuals Q-Q plot;
- The lack/presence of little multicollinearity must be verified by: 1) Inspecting the Pearson's Bivariate Correlation coefficient of the model predictors; 2) Calculating the Tolerance index ( $T < 0.2$  little multicollinearity,  $T < 0.01$  strong multicollinearity), which measures the influence of one IV on the others; 3) Evaluating the Variance Inflation Factor ( $VIF = 1/T > 10$  strong multicollinearity); 4) Calculating the Condition Index ( $10 < CI < 30$  medium multicollinearity,  $CI > 30$  strong multicollinearity);
- The lack/presence of autocorrelation must be checked through the Durbin-Watson's d test ( $1.5 < d < 2.5$  no autocorrelation);
- The lack/presence of homoscedasticity must be verified through a scatterplot of the regression model standardised residuals versus the observed DV.

## **Study I: Neurorehabilitation Scenario**

### **4 Kinematics and muscle activity during robot-mediated motor adaptation of reaching with the upper limb**

#### **4.1 Introduction**

Motor (skill) learning is commonly defined as a progressive improvement in the performance of a given task characterized by a constant retention and consolidation of the newly acquired skill over time (Shadmehr and Wise, 2005). Motor learning features in our daily life from when we are born, when we first learn how to walk and then how to ride a bicycle. However, it is also required in patients that have suffered of a severe brain injury (e.g. stroke) that has damaged the motor areas of the brain (and other regions connected to it) and impaired the performance of natural movements such as walking, reaching and/or grasping. In these situations, an intense re-learning process is therefore needed to recover the lost abilities and minimize the impact of the injury on daily-life. However, brain injuries can be quite variable and therefore recovery can be challenging and different from patient to patient (Semrau et al., 2015). Early ( $< 7$  days) mobilisation after stroke has been shown to promote better recovery than later rehabilitation ( $> 1$  month) (Ottenbacher and Janell, 1993; Musicco et al., 2003, even though very early mobilisation ( $< 24$ h after stroke) might not be associated with significant beneficial effects (Xu et al., 2017) and might even increase mortality rate (Bernhard et al., 2015; Awad et al., 2016; Olkowski and Shah, 2017). Many different types of rehabilitation strategies and protocols are currently available, and there is a wide-spread trend towards personalized therapies and prognostic computational models aiming to optimize the rehabilitation outcome (Kwakkel, 2006; Reinkensmeyer et al., 2016). Physiotherapy is the most common intervention that patients are offered after a brain injury: the passive movement of the paretic limb(s) facilitates the regain of muscles tone and range of movement but is not the most favourable approach for functional recovery. According to the theory proposed by Hebb in the mid-20th century, when two cells are close to each other and one of the two is continuously and persistently firing the other one, some (metabolic) changes happen in one or both cells such that efficiency increases, and a stronger or even new pathway could be generated (Hebb, 1949). This postulate suggests that the purposeful activation of neural pathways would be able to intensify neural connections or even create new ones. Following this theory, a lot of research and rehabilitation protocols have been based on an active engagement of the patients, as even the intention of doing a movement could, in the long-term, result fruitful. Robotic neurorehabilitation is particularly attractive in this field as computational programmes

can be coded so that different level of assistance can be delivered according to the patient's ability (Hunag and Krakauer 2009). Nowadays there are many commercial solutions for rehabilitation robotics (Riener, 2007), from exoskeletons to actuated joysticks, and all of them are equipped with motors, which can be regulated and set to (not-) assist or even resist the movements. Robotic devices are useful as they can deliver higher training dosage at higher intensities than a physiotherapist without getting "tired"; moreover, their embedded sensors allow for reliable measurability of the performed movements and for an accurate assessment of performance, both in healthy and impaired populations (Finley et al., 2009; Zollo et al., 2011; Turner et al., 2013). In parallel, other neurophysiological recording techniques can be employed to simultaneously observe movement, muscles and even neural performance (Sale et al., 2015). Rehabilitation robotics are therefore commonly used to assess patients' movement abilities as well as to train and promote the recovery process (Huang and Krakauer 2009).

Motor adaptation is a motor learning paradigm (i.e. procedural learning; Krebs 1998) easily implemented with rehabilitation robotics via the application of specific external perturbations that alter the natural movement and prevent a good performance. The change in the interacting environment causes an initial decrease of performance (i.e. increased error) followed by an almost-exponential trial-by-trial return to baseline performance (Huberdeau et al., 2015). Motor adaptation also induces the so called "after-effects" (i.e. over-compensating movements towards the opposite directions of the previously applied perturbation) once the environment returns to its natural state, as subjects expect it to be still altered and do not foresee the actual change. Studies have designed experiments so that the external disturbance could generate after-effects that resembled the natural behaviour prior to an injury (Patton et al., 2006). Motor adaptation protocols could therefore induce reactive changes in subjects/patients impaired behaviour that, with consolidation over time and support from physiotherapy, can lead towards the re-learning of the lost functions and recovery. However, robot-mediated rehabilitation paradigms are still not very common: there is in fact the need for a clearer understanding of the neural correlates induced by such practices and the verification of induced actual performance improvements as well as neuronal changes (i.e. neuroplasticity) (Turner 2013). Moreover, given the complexity of neural injuries and the demand for personalized recovery programs, a lot still needs to be done to identify reliable fingerprints of changes in performance and motor control (at both central/neural and peripheral/muscular level) that could then be used to guide the definition of patient-specific rehabilitation needs and future work (Huang and Krakauer, 2009).



In this study a complete experimental setup able to monitor a robot-mediated force field motor adaptation process was implemented and an exhaustive investigation of its behavioural and neurophysiological aspects was carried out. In this chapter, attention was given to the experimental implementation and to the kinematic and muscular characteristics of the induced adaptation process, whereas subsequent chapters will focus on the neural correlates of adaptation. The designed experiments exploited a commonly used motor adaptation paradigm in studies on both healthy and impaired (Krebs et al., 1998; De Xivry et al., 2013; Trewartha et al., 2014). The healthy population sample recruited for the study was expected to adapt to the applied force-field as previously shown in the literature, showing temporary after-effects once the disturbance was removed, and eventually returning to a baseline performance (Shadmehr and Mussa-Ivaldi, 1994; Brashers-Krug et al., 1996; Milner and Franklin, 2005). Protocol-related muscular correlates of adaptation were also investigated, following the assumption that muscle activations are task specific (Throughman and Shadmehr, 1999), and more advanced analyses that could benefit the design of future rehabilitation protocols for the neurologically impaired were pursued (see Appendix IV; Pizzamiglio et al., 2017).

## **4.2 Materials and methods**

### **4.2.1 Ethical approval**

Twenty-three right-handed healthy young adults [age mean ( $\pm$  standard deviation; SD) = 28 ( $\pm$  7), 6 male/17 female, range = 21 – 41 y.o.] with no previous history of neurological, neuromuscular and/or orthopaedic disease(s) (see Appendix II), agreed to participate in this study by giving written informed consent (see Appendix III). The study was approved by the University of East London Ethics Committee (UREC\_1415\_29, see Appendix I) and all experiments were conducted in accordance with the Declaration of Helsinki. Data of five subjects were discarded because of problems during data acquisitions (2 female) and profound movement artefacts (3 female), leaving a total of eighteen subjects [age mean = 28 ( $\pm$  8), 6 male/12 female, range = 21 – 41 y.o.]. Sample size was determined by referring to the previous work done in the lab (Hunter et al., 2009: N = 14, 7 male) and to the relevant literature for this work (e.g. Milner and Franklin, 2005, N = 8, 6 male; Naranjo et al., 2007: N = 9, 6 male; Dipietro et al., 2014: N = 7, gender not specified; Demandt et al., 2012: N = 8, 4 male; Ball et al., 2008: N = 8, 4 male; Formaggio et al., 2013: N = 8, 3 male; Storti et al., 2015: N = 10, 7 male).

#### 4.2.2 Robot equipment

A MIT-Manus robotic manipulandum (IMT2, InMotion Technologies, Cambridge, MA, USA) was employed in this study. The robot has 2 degrees of freedom (x,y, see Figure 4-1 (A)) and allows free movements of the upper limbs within the horizontal plane only (i.e. no vertical movements). The robotic arm has two joints whose angular positions (eventually transformed into Cartesian coordinates) are recorded at a sampling frequency of 200 Hz by 16-bit position encoders placed inside the robot motors. The workstation includes a vertical screen connected to the robot via the control PC on which the task environment is displayed. The end-effector is represented by a cursor of 0.5 cm of diameter whose position on the screen reflects the position of the joystick in the horizontal plane, serving as online feedback for subjects (see Figure 4-2 (A)). The manipulandum can operate in three different modalities:

- NON-ASSISTIVE MODE (motors-off): when performing a task in this mode, subjects are required to voluntarily move the upper-limb whose kinematics is monitored by the position and force encoders;
- ASSISTIVE MODE (motors-on): this is the mode commonly used in neuro-rehabilitation as the robot facilitates the movement or passively moves the upper-limb when subjects find it difficult; assistance can be provided at different levels;
- RESISTIVE MODE (motors-on): in this mode the robot can apply different types of resisting forces (i.e. against the movement) that subjects need to counteract.

In this study the robot was set in the resistive mode to allow subjects to work against a resisting force and adapt. A velocity dependent force field was employed as commonly used in literature (Milner and Franklin, 2005; Thoroughman and Shadmehr, 1999) according to the formula:

$$\begin{bmatrix} F_x \\ F_y \end{bmatrix} = B \cdot \begin{bmatrix} \cos \theta & -\sin \theta \\ \sin \theta & \cos \theta \end{bmatrix} \cdot \begin{bmatrix} V_x \\ V_y \end{bmatrix}$$

Equation 4-1: Robot-mediated velocity dependent force field.

where  $F_x$  and  $F_y$  are the resisting force produced in the respective directions,  $V_x$  and  $V_y$  are the end-effector velocities in the x- and y-direction respectively,  $B$  is the intensity of the force field generated by the robot motors, and the angle  $\theta$  is equal to  $-90^\circ$  or  $90^\circ$  respectively for clockwise or counter-clockwise practice (Brashers-Krug et al., 1996; Bays et al., 2005). It is possible to change values of force field according to the study protocol designed. This robot equipment has been extensively employed in studies of motor adaptation and motor learning (Krebs et al., 1998; Krebs et al., 2001; Finley et al.,

2009) as well as in clinical research for stroke rehabilitation (Dipietro et al., 2007; Zollo et al., 2011; Hunter et al., 2009; Mazzoleni et al., 2014; Ang et al., 2015).

#### **4.2.3 The reaching task**

The subject sat in a comfortable chair directly in front of the robot and was asked to grasp the end-effector handle with the right hand. Careful measurements were taken in order to position the arm in a semi-pronated fashion at 70° of shoulder extension and 120° of elbow flexion. Subject's forearm was placed in a custom-made thermoplastic trough fixed to the joystick, which supported the reaching arm against gravity. Once sat, the subject's height was adjusted in order to have the shoulders at the same level of the end effector. Safety belt straps were fastened to the subject's chest in order to restrict any trunk movements that could have helped the reaching task. The vertical screen situated at eye-level gave online feedback regarding the position of the displaced robot handle. Subjects were instructed to perform a straight reaching movement (15 cm of linear trajectory length) from a central starting point to a peripheral target (1 cm diameter on the screen both) within a period of time of 1.0 – 1.2 seconds. Subjects were told to move only at the appearance of a visual cue defined by the peripheral target cursor turning from black to red (see Figure 4-2 (A)). On the vertical screen a feedback on the time of each performed movement was given to the subject, specifically: "GOOD", if the movement was carried out within the requested time period ( $1.0 \text{ sec} < \text{time} < 1.2 \text{ sec}$ ); "SLOW", if the movement slower than requested ( $1.2 \text{ sec} > \text{time}$ ); "FAST", if the movement was faster than requested ( $\text{time} < 1.0 \text{ sec}$ ). After each movement, subjects were told to relax the arm as the robot repositioned it to the central point: this passive arm return was undertaken to not to interfere with the motor adaptation process. Moreover, subjects were asked to avoid any big movements and try to blink their eyes in the period between two consecutive reaching movements in order to minimize the number of artefacts within the physiological recordings.

#### **4.2.4 The experimental protocol**

One trial was composed by a voluntary reaching movement towards the peripheral target and the passive return to the central position. The protocol designed for the current experiments is in line with standard paradigms found in literature (Della-Maggiore et al., 2015 for a review). As shown in Figure 4-2 (B), the experimental protocol was based on 3 conditions, each composed of 96 reaching trials for a total of 288 trials per experiment. The first condition (Familiarization, 96 trials total) was performed in a null force-field and was intended to enable naive subjects to become familiar with the reaching task.

During the second condition (Motor Adaptation, 96 trials total), the robot applied a velocity-dependent force-field in the counter-clockwise direction of 25 Ns/m absolute intensity, perpendicular to the trajectory of the joystick. The third condition (Wash Out, 96 trials total) was performed in a null force-field once again. Movements along the 135° direction and disturbed reaches with a counter-clockwise force-field perturbation were scheduled in order to mostly activate upper limb extensors (Throughman and Shadmehr, 1999; Pizzamiglio et al., 2017). Longer periods of rest at the beginning of the experiment, between each condition and at the end of the experiment were provided, during which 6 minutes of resting-state electroencephalography (EEG) was recorded. In these periods subjects sat with the arm supported by the thermoplastic trough, thus biomechanical properties are comparable with the task-related data. Specifically, resting-state EEG was recorded for 3 minutes with eyes-open (EO, looking at the centre of the screen) and 3 minutes with eyes-closed (EC): EO and EC sequence was randomized across subjects, but maintained consistent within the same subject. Resting-state data have been the focus of a separate work and results are presented elsewhere (see Appendix IV; Faiman, Pizzamiglio and Turner 2017, in preparation).

#### **4.2.5 Recording techniques**

Figure 4-1 represents the experimental setup workflow diagram and actual laboratory environment and instrumentations employed. The robot PC was connected to the vertical screen in front of the subject and displayed the selected protocol. Kinematic measures of each reaching trial were recorded by the encoders embedded within the two joystick joints as previously mentioned (see paragraph 4.1.2). The end-effector position (m) and velocity (m/s) within the horizontal plane (i.e. along the x and y axes), as well as the forces exerted by the subject in the 3D space (i.e. along the x, y and z axes; N) were sampled at 200 Hz and stored on the computer PC for offline analyses. Electromyographic activity (EMG;  $\mu$ V) was recorded from the right arm Anterior Deltoid (AD), Posterior Deltoid (PD), Biceps Brachii (BB), Triceps Brachii (TB), Extensor Carpi Radialis (ECR), Flexor Carpi Radialis (FCR), and Brachioradialis (BR) muscles (see Figure 4-3). Additional recordings were obtained from the left arm Biceps Brachii to control for potential activation of the contralateral arm as aid to counteract the resisting force field during motor adaptation. Bipolar superficial electrodes with a fixed 1.5 cm inter-electrode distance were positioned on each muscle according to the belly-belly montage following the SENIAM guidelines (Hermens et al., 2000). Data were sampled at 1 kHz and digitized via a 14-bit analog-to-digital converter (DataLog W4X8 EMG system, Biometrics Ltd, Newport, UK, see Figure 4-1 (C)). Brain activity (EEG;  $\mu$ V) was recorded through a 64-channel Waveguard

cap and amplified by a TMSi Ref-Ext amplifier (ANT Neuro, Enschede, Netherlands, see Figure 4-1 (C)), digitized at 1024 Hz and band-pass filtered from 0.1 to 500 Hz. During the recording, data were referenced to the Fz electrode and impedances were kept below 5 k $\Omega$ . To synchronize the three simultaneously recorded signals, the robot PC sent a TTL pulse at each visual cue (i.e. trigger at the beginning of a trial, time = 0 sec) via a double - split BNC cable to the EMG and the EEG recording systems (see Figure 4-1 (A) thin red lines).

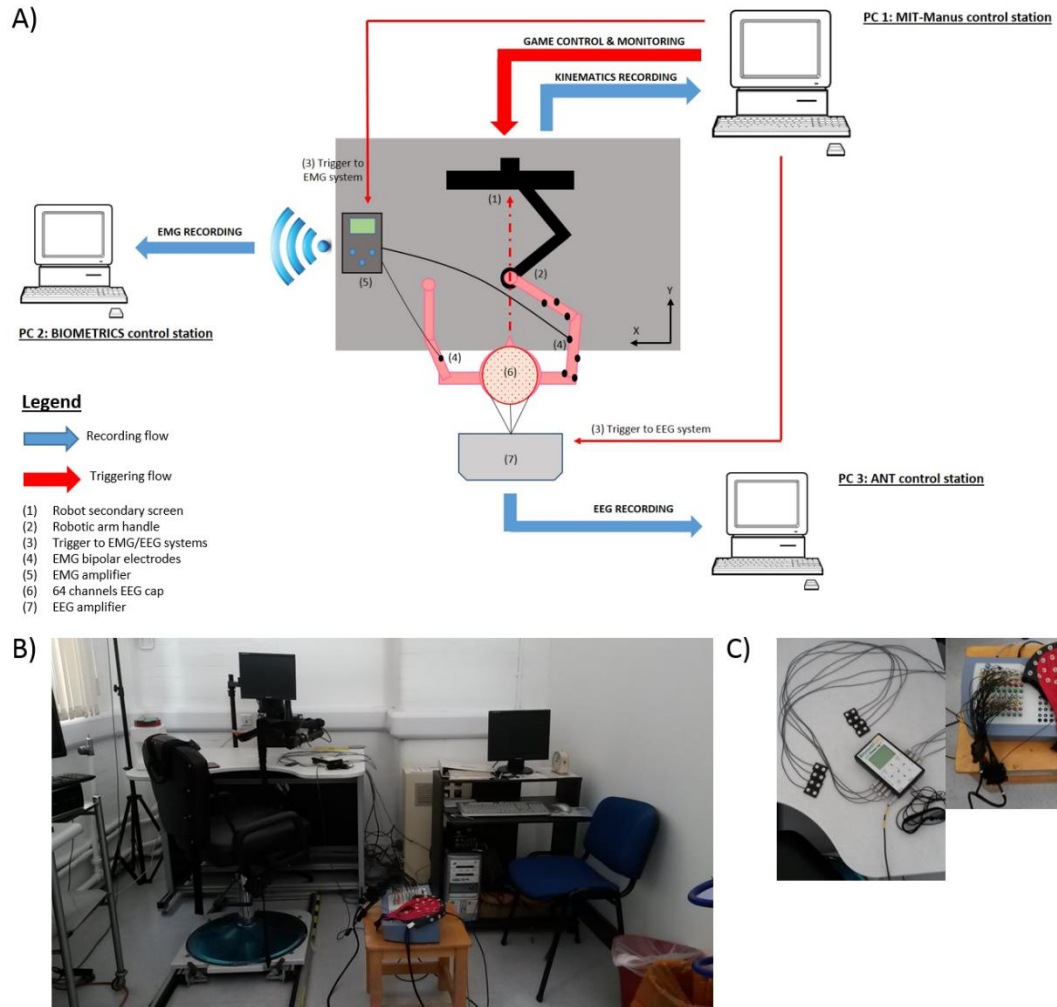


Figure 4-1: Experimental setup workflow and single components.

**A)** Experimental setup diagram. The subject sat in front of the robot workstation and grasped with the right hand the joystick end-effector (2). The task environment is reproduced on a vertical screen (1) connected to the robot PC and online feedback on the position of the end-effector during each movement is here displayed. The robot has 2 degrees of freedom (x,y) and allows movements only within the horizontal plane. Kinematics of each movement is recorded by the encoders embedded in each joint of the robotic joystick and saved in .csv files on the PC. At the beginning of each trial (i.e. reach movement), a TTL pulse (3) is sent via a double-split BNC cable to the EMG (5) and the EEG (6) recording systems. These triggers allow to have all the recordings synchronized for offline accurate analyses. Muscle activity of 8 upper-limb muscles (4) is recorded via surface electrodes and sent via Bluetooth to a second PC for saving. 64-channel EEG (6, 7) is recorded and saved on a third PC. **B)** Experimental setup picture. **C)** EMG DataLog (left) and EEG 64-channel Waveguard cap with TMSi Refa-Ext amplifier (right) employed for this study.

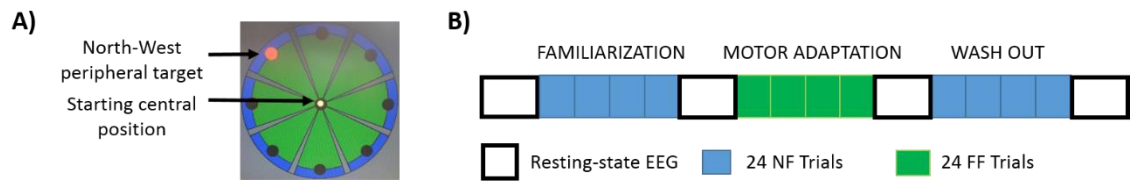


Figure 4-2: Experimental task environment and protocol.

**A)** Subjects were asked to reach towards a peripheral target ( $135^\circ/\text{NW}$  direction) projected on a vertical display in front of them as soon as the cue (i.e. target turning red) appeared. Online feedback (yellow cursor) was given to subjects throughout the whole trial (i.e. reach) duration. **B)** The experimental protocol was based on 3 conditions, each of 96 trials: Familiarization (no force-field), Motor Adaptation (force-field) and Wash Out (no force-field). A period of rest was given between conditions in order to avoid muscles fatigue. 6 minutes resting-state EEG (3 minutes eyes open, 3 minutes eyes closed randomized across subjects) was recorded at the very beginning, between each condition and at the very end of the experiment.

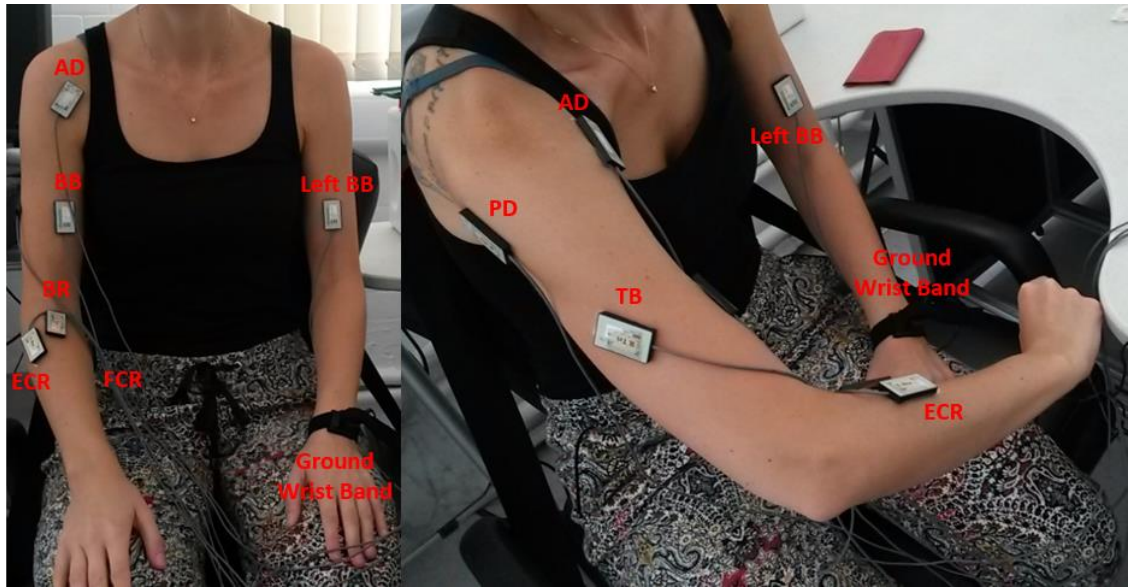


Figure 4-3: Upper limb muscles.

The activity of 8 upper limb muscles was monitored during the experiments, specifically the right arm Anterior Deltoid (AD), Posterior Deltoid (PD), Biceps Brachii (BB), Triceps Brachii (TB), Extensor Carpi Radialis (ECR), Flexor Carpi Radialis (FCR) and Brachioradialis (BR), and the left arm Biceps Brachii (left BB) as control. The ground electrode was positioned on the left arm wrist Ulna bone peripheral extremity.



#### **4.2.6 Data analyses**

Offline data analyses were run in MatLab 2013b (The MathWorks, Inc.). In this chapter a detail description of kinematic and EMG analyses methodologies is covered, but for more details on EEG data analyses techniques see chapter 5, paragraph 5.2.2.

##### **Reaching kinematics**

Kinematic data from the robot were interpolated to match the EMG sampling rate of 1 kHz. The starting of a reaching movement was defined as Movement Onset and calculated as the time point at which speed exceeded the threshold of 0.03 m/s as previously used in literature (Hunter et al., 2009); the end of a reaching movement was defined as Movement Offset and calculated as the time point after Movement Onset at which movement velocity lowered below the threshold of 0.03 m/s. Trial-by-trial trajectory error was assessed through the measure of Summed Error (m), defined as the absolute cumulative perpendicular distance between the actual trajectory and the ideal straight line connecting the central starting point with the peripheral target. Summed Error values are always positive as, by definition, it does not take into account path directionality and is a measure of error for the whole duration of the reaching movement, from Movement Onset to Movement Offset (Osu et al., 2003; Hunter et al., 2009). The measure of Peak Velocity (m/s) described the trial-by-trial maxima of compound velocity (i.e. the overall velocity magnitude across both x and y axes), whereas the measure of Peak Force (N) represented the trial-by-trial maxima of compound force (i.e. the overall force magnitude across both x and y axes).

##### **EMG pre-processing and basic muscle activity**

Trial-by-trial raw EMG data were first de-trended, high-pass filtered at 45 Hz (Butterworth, order 3), notch filtered (50Hz) and rectified. The high-pass filter choice was based on the commonly accepted knowledge that EMG signals may be contaminated by intrinsic low-frequency noise sources (De Luca et al., 2010) and ensures that all the possible noise and movement artefacts are excluded from the signal. Each muscle activity was normalized to the maximum value registered in that muscle across the whole experimental recording (i.e. activation ratio, %) in order to minimize variability across subjects due to possible variation in electrode-skin impedances. After pre-processing of the data, maximum EMG activation (Peak EMG;  $\mu\text{V}$ ) and latency (Peak EMG latency relative to movement onset; ms) were firstly calculated for each trial within a time period ranging from Movement Onset and Movement Offset. Secondary advanced analyses of muscles co-activation in both the time (measures of Wasted Contraction; Huang and

Ahmed, 2014) and in the frequency domain (measures of Intermuscular Coherence, Grosse and Brown, 2002) have been performed to investigate muscular correlates of robot-mediated motor adaptation. Results are reported elsewhere (see Appendix IV; Pizzamiglio et al., 2017; Pizzamiglio et al., 2017).

#### **4.2.7 Statistics**

Statistical analyses were performed with SPSS 23 (IBM). All measures of motor adaptation were assessed trial-by-trial for each subject and then averaged for 16 trials across each condition (i.e. 6 blocks per condition) and across subjects ( $N = 18$ ). Statistical analysis of motor adaptation measures then focused on differences between 8 blocks of major interest: block 6 (Familiarization trials 81-96), block 7 (Motor Adaptation trials 1-16), block 8 (Motor Adaptation trials 17-32), block 9 (Motor Adaptation trials 33-48), block 10 (Motor Adaptation trials 49-64), block 11 (Motor Adaptation trials 65-80), block 12 (Motor Adaptation trials 81-96) and block 18 (Wash Out trials 81-96). Statistical analyses were run through SPSS 23 (IBM) and MatLab 2013b. Averaged block data were first tested for normality with the Kolmogorov-Smirnoff test. The vast majority of data were normally distributed thus parametric tests were performed. For each measure, one way repeated measures analysis of variance with factor “block” (repeated measures ANOVA; 8 blocks) was performed in order to highlight the presence of any variance across blocks. For each kinematic measure, peak force or basic muscle activity measures, paired-sample T-tests with Bonferroni correction for multiple comparisons were used to define differences between block 6 (familiarization) and blocks 7-12 during adaptation and at the end of washout (block 18). Significance level was set at  $\alpha = 0.05$ , thus paired-samples T-tests were considered statistically significant if  $p < 0.0071$  (according to Bonferroni correction:  $0.05/7$ , with number of repeated tests = 7).

### **4.3 Results**

Figure 4-4 shows an exemplary single-subject motor adaptation process. Blue lines represent the ideal straight line connecting the central starting point with the peripheral target positioned at  $135^\circ$ , whereas black lines represent single-trial actual trajectories performed by the subject. During the Familiarization condition, the subject familiarized with the reaching task and the setup: here no resisting force field was applied by the robot motors, and indeed the single-trial trajectories have only a small deviation from the ideal straight-blue line. During the Motor Adaptation condition, when the robot applied a counter-clockwise resisting force field, bigger deviations towards the left-hand side can be seen: in the very first trials the arm is markedly pulled away from the straight line;

however, a trial-by-trial reduction of movement error can be seen, with trajectories getting closer to the ideal straight-blue line. The reduction of movement error is representative of a successful adaptation process. In the Wash Out condition the robot again applied no resisting force to the movements: moderate deviations towards the opposite force-field direction can be seen in the very first trials (i.e. over-compensation), with a quick trial-by-trial reduction of actual movement deviation from the ideal straight-blue line. Altogether, the above describes a successful motor adaptation followed by a de-adaptation process.

#### **4.3.1 Kinematics measures of motor adaptation**

Each measure is represented by an averaged trial-by-trial trend (Figure 4-5) and block-by-block mean ( $\pm$  standard deviation) across the three conditions (Table 4-1). Repeated measures ANOVA values were significant for all the kinematic and kinetic measures (all  $F > 8.11$ ; all  $p < 0.001$ ). According to paired-samples T-tests, all motor adaptation blocks were significantly higher than block 6 for summed error (all  $p < 0.001$ ), peak velocity (all  $p < 0.007$ ) and peak force (all  $p < 0.001$ ). Movement Onset and Movement Offset only decreased in block 7 compared to block 6 (corrected paired T-test:  $p = 0.005$ ). All measures returned to baseline after wash out as demonstrated by the comparison between block 6 and block 18.

#### **4.3.2 Basic muscle activity measures of motor adaptation**

Some muscles demonstrated increases in peak EMG amplitude across conditions on a block-by-block basis whilst others had more complex patterns of activity change (Figure 4-6). Table 4-2 presents the results of the 1 way repeated measures ANOVA for Peak EMG amplitude, whereby ECR ( $F = 34.52$ ,  $p < 0.001$ ), PD ( $F = 31.13$ ,  $p < 0.001$ ), BB ( $F = 24.73$ ,  $p < 0.001$ ), BR ( $F = 19.46$ ,  $p < 0.001$ ), FCR ( $F = 16.33$ ,  $p < 0.001$ ), TB ( $F = 12.06$ ,  $p < 0.001$ ) and AD ( $F = 7.72$ ,  $p = 0.001$ ) were statistically different across blocks, but left BB was not ( $F = 1.92$ ,  $p > 0.05$ ). Paired-sample T-tests demonstrated that PD peak EMG amplitude ( $p < 0.001$ ) increased during early adaptation compared to baseline and did not show any further change during later adaptation and wash out. BB and ECR peak EMG amplitude increased in the early adaptation period with respect to baseline (all  $p < 0.007$ ) and did not show any further change during later adaptation; ECR peak EMG amplitude during late wash out significantly decreased with respect to baseline ( $p < 0.007$ ). FCR, TB and BR peak EMG amplitude increased during early adaptation ( $p < 0.007$ ), but then progressively decreased towards baseline again by block 7 for FCR, block 8 for TB and block 11 for BR. On the contrary, a sustained decrease of EMG peak

activity was recorded in the AD muscle during early adaptation (all  $p < 0.007$ ) with no further changes during later adaptation but a return to normal activity by end of wash out. The increase of peak EMG amplitude during adaptation was accompanied by changes of Peak EMG amplitude latency in all the muscles except for AD and left BB ( $F < 3.15$ ,  $p > 0.018$  with no significant paired samples t-Tests). BR ( $F = 21.43$ ,  $p < 0.001$ ), TB ( $F = 12.67$ ,  $p < 0.001$ ), and ECR ( $F = 12.04$ ,  $p < 0.001$ ) peak EMG amplitude latency shortened in early adaptation with no further changes during later adaptation (all  $p < 0.001$ ). PD ( $F = 11.10$ ,  $p < 0.001$ ) peak EMG amplitude latency shortened in early adaptation from block 8 with no further changes during later adaptation (all  $p < 0.007$ ), whereas BB ( $F = 5.05$ ,  $p = 0.004$ ) peak EMG amplitude latency significantly shortened only during later adaptation (block 12  $p < 0.007$ ). On the contrary, a delayed peak EMG amplitude latency was reported for muscle FCR ( $F = 9.14$ ,  $p = 0.001$ ) during early adaptation which then progressively decreased towards baseline again by block 9 (first three blocks  $p < 0.007$ ).

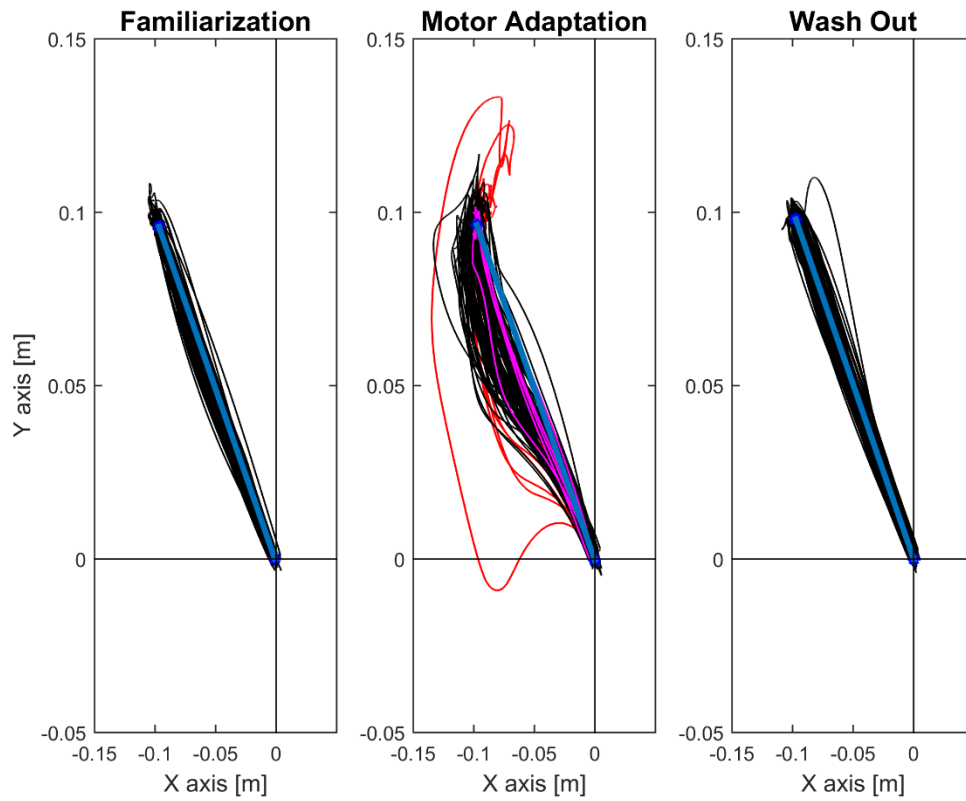


Figure 4-4: The motor adaptation process.

Single-subject trial-by-trial actual trajectories (i.e. thin black lines) performed in the three experimental conditions of Familiarization, Motor Adaptation and Wash Out. Thick blue lines represent the ideal straight line connecting the central starting point ( $x = 0$ ;  $y = 0$ ) with the peripheral target. During Familiarization trajectories are very close to the ideal straight line as no disturbance is applied; when the counter-clockwise force is on (Motor Adaptation), deviations from the ideal straight line are pronounced towards the left-hand side in the beginning (red trajectories = first 5 trials) and slowly reduced trial-by-trial (pink trajectories = last 5 trials); during Wash Out, no external force field is applied and a first overcompensation towards the force field opposite direction (i.e. right-hand side) is then followed by trajectories with very small deviations from the straight line.

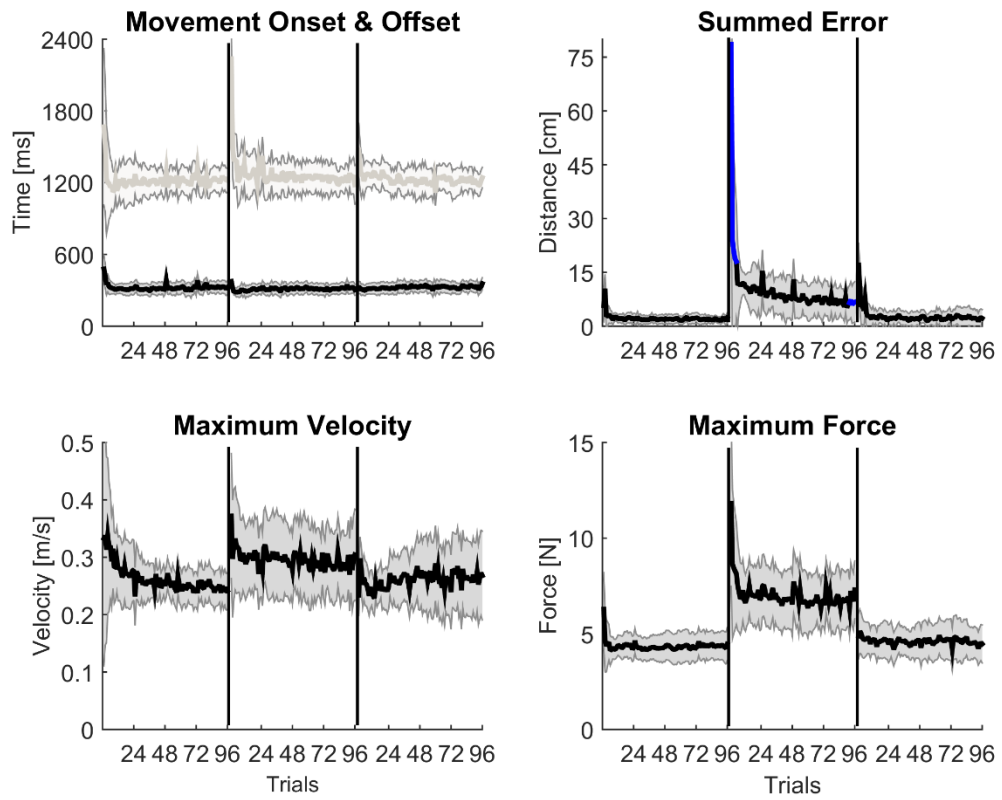


Figure 4-5: Trial-by-trial kinematic measures of motor adaptation.

A trial-by-trial population average ( $N = 18$ ) profile with shaded standard deviation for each kinematic measure across the three experimental conditions. Top Left: Movement Onset (black line) and Offset (grey line) are almost constant across the whole experiment. Bottom Left/Right: Peak Velocity and Planar Force show a typical constant increase of values during the motor adaptation condition. Top Right: movement Summed Error slowly decreases during the adaptation condition, with blue lines representing first and late 5 trials averages during adaptation to highlight changes in error.

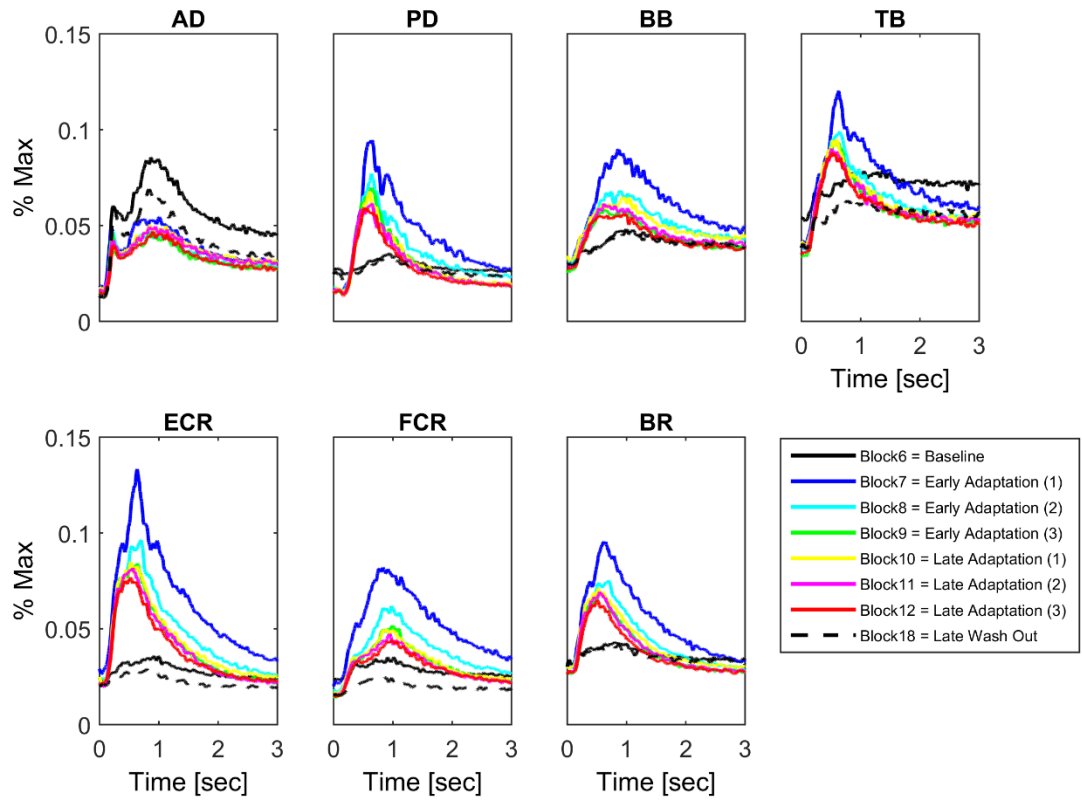


Figure 4-6: Block-by-block muscle specific activation profiles.

Block-by-block average ( $N = 18$ ) activation profiles (from visual cue,  $t = 0$ , to 3 seconds afterwards) have been colour coded to describe the evolution of muscle specific activation over the adaptation period. Represented muscles are Anterior Deltoid (AD), Posterior Deltoid (PD), Biceps Brachii (BB), Triceps Brachii (TB), Extensor Carpi Radialis (ECR), Flexor Carpi Radialis (FCR) and Brachioradialis (BR). A clear pattern of adaptation to the counter-clockwise force field can be seen in the Triceps Brachii and extensor Carpi Radialis muscles.

Table 4-1: Kinematics results.

Block-by-block (n = 8) of the five kinematic measures (Movement Onset, Movement Offset, Peak Velocity, Peak Planar Force, Summed Error). Repeated measures ANOVA F and p-values are reported in the last two columns on the right, and statistically significant paired samples t-Tests with Bonferroni correction for multiple comparisons are highlighted with \* (N = 18, Block 6 vs. Blocki with I = 7, ..12, 18; 7 comparisons and corrected p < 0.0071).

	Null Field	Force Field	Force Field	Force Field	Force Field	Force Field	Force Field	Null Field	Anova	
	Block 6	Block 7	Block 8	Block 9	Block 10	Block 11	Block12	Block18	F	p
<b>Movement Onset (ms)</b>	325 ( $\pm$ 32)	296 ( $\pm$ 27) *	311 ( $\pm$ 26)	312 ( $\pm$ 31)	317 ( $\pm$ 31)	309 ( $\pm$ 25)	318 ( $\pm$ 24)	332 ( $\pm$ 24)	8.60	0.001
<b>Movement Offset (ms)</b>	1219 ( $\pm$ 28)	1329 ( $\pm$ 88) *	1267 ( $\pm$ 77)	1245 ( $\pm$ 50)	1241 ( $\pm$ 56)	1239 ( $\pm$ 36)	1225 ( $\pm$ 45)	1216 ( $\pm$ 49)	9.91	0.001
<b>Peak Velocity (m/s)</b>	0.25 ( $\pm$ 0.02)	0.3 ( $\pm$ 0.06) *	0.3 ( $\pm$ 0.06) *	0.3 ( $\pm$ 0.06) *	0.3 ( $\pm$ 0.06) *	0.3 ( $\pm$ 0.05) *	0.3 ( $\pm$ 0.06) *	0.26 ( $\pm$ 0.06)	8.11	0.001
<b>Peak Planar Force (N)</b>	4.4 ( $\pm$ 0.7)	7.4 ( $\pm$ 1.7) *	7.1 ( $\pm$ 1.3) *	6.8 ( $\pm$ 1.3) *	6.9 ( $\pm$ 1.5) *	6.8 ( $\pm$ 1.2) *	6.9 ( $\pm$ 1.3) *	4.5 ( $\pm$ 0.8)	40.66	0.001
<b>Summed Error (m)</b>	1.9 ( $\pm$ 0.5)	14.9 ( $\pm$ 5.7) *	9.9 ( $\pm$ 4.1) *	8.3 ( $\pm$ 3.9) *	7.6 ( $\pm$ 4) *	7.1 ( $\pm$ 3.4) *	6.7 ( $\pm$ 3.1) *	2.3 ( $\pm$ 2.4)	50.64	0.001



Table 4-2: EMG results.

Block-by-block (n = 8) of two EMG measures (Peak EMG, Peak EMG Latency relative to Movement Onset) for all muscles (Anterior Deltoid (AD), Posterior Deltoid (PD), Biceps Brachii (BB), Triceps Brachii (TB), Extensor Carpi Radialis (ECR), Flexor Carpi Radialis (FCR), Brachioradialis (BR) and left Biceps Brachii (left BB)). Repeated measures ANOVA F and p-values are reported in the last two columns on the right, and statistically significant paired samples t-Tests with Bonferroni correction for multiple comparisons are highlighted with \* (N = 18, Block 6 vs. Blocki with I = 7, ..12, 18; 7 comparisons and corrected p < 0.0071).

	Null Field	Force Field	Force Field	Force Field	Force Field	Force Field	Force Field	Null Field	Anova	
	Block 6	Block 7	Block 8	Block 9	Block 10	Block 11	Block12	Block18	F	p
<b>Peak EMG (%)</b>										
AD	0.45 (± 0.15)	0.33 (± 0.17) *	0.28 (± 0.15) *	0.27 (± 0.16) *	0.29 (± 0.17) *	0.29 (± 0.15) *	0.27 (± 0.13) *	0.36 (± 0.17) *	7.72	0.001
PD	0.17 (± 0.06)	0.53 (± 0.12) *	0.42 (± 0.18) *	0.39 (± 0.16) *	0.36 (± 0.16) *	0.65 (± 0.17) *	0.33 (± 0.15) *	0.17 (± 0.09) *	31.13	0.001
BB	0.22 (± 0.07)	0.50 (± 0.11) *	0.41 (± 0.11) *	0.36 (± 0.12) *	0.36 (± 0.12) *	0.36 (± 0.11) *	0.32 (± 0.11) *	0.23 (± 0.13)	24.73	0.001
TB	0.40 (± 0.12)	0.58 (± 0.13) *	0.48 (± 0.16) *	0.47 (± 0.15)	0.46 (± 0.15)	0.44 (± 0.14)	0.44 (± 0.15)	0.33 (± 0.19)	12.06	0.001
ECR	0.21 (± 0.14)	0.60 (± 0.16) *	0.49 (± 0.18) *	0.45 (± 0.16) *	0.44 (± 0.16) *	0.42 (± 0.16) *	0.4 (± 0.16) *	0.17 (± 0.15) *	34.52	0.001
FCR	0.23 (± 0.17)	0.47 (± 0.14) *	0.36 (± 0.13)	0.31 (± 0.14)	0.29 (± 0.11)	0.28 (± 0.10)	0.28 (± 0.12)	0.15 (± 0.11)	16.33	0.001
BR	0.22 (± 0.10)	0.49 (± 0.12) *	0.38 (± 0.13) *	0.34 (± 0.11) *	0.35 (± 0.13) *	0.34 (± 0.13) *	0.32 (± 0.13)	0.21 (± 0.15)	19.46	0.001
Left BB	0.07 (± 0.03)	0.14 (± 0.19)	0.10 (± 0.06)	0.09 (± 0.05)	0.09 (± 0.05)	0.08 (± 0.05)	0.08 (± 0.05)	0.07 (± 0.04)	1.92	N.S.
<b>Peak EMG Time – Mov. Onset (ms)</b>										
AD	575 (± 83)	526 (± 149)	495 (± 152)	504 (± 165)	508 (± 161)	509 (± 155)	497 (± 169)	532 (± 108)	1.76	N.S.
PD	524 (± 90.4)	483 (± 102)	416 (± 95) *	382 (± 72) *	400 (± 113) *	376 (± 102) *	357 (± 92) *	519 (± 114)	11.10	0.001
BB	584 (± 92)	580 (± 177)	540 (± 136)	474 (± 135)	463 (± 158)	485 (± 123)	460 (± 113) *	537 (± 98)	5.05	0.004
TB	556 (± 115)	442 (± 116) *	431 (± 115) *	356 (± 95) *	363 (± 88) *	393 (± 73) *	365 (± 105) *	537 (± 150)	12.67	0.001
ECR	454 (± 89)	365 (± 67) *	326 (± 115) *	304 (± 74) *	287 (± 99) *	304 (± 101) *	265 (± 102) *	424 (± 145)	12.04	0.001
FCR	478 (± 122)	670 (± 147) *	622 (± 119) *	606 (± 126) *	540 (± 138)	548 (± 167)	553 (± 144)	449 (± 113)	9.14	0.001
BR	490 (± 68)	383 (± 100) *	341 (± 82) *	303 (± 82) *	314 (± 97) *	305 (± 87) *	292 (± 79) *	480 (± 100)	21.43	0.001
Left BB	460 (± 66)	534 (± 113)	470 (± 85)	446 (± 90)	444 (± 82)	428 (± 120)	442 (± 87)	465 (± 80)	3.15	0.018

## **4.4 Discussions**

### **4.4.1 Novel findings**

A typical motor adaptation paradigm was here described through evidence of kinematics and multiple muscle activity: an extended number of upper-limb muscles was studied and a detailed description of muscular correlates of motor adaptation was offered. Previous investigations have focused on upper-arm and trunk muscles during adaptation to robot-mediated force fields (Osu et al., 2003; Franklin et al., 2003; Milner and Franklin, 2005). However, in this study the trunk of the subject was constrained by seatbelts, thus it was opted to investigate if and how forelimb muscles could instead play a role in the adaptation process. Indeed, a typical and successful robot-mediated velocity-dependent force field motor adaptation process (Huang and Krakauer, 2009) was here reported, described by standard kinematics measures, and in parallel supported by specific patterns of upper-limb muscle activation.

### **4.4.2 The motor adaptation process**

#### **Kinematics and behaviour**

Subjects performed a controlled reaching task within the horizontal plane both in a null force field and in a velocity-dependent force field environment. First, subjects completely familiarized with the setup and the task as errors of deviation of the actual movement from the ideal straight lines reached very small values (Summed Error =  $1.9 (\pm 0.5)$  ms in block 7). Subsequently, a counter-clockwise velocity dependent force field disrupted the natural movement causing big deviations from the ideal straight line. Trial-by-trial, the initial big deviations were slowly replaced by smaller errors according to a nearly-exponential trend as previously reported in literature (Huberdau et al., 2015). The removal of the force-field showed strong after-effects as subjects over-compensated in the direction opposite to the previous-applied force field in the very first trials of wash out. However, adaptation decay quickly evolved during the wash out condition as subjects performed good reaching movement with little error already after few trials. Our results are in line with the assumption that motor adaptation is a reaction to specific changes in the environment with which the subject is interacting, consisting of a gradual reduction of performance error and a return to baseline performance (Shadmehr and Wise, 2005; Huang and Krakauer, 2009). The designed task had a higher level of complexity than those employed in previous work as a high force-field intensity was programmed (25 Ns/m) and the movement direction was fixed at  $135^\circ$  (i.e. North-West). Other studies have successfully employed higher level of resisting force (Focke et al., 2013),

demonstrating that standard motor adaptation features could be extended to more complex study designs. Moreover, the choice of the north-west direction was dictated by previous literature investigation according to which different levels of difficulty could be obtained by reaching towards different directions (Schawobsky et al., 2007), with the chosen direction as one of the most difficult to follow through a motor adaptation paradigm. Despite the planned difficulty, subjects showed a typical adapting curve even within less than 100 trials. The stronger force (with respect to that produced during a natural reaching) constantly exerted during the adaptation condition is symbolic of an active compensatory action generated by the subjects. Higher-velocity profiles were also observed throughout the whole adaptation process: subjects were required to reach out towards the peripheral target always between 1-1.2 seconds, therefore it is reasonable that a higher speed was employed to smoothly move within the requested time range. The disturbance of reaching trajectory by a velocity-dependent force field has been extensively studied in literature (Shadmehr and Mussa-Ivaldi, 1994; Brashers-Krug et al., 1996; Krebs et al., 1998; Bays et al., 2005; Milner and Franklin, 2005; Hunter et al., 2009; Focke et al., 2013; Yeo et al., 2015). The typical trial-by-trial exponential decay of movement error has also been subject to many different theoretical models (Smith et al., 2006; Lonini et al., 2009; Wei and Körding 2010). Moreover, the over-compensating after-effect here observed has been extensively reported in literature (Huang and Krakauer, 2009): subjects persisted in the adapted state as if the environment was still altered. This effect has been pointed out as very important during rehabilitation after neural injuries as one could adjust the training environment so that after effects resembled natural behaviour (Patton et al., 2006). Moreover, it is symbolic of an anticipatory elaboration of the expected state of the environment from the subjects, validating the hypothesis of the creation of an internal neural model during adaptation (Milner and Franklin, 2005; Lonini et al., 2009).

### **Muscle activations**

In the current study previous findings were successfully replicated and novel evidences on specific muscle activation patterns supporting the adaptation process were presented. Indeed, previous studies have demonstrated how different muscles contribute to the motor adaptation process (Osu et al., 2003; Franklin et al., 2003; Milner and Franklin, 2005; Darainy and Ostry, 2008; Huang and Ahmed, 2014). In this study however, forearm muscles were also included in the investigation and shown to play an active role during reaching adaptation. Muscle activities increased significantly with respect to a normal

reach and remained higher throughout the whole adaptation duration in those muscles mostly required to compensate for the counter-clockwise force-field applied, which is Posterior Deltoid, Triceps Brachii, Biceps Brachii and Extensor Carpi Radialis (Table 4-2, Figure 4-6). In parallel, some muscles also anticipated the time of maximum activity during adaptation as likely mostly involved in the compensation process, specifically Triceps Brachii, Extensor Carpi Radialis and Brachioradialis (Table 4-2). Resisting a counter-clockwise force field during reaching thus engages mostly upper-limb extensors with the exception of the Biceps Brachii, which is likely involved to support the other muscles during adaptation (Pizzamiglio et al., 2017). Forearm muscles were also involved in the opposition to the external perturbation, especially the ECR which is not directly involved in the movement of shoulder and elbow joints (since it mostly promotes wrist extension) but is more likely stabilizing the lower arm. Of note, despite being always higher than during a natural reaching, the maximum EMG values of all muscles decreased block-by-block during adaptation, in line with theories of mechanisms of early and late stages of adaptation (Milner and Franklin, 2005). Indeed, initial reactions to an external perturbation are orchestrated by feedback drives and reflexes implying strong muscles activities and co-contraction profiles, whereas feedforward models take over control at later stages of adaptation and optimize the behaviour by programming the activation of only the necessary muscles for the necessary amount in order to save metabolic cost (Huang and Ahmed, 2014; Pizzamiglio et al., 2017). Of note, trunk movements were kept minimal by using seatbelts, whereas activity of the contralateral arm was monitored throughout the whole experiment duration. No differences in the activity of the Biceps Brachii muscle of the left arm were reported: this is symbolic of no contraction of the contralateral arm as leverage to counteract the applied force field. The lack of sustained activity in the left arm paves the path for reliable future investigations of the neural correlates of motor adaptation. Indeed, the bilateral activation of the upper-limbs would have induced bilateral complex neural patterns, thus the electrophysiological features of the motor adaptation process per se would have been difficult to disentangle. Subsequent analyses (see chapters 5 and 6) will focus on the neural aspects of simple reaching and of reaching in the robot-mediated force-field environment.

#### **4.4.3 Further insights into muscular correlates for rehabilitation**

More thorough investigations of motor adaptation co-contraction muscle patterns were also performed in separate settings (see Appendix IV; Pizzamiglio et al., 2017) pursuing theories claiming that muscles activities are task specific (Feldman 1998; Throughman and Shadmehr, 1999; Milner and Franklin, 2005). Subjects were asked to adapt to either

the counter-clockwise either to a clockwise robot-mediated force-field (of the same intensity, i.e. 25 Nm/s) and the respective muscle activations and muscle-pairs co-contractions patterns were compared. These analyses demonstrated that muscular activity is indeed related to the resisting force applied by the robot, specifically to the direction of the velocity-dependent force-field (Pizzamiglio et al., 2017). For the right arm, pairs including the flexors muscles were co-contracted earlier in the clockwise condition, whereas pairs always including one of the extensor muscles were co-contracted earlier in the counter-clockwise condition. It therefore appears that during robot-mediated motor adaptation, the force-field direction can modulate muscle activation and co-contraction profiles. It has been previously shown that, in early stages of motor adaptation, an elevated muscle co-contraction level is engaged in different populations (Huang & Ahmed, 2014; Thoroughman & Shadmehr, 1999). Despite the considerable metabolic cost, this is still a valuable strategy employed in order to improve performance and reduce movement error (Huang & Ahmed, 2014; Oscari et al., 2016). In neurological populations however, muscle co-contraction is often considered a pathological factor. In stroke patients for example, high levels of antagonist muscle co-contraction is considered as an expression of impaired stiffness of the joints (Hammond et al., 1988). How the pathological co-contraction level might influence the level of motor impairment in neurological populations is still under debate (Busse et al., 2006; Chae et al., 2002; Gowland et al., 1992). Recent studies have proposed the use of muscle coupling as a marker during neurofeedback training in neurological populations (Wright et al., 2014). Targeting the normalization of muscle co-contraction patterns seems in fact a valuable rehabilitation target given the easy to follow EMG-based feedback patterns. Relying on simple indicators of activity, such as muscle co-contraction levels in different adaptation settings (i.e., clockwise vs. counter-clockwise protocols), could be a valuable strategy to promote recovery during neurorehabilitative interventions. Previous studies demonstrated that some patients require restoring lost muscle couplings, whereas others would need the attenuation of excessive muscle couplings (Cheung et al., 2012). Relevant individualised therapeutic targets and precise therapeutic programs could be designed, for example by modifying the direction of movement or force field to induce specific co-contraction patterns. It remains to be established how an intervention inducing muscle co-contraction changes in an impaired population would affect the upper-limb function per se: further research including neuropathological populations is needed to eventually establish a recommended strategy for individual practice.

#### **4.4.4 Limitations**

The number of subjects recruited in this investigation is in line with studies found in literature. Given the high repeatability of adaptation behaviour across different subjects we considered the recruited sample meaningful for the study purpose. However, future studies should perform a priori sample size analyses with respect to the hypothesised results in order to more consistently determine the minimum number of subjects needed. Even though subjects exponentially adapted to the applied counter-clockwise force field, a complete adaptation did not happen as group-level error in the last trials was still significantly different from the baseline (see Table 4-1). The choice of employing 96 trials in total for each condition was a trade-off between accomplishing adaptation and avoiding fatigue and exhaustion. Future studies should provide more trials, at least during the adaptation condition, in order to accomplish a full adaptation. Moreover, recent investigations have shown that complex setups (e.g. movement of the arm in the 3D space, no forearm support against gravity, etc.) could undermine the translation of standard adaptation features (Focke et al., 2013). Indeed, an over controlled experimental setup prevents the observation of real natural behaviours: it is possible that either the adaptation process could manifest itself differently, either other not-yet-considered factors could play a role in the process. This has repercussions on the translation of rehabilitation into daily-life activity performance: it has been reported that neurologically impaired patients undergoing a passive/active rehabilitation might overcome impairments through rehabilitation but not fully recover functionality (Huang and Krakauer, 2009). Future studies should investigate more complex experimental setup and natural setting to disentangle the concepts of impairments and functional recovery and identify how to optimize recovery of natural behaviours after neurological injuries. As per our investigation, the employment of a simple setup with movements constrained in the horizontal plane resembles typical rehabilitation paradigms currently performed in hospitals with hemiparetic subjects (Turner 2013). Our goal was indeed to investigate a typical rehabilitation protocol and provide further support and evidence of the adaptation process that could be then implemented in clinical rehabilitation practice.

## **5      Sensor-level neural correlates of robot-mediated motor adaptation during reaching with the upper-limb**

### **5.1    Introduction**

Healthy individuals perform upper-limb reaching naturally, “not thinking about it”, however it is a complex movement that requires the activation of different body parts (brain, muscles, joints) as per instructions of an accurate plan quickly scheduled by the Central Nervous System (CNS). For example, reaching for a box on a shelf requires the definition of both kinematics and dynamics instructions: the former describes the best trajectory, velocity and joint torques necessary to achieve the goal; the latter defines the required forces to shift or lift the box, thus also involves muscle activations. The CNS accomplishes all of this by solving complex problems with numerous variables and choosing the plan that minimizes energy and efforts (Shadmehr and Wise, 2005). The best solution to this complex problem is computed in the order of milliseconds by recruiting specific areas both in parallel and in sequence, each one of them apt to a given function within the pipeline. It has been previously hypothesised and demonstrated that the reaching movement activates a frontal-parietal network called the “dorsal-visual stream” (Grafton et al., 1996; Battaglia-Mayer et al., 2003), which recruits parietal, premotor, motor and frontal areas. The introduction of a velocity-dependent force-field that disturbs the reaching movement induces movement deviations (errors) from the ideal straight planned trajectory followed by augmented co-contraction between the upper-limb muscles (Pizzamiglio et al., 2017). The initial large error and high co-contraction are slowly reduced over time, trial-by-trial, with practice, thanks to feedback and feedforward adapting processes and internal models developing within the CNS (Milner and Franklin, 2005). Studies employing techniques with high spatial resolution, such as fMRI and PET, have previously demonstrated that different phases of motor adaptation and motor learning recruit specific brain areas (Della Maggiore and McIntosh, 2005). At early stages of adaptation a cortical-striatal loop is involved (Krebs et al., 1998), whereby the frontal cortex plays a major role as temporary storage of sensorimotor information for imminent use (Shadmehr and Holcomb, 1997). As adaptation takes over and performance improves, a different, cortico-cerebellar loop enters the game (Krebs et al., 1998), in which the parietal cortex as well as the cerebellum act as long-term memory storages (Shadmehr and Holcomb, 1997). The passage from novice to skilled performer is therefore conveyed by a switch from cortico-striatal to cortico-cerebellar control of the performed motor action and practice; the long-term learning of new skills, commonly believed to be obtained through the formation of new internal motor models proper of the new skill, is

then believed to happen within the parietal and motor cortices (Villalta et al., 2013; Della Maggiore et al., 2015). Despite the high spatial resolution of these techniques, these findings are limited in temporal resolution as only slow changes in brain blood-oxygen activity could be recorded.

More recent investigations have employed EEG for its high temporal resolution (ms) in order to study fast changes in brain dynamics during numerous motor tasks. Specific spatial activations can be identified through measures of 1) Event-Related Potentials (ERPs), automatic responses of the brain to external stimuli obtained as mathematical average of the recorded signal in the time domain, and 2) Event-Related Spectral Perturbations (ERSPs), induced dynamics in the EEG spectrum by the onset of external stimuli (Makeig, 1993) described as increases or decreases of the power of the EEG signal of a specific frequency at a given time point with respect to a pre-stimulus undisturbed period. Many studies have analysed the time-frequency EEG correlates of hand/finger movements (Babiloni et al., 2016; Pollok et al., 2014; Derosiére et al., 2014; Manganotti et al., 1998) as well as of arm reaching (Storti et al., 2015; Formaggio et al., 2013; Formaggio et al., 2014). Typical voluntary upper-limb movements are characterised by a decrease of the power in low frequency ranges ( $\alpha$  (8 – 12 Hz),  $\beta$  (15 – 30 Hz)), called Event-Related Desynchronization (ERD), during movement execution (or imagination) mainly in the primary sensorimotor cortex of the hemisphere contralateral to the moved limb, and most of the time also in the ipsilateral hemisphere (Van Wijk et al., 2012). The end of the voluntary movement is usually accompanied by an increase of  $\beta$  power called Event-Related Synchronization (ERS) previously demonstrated to be symbolic of trial-by-trial motor learning and internal models update (Tan et al., 2014; Torrecillos et al., 2015; Fry et al., 2016; Tan et al., 2016). Very little has been studied on the effects of force field motor adaptation with a focus on the movement preparation and execution period: given the potentiality of this type of motor adaptation protocol in robot-mediated rehabilitation for the neurologically impaired (Huang and Krakauer 2009; Turner 2013), it would be useful to investigate the effects this type of rehabilitation practice has on the human brain.

The neural correlates of the robot-mediated motor adaptation protocol described in chapter 4 were therefore investigated through different descriptors of the recorded EEG signals recorded at the scalp level. Our goal was to identify specific changes within the brain activations that could be related to 1) the applied external force field the subjects had to face, and/or 2) the development of adaptive or compensatory strategies optimizing



the behaviour and/or the performance. Positive findings could pave the path for more advanced investigations of the neural correlates of this motor adaptation protocol as well as be translated into real rehabilitation practice and used as potential fingerprint of a healthy behaviour for recovery.

## **5.2 Materials and methods**

### **5.2.1 Data collection and experimental protocol**

The raw EEG data were obtained in the experiments described in chapter 4. For details on subjects' recruitment, experimental setup and protocol, see chapter 4, paragraph 4.2.1 to 4.2.5.

### **5.2.2 Data analyses**

Data analyses were carried out with MatLab 2015b (The MathWorks, Inc.), with the support of EEGLab and FieldTrip open-source toolboxes for the analysis of EEG data (Delorme and Makeig, 2004; Oostenveld et al., 2010).

#### **EEG pre-processing**

EEG data are very sensitive to external (i.e. environmental) and internal (i.e. physiological) sources of artefacts, therefore the first step of the data analyses consists of cleaning the signals from spurious noise and removing those elements that could affect further analyses and lead towards biased results. A meticulous pre-processing pipeline for EEG data has been developed with EEGLab toolbox (Delorme and Makeig, 2004) following guidelines found in literature and customising it according to our specific protocol. First, for each subject and each condition separately, data were band-pass filtered between 0.5 Hz and 100 Hz (FIR filter, order automatically set by EEGLab), notch filtered at 50 Hz (FIR notch filter, order = 3302) to remove the power line noise, and again notch filtered at 25 Hz (FIR notch filter, order = 3302) to remove an electrical noise present within the laboratory setup. Data were then segmented into epochs of 3 seconds each from -1000 ms to 2000 ms with respect to each trigger (i.e. visual cue). From now on, the segmented data will be referred as *trials*. Visual inspection was performed on segmented data and served to identify 1) EEG channels affected by sustained noise throughout the whole experiment duration (i.e. bad channels), and 2) trials heavily corrupted by non-stereotypical artefacts (i.e. bad trials). Bad channels were marked and later on temporarily removed from the data, whereas bad trials were permanently deleted from the dataset. Subsequently, a period of 900 ms between -1000 ms and -100 ms before the visual cue in each trial was defined as *baseline*, which represents a period of reference for the task-related signal (i.e. data after the visual cue). For each channel in each trial,

baseline was removed from the task-related data, bad channels were temporarily removed, and data were re-referenced to a common average reference. Data were subsequently decomposed using Independent Component Analysis (ICA) with the extended Infomax algorithm as provided by EEGLab (Cardoso, 1997; Delorme et al., 2007). Spectral, spatial and temporal features of each Independent Component (IC) were inspected and those symbolic of stereotypical artefacts (e.g. electrical noise, blink, neck muscles, etc.) were removed from the data (see Figure 5-1 for examples). The remaining components were back-projected to the scalp channels and previously removed channels were eventually reconstructed from the cleaned dataset through interpolation of the neighbouring electrodes (method = 'spherical' as implemented in EEGLab, which uses superfast spherical interpolation) (Perrin et al., 1989; Ferree, 2000). Data were then re-referenced again to common average and one last visual inspection was performed to check the quality of the cleaned data and eventually remove still noisy trials. At the end of the pre-processing step, a total of 64 electrodes were available for each subject in each condition, even though the two mastoids channels were never considered in more advanced analyses.

### **Event-Related Potentials (ERPs)**

Event-Related Potentials (ERP) are the measured brain responses to specific sensory, cognitive or motor events (Luck, 2014) and are usually classified in Negative (N) or Positive (P) components (i.e. deflections). The timing of these responses is thought to provide a measure of the timing of the brain's communication or timing of information processing. Moreover, ERPs are well-known for their consistency to novel stimuli, which make them a reliable variable for analysis. ERPs were calculated for each subject, block and channel as simple mathematical averages across trials. This analysis aimed to investigate ERPs correlates of the natural reaching movement and demonstrate the presence/lack of significantly different neural responses to the reaching task between perturbed and unperturbed conditions. After visual inspection of the ERPs data and specific literature investigation component-specific time windows of interest were defined as follow: N/P100 (90-110 ms), N/P170 (160-190 ms) and N/P300 (280-360 ms) (Naranjo et al., 2007). It was hypothesised that early components (N/P100) wouldn't change across conditions because they are more related to the visual cue reaction (i.e. constant across conditions), but that later components associated to information processing (mainly N/P300) would show statistically significant changes between conditions. Considering only the cleaned trials remained after pre-processing, ERPs were evaluated for Late Familiarization (average of second half of left trials in *Familiarization*,

Late Fam = 42 ( $\pm$  2) trials), Early Motor Adaptation (average of first half of remaining trials in *Motor Adaptation*, Early MA = 42 ( $\pm$  2) trials), Late Motor Adaptation (average of second half of remaining trials in *Motor Adaptation*, Late MA = 42 ( $\pm$  2) trials), and Late Wash Out (average of second half of remaining trials in *Wash Out*, Late WO = 41 ( $\pm$  2) epochs). ERPs data were averaged across a higher number of trials in comparison to kinematics and EMG data (averaged in a 16-trials blocks) because of the higher variance of electroencephalographic data.

### **Event-Related Spectral Perturbations (ERSPs)**

Time-Frequency (TFr) analysis represents a decomposition of the EEG signal into amplitude and phase information for each frequency within the EEG (so-called “spectral decomposition”), and it describes changes of power in specific frequencies over time with respect to task events (in our case, a visual cue). In order to quantify the responses in the time-frequency domain, for each subject, separately for the three conditions, for each electrode (except for the mastoids), Event-Related Spectral Perturbation (ERSP) changes in the power spectrum in each trial were measured using Morlet wavelet decomposition (function *pop\_newtimef* in EEGLab) with the following parameters:

- High frequency: 80 Hz;
- Wavelet width at lowest frequency: 3 oscillation cycles;
- Wavelet width at highest frequency: 18 cycles;
- Hanning window size: 437 ms;
- Time steps: 10 ms.

Single-trial spectrograms were normalized by subtracting the mean baseline power spectrum, with baseline defined as a window of 900 ms from -1000 ms to -100 ms before the visual cue in each trial. Significant deviations in each task-related power spectrum were evaluated by applying a bootstrap statistical method based on a surrogate distribution randomly derived from the pre-stimulus baseline. Statistical significance level was set at  $p < 0.01$  and only significant values were considered in the analysis. This method (single-trial-based ERSP baseline correction method with bootstrap) has been shown to minimize contribution from artefactual data and to be robust to outliers, yielding more reliable results than standard baseline correction methods (Grandchamp and Delorme, 2011). Baseline correction in time-frequency analysis is crucial for distinguishing event-related contribution to the EEG power from background noise or non-related activities. Again, considering only the cleaned trials remained after pre-processing, ERSPs were averaged for each subject across trials for Late Familiarization

(average of second half of left trials in *Familiarization*, Late Fam = 42 ( $\pm$  2) trials), Early Motor Adaptation (average of first half of left trials in *Motor Adaptation*, Early MA = 42 ( $\pm$  2) trials), Late Motor Adaptation (average of second half of left trials in *Motor Adaptation*, Late MA = 42 ( $\pm$  2) trials), and Late Wash Out (average of second half of left trials in *Wash Out*, Late WO = 41 ( $\pm$  2) epochs) conditions. ERSPs data were also averaged across a higher number of trials in comparison to kinematics and EMG data (averaged in a 16-trials blocks) because of the higher variance of electroencephalographic data. As an example, Figure 5-2 shows a typical output of this method, here specifically applied to the Late Fam condition: the frequency range considered in the analyses was from 8.01 Hz to 80 Hz and the time range covered from -0.706 sec to 1.7 sec around each visual cue. Such ranges are the result of the algorithm optimization as implemented in EEGLab and allow us to observe changes in power spectrum over the full period of movement. This approach allows us to identify typical power changes during natural reaching (Late Fam) as the task-related data are statistically tested against a null-mean pre-stimulus baseline, during which the arm is still and the subject relaxed.

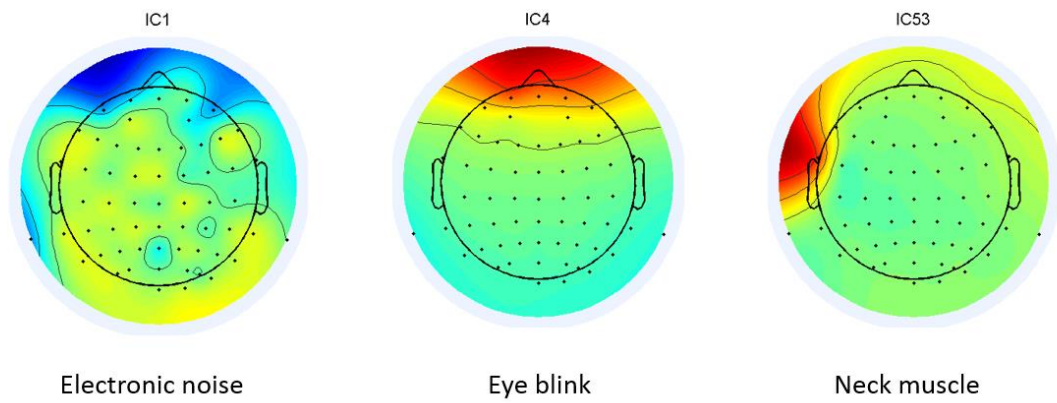


Figure 5-1: Stereotypical artefactual Independent Components topoplots.

These brain activations plots show the activity intensity (colours) and location from which typical artefactual components can be recognised. Electronic noise was caused by a 25 Hz interference due to lab setting and is represented by a scattered/dotted topographical representation with no specific dipole. Eye blinks are stereotyped by a strong frontal activation only. Neck muscles are represented by sharp strong activations at the edge of the head.

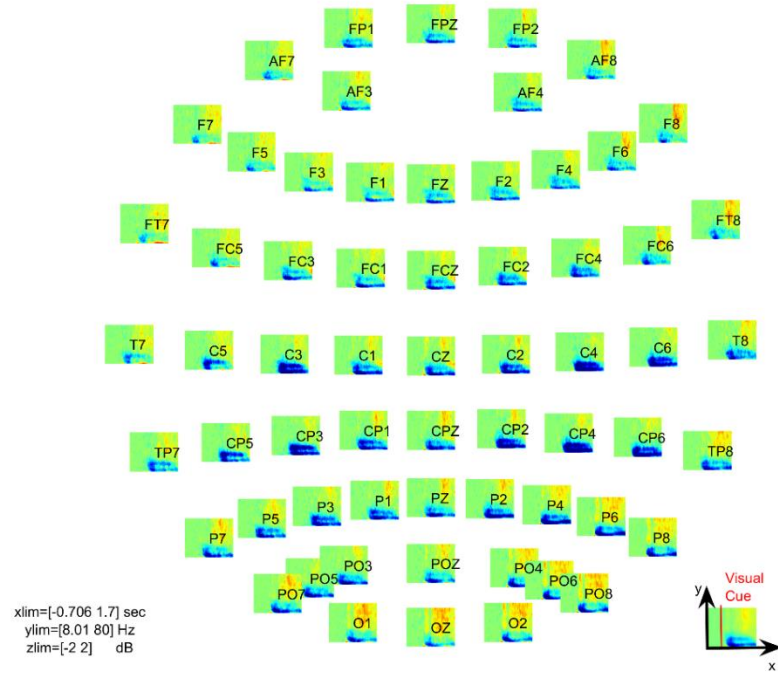


Figure 5-2: Group grand average whole-brain Event-Related Spectral Perturbation changes during natural undisturbed reaching.

62 channel time-frequency spectral power during Late Fam are represented according to the used Waveguard cap layout. Bottom right: plot legend for each channel. Bottom left: axes limits details (xlim = -0.706 – 1.7 sec; ylim = 8 – 80 Hz; zlim = -1.5 – 1.5 dB). Changes in the time-frequency domain are assessed through mean of statistical bootstrapping between baseline (900 ms before visual cue) and task-related data (whole period after visual cue). Significant decrease of power with respect to baseline is colour-coded with light-blue/blue. Significant increase of power with respect to baseline is colour-coded with yellow/red. Colour intensity is proportional to the value of ERSs in dB. Not-significant time-frequency data are green masked.

### 5.2.3 Statistics

#### ERPs

First, typical natural reaching ERPs components were investigated by comparing Late Fam vs. a zero-baseline (as previously reported in literature; Naranjo et al., 2007) and vs. the pre-familiarization resting-state with eyes open (as per similar subject and arm position and vision towards the centre of the screen). Secondly, differences of sensor-level ERPs across conditions (Late Fam vs. Early MA, Late MA and Late WO) were assessed. In both instances, non-parametric cluster based permutation tests as implemented in FieldTrip were employed to correct for multiple comparisons (i.e. electrodes, time points) (Maris and Oostenveld, 2007). In line with previous EEG studies (Negrini et al., 2017), to analyse sensor-level EEG data, multiple dependent sample t-Tests were applied on each channel separately for the three components of interest. In particular, a paired sample t-Test was conducted for each electrode at each time bin within the components specific time windows. T-values exceeding an a priori threshold of  $p < 0.01$  were clustered based on adjacent time bins and neighbouring electrodes. Cluster-level statistics were computed by taking the sum of the t-values within every cluster. The statistical comparisons were done with respect to the maximum values of summed t-values. By means of a permutation test (i.e. randomizing data across conditions and rerunning the statistical test 1500 times, Monte-Carlo approximation) a randomization distribution of the maximum of summed cluster t-values was obtained to evaluate the statistics of the actual data. Clusters in the original dataset were considered to be significant at an alpha level of ( $\alpha_{\text{cluster}}$ ) 5% if less than the 5% of the permutations ( $\alpha_{\text{cluster}} = 0.05$ ,  $\alpha = 0.025$  for 2-tailed tests,  $N = 1500$ ) used to construct the reference distribution yielded a maximum cluster-level statistic larger than the cluster-level value observed in the original data. As three different tests were carried out (Late Fam vs. Early MA, vs. Late MA and vs. Late WO), further correction for multiple comparison was run with Bonferroni method ( $p = 0.025/3 = 0.0083$  for two-tailed test). Between-condition contrasts were performed on all electrodes (total of 62 electrodes, except for the mastoids) due to exploratory nature of the investigation.

#### ERSPs

The same cluster-based permutation statistical approach previously used has been then employed also for the evaluation of ERSs changes across conditions (for a total of three comparisons as in paragraph 4.3.1). Multiple dependent sample t-Tests were applied on each channel separately for the four FOIs,  $\alpha$  (8 – 12 Hz),  $\beta$  (15 – 30 Hz), low  $\gamma$  (31 – 45 Hz) and high- $\gamma$  (46 – 80 Hz), and in five separated 300 ms – windows of interest from 0

sec (i.e. visual cue) to 1.5 sec afterwards (as a control, a 300 ms – window pre-stimulus was tested to confirm that no changes in the baseline occurred across conditions). In particular, a paired sample t-Test was conducted for each electrode at each time-frequency bin within the components specific time windows. T-values exceeding an a priori threshold of  $p < 0.05$  were clustered based on adjacent time-frequency bins and neighbouring electrodes. Cluster-level statistics were computed by taking the sum of the t-values within every cluster. The statistical comparisons were done with respect to the maximum values of summed t-values. By means of a permutation test (i.e. randomizing data across conditions and rerunning the statistical test 1500 times, Monte-Carlo approximation) a randomization distribution of the maximum of summed cluster t-values was obtained to evaluate the statistics of the actual data. Clusters in the original dataset were considered to be significant at an alpha level of ( $\alpha_{\text{cluster}}$ ) 5% if less than the 5% of the permutations ( $\alpha_{\text{cluster}} = 0.05$ ,  $\alpha = 0.025$  for 2-tailed tests,  $N = 1500$ ) used to construct the reference distribution yielded a maximum cluster-level statistic larger than the cluster-level value observed in the original data. Due to the lack of any “a priori” predictions about the location from where potential conditions effect could rise, and since fMRI/PET literature highlighted activity in several cortical and subcortical areas (Krebs et al., 1998), all the channels were simultaneously entered in the analysis (total of 62 electrodes, except for the mastoids). As three different tests were carried out (Late Fam vs. Early MA, vs. Late MA and vs. Late WO), further correction for multiple comparison was run with Bonferroni method ( $p = 0.025/3 = 0.0083$  for two-tailed test).

### 5.3 Results

#### 5.3.1 ERPs during natural undisturbed reaching

Figure 5-3 presents typical ERPs over time at each channel during undisturbed reaching (Late Fam), as well as topographical activations at each window of interest. For a clear understanding of the ERP time evolution within the trial period, a group-level average of undisturbed reaching movement velocity profile is also provided. In Figure 5-3 (A), highlighted electrodes (\*) represents the scalp location in which the detected EEG activity significantly differed from a dummy activation (i.e. zero activity). Specifically, significant activations were found in:

- 90-110 ms time window:

Positive Cluster = {F7, F3, FC5, FC1, FC2, T7, C3, CZ, AF7, F5, FC3, FCZ, C5, C1},  $p = 0.007$



Negative Cluster = {T8, CP6, P4, P8, POZ, O1, OZ, O2, C6, CP4, P2, P6, PO4, PO6, FT8, PO8},  $p = 0.008$

- 160-190 ms time window:

Positive Cluster = {FP1, FPZ, F7, F3, FC5, AF7, AF3, AF4, F5, F1, FC3, C5, FT7},  
 $p = 0.021$

- 280-360 ms time window:

Positive Cluster = {C4, CP5, CP2, CP6, P3, PZ, P4, P8, POZ, O2, CP4, P5, P1, P2, P6, PO5, PO3, PO4, PO6, PO8},  $p = 0.001$

Negative Cluster = {FPZ, FP2, F3, FZ, F4, F8, FC1, FC2, FC6, AF3, AF4, AF8, F1, F2, F6, FC3, FCZ, FT8},  $p = 0.001$

A positive cluster represents a statistically significant increase of activity in the first term of one comparison with respect to the second term. A negative cluster represents a statistically significant decrease of activity in the first term of one comparison with respect to the second term. From the above it can be said that, with respect to a zero-activity:

- There is a statistically significant positive deflection of activity in a left-medial pre-frontal-central cluster in a period of time between 90 ms and 100 ms after the visual cue (P100);
- There is a statistically significant negative deflection of activity in a right-medial temporal-parietal-occipital cluster in a period of time between 90 ms and 100 ms after the visual cue (N100);
- There is a statistically significant positive deflection of activity in a left-medial pre-frontal cluster in a period of time between 160 ms and 190 ms after the visual cue (P170);
- There is a statistically significant positive deflection of activity in a bilateral parietal-occipital cluster in a period of time between 280 ms and 360 ms after the visual cue (P300);
- There is a statistically significant negative deflection of activity in a bilateral pre-frontal cluster in a period of time between 280 ms and 360 ms after the visual cue (N300);

In Figure 5-3 (B), highlighted electrodes (\*) represents the scalp location in which the detected EEG activity significantly differed from the pre-familiarization resting-state with eyes open. Specifically, significant activations were found in:

- 90-110 ms time window:

Positive Cluster = {F7, FC5, FC1, FC2, T7, C3, CZ, AF7, F5, FC3, FCZ, C5, C1, FT7},  $p = 0.009$

- 160-190 ms time window:

Positive Cluster = {FP1, FPZ, F7, F3, FC5, AF7, AF3, F5, F1, FC3, FT7},  $p = 0.047$

- 280-360 ms time window:

Positive Cluster = {C4, CP5, CP2, CP6, P3, PZ, P4, P8, POZ, O2, CP4, P5, P1, P2, P6, PO5, PO3, PO4, PO6, PO8},  $p = 0.001$

Negative Cluster = {FPZ, FP2, F3, FZ, F4, F8, FC1, FC2, FC6, AF3, AF4, AF8, F1, F2, F6, FC3, FCZ, FT8},  $p = 0.001$

From the above it can be said that, in comparison to a pre-experimental resting-state with eyes-open condition:

- There is a statistically significant positive deflection of activity in a left-medial pre-frontal-central cluster in a period of time between 90 ms and 100 ms after the visual cue (P100);
- There is a statistically significant positive deflection of activity in a left-medial pre-frontal cluster in a period of time between 160 ms and 190 ms after the visual cue (P170);
- There is a statistically significant positive deflection of activity in a bilateral parietal-occipital cluster in a period of time between 280 ms and 360 ms after the visual cue (P300);
- There is a statistically significant negative deflection of activity in a bilateral pre-frontal cluster in a period of time between 280 ms and 360 ms after the visual cue (N300).

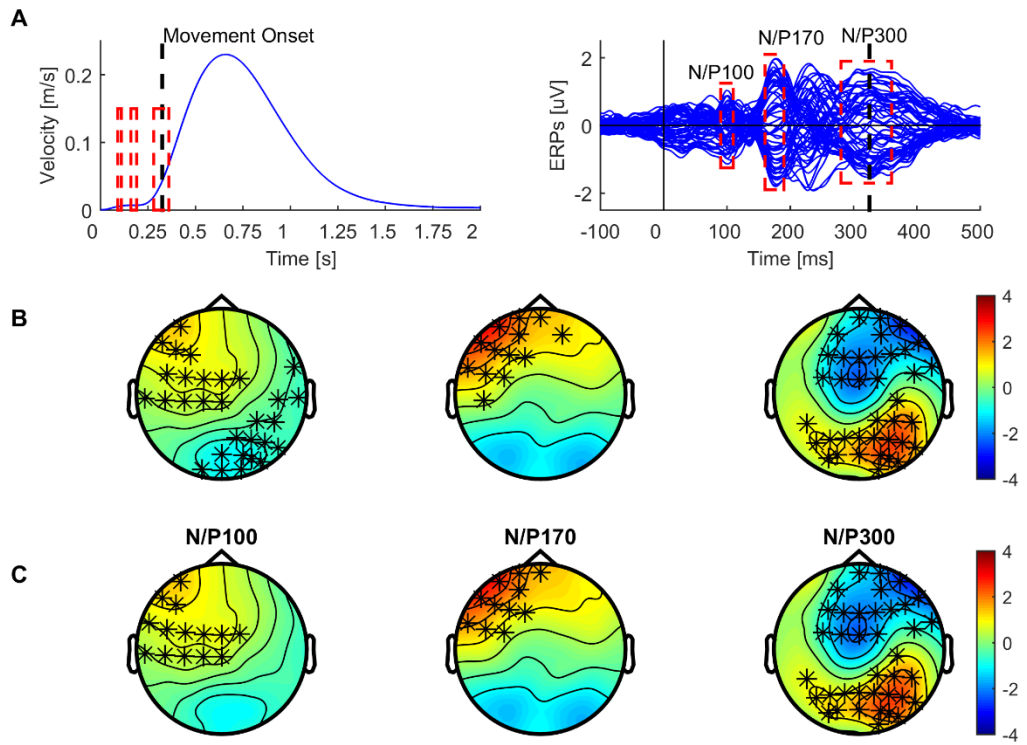


Figure 5-3: ERPs during natural reaching.

Group-level grandaverage of ERPs time evolution and topographical plots during Late Fam represent typical activations during undisturbed reaching movements. Three time-windows of interest have been identified according to literature: 90-110 ms (N/P100), 160-190 ms (N/P170) and 280-360 ms (N/P300), highlighted with the three dashed squares. As shown here, ERPs temporal evolutions take place before or straddling movement onset. A) Left: Group-level velocity profile average is reported for a better understanding of time of ERPs in comparison to time of movement. Right: 62 channels ERPs profiles are reported together with Movement Onset trace (vertical dashed black line). B) Significant activations with respect to a null distribution (as reported in previous literature). C) Significant activations with respect to pre-familiarization resting-state with eyes open (as nowadays common practice).

### 5.3.2 ERSPs during natural undisturbed reaching

Figure 5-2 showed statistically significant changes in spectral power during natural reaching (Late Fam) in comparison to the pre-stimulus baseline for each channel. Time-frequency representations are colour coded so that statistically significant decreases of power with respect to the baseline (Event-Related Desynchronization, ERD,  $p < 0.01$ ) are coded with cold colours (i.e. light-blue/blue), whereas statistically significant increases of power in comparison to the baseline (Event-Related Synchronization, ERS,  $p < 0.01$ ) are coded with warm colours (i.e. yellow/red). A significant ERD is visible at low frequency ( $\alpha$  and  $\beta$ ) after the visual cue and sustained for the whole trial duration. A significant ERS is visible at high frequencies (low and high  $\gamma$ ) later during the trial. Figure 5-4 shows the temporal evolution of the group-level grand average of ERSPs, averaged across trials within the Late Fam condition, during natural reaching in each FOI and in time windows of 300 ms from -0.3 sec to 1.5 sec around the visual cue. Baseline activity (-0.3 – 0 sec) is masked in green, symbolic of no significant activity in the pre-stimulus interval; significant changes of spectral power with respect to the baseline are visible from 0.3 sec after the visual cue, when a whole-brain-spread  $\alpha$  ERD appears and remains sustained throughout the whole trial duration;  $\beta$  ERD is also visible from this time point but mainly localized bilaterally over the sensorimotor areas. Ultimately, no specific changes in both low and high  $\gamma$  frequency bands are observed.

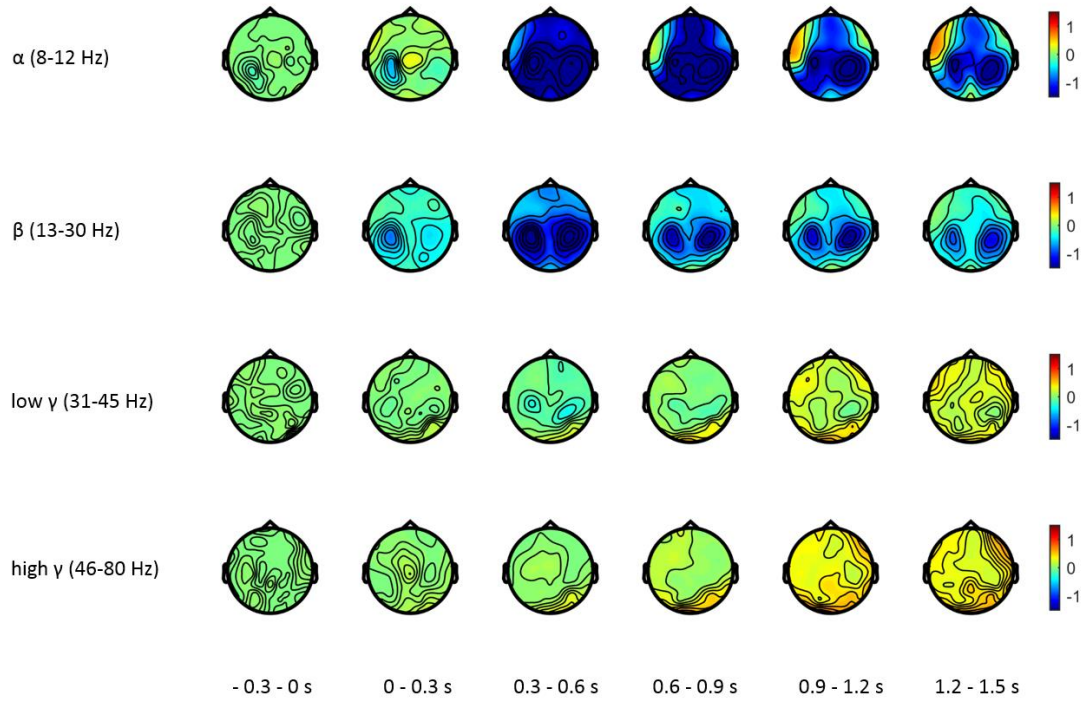


Figure 5-4: ERSPs during natural undisturbed reaching in each FOI.

ERSPs during Late Fam condition divided into windows of 300 ms each starting from -0.3 sec before visual cue ( $t = 0$  sec) till 1.5 sec after. No significant activity is detected before the visual cue, confirming the reliability of the baseline. By 0.3 sec after visual cue, a strong and persistent  $\alpha$  and  $\beta$  ERD (desynchronization) with respect to the baseline is visible mainly over the bilateral sensorimotor areas (colour-coded values are in dB).

### 5.3.3 ERPs changes during robot-mediated motor adaptation with respect to natural reaching

The analysis of the N/P100 and N/170 did not show any statistically significant difference between Late Fam and any subsequent condition (all  $p > 0.05$ ). The analysis of P/N300 reported significant differences when comparing Late Fam vs. Early and Late Fam vs. Late MA, but no differences between Late Fam and Late WO. Specifically, significant differences were found in:

- Early MA. vs. Late Fam N300:

Negative Cluster = {FZ, F4, FC1, FC2, FC6, C3, CZ, C4, CP2, AF4, F1, F2, F6, FC3, FCZ, FC4, C1, C2, C6, CPZ},  $p = 0.008$ ;

- Late MA vs. Late Fam N300:

Negative Cluster = {F3, FZ, F4, FC1, FC2, C3, CZ, C4, AF3, AF4, F1, F2, FC3, FCZ, FC4, C1, C2},  $p = 0.004$ .

Figure 5-5 shows the actual activations during each condition of interest and the topographical location of the statistical significant clusters. As also shown in the last row of Figure 5-5, from the above it can be observed that there is a significantly more negative deflection during both Early MA and Late MA in comparison to Late Fam in a bilateral frontal-central cluster in a period of time between 280 ms and 360 ms after the visual cue (N300).

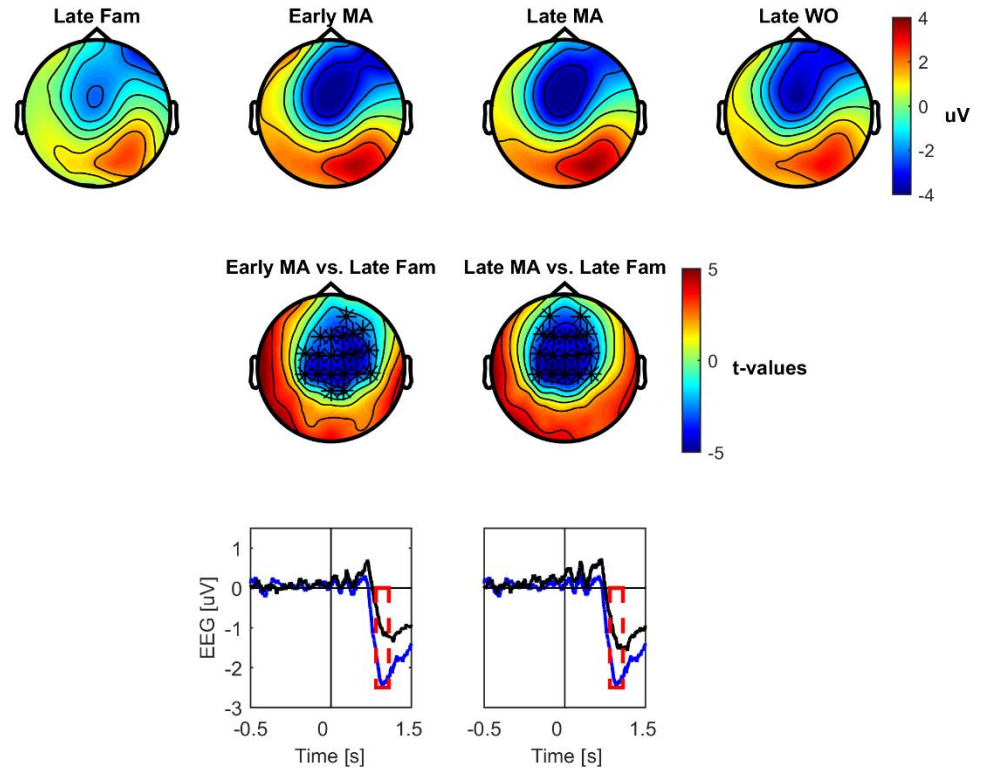


Figure 5-5: ERPs activations and statistical comparisons for the N300 component.

ERPs activations ( $\mu\text{V}$ ) in the four conditions of interest are represented in the first row. Statistical significance was obtained through non-parametric cluster-based permutation tests only when comparing Early MA vs. Late Fam and Late MA vs. Late Fam. Electrodes that passed the non-parametric test and the subsequent correction for multiple comparisons ( $p < 0.0083$ ) are highlighted with \* in the second row. Average activity of the significant electrodes per each comparison are showed in the third row: the black line always represents Late Fam ERP, the blue line represents the Early MA and Late MA respectively, and the red dashed square identifies the time-window of interest (280 – 360 ms after the visual cue,  $t = 0$  s).

### 5.3.4 ERSPs changes during robot-mediated motor adaptation with respect to natural reaching

Figure 5-6, 5-7 and 5-8 show the temporal evolution of the group-level grand-average of the ERSPs, averaged across trials within each condition (i.e. Early MA, Late MA, Late WO), over the duration of a reaching trial for each FOI. Electrodes whose spectral power significantly changed in each condition in comparison to Late Fam ( $p < 0.0083$  per Bonferroni correction), according to the employed non-parametric tests, are highlighted with \*. Specifically, significant differences were found in:

- Early MA vs. Late Fam  $\beta$ , 300 – 600 ms time window:

Positive Cluster = {T7, C3, CP5, CP1, P7, P3, C5, CP3, P5, PO5, TP7, PO7},  $p = 0.001$

- Late MA vs. Late Fam  $\beta$ , 300 – 600 ms time window:

Positive Cluster = {T7, C3, CP5, P7, P3, FC3, C5, CP3, P5, P1, PO5, PO3, TP7, PO7},  $p = 0.004$

From the above it can be said that a significantly higher  $\beta$  spectral power (i.e. less intense ERD) in Early MA and Late MA in comparison to Late Fam is detected over the contralateral (i.e. left) sensorimotor cortex in a period of time between 300 ms and 600 ms after the visual cue. Table 5-1 reports all the results from the cluster-based non-parametric tests: no significant changes were obtained in the frequency bands of  $\alpha$  and  $\gamma$ .

### 5.3.5 ERSPs during robot-mediated motor adaptation

As a control analysis, a cluster-based permutation test was also run to test whether any changes took place from early to late adaptation. Figure 5-9 shows the ERSPs difference between Late MA and Early MA (group-level grand-average) over the duration of a reaching trial for each FOI. The non-parametric statistics revealed a positive cluster ( $p = 0.021$ ) including electrodes bilaterally located over the frontal-premotor cortex ({FZ, FC1, FC2, AF4, F1, F2, FC3, FCZ}), resembling an increase of  $\beta$  spectral power (i.e. less intense ERD) in the late phase of adaptation in comparison to the early stages.



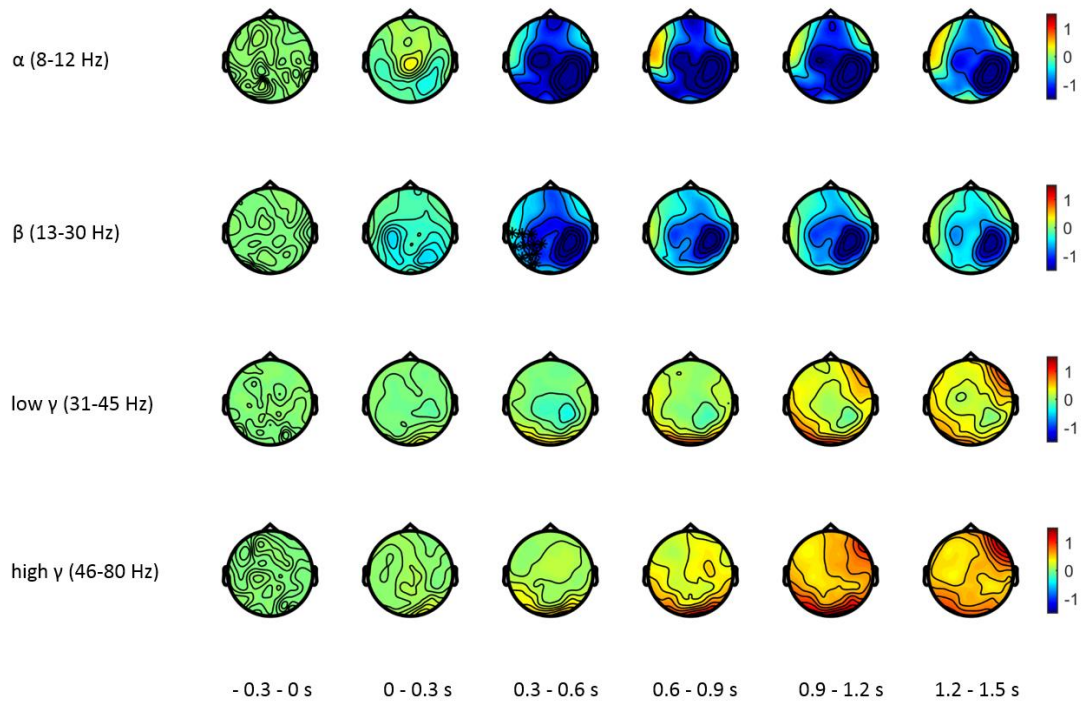


Figure 5-6: ERSPs changes during early adaptation to the robot-mediated force field in each FOI.

ERSPs during Early MA condition divided into windows of 300 ms each starting from -0.3 sec before visual cue ( $t = 0$  sec) till 1.5 sec after. No significant activity is detected before the visual cue, confirming the reliability of the baseline. Cluster-based permutation tests assessed the difference between Early MA vs. Late Fam in each window and FOI, and statistically significant electrodes are highlighted with \* ( $p < 0.0083$ ). In the time window 0.3 – 0.6 sec after visual cue, a significant increase of  $\beta$  power during Early MA with respect to Late Fam is detected over the left sensorimotor region (colour-coded values are in dB).

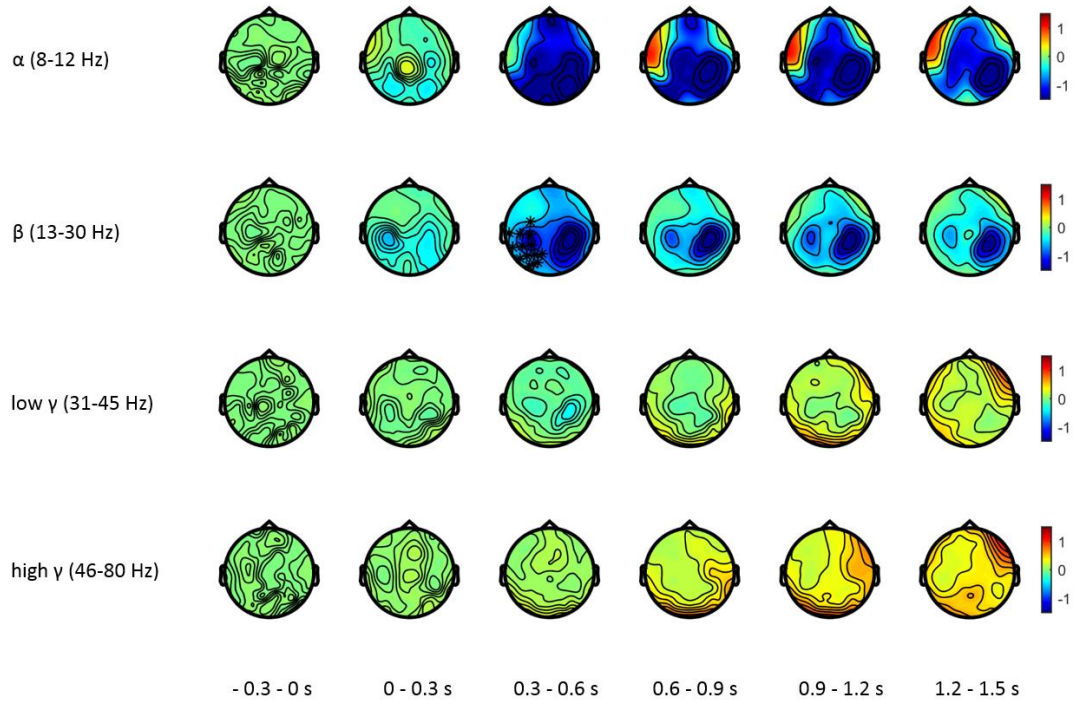


Figure 5-7: Event-Related Spectral Perturbations changes during late adaptation to the robot-mediated force field in each FOI.

ERSPs during Late MA condition divided into windows of 300 ms each starting from -0.3 sec before visual cue ( $t = 0$  sec) till 1.5 sec after. No significant activity is detected before the visual cue, confirming the reliability of the baseline. Cluster-based permutation tests assessed the difference between Late MA vs. Late Fam in each window and FOI, and statistically significant electrodes are highlighted with \* ( $p < 0.0083$ ). In the time window 0.3 – 0.6 sec after visual cue, a significant increase of  $\beta$  power during Late MA with respect to Late Fam is detected over the left sensorimotor region (colour-coded values are in dB).

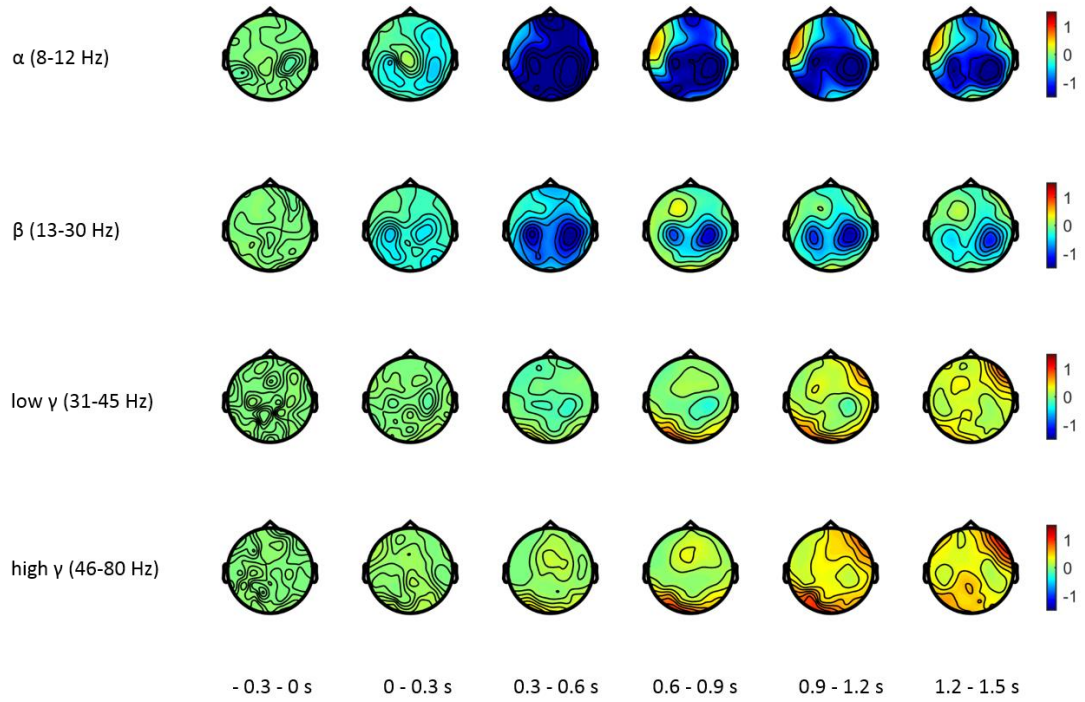


Figure 5-8: Event-Related Spectral Perturbations during late wash out of the adaptation effects in each FOI.

ERSPs during Late WO condition divided into windows of 300 ms each starting from -0.3 sec before visual cue ( $t = 0$  sec) till 1.5 sec after. No significant activity is detected before the visual cue, confirming the reliability of the baseline. Cluster-based permutation tests assessed the difference between Late WO vs. Late Fam in each window and FOI: no statistically significant electrodes were found (colour-coded values are in dB).

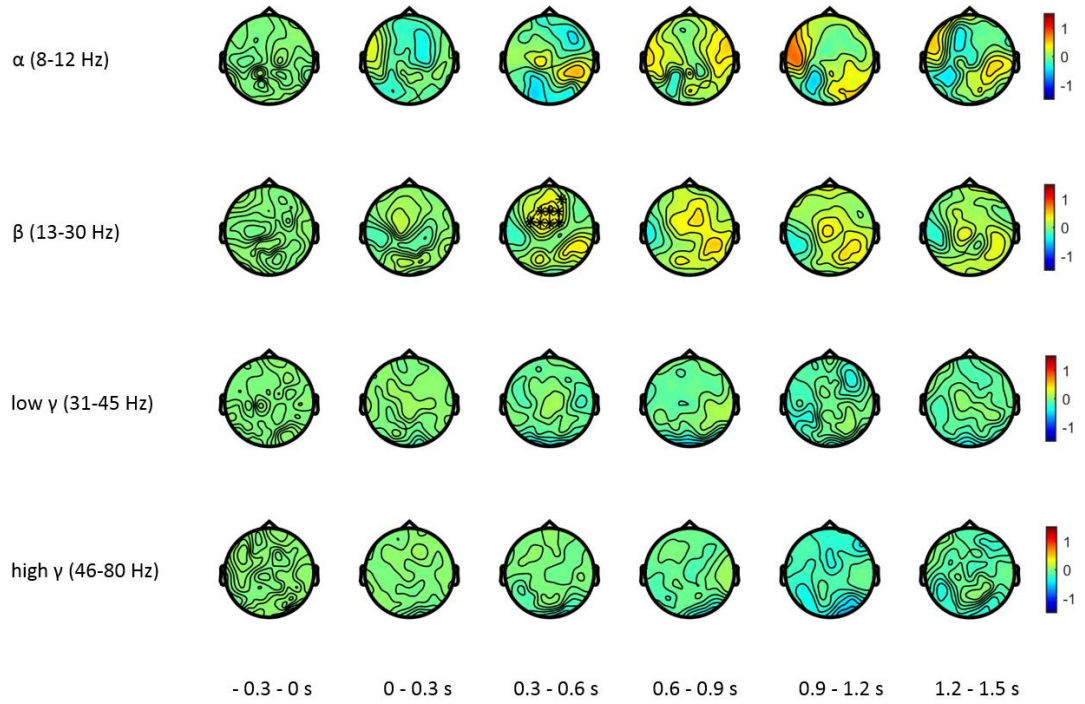


Figure 5-9: Event-Related Spectral Perturbations differences between late and early adaptation in each FOI.

Difference ERSPs between Late MA and Early MA conditions divided into windows of 300 ms each starting from -0.3 sec before visual cue (t = 0 sec) till 1.5 sec after. Cluster-based permutation tests assessed the difference between the two adaptation phases in each window and FOI, and statistically significant electrodes are highlighted with \*. In the time window 0.3 – 0.6 sec after visual cue, a significant increase of  $\beta$  power during Late MA with respect to Early MA is detected over the central frontal-premotor region (colour-coded values are in dB).

Table 5-1: Non-parametric cluster-based permutation test on Event-Related Spectral Perturbations changes with respect to natural reaching.

For the  $\beta$  frequency band comparisons are made within time windows of 300 ms from visual cue ( $t = 0$  sec) to 1.5 seconds after; only significant comparisons are reported. Clusters of electrodes whose ERSP is significantly different between the two compared conditions are highlighted (\* for  $p < 0.0083$  according to Bonferroni correction for two-tailed test).

Comparison	0 – 0.3 sec	0.3 – 0.6 sec	0.6 – 0.9 sec	0.9 – 1.2 sec	1.2 – 1.5 sec
$\beta$ (13 – 30 Hz)					
EarlyMA vs. LateFam	N.S.	<b>p = 0.001*</b> {T7, C3, CP5, CP1, P7, P3, C5, CP3, P5, PO5, TP7, PO7}	N.S.	N.S.	N.S.
LateMA vs. Late Fam	N.S.	<b>p = 0.004*</b> {T7, C3, CP5, P7, P3, FC3, C5, CP3, P5, P1, PO5, PO3, TP7, PO7}	N.S.	N.S.	N.S.

## **5.4 Discussions**

### **5.4.1 Novel findings**

In this chapter, the neural correlates of a typical reaching movement were described in both the time- and frequency-domain. Complex patterns of neural activations are reported altogether, whereas previous studies have focused on only one aspect of this behaviour. Moreover, changes in cortical activations of disturbed reaching movements during a robot-mediated force-field adaptation task were also reported through means of EEG recording technique and the implemented robust statistical method. The employed measures of Event-Related Potentials (ERPs) and Event-Related Spectral Perturbations (ERSPs) are here confirmed as valid assessment tools and pave the path for more complex investigations of the undertaken motor adaptation process.

### **5.4.2 The natural reaching movement**

Previous work has shown that a reaching movement recruits a frontal-parietal network called the “dorsal-visual stream” (Grafton et al., 1996; Battaglia-Mayer et al., 2003), which includes parietal, premotor, motor and frontal areas. Many techniques have been previously employed to study the reaching movement and its neural correlates and, among those, EEG is able to describe the subsequent and parallel neural activations of the aforementioned areas with an excellent temporal resolution. ERPs are spontaneous responses of the brain to external stimuli (i.e. auditory, mechanical, visual, etc.) and are very reliable and repeatable within subjects and conditions (Luck, 2014). The time and direction of a given ERP can be informative of specific brain activations and could be also related to certain behavioural aspects. Spontaneous brain activity during cued reaching movement has been studied before in different settings (Naranjo et al., 2007; Dipietro et al., 2014) and results are in line with what is reported here. In the early period after the visual cue and before movement onset (0 – 200 ms) there is an increased negativity in electrodes over the occipital-parietal areas (bilaterally) paralleled by a significant positive potential in electrodes located over frontal-premotor and motor areas contralateral to the engaged arm. These activations have been previously shown to be not-sequential (Naranjo et al., 2007) and involved in target (~ 170 ms) and movement (~ 200 ms) selection both in humans and monkeys (Hoshi and Tanji, 2004). An inversion of polarity is then visible from 300 ms afterwards: a significant negative deflection is indeed observed in a cluster of electrodes over frontal-premotor regions, whereas a significant positive potential is shown in a parietal-occipital cluster, in both cases bilaterally in line with previous work (McDowell et al., 2002; Dipietro et al., 2014). The time of these last

activations is crucial, as it straddles Movement Onset (~ 325 ms after visual cue during Late Fam as reported in chapter 4, see Figure 5-3 (A)), for which these areas are believed to play a role in the transition from movement planning to movement execution (Naranjo et al., 2007). The validity of previous claims and of our results was here assessed by investigating neural potentials during natural reaching against a dummy-null activation (as previously reported in literature, Naranjo et al., 2007) as well as with respect to spontaneous activations during a period of resting-state prior to the experiment start. During resting-state recording, subjects maintained the same posture and fixation point as during the robot-mediated task. Consequently, differences in neural potentials with respect to the resting-state condition would be due to the planning and execution of the reaching movement itself. As a matter of fact, the two analytical approaches undertaken returned very similar results, with only one difference in the window of N/P170. As a good common practice, future investigations should include a period of resting-state EEG prior to the task to be used as “baseline” and as a term of comparison in subsequent statistical analyses.

Time-Frequency (TFr) analysis of EEG data is a technique operating in both the time and the frequency domain, more advanced than ERPs (operating in the time domain only), that evaluates the energy (power) of certain waves oscillating at a given frequency at a specific time point of interest. Advanced TFr methodology based on Morlet wavelet decomposition were here employed (Grandchamp and Delorme, 2011) and statistically significant changes (according to a bootstrap method) in energy/power (ERSPs) were observed during the performing of natural reaching movements in comparison to a period of stillness (i.e. baseline pre-stimulus). Specifically, a sustained decrease of power during movement execution (also called ERD, Event-Related desynchronization) with respect to the pre-stimulus baseline was observed in both  $\alpha$  and  $\beta$  frequency bands mainly in electrodes located bilaterally over the sensorimotor areas (see Figure 5-4), but also spread over the whole head (see Figure 5-2) (Jurkiewicz et al., 2006; Babiloni et al., 2016). Bilateral low frequency ERD during reaching has been extensively reported via surface (Pfurtscheller and da Silva, 1999; Pfurtscheller, 2001; Demandt et al., 2012; Storti et al., 2015) or cortical EEG recordings (Babiloni et al., 2016), as well as during other visual-guided manual tasks such as hand-grip (Derosiere et al., 2014) and sequential finger movements (Manganotti et al., 1998).  $\beta$  band oscillations are thought to be of an inhibitory nature and are required to desynchronize in order to promote an “active state”, subserving sensorimotor integration and voluntary movements (Engel and Fries, 2010).  $\beta$  ERD has been observed in both voluntary, passively performed and imagined movements

(Formaggio et al., 2013), which makes it a suitable neural marker for Brain-Computer Interfaces. Moreover, it has been recently shown to be highly reproducible within subjects across different experimental sessions (Esenhahn et al., 2017), which makes it also an ideal candidate as an individual descriptor in clinical evaluations. Despite the uni-manual movement performed in our study, a bilateral  $\beta$  ERD over the two sensorimotor cortices is visible, in line with previous findings: the simultaneous desynchronization of the ipsilateral motor areas (i.e. right hemisphere in our case) is thought to be a result of an inter-hemispheric cross-talk required to handle task of high difficulty (Desorriere et al., 2014; Formaggio et al., 2013), or of inhibitory processes towards the opposite upper limb (Van Wijk et al., 2012). At the same time, a temporary increase of power after movement onset (also called ERS, Event-Related Synchronization) with respect to the pre-stimulus baseline is reported in low and high  $\gamma$  frequency ranges, spread over a broad area including frontal, sensorimotor and occipital-parietal electrodes bilaterally (see Figure 5-2 and Figure 5-4). Increased high  $\gamma$  activity time-locked to movement onset has been previously reported during both upper- and lower-limb voluntary movements as recorded from the contralateral motor cortex (Ball et al., 2008; Cheyne et al., 2008; Babiloni et al., 2016) and thought to be involved in online feedback during movement. Moreover, fronto-parietal  $\gamma$  activity has also been attributed to mechanisms of top-down attention (Corbetta and Shulman, 2000; Gonzalez Andino et al., 2005).

In summary, the natural reaching movement performed in our experimental setup exhibited typical motor and fronto-parietal neural activations in line with the theory of the “dorso-visual stream” (Naranjo et al., 2007). The positive outcome of this first analysis confirms the validity of our experimental setup and of the analytical pipeline for the investigation of the spatio-temporal neural correlates of the reaching movement in the neurorehabilitation robotics context.

#### **5.4.3 The disturbed reaching movement and the motor adaptation process**

As a first step, any changes that the applied perturbation might have caused in the typical neural parallel and sequential activations of reaching were investigated. For both ERPs and ERSPs, differences between the adaptation condition with respect to the natural reaching were statistically tested. As expected, no changes in spontaneous EEG potentials were detected in the period straight after the visual cue (N/P100, N/P170). Indeed, the same visual cue (i.e. peripheral target turning red as described in chapter 4, paragraph 4.2.3) was provided throughout the whole experiment, thus the same visual processing was likely activated. Moreover, target location was also constant, thus target and



movement selection processes were likely to be the same. A significant reduced N300 was however found in a wide cluster of electrodes located over the frontal-premotor and motor bilateral areas (see Figure 5-5), sustained for the whole adaptation condition. These areas are commonly involved in processes of movement selection, planning and execution (Hardwick et al., 2013; Hardwick et al., 2015; Lefebvre et al., 2012; Lage et al., 2015): the sustained increase of cortical activation during adaptation with respect to natural reaching could represent a state-dependent process via which the brain handles a more complex motor task. Given the higher task complexity, it is likely that, within this window of time, these areas receive more feedback from the periphery to online update the movement allowing the counteraction (Scott et al., 2015; Pruszynski and Scott, 2012). On the other hand, ERSPs changes during adaptation showed a reduced  $\beta$  ERD sustained for the whole adaptation condition in electrodes over the left (contralateral) sensorimotor cortex in a period corresponding to the initiation of the movement (300 – 600 ms after visual cue). To the author's knowledge, very little has been previously reported on differences between natural and disturbed reaching movements. Studies on both humans (Pollok et al., 2014) and monkeys (Khanna and Carmena, 2017) have successfully described a correlation between reduced  $\beta$  ERD and faster movement onsets in self-paced movements, as it would allow for the search of new strategies. However, in this study subjects were explicitly asked to move within a predefined period of time and group-level values of movement onset did not show prominent differences across conditions (see chapter 4, Table 4-1). Studies on the maintenance of a finger steady-state motor output claimed that higher cortical motor  $\beta$  power correlated with better performance (Kristeva et al., 2007). Despite the different context (isometric contraction recruiting stronger  $\beta$  activity) and motor task involved, control analyses were also performed to inspect any potential relationships between reduced  $\beta$  ERD and changes in performance, however there was none. Moreover, the increase in relative  $\beta$  power is sustained for the whole adaptation duration, thus it is likely to be related to the task itself and its complexity, and not to an adaptation process underlying. This is further supported by intra-cortical recordings in monkeys which showed that neurons in the primary motor cortex are tuned to a preferred movement direction during reaching (Georgopoulos et al., 1982), which is however altered during reaching in a force field as neurons decode the direction of the required compensatory force (Gandolfo et al., 2000), supporting the hypothesis of cortical changes due simply to the applied load and not to adaptation or plasticity processes. Interestingly, it is known that patients suffering of neurological deficits and impairments, such as stroke or Parkinson's disease, show an anomalous increase of  $\beta$  power (reduced

$\beta$  ERD) during voluntary movements (Rossiter et al., 2014; Shiner et al., 2015; Moisello et al., 2015). This pathological increase of  $\beta$  power has been suggested to be symbolic of less flexible sensorimotor and cognitive control of voluntary actions (Engel and Fries 2010). This is in line with uni- and bi-manual learning tasks that claimed that a proper  $\beta$  modulation is necessary to maintain movement stability (Houweling et al., 2010). A recent investigation also demonstrated that the level of motor functions after stroke negatively correlated with the intensity of the  $\beta$  rhythm recorded from the central sensorimotor regions of the affected hemisphere (Thibaut et al., 2017). A similar principle is here suggested: it is indeed possible that the applied novel strong perturbation causes movement instability and, subsequently, a stronger sensorimotor  $\beta$  range synchrony due to the reduced control of voluntary movements available to the subjects.

The adaptation condition per se was then analysed in order to investigate if any correlates of the adaptation process itself could be observed. No changes in ERPs and in low ( $\alpha$ ) or high ( $\gamma$ ) time-frequency ERSs were detected between early and late adaptation. However, a statistically significant reduction of  $\beta$  ERD (i.e. increase of  $\beta$  power) in a cluster of electrodes located over the frontal-premotor bilateral regions was successfully identified during late with respect to early adaptation in the period of movement initiation (300 – 600 ms). As aforementioned, the frontal cortex (FC), the DLPFC and the Supplemental Motor Area (SMA) are indeed altogether involved in the early stages of motor learning and adaptation (Lefebvre et al., 2012; Shadmehr and Holcomb, 1997) in movement selection and initiation as well as in motor memory consolidation (Lage et al., 2015). A variety of studies have previously reported a similar reduction over learning in both healthy (Kranczioch et al., 2008; Studer et al., 2010) and neurologically impaired populations (Moisello et al., 2015). According to their findings, the reduced  $\beta$  ERD resembles decreased motor-related cortical activations, which could be symbolic of less effort needed to perform the task and of a newly acquired automaticity. It is therefore likely that an increased cortical activation in the frontal regions is symbolic of the creation of internal models specific to the disturbed reaching (Shadmehr and Holcomb, 1997). Optimization strategies are not confined to the brain only, but also develop at the periphery, whereby reduced co-contraction across muscles is replaced by a more orchestrated synchrony (i.e. higher inter-muscular coherence) exactly in the period of movement initiation (Pizzamiglio et al., 2017). Altogether, these findings support the hypothesis that our nervous system optimizes activations and behaviour in order to minimize efforts and save energy.

#### **5.4.4 Error-Related Negativity during motor adaptation**

A valid alternative interpretation to the reported findings, specifically to the sustained increase of ERP negative deflection at 300 ms after the visual cue during adaptation to the counter-clockwise force-field, can be found within the theory of Error-Related Negativity (ERN). ERN was first introduced during studies on error processing during discrete response (Falkenstein et al., 2000) and prism adaptation protocols (MacLean et al., 2015). Two specific event-related deflections were identified in these studies, both at around 300 ms: a positive potential (P300), linked to learning processes, and a negative potential, eventually related to error processing (ERN). Investigations based on motor control tasks also identified an ERN component starting right before the movement onset, likely from the anterior cingulate cortex (ACC), (Krigolson and Holroyd, 2006), and eventually suggested to be related to the creation of predictive feedback models during the error-based tasks. The findings reported in this chapter appear to be in line with this theory as the timing (around 300 ms) and location (medial frontal, likely capturing activity coming also from ACC sources) of the significantly increased negative ERP component during adaptation (condition during which subjects performed movement errors on a trial basis) resemble those of a typical ERN. This is further supported by the fact that subjects did not completely adapt to the external perturbation (see chapter 4, paragraph 4.3.1, figure 4-5 and table 4-1), which could have caused the sustained ERN during adaptation. It could be therefore argued that this sustained negative component is the signature of an error processing strategy developed by a predictive model. Previous studies defined motor learning and adaptation as guided by prediction errors (Shadmehr et al., 2010), whereby an internal forward model is usually developed which foresees the consequences of each movement based on the actual state of the system (Wolpert and Miall, 1996; Shadmehr and Holcomb, 1997; Krebs et al., 1998). Interestingly, a concurrent increased cortical activation (i.e. reduced  $\beta$  ERD) was observed in the current investigations and discussed (see paragraph 5.4.3) as a potential indicator of the creation of an internal model specific to the disturbed reaching. ERN could therefore be likely considered as a marker of the error processing functions the motor system develops during learning and activates immediately before the actual error commission in a predictive fashion, in contrast to the typical ERN response (detected when performing errors during reaction time tasks) and ERN feedback (detected when the result of an action is not as expected) which both appear after the actual error commission (Krigolson & Holroyd, 2006; Völker et al., 2018). As abovementioned, subjects did not completely adapt to the external perturbation (i.e. summed error values did not return to baseline level), which

explains the observation of a sustained ERN during adaptation, because a constant error processing was required. Neural activations have been shown to shift from the prefrontal cortex (early adaptation) to the posterior parietal cortex and cerebellum (late adaptation) (Shadmehr and Holcomb, 1997; Krebs et al., 1998). Such a shift in neural activations was not observed in the current investigation, confirming the nature of the employed paradigm as of “short-adaptation”. The ERN could be a valid and strong marker of learning processes in pathological conditions as it was demonstrated that ERN levels are significantly reduced in patients with medial frontal lesions (Hogan et al., 2006; Stemmer et al., 2004; Swick and Turken, 2002) and in healthy but elderly subjects (Colino et al., 2017). Moreover, investigations with stroke patients demonstrated that neural infarcts can selectively impair motor preparation functions executed by the pre-frontal areas and the ACC (Wiese et al., 2015). ERN could be employed as valid marker of motor learning in pathological conditions not only as an assessment measure but also as a target for specific rehabilitation protocols such as neurofeedback training. Interestingly, ERN has been demonstrated not to be influenced by stimulus modality (Falkenstein et al., 2000), output differences (Holroyd et al., 1998) and even robot-mediated force-field direction (Desowska, Pizzamiglio and Turner, 2018 *Journal of Neuroscience under review*). This would make the ERN a reliable indicator of the learning levels of patients during rehabilitation, independently of the specific motor task and output.

#### **5.4.5 Limitations**

As previously mentioned (see chapter 4, paragraph 4.4.4), even though subjects showed a typical adaptation profile in movement error, no complete adaptation was reached at the end of the condition. This is further supported by the neural findings: more trials would allow subjects to completely adapt to the novel environment, promoting  $\beta$  ERD over the primary motor cortex to return to its natural values and eventually developing other specific neural activations directly correlated to performance improvement. Moreover, as per our study design, no long-term memory could be assessed after this single adaptation session: consolidation and novel internal model creation has been demonstrated to take place in primary motor and posterior parietal regions (Della Maggiore et al., 2015), thus future studies should comprehend multiple testing sessions in order to evaluate long-term memory formation. Repetitive sessions would also facilitate the disentanglement of neural correlates of adaptation from those of simple reaction to the applied perturbation. An alternative approach was here followed by which adaptation correlates could be identified in spontaneous neural oscillations recorded during resting-state EEG before and after adaptation, the results are reported elsewhere (see Faïman, Pizzamiglio and

Turner 2017, master thesis and paper in preparation). Future studies should also involve neurologically impaired patients, such as stroke survivors, and investigate how their neural correlates during this motor adaptation task are shaped in comparison to the healthy populations', thus to eventually define specific marker of adaptation and/or optimization and adjust the rehabilitative process to maximize recovery. Moreover, more advanced techniques of functional connectivity should be implemented to define a proper relationship between brain and behaviour and find mechanisms of motor control shaping through motor adaptation. A very recent study investigating cortico-muscular correlates of isometric and dynamic motor tasks showed that, at high level of forces,  $\beta$  band cortico-muscular coherence (CMC) as well as inter-muscular coherence (IMC) are reduced in dynamic with respect to isometric contractions and resemble task-specific synergistic control strategies (Reyes et al., 2017). Very similar findings were found (Pizzamiglio et al., 2017), whereby  $\beta$  IMC was reduced during the dynamic reaching movement and eventually replaced by higher frequencies activations. On the other hand,  $\beta$  CMC has gained a lot of interest in stroke rehabilitation (Rossiter et al., 2013) as a measure of the relationship between cortical changes and muscle activations during recovery. This background encourages the study of the cortico-muscular correlates of disturbed reaching movements during the motor adaptation task as it could shed some light on the relationship between brain and muscles during adaptation and how this changes with respect to a natural reaching behaviour (see chapter 6).

## **6 Source-level neural correlates of robot-mediated motor adaptation during reaching with the upper-limb**

### **6.1 Introduction**

Brain oscillations are subject- and task-specific, with peaks in the  $\alpha$  (8-12 Hz),  $\beta$  (15-30 Hz) and  $\gamma$  (35-up to 80 Hz) commonly observed (Baker, 2007). It has been shown that oscillations within the  $\beta$  band in the sensorimotor cortex are coherent with electromyogram activities at similar frequencies in contralateral musculatures, mostly during isometric contractions (Conway et al., 1995; Halliday et al., 1995; Kilner et al., 1999; Kilner et al., 2000; Kristeva et al., 2007). This brain-muscle synchronization shifts towards higher oscillatory frequencies when, during isometric contractions, dynamic forces or movement are introduced (Marsden et al., 2000; Omlor et al., 2007; Mehrkanoon et al., 2014). The measure commonly used to evaluate the strength and quality of the brain-muscle relationship is Cortico-Muscular Coherence (CMC) (Rosenber et al., 1989), a methodology extensively employed in studies with both primates (Murthy and Fetz, 1992; Takei and Kazuhiko, 2008; Witham et al., 2010) and humans (Kamp et al., 2013; Babiloni et al., 2008; Dal Maso et al., 2012; Mendez-Balbuena et al., 2011; Reyes et al., 2017). Amplitude of CMC can convey information on the quality of the brain-muscle communication and integrity of the pyramidal system (Mima et al., 1999), on the synchronization between cortical and spinal cord during movement (Mima and Hallet, 1999), and it is indeed altered in neuro-degenerative disorders and after neural injuries (Fang et al., 2009; Kamp et al., 2013; Rossiter et al., 2013; Airaksinen et al., 2015; Belardinelli et al., 2017). CMC phase has the potentiality to measure the communication delay between brain and muscles as well as its directionality, disentangling between feedforward and feedback drives (Witham et al., 2010; Mehrkanoon et al., 2014). CMC in low frequencies such as  $\alpha$  (8-12 Hz) have been attributed to a pulsatile communication between brain and muscles (Vallbo and Wessberg, 1993) and to feedback motor processing functions when transiting from two steady states (Mehrkanoon et al., 2014);  $\beta$  CMC drives have always been attributed a feedforward role guiding muscles, required to maintain the status-quo (Engel and Fries, 2010) and the steady state motor output, or enrolled in more complex sensorimotor (Baker, 2007) and muscular binding (Reyes et al., 2017) processes;  $\gamma$  cortico-muscular coherence has been linked to higher processes of sensorimotor integration (Mehrkanoon et al., 2014), promotion of voluntary movements (Fang et al., 2009) and focused attention (Schoffelen et al., 2005).

CMC has been used in clinical practice to assess the grade and quality of recovery after neural injuries as well as of degenerative processes. On the one hand, studies on stroke survivors investigated the reliability of CMC to assess 1) the quality of the recovering communication between brain and muscles (Fang et al., 2009), 2) the cortical changes occurring after stroke (Rossiter et al., 2013; Belardinelli et al., 2017), and 3) the cortical changes as patients move from the acute to the chronic stage (von Carlowitz-Ghori et al., 2014). On the other hand, studies on Parkinson's disease patients employed the CMC method to assess the potential positive effects of different therapies on tremor entity and motor performance (Caviness et al., 2006; Park et al., 2009; Airaksinen et al., 2015), however not reaching a common conclusion. Lastly, investigations on the effects of degenerated cortical executive functions and motor control in elderly utilized CMC to extract information on potential compensatory strategies used to preserve motor performance (Kamp et al., 2013; Bayram et al., 2015). In summary, cortico-muscular coherence could be a valid methodology in clinical practice for example, 1) to assess the entity of abnormal bilateral or ipsilateral activations when executing a movement after stroke, 2) to evaluate the benefits of certain drug- or stimulation-based therapies for tremor reduction in Parkinson's disease and other tremor-based disorders, as well as 3) to assess the entity and progress of cortical inefficiency in ageing.

In this study the coherent neural-muscular drives during natural reaching in healthy subjects and their changes due to the robot-mediated motor adaptation process were investigated. Given the poor spatial resolution typical of EEG signals, a source-reconstruction methodology was employed to transfer the scalp electrical signals to the cortex and locate the sources of the neural activity. Moreover, investigations were restricted specifically to the relationships between the brain and those muscles most recruited during adaptation to the applied counter-clockwise force-field, specifically Triceps Brachii (TB), Biceps Brachii (BB) and Extensor Carpi Radialis (ECR) muscles (Pizzamiglio et al., 2017). Given the previous evidence of CMC during reaching in healthy subjects (Fang et al., 2009),  $\beta$  and/or  $\gamma$  CMC activity was expected to arise in the contralateral (left) sensorimotor cortex during natural reaching. However, as there is no precedent on the investigation of cortico-muscular coherence during a robot-mediated motor adaptation protocol, condition-specific changes in CMC were hypothesised to happen within the primary motor cortex and areas involved in 1) the integration of sensory feedback from the periphery (i.e. sensory cortex) and in 2) the planning/execution of the movement (i.e. frontal and premotor cortices). According to the theories of motor learning, the early stages of a motor adaptation process are characterised by a strong

cortico-striatal activity, whereby the frontal cortex is mostly involved as temporary storage of info and memories (Shadmehr and Holcomb, 1997; Krebs et al., 1998). Thus, changes in frontal, premotor and subsequently parietal areas were expected to be significant during the adaptation process. Positive results of this advanced analysis will shed some light on the coherent cortico-muscular drives during the adaptation process and will validate the employment of CMC in clinical practice with neurologically impaired patients.

## **6.2 Materials and methods**

### **6.2.1 Data collection and experimental setup**

The raw EEG data were obtained in the experiments described in chapter 4. For details on subjects' recruitment, experimental setup and protocol, see chapter 4, paragraph 4.2.1 to 4.2.5.

### **6.2.2 Data analyses**

Data analyses were performed with MatLab 2015b (The MathWorks, Inc.), with the support of FieldTrip open-source toolbox (Oostenveld et al., 2010).

#### **Cortico-Muscular Coherence (CMC) at sensor-level**

To observe the changes in cortico-spinal synchronization during the reaching movement across different conditions, Cortico-Muscular Coherence (CMC) was estimated between all EEG channels and the EMG signals from TB, BB and ECR muscles. Analyses focused on these three muscles only as previously shown to be most recruited during adaptation to counter-clockwise force-field (Thoroughman and Shadmehr, 1999; Pizzamiglio et al., 2017). To assess CMC, raw EEG data previously pre-processed (see chapter 5, paragraph 5.2.2) were used, whereas raw EMG data were de-trended, band-pass filtered between 2 Hz and 100 Hz (Butterworth, order 3, dual-pass fashion to avoid phase lag) and notch filtered (50 Hz, IIR Comb Notching filtered as designed in MatLab, order 20). No rectification was implemented to calculate CMC as it was previously demonstrated not to be necessary and valuable when high forces are involved (McClelland et al., 2012; Farina et al., 2013). Filtered EMG data were then segmented into epochs of 3 seconds each from -1000 ms to 2000 ms with respect to each trigger (i.e. visual cue) in line with the pre-processed EEG, and the same subject-condition-specific epochs removed from the neural signals were discarded also in the muscular signals for consistency. Spectral analysis of EEG and EMG signals was performed with the support of FieldTrip toolbox for MatLab (Oostenveld et al., 2010) on data segments of 1 second for each trial (0.3 – 1.3 sec after visual cue). This period of time was considered according to kinematic evidences of



start/end of movement (see chapter 4, paragraph 4.3.1 and Table 4-1) in order to specifically investigate cortico-muscular correlates during a complete reaching movement. The auto- and cross-spectra were assessed within a frequency range from 2 Hz to 80 Hz for the entire data length of 1 second via Fast Fourier Transform (FFT) with a multi-taper fashion (Muthuraman et al., 2012) as implemented in FieldTrip with the function *ft\_freqanalysis*, method = 'mtmfft'. The methodology analyses an entire spectrum for the entire data length (i.e. no time-domain, only frequency results), using discrete spheroidal sequences (Slepian sequences, method *dpss* as implemented in MatLab) as tapers by default (Slepian, 1978). Coherence between EEG ( $x(t)$ ) and EMG ( $y(t)$ ) signals was computed according to the Equation 5, whereby  $S_{xx}$  and  $S_{yy}$  are the individual power spectra (i.e. of an EEG channel and an EMG muscle respectively), whereas  $S_{xy}$  is the cross-spectrum between the two signals. The obtained coherence values at each frequency are normalized between 0 (i.e. lack of correlation between the two signals) and 1 (i.e. complete correlation between the two signals). To inspect if obtained values of CMC during natural reaching (i.e. Late Fam condition only) were statistically significant, for each subject a Confidence Limit was defined according to the formula (Rosenberg et al., 1989):

$$CL = 1 - (1 - \alpha)^{\frac{1}{L-1}}$$

Equation 6-1: Confidence Interval formula.

with  $\alpha$  being the significance level (95%) and L being the number of disjoint segments used (i.e. number of trials). The cross-spectrum results, or Cross-Spectral Density matrix (CSD) between neural and muscular signals was saved and further used for source level localization of cortico-spinal coherent activities.

### Source localization

The Beamformer technique with Dynamic Imaging of Coherent Sources (DICS) methodology as implemented in FieldTrip was employed in order to localize sources responsible for producing coherent activity with the arm muscles of interest (i.e. TB, BB and ECR) in  $\beta$  (15-25 Hz) and low  $\gamma$  (35-45 Hz) frequency bands. This technique estimates the amount of activity at a given location in the brain via a linear projection of the sensor data using a spatially adaptive filter computed from the lead fields of the sources and the cross spectral density matrix between neural and muscular signals previously calculated (Gross et al., 2001). The brain volume is filled with regularly spaced dipoles defined on a 3D grid and the source strength for each grid point is computed,

producing a 3D spatial distribution of the power of the neuronal source. This distribution is then usually overlaid on a structural image of each subject's brain in order to optimize the results to the individual anatomy. As none of the healthy adults recruited in the study have ever had a brain MRI scan before, a template 3D grid based on a template anatomical volume in Montreal Neurological Institute (MNI) space with dipole spacing of 8 mm as provided in FieldTrip was here used in order to have dipole locations directly comparable across participants and conditions. Individual maps of CMC were spatially normalized and interpolated on a template T1-weighted MRI scan as provided in FieldTrip.

### **6.2.3 Statistics**

#### **Cluster-based permutation tests**

The cluster-based non-parametric statistical approach previously used has been employed here again for the evaluation of changes in coherent activity between brain and the muscles of interest (i.e. TB, BB and ECR) across conditions for a total of three comparisons (Late Fam vs. Early MA, vs. Late MA and vs. Late WO). CMC with each muscle in each frequency band were assessed separately and the effects of interest were evaluated by means of multiple dependent sample t-Tests applied to each 3D voxel. T-values exceeding an a priori threshold of  $p < 0.05$  were clustered based on adjacent voxels exhibiting the same effect. Cluster-level statistics were computed by taking the sum of the t-values within every cluster. The statistical comparisons were done with respect to the maximum values of summed t-values. By means of a permutation test (i.e. randomizing data across conditions and rerunning the statistical test 1500 times, Monte-Carlo approximation) a randomization distribution of the maximum of summed cluster t-values was obtained to evaluate the statistics of the actual data. Clusters in the original dataset were considered to be significant at an alpha level of ( $\alpha_{\text{cluster}}$ ) 5% if less than the 5% of the permutations ( $\alpha_{\text{cluster}} = 0.01$ ,  $\alpha = 0.025$  for 2-tailed tests,  $N = 1500$ ) used to construct the reference distribution yielded a maximum cluster-level statistic larger than the cluster-level value observed in the original data. As three different tests were carried out (Late Fam vs. Early MA, vs. Late MA and vs. Late WO), further correction for multiple comparison was run with Bonferroni method ( $p = 0.025/3 = 0.0083$  for two-tailed test).

#### **Regions of Interest (ROIs)**

Preliminary investigations not reported here handled the statistical problem aforementioned with a whole-brain approach. On the one hand, this approach is not optimal, as too many voxels are included in the analysis increasing the number of multiple

comparisons to a non-realistic number. On the other hand, the definition of an a priori hypothesis would promote the exclusion from the statistical analysis of those brain areas a priori known not to be involved in the control of peripheral muscles. Therefore, different comprehensive meta-analyses on the neural correlates of voluntary upper-limb movements (Witt et al., 2008; Pool et al., 2013; Turesky et al., 2016) and motor learning (Lohse et al., 2014) have been cross-checked to define a reduced number of Regions of Interest (ROIs) on which to explore changes of CMC during motor adaptation. At first, the identified ROIs included:

- Left Premotor Cortex (PM);
- Bilateral Supplementary Motor Area (SMA);
- Bilateral Primary Motor Cortex (M1);
- Left Sensorimotor Cortex (S1);
- Right Inferior Parietal Lobule (IPL);
- Bilateral cerebellum (forearm and upper arm areas, Mottolese et al., 2013);
- Left Putamen;
- Right Insula.

Despite the potentiality of source-localization techniques in improving the spatial resolution of EEG data and identify specific cortical/cerebellar activations, it is far beyond its possibilities to reliably reconstruct activities generated in deeper structures than the cortex, such as the Striatum or the Basal Ganglia. Therefore, deep structures were excluded from the statistical analysis (i.e. left Putamen and right Insula), which eventually resulted in 17 ROIs defined according to FieldTrip toolbox, specifically:

- Left Superior Frontal Cortex;
- Left Medial Frontal Cortex;
- Bilateral M1;
- Bilateral SMA;
- Left S1;
- Bilateral Cerebellar Area 6;
- Bilateral Cerebellar Area 7b;
- Bilateral Cerebellar Area 8;
- Bilateral Cerebellar Area 9;
- Bilateral Paracentral Lobule.

## 6.3 Results

### 6.3.1 Sensor- and source-level CMC during reaching in different conditions

Figure 6-1 shows a typical subject CMC behaviour during natural reaching (i.e. Late Fam condition) for both  $\beta$  and low  $\gamma$  frequency bands where not-significant values have been put equal to zero. The significant threshold of coherence for this specific subject was 0.0618, thus values reported on the colour-bar are all significant. Clusters of  $\beta$  and low  $\gamma$  CMC can be seen over the contralateral sensorimotor cortex in almost all the CMC frequency-muscle combinations. The number of trials averaged during Late Fam condition ranged from 38 to 47 (mean ( $\pm$  std) = 43 ( $\pm$  2)), thus the threshold values for CMC ranged from 0.0618 to 0.0758 (mean ( $\pm$  std) = 0.0682 ( $\pm$  0.0036)). Only a few ( $n = 5$ ) subjects didn't show a significant CMC for any muscle-frequency combinations during natural reaching thus analyses were carried on as repetitive practice of a motor task has been shown to induce changes in CMC (Perez et al., 2006; Mendez-Balbuena et al., 2011; Fu et al., 2014). Figure 6-2, 6-3 and 6-4 represent the source-level results in both the  $\beta$  and low  $\gamma$  frequency bands of CMC with TB, BB and ECR respectively across each condition. The obtained source-localized activity is a volumetric reconstruction specified in head-coordinates and, in order to be able to visualise the results, functional data needed to be interpolated to the anatomical MRI template. The passage from sensor- to source-level consistently improved the spatial-resolution of the data: for example, higher values (i.e. yellow) of CMC with all the three muscles in the  $\beta$  band during Late Fam are indeed localized in the left sensorimotor cortex as expected. During the motor adaptation condition muscle specific CMC patterns develop and by the end of the wash out condition  $\beta$  CMC remains high in the left motor sensorimotor regions. Low  $\gamma$  CMC show more variable patterns across muscles, with however a common increase in values during different stages of adaptation across muscles.

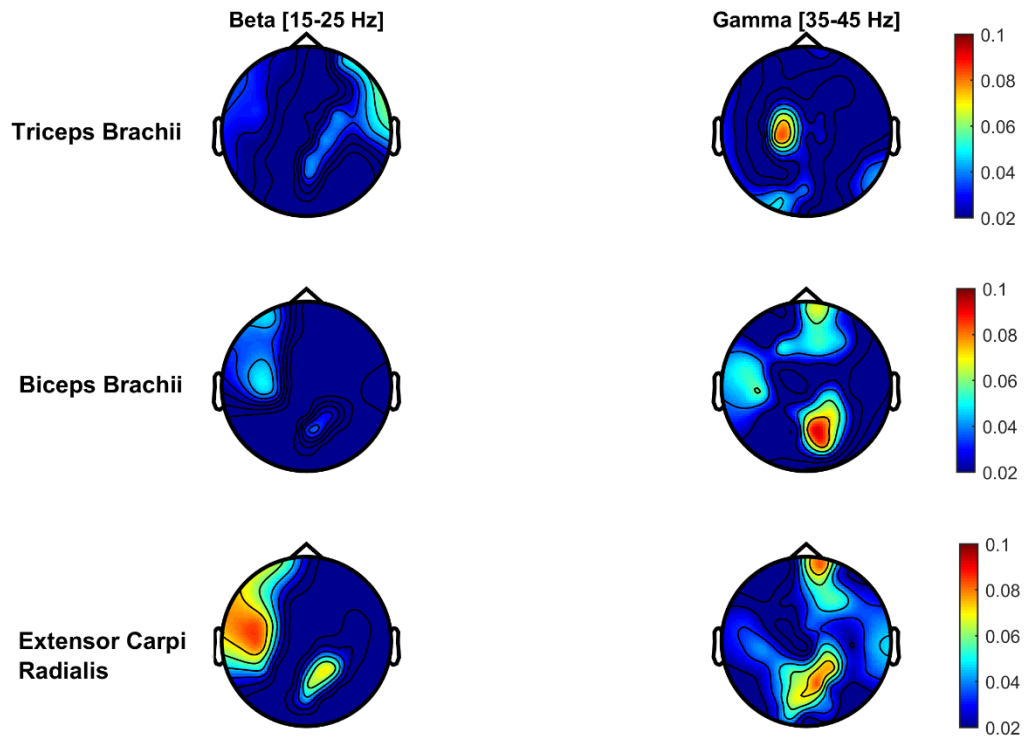


Figure 6-1: Sensor-level plots of an exemplary single subject cortico-muscular coherence between all EEG electrodes and the Triceps Brachii (first row), the Biceps Brachii (second row) and the Extensor Carpi Radialis (third row) muscles in both  $\beta$  and low  $\gamma$  frequency bands during natural reaching.

Topoplots of a single-subject  $\beta$  (left column) and low  $\gamma$  (right column) CMC at sensor-level for each muscle of interest are reported for Late Fam condition only (i.e. natural reaching). Values of CMC are colour-coded so that warm (i.e. red) colours represent high values, whereas cold (i.e. blue) colours represent low values. Dark blue areas are masked as not above the specific subject threshold (0.0618).

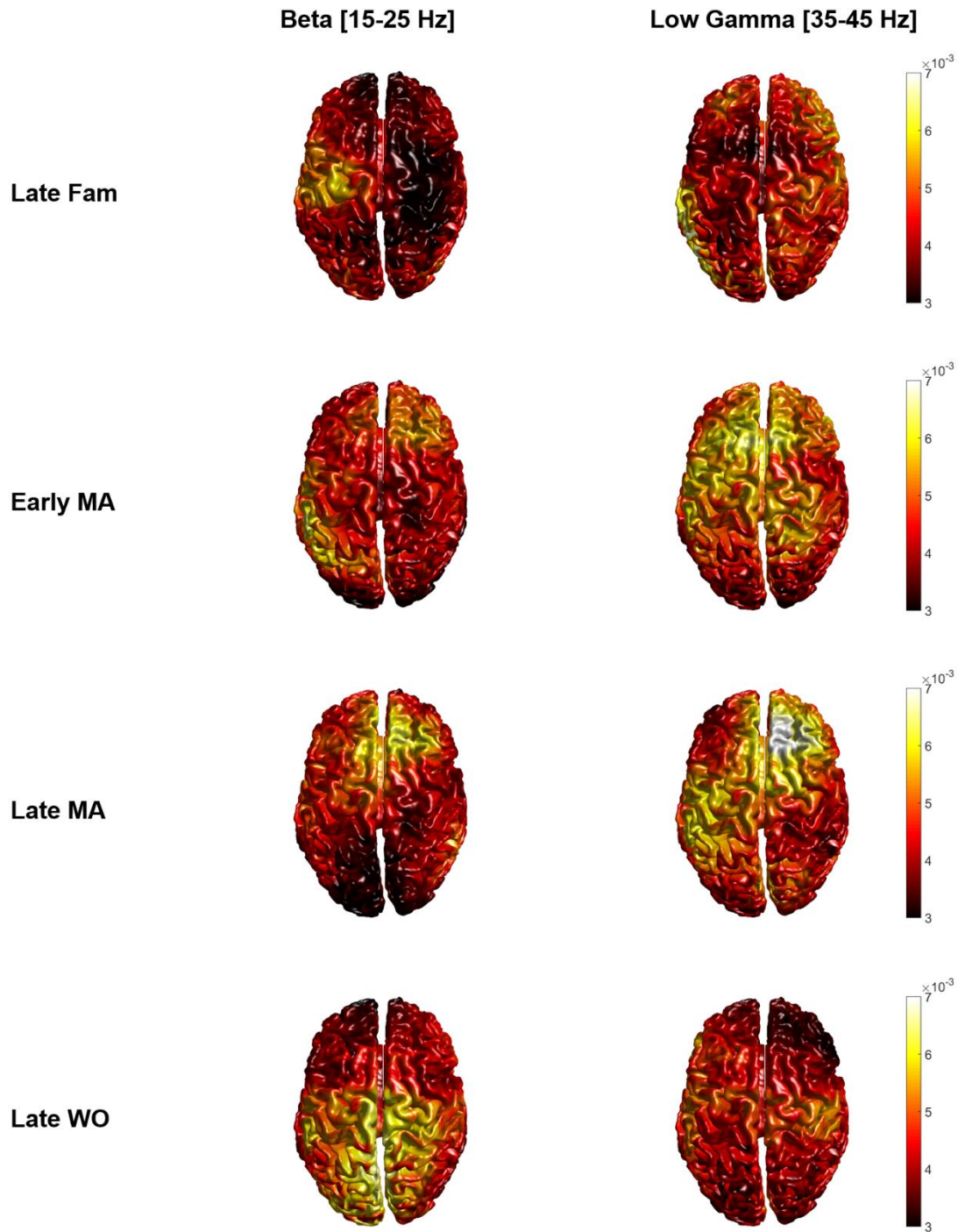


Figure 6-2: Source-level plots of all subjects grand average of cortico-muscular coherence between all EEG electrodes and the Triceps Brachii muscle.

Surface-plots of group-level  $\beta$  (left column) and low  $\gamma$  (right column) CMC at source-level for the Triceps Brachii muscle are reported for each condition. Values of CMC are colour-coded so that black-red colours represent low values, whereas yellow-white colours represent high values.

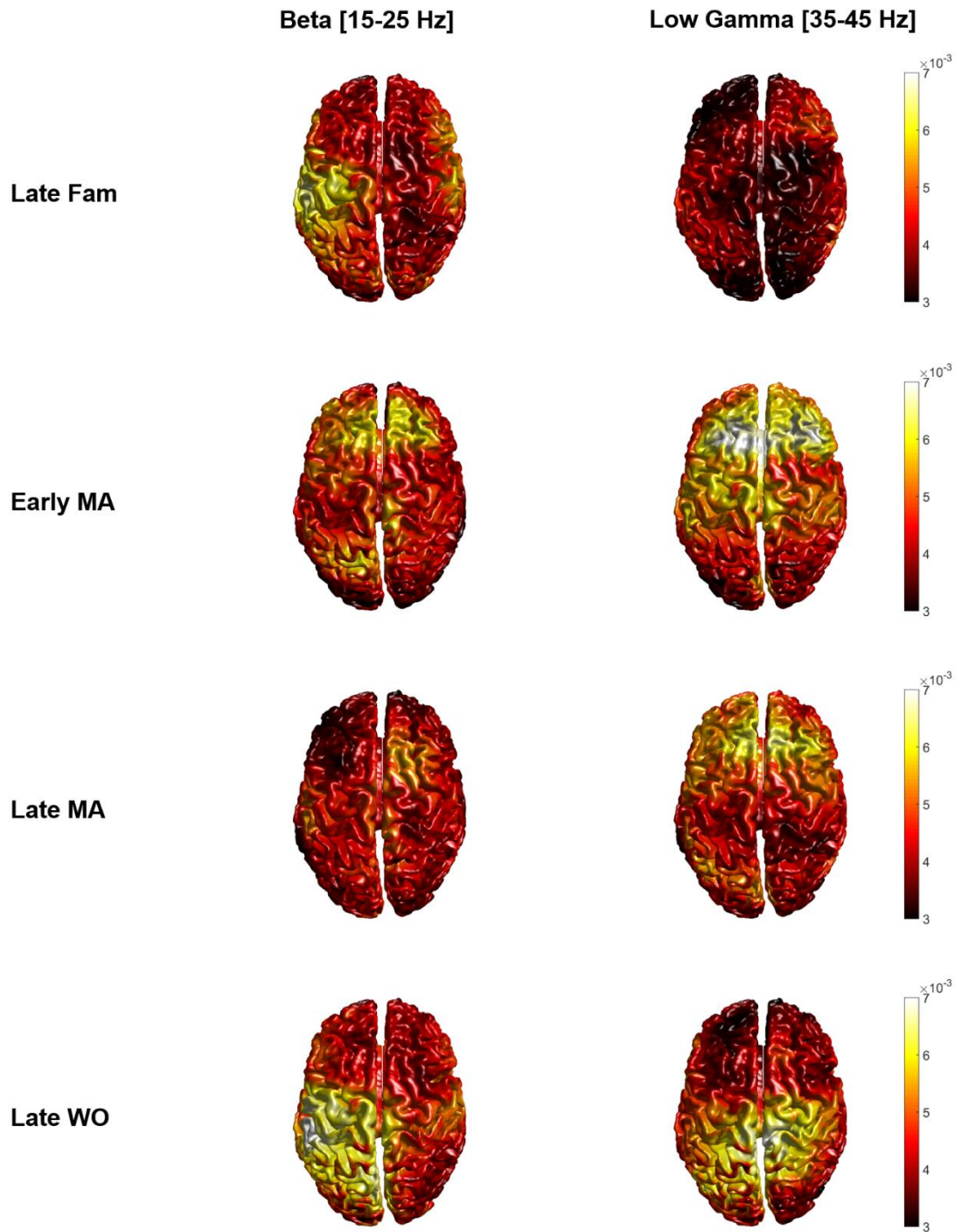


Figure 6-3: Source-level plots of all subjects grand average of cortico-muscular coherence between all EEG electrodes and the Biceps Brachii muscle.

Surface-plots of group-level  $\beta$  (left column) and low  $\gamma$  (right column) CMC at source-level for the Biceps Brachii muscle are reported for each condition. Values of CMC are colour-coded so that black-red colours represent low values, whereas yellow-white colours represent high values.

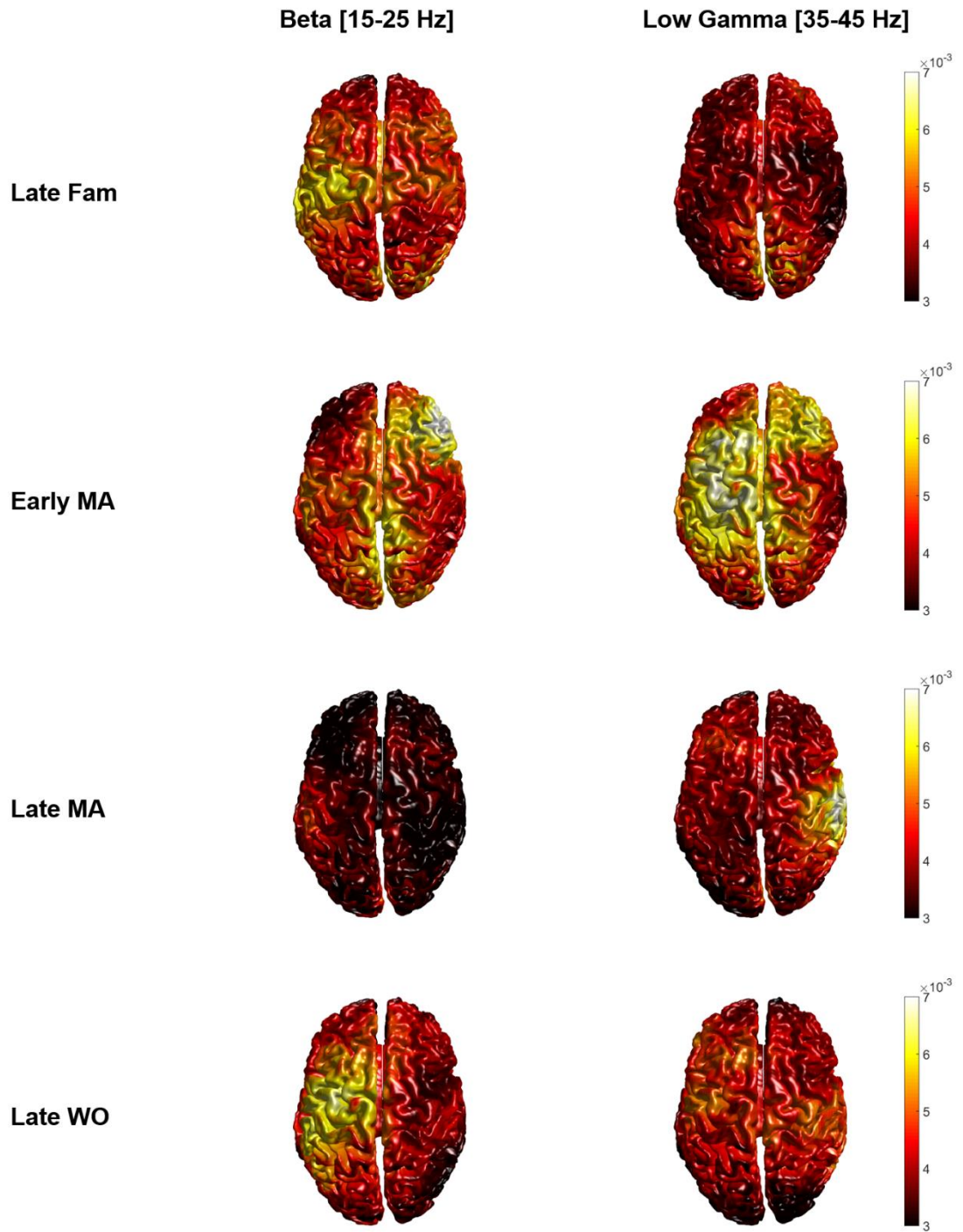


Figure 6-4: Source-level plots of all subjects grand average of cortico-muscular coherence between all EEG electrodes and the Extensor Carpi Radialis muscle.

Surface-plots of group-level  $\beta$  (left column) and low  $\gamma$  (right column) CMC at source-level for the Extensor Carpi Radialis muscle are reported for each condition. Values of CMC are colour-coded so that black-red colours represent low values, whereas yellow-white colours represent high values.



### 6.3.2 CMC correlates of robot-mediated motor adaptation

The non-parametric statistical analysis yielded muscle specific results which are all reported in Table 6-1. No significant changes during adaptation with respect to natural reaching were observed for the TB muscle. Instead, a significant increase of BB-low  $\gamma$  CMC ( $p = 0.006$ , positive cluster) was observed during Early MA with respect to Late Fam in left frontal-, bilateral premotor- and motor-, left sensory- and bilateral medial central areas. Figure 6-5 shows the statistically significant cluster t-maps of BB-low  $\gamma$  CMC on a brain surface (i.e. surface-plot) and over an MRI template sliced along the three main axes of the head coordinate system for improved visualization (i.e. ortho-plot). Moreover, a statistically significant decrease of ECR- $\beta$  CMC ( $p = 0.008$ ) was observed during Late MA with respect to Late Fam in left frontal-, bilateral premotor- and motor- and bilateral medial central areas. Figure 6-6 shows the statistically significant cluster t-maps of ECR- $\beta$  CMC through both a surface- and an ortho-plot. Despite the different results obtained, some areas are commonly involved in the changes of CMC across condition, frequency bands and muscles, specifically: left M1, left Superior Frontal Cortex (FC), left Medial FC and bilateral SMA.

### 6.3.3 CMC changes during adaptation

Given the positive results of the previous analysis and the definition of a set of ROIs commonly involved in the changes of CMC during adaptation with respect to natural reaching (i.e. right/left M1, right/left SMA, right/left Paracentral Lobule, left superior/medial FC), a further cluster-based permutation test was run to test whether any changes took place from early to late adaptation only. A statistically significant decrease of BB- $\beta$  CMC ( $p = 0.015$ ) was observed during Late MA with respect to Early MA in left frontal areas (superior and medial). Moreover, a significant decrease of ECR- $\beta$  CMC ( $p = 0.045$ ) was reported during adaptation in bilateral SMA. Figure 6-7 shows the statistically significant clusters t-maps of (A) BB- $\beta$  and (B) ECR- $\beta$  CMC through an ortho-plot. No significant changes were observed in TB- $\beta$  CMC and for low  $\gamma$  CMC of any muscles. Results summary is reported in Table 6-2. CMC, by definition, describes the relationship between a certain brain area and a given muscle therefore, in order to investigate if the observed cortico-muscular changes during adaptation were symbolic of specific behavioural changes, linear regression models were attempted to describe kinematic variables. For each subject and each condition (i.e. Late MA and Early MA), the average BB- $\beta$  CMC was extracted from the left superior and medial FC ROIs and the average ECR- $\beta$  CMC was obtained from the left and right SMA ROIs. Only the difference

between Late MA and Early MA was further considered. Kinematics data of Summed Error, Movement Onset and Peak Force, previously discussed (see chapter 4, paragraph 4.3.1), were considered as Dependent Variables (DVs) in regression models:  $\beta$  CMC changes correlating with movement error changes during practice would resembled an adaptive strategy;  $\beta$  CMC changes correlating with movement onset changes during training would be symbolic of a faster-movement strategy;  $\beta$  CMC changes correlating with maximum force changes during adaptation would show a partial adaptive strategy simply based on force production. Multiple Regression models were stepwise created with the format:

$$\Delta Kinematics = \beta_0 + \beta_i \cdot \Delta \beta\_CMC_{mus,ROI} + \varepsilon$$

Equation 6-2: Multiple regression models formula.

where  $\Delta Kinematics$  is the difference between Late MA and Early MA values of any of the three kinematic variables considered (i.e. Summed Error, Movement Onset and Peak Force),  $\Delta \beta\_CMC_{mus,ROI}$  are the differences between Late MA and Early MA of the average  $\beta$  CMC values from the specific muscle and ROI (Left Superior FC for BB, Left Medial FC for BB, Left SMA and Right SMA both for ECR) entered into the model as Independent Variables (IVs),  $\beta_n$  are the intercept and coefficient associated to each model predictor, and  $\varepsilon$  is the error. Data were first centred (i.e. the mean score was subtracted from each observation) and scaled (i.e. standard deviation was set equal to 1) in order to reduce the chance of multicollinearity. Only one regression model was successfully created for  $\Delta Peak Force$  (R-squared = 0.234,  $p = 0.042$ ) for which all assumptions were met (no multicollinearity, no auto-correlation, no homoscedasticity). Specifically, only the IVs significantly contributing to the prediction of Peak Force were entered stepwise into the model. The final model predicts the DV based only on Left SMA – ECR- $\beta$  CMC ( $B = -0.432$ ,  $p = 0.042$ ) as shown in Figure 6-8. The final model equation can therefore be written as follow:

$$\Delta Peak Force = -0.108 - 0.432 \cdot \Delta leftSMA\_ECR\_ \beta CMC$$

Equation 6-3:  $\Delta Peak Force$  multiple regression model formula.

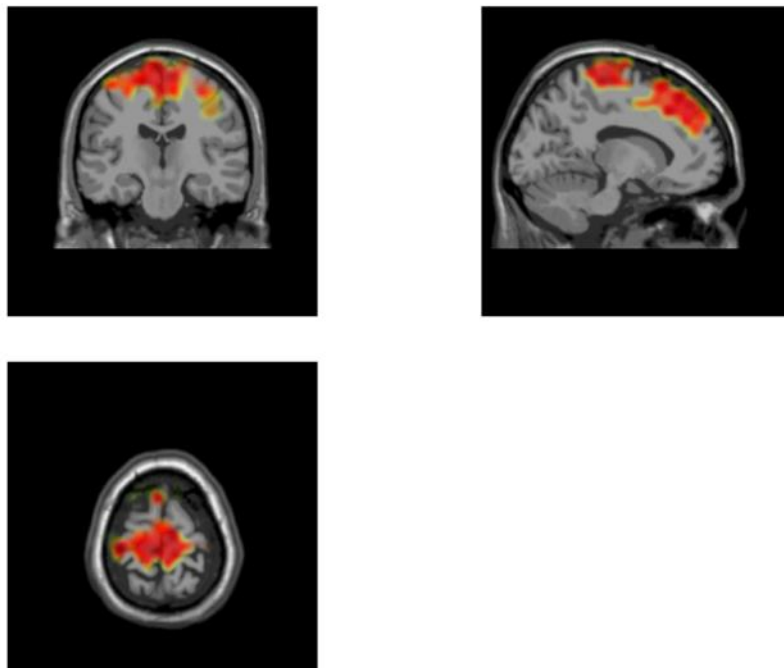
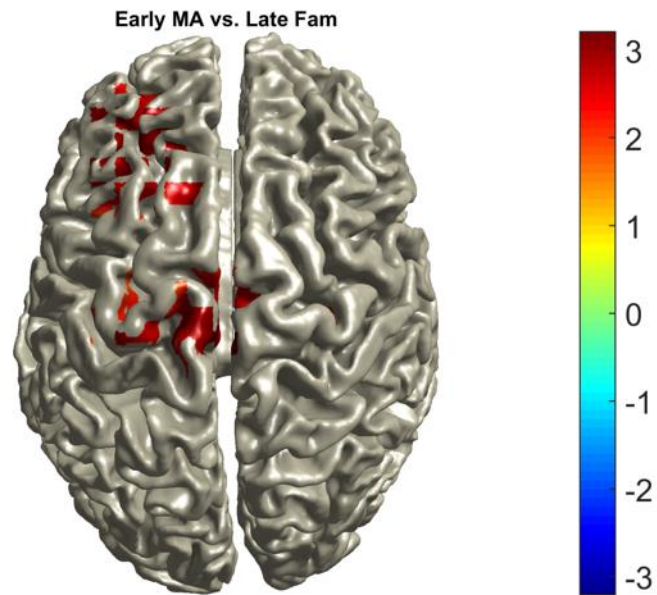


Figure 6-5: Source-level non-parametric permutation test on  $\gamma$  CMC with Biceps Brachii muscle when comparing Early MA vs. Late Fam.

Surface- and ortho-plots of group-level positive clusters during Early MA with respect to Late Fam in low  $\gamma$  frequency band. Colour-coded areas represent significant changes (i.e. increase,  $p < 0.0083$ ) in CMC of the Biceps Brachii muscle between the two conditions.

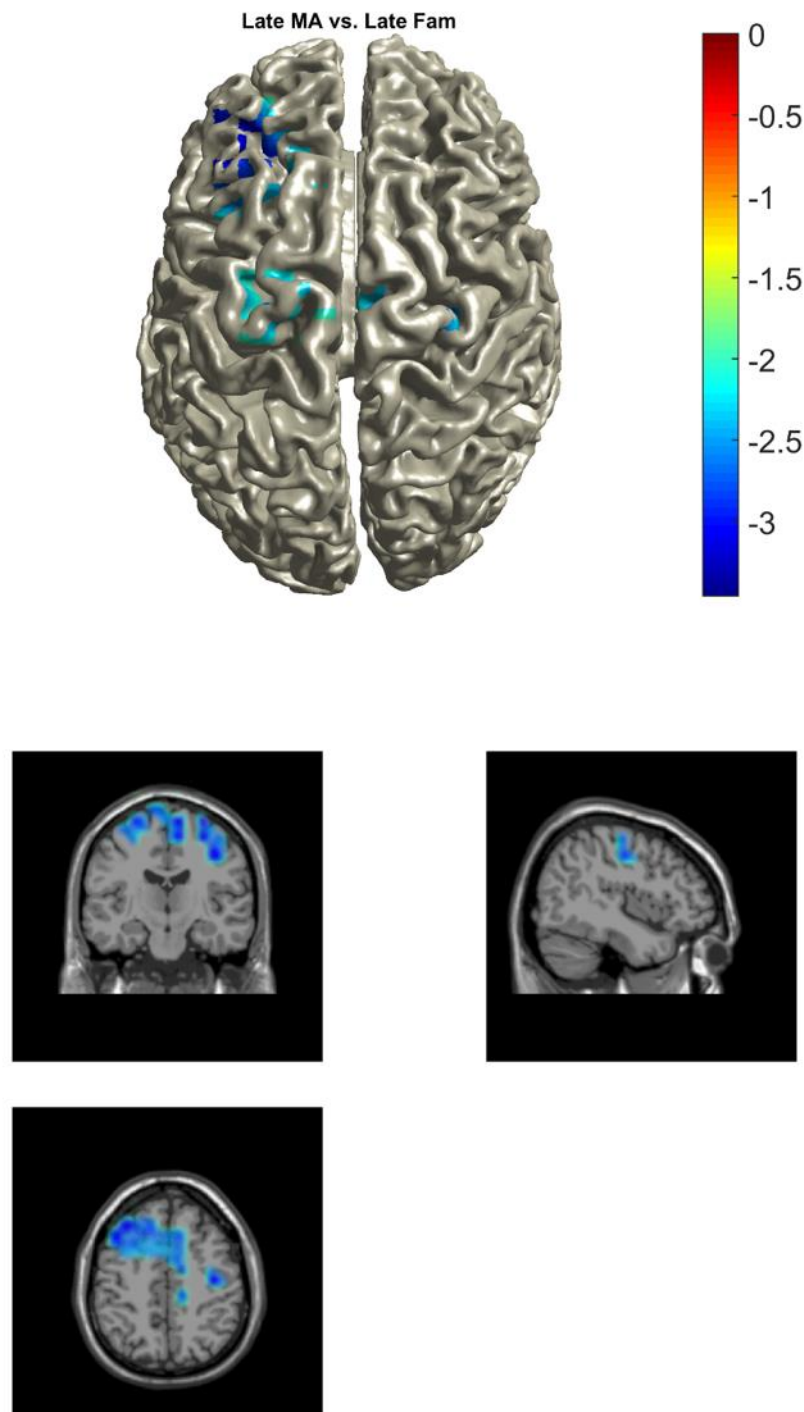
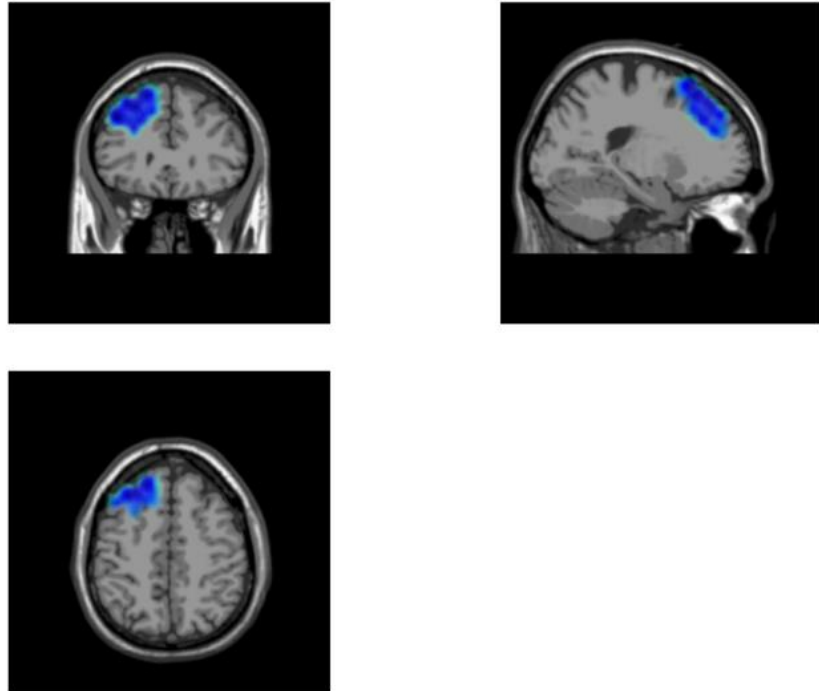


Figure 6-6: Source-level non-parametric permutation test on  $\beta$  CMC with Extensor Carpi Radialis muscle when comparing Late MA vs. Late Fam.

Surface- and ortho-plots of group-level negative clusters during Late MA with respect to Late Fam in  $\beta$  frequency band. Colour-coded areas represent significant changes (i.e. decrease,  $p < 0.0083$ ) in CMC of the Extensor Carpi Radialis muscle between the two conditions.

**A)**



**B)**

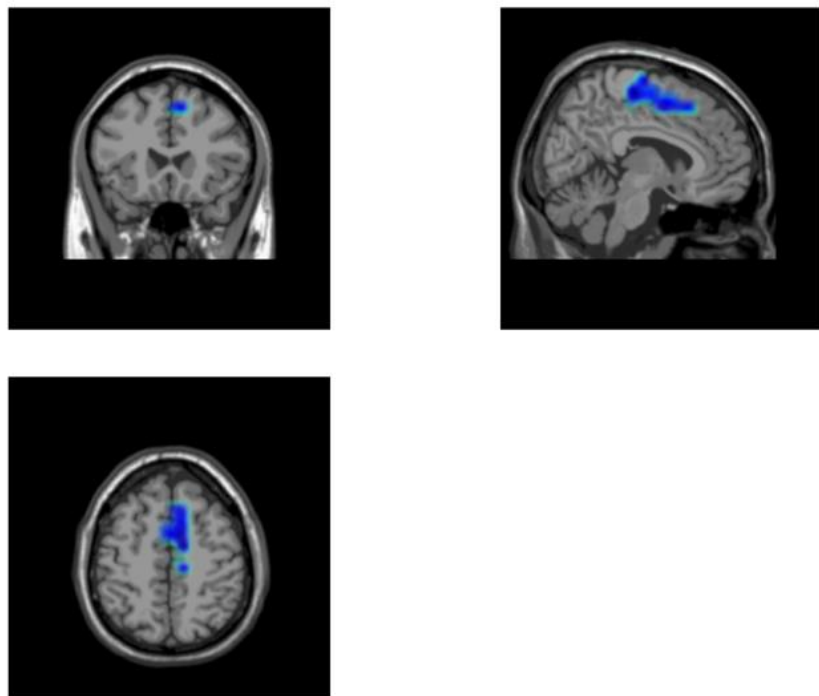


Figure 6-7: Source-level non-parametric permutation test on  $\beta$  CMC with Biceps Brachii (A) and Extensor Carpi Radialis (B) muscle when comparing Late MA vs. Early MA.

Ortho-plots of group-level negative clusters during Late MA with respect to Early MA in  $\beta$  frequency band. Colour-coded areas represent significant changes (i.e. decrease) in CMC of the Biceps Brachii (A) and of the Extensor Carpi Radialis (B) muscle during adaptation.

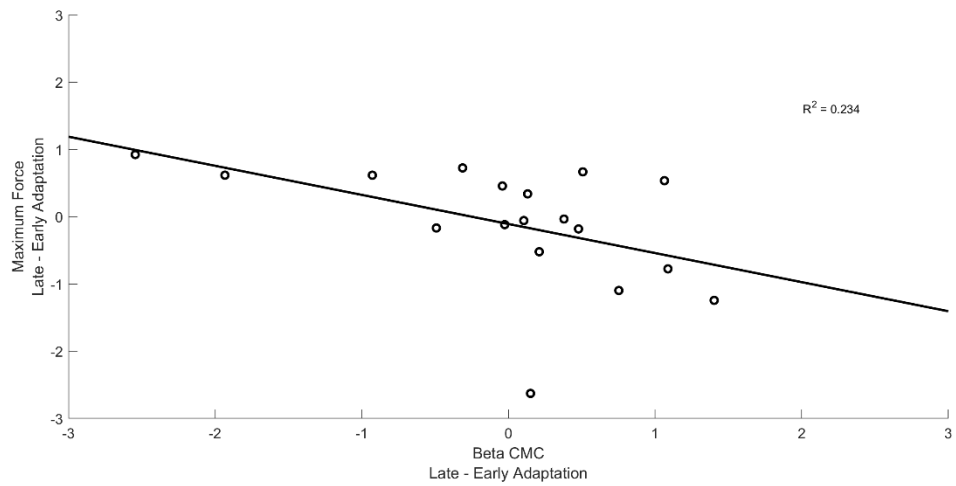


Figure 6-8: Changes in ECR-left SMA  $\beta$  CMC average between late and early adaptation correlate with differences in maximum exerted force.

Single-subjects maximum force values (difference between Late MA and Early MA) are plotted against the ECR-left SMA  $\beta$  CMC average values (difference between Late MA and Early MA). This correlation shows that a reduction of  $\beta$  CMC in left SMA moderately contributes to the stabilization and regulation of the maximum exerted force: subjects that needed to diminish their force indeed increased cortical activations ( $\beta$  CMC).

Table 6-1: Non-parametric cluster-based permutation test on CMC changes with respect to natural reaching.

For each significant comparison ( $p < 0.0083$ ) the statistically significant ROIs, the number of voxels found significant per each ROI and their percentage with respect to the total within the ROI are reported

<b>Early MA vs. Late Fam, low <math>\gamma</math> (35-45 Hz)</b>				
<b>Muscles</b>	<b>ROIs</b>	<b>Num. Sig. Voxels</b>	<b>Num. Sig. Voxels (%)</b>	<b>ROI Voxels</b>
<b>Biceps Brachii</b>	Left M1	14	23.7	
	Right M1	17	28.3	
	Left Superior FC	37	53.6	
	Left Medial FC	55	75.3	
	Left SMA	22	84.6	
	Right SMA	30	66.7	
	Left S1	5	8.3	
	Left Paracentral Lobule	21	100	
	Right Paracentral Lobule	13	81.2	
<b>Late MA vs. Late Fam, <math>\beta</math> (15-25 Hz)</b>				
<b>Extensor Carpi Radialis</b>	Left M1	14	23.7	
	Right M1	22	36.7	
	Left Superior FC	25	36.2	
	Left Medial FC	46	63.0	
	Left SMA	6	23.1	
	Right SMA	24	53.3	
	Left Paracentral Lobule	3	14.3	
	Right Paracentral Locule	2	12.5	

Table 6-2: Non-parametric cluster-based permutation test on CMC changes during adaptation.

For each significant comparison the statistically significant ROIs, the number of voxels found significant per each ROI and their percentage with respect to the total within the ROI are reported.

<b>Late MA vs. Early MA, <math>\beta</math> (15-25 Hz)</b>				
<b>Biceps Brachii</b>	<b>ROIs</b>	<b>Num. Voxels</b>	<b>Sig.</b>	<b>Num. Sig. Voxels (%)</b>
	Left Superior FC	28		40.6
	Left Medial FC	55		75.3
<b>Extensor Carpi Radialis</b>	Left SMA	2		7.7
	Right SMA	30		66.7

## **6.4 Discussions**

### **6.4.1 Novel findings**

Evidence of cortico-muscular communication during a robot-mediated force-field motor adaptation task was identified in the current study. The primary goal of the investigation was to observe changes in cortico-muscular coherence over time across different stages of motor adaptation and with respect to a natural reaching behaviour. Sensor-level CMC data were projected back from the scalp to the cortex via beamforming techniques, which allowed for a better localization and higher spatial resolution of the coherence evidence. At source level, changes in CMC across different stages of adaptation in comparison to natural reaching were identified in multiple brain regions as frontal, premotor and sensorimotor areas, in line with previous findings (Baker, 2007; Babiloni et al., 2008; Fang et al., 2009; Whitam et al., 2010; Rossiter et al., 2013; Gentili et al., 2015; Belardinelli et al., 2017). Moreover, CMC differences observed specifically during the motor adaptation process were confined to frontal areas (i.e. superior frontal cortex, medial frontal cortex and SMA) and successfully correlated with the maximum force exerted by subjects, thus showing a direct link between cortical oscillations and muscular activations required to properly perform the task. These findings consolidate the belief that CMC is a valid assessment tool for motor impairments, integrity of the cortico-muscular communication line and recovery after neural injuries (Mima et al., 2000; Fang et al., 2009; Rossiter et al., 2013; von Carlowitz-Ghori et al., 2014; Belardinelli et al., 2017), for degenerative processes such as ageing (Kamp et al., 2013; Bayram et al., 2015), as well as a potential reference measure for BCI rehabilitation applications (von Carlowitz-Ghori et al., 2015), and could be used to evaluate progress in recovery with motor adaptation paradigms in clinical practice.

### **6.4.2 The natural reaching movement**

An exemplary subject sensor-level CMC results showed muscle- and frequency specific activations above the subject-specific threshold (Rosenberg et al., 1989) (Figure 6-1): only a few subjects ( $n = 5$ ) did not present significant coherence values in line with previous literature, confirming the observation that not all individuals present CMC during both upper- and lower-limb motor task (Perez et al., 2006; Fu et al., 2014), likely due to differences in cortical wiring and efficiency, and that a period of practice and adaptation can enhance the cortico-muscular relationship (Mendez-Balbuena et al., 2011). Accordingly, attention was given to the differences that the planned motor adaptation paradigm was able to induce rather than the absolute coherence values per-se (same



approach as Gentili et al., 2015), thus all subjects were included in the subsequent analyses. Source-localized activities during natural reaching show a prominent peak of CMC on the contralateral (left) sensorimotor cortex in  $\beta$  band for each muscle of interest (Figure 6-2, 6-3 and 6-4, first row), with less contribution from the  $\gamma$  band.  $\beta$  band CMC is known to reflect mainly efferent drives from the motor cortex to muscles (Mehrkanoon et al., 2014) and to be context specific (Baker, 2007), thus multiple theories have been proposed to account for its activity. Extensive work has been done on the maintenance of a steady motor output through isometric contraction tasks (Conway et al., 1995; Halliday et al., 1995; Kilner et al., 1999; Kilner et al., 2000; Kristeva et al., 2007; Witte et al., 2007), whereby  $\beta$  band CMC is stronger when compensating for a static perturbation and disappears in favour of  $\gamma$  CMC when counteracting a dynamic force (Kilner et al., 1999; Marsden et al., 2000; Omlor et al., 2007; Kamp et al., 2013). According to this line of research,  $\beta$  band oscillations represent a cortical state promoting maintenance of the “status-quo” and the steady state motor output in terms of muscles force (Engel and Fries 2010). An increase of  $\beta$  CMC was linked to augmented isometric contraction and performance (Kilner et al., 2000; Kristeva et al., 2007; Mehrkanoon et al., 2014), but its decrease when compensating for a dynamic force in an isometric fashion suggests that the maintenance of the motor output is not its only function. Moreover, the task performed in the current study was dynamic and more complex: reaching requires target definition, planning and movement accuracy to be precisely executed. The cortico-muscular relationship in both the  $\beta$  and  $\gamma$  frequency bands have been previously reported for dynamic complex movements such as reaching (Fang et al., 2009) and hand grip (Rossiter et al., 2013) in both healthy and stroke populations, as well as during a pick-up task in monkeys (Murthy and Fetz, 1992), finger movements (Fu et al., 2014) and dynamic bilateral ankle dorsi-flexion movements (Yoshida et al., 2017) in humans. In more complex contexts, it is likely that cortico-muscular coherence is symbolic of the integration of both the central (feedforward, motor) and peripheral (feedback, sensory) drives (Baker, 2007) for the optimal fulfilment of the task. The  $\beta$  band CMC observed during natural reaching is here suggested as not merely indicative of cortical motor commands guiding muscle activity but instead symbolic of a sensorimotor integration phenomenon, whereby motor and sensory drives are integrated to accomplish an optimal performance.

### **6.4.3 The disturbed reaching movement and the adaptation process**

At the early stages of adaptation an increase of  $\gamma$  CMC occurred in frontal (i.e. superior frontal cortex, medial frontal cortex), premotor (i.e. SMA) and sensorimotor (i.e. M1 and S1) areas for the Biceps Brachii, muscles (see Figure 6-5 and Table 6-1), a muscle actively involved in counteracting the applied perturbation (Pizzamiglio et al., 2017). The areas showing increased  $\gamma$  cortico-muscular coupling have been previously identified as playing a major role during visuomotor adaptation (Brovelli et al., 2015). As previously mentioned, also  $\gamma$  CMC involves mainly efferent drives to muscles (Mima et al., 2000; Schoffelen et al., 2005; Witham et al., 2010; Mehrkanoon et al., 2014) and represents a complex process by which sensory feedback drives and motor feedforward commands are integrated to organise voluntary motor actions (Brown et al., 1998; Omlor et al., 2007; Fang et al., 2009). The increased  $\gamma$  CMC could therefore be attributed to changes in both feedforward and feedback drives (Riddle and Baker, 2005; Baker, 2007). The introduction of an external force-field changed how muscles and joints were stimulated with respect to a natural reaching movement, thus more feedback information was likely to be sent to the central system in order to properly plan and counteract the perturbation. Increased  $\gamma$  CMC could therefore be the result of a stronger sensorimotor integration due to the increased amount of sensory feedback coming from the periphery. This argument implies that the changes are simply task- and condition-related: as the perturbation is constant for the all trials of MA, the change in CMC should have persisted in both early and late stages of adaptation. However, this is not the case, as during late adaptation  $\gamma$  CMC is not significantly higher than during natural reaching. Therefore, stronger  $\gamma$  CMC is likely the result of an increase in both sensory feedback and feedforward motor commands at early stages of adaptation when subjects are still naïve to the perturbation and the reaction is based on strong muscle co-contraction and reflexes rather than on strategic adaptive compensation (Milner and Franklin, 2005; Pizzamiglio et al., 2017). This is further validated by the fact that at later stages of adaptation  $\gamma$  CMC is visibly stronger than during natural reaching: here feedback drives are constantly higher than during natural reaching, but subjects are progressively adapting and need less control over the task (i.e. from controlled and naïve to automatic and skilled). Indeed, increased  $\gamma$  CMC occur in a wide cortical cluster including frontal, premotor and sensorimotor areas which are either directly (M1) either indirectly connected to the muscles. This confirms CMC as a symbol of complex processes that, through integration of sensory and motor information (M1/S1) (Witham et al., 2010), plan the required muscle activation to

compensate for the perturbation (Babiloni et al., 2008), minimizing error and optimizing performance. Moreover, previous work has demonstrated that CMC can be modulated by motor as well as cognitive demands: more focused attention and cognitive efforts (Safri et al., 2006; Safri et al., 2007; Schoffelen et al., 2005) enhance  $\gamma$  CMC, whereas the execution of simultaneous secondary tasks and divided attention (Safri et al., 2007; Kristeva-Feige et al., 2002) reduces it. In this study, subjects were likely to be more attentive at the beginning of the adaptation condition, when naïve to the perturbation, and then release the attention at later stages when the task became more automatic thanks to ongoing adaptive strategies. Therefore, the increased  $\gamma$  CMC during early stages of adaptation could be the result of a stronger sensorimotor integration process combined with more focused attention to the task from which specific muscle activations and inter-synchronizations would result for a better performance (Reyes et al., 2017; Pizzamiglio et al., 2017).

With respect to natural reaching, during late stages of adaptation a decrease of  $\beta$  CMC was observed for the Extensor Carpi Radialis muscle (see Figure 6-6 and Table 6-1). TB, BB and ECR are all actively involved in counteracting the applied perturbation: if the upper-arm muscles are the “propeller” and major actuators of the reaching movement, the forearm muscle is likely to be involved in the stabilization of the forearm during the disturbed movement. It was previously demonstrated that muscles specifically involved in the promotion of the reaching movement and in the counteraction of the perturbation share a coherent intermuscular coupling at high frequencies which enable a reduction of useless co-contraction and the saving of energy (Pizzamiglio et al., 2017). In parallel, recent findings have shown that the cortico-muscular relationship resembles a complex mechanism of intermuscular binding at the cortical level whereby reduced  $\beta$  CMC represents a muscular unbinding process required to handle the requested motor task through independent (not synergetic) muscle activations (Reyes et al., 2017). A decrease of  $\beta$  intermuscular coherence is thus likely to occur in unstable situations (i.e. perturbed reaching movement and spring compression at high level of force) (Houweling et al., 2010), when novel intermuscular collaborations need to be developed or independent control of muscles takes over synergetic mechanisms. In line with what was previously mentioned, the reduced  $\beta$  CMC in a wide cortical cluster (including frontal, premotor and sensorimotor areas) is here suggested to be the result of sensorimotor integration and planning processes according to which less forearm activation (co-contraction) is required to compensate for the force in later stages of adaptation, when performance is improving thanks to ongoing adaptive strategies.

The cortical areas that showed both an increase in  $\gamma$  CMC and a decrease of  $\beta$  CMC during early and late stages of adaptation respectively were further tested for changes during the adaptation process only. A decrease of BB- $\beta$  CMC was found in the superior and medial frontal cortex, whereas a decrease of ECR- $\beta$  CMC was observed in the bilateral SMA (see Figure 6-7 and Table 6-2). Interestingly, the reduction of  $\beta$  CMC during adaptation occurs not in the primary motor cortex but in the frontal (superior-medial) and SMA regions, indirectly connected to muscles through connections to M1 (Darian-Smith et al., 1993). Frontal and premotor areas (extending from superior to medial inferior frontal gyrus) have been previously shown to be recruited during hand flexion-extension movements in stroke survivors after 4-weeks BCI rehabilitation (Belardinelli et al., 2017). These areas are therefore likely to be indirectly involved in the control of voluntary movements, and more specifically in the early stages of the motor adaptation process as extensively described in literature (Krebs et al., 1998; Shadmehr and Holcomb, 1997; Lage et al., 2015). The anterior prefrontal cortex (namely the BA10 area; Carlen, 2017) has been previously shown to indirectly control cognitive-motor performance (Babiloni et al., 2008).  $\beta$  cortico-cortical coherence between FZ and F3 electrodes (positioned over SMA and dlPFC areas) was reduced during a visuomotor adaptation task whereby subjects had to draw lines in a centre-out fashion, suggesting the involvement of medial-left prefrontal cortex in the modulation of adaptation control (Gentili et al., 2015). This phenomenon of “cortical refinement” was attributed to a progressive disengagement of not-essential frontal executive processes as a result of practice. Our findings cannot speculate on the formation of internal models of adaptation and on the progressive transfer of the control of learning from the cortico-striatal to the cortico-cerebellar loop (Krebs et al., 1998), but can convey information on the changes in control on the activation of muscles during the adaptation process. Indeed, a linear relationship was found between changes in ECR- $\beta$  CMC in the left SMA and changes in the maximum exerted force (Figure 6-8). ECR- $\beta$  CMC in the left SMA is moderately correlated with the maximum exerted force so that stronger cortical activations (i.e. increased  $\beta$  CMC) are needed to reduce the exerted force, if exceeding the minimum needed. Previous work has found a linear relationship between CMC and output force in both healthy and elderly (Bayram et al., 2015; Brown et al., 1998; Mima et al., 1999). SMA is known to provide input to the primary motor cortex (Witham et al., 2010; Darian-Smith et al., 1993) and to be involved in the motor adaptation process: it is likely to be recruited to plan the muscle activation required during the task to produce the needed counteracting force and minimize the energy costs.  $\beta$  CMC in SMA is therefore here suggested to resemble a force

modulation process operating through changes in muscular activations (Reyes et al., 2017) during which natural synergetic strategies are disrupted and new ones are created to optimize performance and minimize energy expenses.

#### **6.4.4 Cortico-muscular and intermuscular coherence in rehabilitation**

Evaluating CMC allows assessment of the integrity and functionality of the neural pathways linking the brain and the muscles, in both descending and ascending directions. To further strengthen the validity of the presented cortico-muscular findings, parallel investigations evaluated intermuscular coherence (IMC), a measure of the neural coupling between muscles evaluated in the frequency domain. IMC likely encompasses efferent and afferent inputs from both the cortical (i.e. cerebellar, reticulospinal) and the local peripheral (i.e. spinal, motoneuronal) circuits (Brown et al., 1999; Grosse et al., 2002; Lemon, 2008; Narzarpour et al., 2012). Given the broad spectrum of influences embedded within measures of intermuscular evidence, it is a valid argument in support of cortico-muscular claims made here when aiming to disentangle the effects of cortical inputs on muscles activity (Boonstra, 2013). Recent studies claimed that movements performed in unstable situations require the disruption of actual muscular couplings in favour of the creation of novel binding mechanisms able to sustain the requested motor tasks; at this regard, reduced  $\beta$  intermuscular and cortico-muscular coherence were suggested as potential indicators of such decoupling processes (Houweling et al., 2010; Reyes et al., 2017). A preliminary investigation of intermuscular coherence during motor adaptation to an external clockwise robot-mediated force field was undertaken during this work of thesis but in separate settings (Pizzamiglio et al., 2017). Time-frequency mapping of IMC during the period from visual cue to 3 seconds afterwards showed a progressive significant increase of IMC from early to late adaptation in high  $\gamma$  frequencies (40-100 Hz) in those pairs of muscles mostly recruited to promote the reaching movement and concurrently counteract to the external perturbation. Interestingly, the progressive increase of high  $\gamma$  IMC occurred in parallel to the decrease of movement error and co-contraction profiles. It was postulated that the observed IMC changes were symbolic of an underlying neural strategy coordinating multiple muscles together in order to optimize performance (Mohr et al., 2015), while minimizing co-contraction levels, effort and metabolic costs (Huang and Ahmed, 2014; Watanabe and Kohn, 2015). Little attention was at that time given to IMC changes in lower frequency bands, whereby a reduction of IMC was observed during the dynamic stage of the movement with respect to the static isometric initial and final phases (Pizzamiglio et al., 2017, see Figure 6 for example). Additional analyses will be carried out in the current investigation in order to focus on

the changes in IMC during adaptation in the  $\beta$  frequency (Pizzamiglio, Belardinelli, Ziemann and Turner, 2018, in preparation): in line with the theories reported above, a significant decrease of  $\beta$  IMC is expected during adaptation among muscles undergoing an unbinding process, further validating the findings of reduced  $\beta$  CMC. All these arguments reveal an added value of the IMC approach with respect to other methodologies, such as co-contraction analyses. As previously demonstrated (Pizzamiglio et al., 2017), during adaptation all muscles exhibit high levels of co-contraction in early stages of adaptation and only the time of maximum co-contraction seems to reliably disentangle the effects of specific motor tasks (i.e. opposite force-field directions). Therefore, IMC seems a more valid technique to evaluate the most relevant functional contribution during specific motor tasks (De Marchis et al., 2015). Moreover, IMC has been shown not to depend on age, consequently representing another strong eligible biomarker for neurological changes in muscle activation (Jaiser et al., 2016). Consequently, IMC as well as CMC might be appointed as reliable assessment measures during rehabilitative interventions. Interestingly, online modulation of cortico-muscular coherence has been recently tested in a neurofeedback experiment with a cohort of healthy adults (von Carlowitz-Ghori et al., 2015). Subjects were requested to move a lever with their right thumb against a load and hold it maintaining a constant level of generated force whilst receiving feedback on a screen based on the level of CMC produced [0-1]. The task required them to either increase either decrease the level of CMC through a self-chosen mental strategy without changing the motor outcome (i.e. the level of generated force). Outstandingly, subjects successfully modified their CMC level through the neurofeedback provided without changing the level of force produced, suggesting that no functional changes occurred between the cortex and the spinal cord, but that specific neurophysiological mechanisms were developed only cortically. These findings are quite promising as rehabilitation based on the online modulation of cortico-muscular or even intermuscular couplings could induce the repair and/or the creation of neural mechanisms in the affected areas (i.e. both cortex and cortico-spinal pathways), promoting neuroplasticity and recovery. Indeed, the mental strategies that would most effectively promote online modulation of these features are still to be reliably identified, thus further research with both healthy individuals and, for example, stroke survivors is needed to consolidate such approaches. In conclusion, both CMC and IMC could be used as reliable markers during rehabilitation, whereby specific neural and muscular couplings could be the targets of specific individualised therapies.

#### **6.4.5 Limitations**

As previously mentioned (see chapter 4, paragraph 4.4.4, and chapter 5, paragraph 5.4.5), subjects did not show a complete adaptation by the end of the condition. This is further supported by the cortico-muscular findings: more trials would result in more reliable coherence evidence (in terms of subject-specific threshold calculation) and would allow subjects to completely adapt to the novel environment, likely promoting stronger and more specific CMC changes. Moreover, despite the positive results obtained through the localization of cortico-muscular neural source, only 62 channels (mastoids excluded) and a template T1-MRI scan were used in the beamforming algorithm. Future studies should consider employing a higher number of electrodes (e.g. 128) and individual structural MRI in order to optimize the process of localization of cortical sources.

## Study II: Real-world Scenario

### 7 Neural correlates of single- and dual-task walking in the real-world

#### 7.1 Introduction

The study of human behaviour in its natural environment has always been hindered by limited technology and the large number of external influences one would have to account for. On the other hand, the laboratory-based approach undertaken in the last decades by the neuroscientific community have enabled a better understanding of specific (neuro-) physiological control mechanisms in the human brain responsible for locomotion. The advantage of having a fully-controlled lab environment that requires the subjects to focus only on one specific task however pays the cost of leaving the “real-world” context excluded (i.e. not-ecologically valid). Furthermore, using un-natural stimuli and experimental designs was of significant concern in the past (Brunswick, 1943; Bronfenbrenner, 1977) and is currently regaining much attention because of the translation of assistive and supportive technologies into daily-life applications (Gramann et al., 2014; Gramann et al., 2017). Indeed, studying behavioural and psychological phenomena abstracted from the environment in which they usually take place results in an uncomplete understanding of the mechanisms behind them. Animal studies have demonstrated how the same behaviour is obtained with different neurophysiological mechanisms when performed in the over-controlled laboratory compared to the natural environment and/or when moving (Chen et al., 2013; Arenz et al., 2017). Recent technology developments have focused on the production and validation of “mobile” instrumentation: light-weight, easy to mount and nearly-wireless and some studies have adopted this “mobile lab” approach allowing subjects to move freely and thus enabling the study of their behaviour in a more natural framework (Ehinger et al., 2014; Jungnickel and Gramann, 2016; Wagner et al., 2016). The further development of robustly designed mobile technology for the recording of body movement and dynamics (e.g. inertial sensors), muscles activities (e.g. electromyography) and brain neural and hemodynamic oscillations (e.g. electrophysiology and spectroscopy) now allows the researcher to venture outside the laboratory and observe human natural behaviour in the real-world.

Bipedal walking is the most important behaviour typical of the human species and has been extensively investigated from a biomechanical perspective in the healthy young population and older and neurologically impaired individuals (Beyart et al., 2015; Del Din et al., 2016). For healthy individuals, walking is one of the most natural activities to perform and for a significant proportion of time further tasks such as navigating,



conversing or listening to music are often undertaken. However, even healthy subjects demonstrate decreased gait performance when walking and engaging in a challenging secondary task such as messaging over a smartphone (Schabrun et al., 2014; Agostini et al., 2015). Therefore, the human habit of walking and simultaneously doing something else should raise some concerns on the level of attention required for each task and how this would affect alertness of the surroundings (e.g. when walking and texting while navigating on a crowded sidewalk). For neurological impaired patients (e.g. hemiplegic stroke survivors, Parkinson's disease patients, elderly with executive functions deficits) walking itself can be challenging or even impossible without external support (Iosa et al., 2014; Menz et al., 2003; Latt et al., 2009; Maidan et al., 2016). If engaged in a secondary task or in a more complex path / route, even the well-recovering neurological patients can show greater attention and effort paired with gait speed reduction and a tendency towards impaired locomotion (Maidan et al., 2017). Therefore, understanding the neural correlates of dual-task walking could shed some light on the potential side effects and risks it conveys for healthy subjects, as well as consolidate the understanding of the limits of the neurologically impaired brain. The final goal would be identifying new opportunities for assistive and supportive technologies for daily-life real-world activities. Thanks to the progress in mobile technologies, the neural correlates of gait in the healthy young population have been recently investigated with high-density electroencephalography (Gwin and Ferris, 2012; Seeber et al., 2014; Wagner et al., 2012; Wagner et al., 2014; Wagner et al., 2016). In parallel, many studies have observed the impact of walking while performing a secondary task on brain hemodynamics through means of functional near-infrared spectroscopy (fNIRS), both in healthy young and old adults and neurological groups (Al-Yahya et al., 2016; Lin and Lin, 2016; Maidan et al., 2016; Maidan et al., 2017). The challenge of being able to record natural human behaviour in the real-world is now possible to overcome, however much still needs to be done to understand how our brain and behaviour are linked in their natural environment.

In this study, a fully-mobile setup for real-world applications was designed, implemented and further validated by investigating neural correlates of natural single- and dual-task walking in an open-space, outside the laboratory environment. In order to insert subjects within the most natural settings and mimic daily-life experiences, secondary tasks consisted in either having a conversation with the experimenter or reading and replying to an email from a smartphone. Gait performance was expected to decrease from single-task to dual-task walking as previously and extensively described (Menz et al., 2003; Francis et al., 2015; Schabrun et al., 2014; Caramia et al., 2017; Yogev-Silgeman et

al., 2010). Neural correlates of single-task walking were expected to replicate previous findings obtained within the laboratory environment (Gwin et al., 2010; Seeber et al., 2014) as representing the neurophysiological bases of walking per se. However, predicting how the brain would react to a simultaneous and continuous secondary task while walking (i.e. moving) in the real-world is challenging, as most dual-task studies have been carried out within the laboratory environment with highly restrictive experimental settings (Wahn and König, 2017). We hypothesized that real-world dual-task conditions would engage brain areas related to higher executive functions and planning (e.g., anterior and dorso-lateral pre-frontal cortex, PFC; Ford et al., 2002; Giraud et al., 2007) and areas involved in complex sensorimotor integration and spatial navigation (e.g., sensorimotor cortex, SMC; posterior parietal cortex, PPC; Buneo and Andersen, 2006; Engel and Fries, 2010; Sipp et al., 2013; Beurskens et al., 2016; Bradford et al., 2016; Wagner et al., 2016). The results suggested that there were condition-specific patterns of neural activation that differed with the nature of the secondary task and that there were frequency specific neural biomarkers for different real-world ambulatory scenarios.

## **7.2 Materials and methods**

### **7.2.1 Ethical approval**

Eighteen right-handed healthy young adults [age mean ( $\pm$  standard deviation; SD) = 25 ( $\pm$  3), 7 male/11 female, range = 20-31] with no previous history of neurological, musculoskeletal or gait disorders (see Appendix II), agreed to participate in this study by giving written informed consent (see Appendix III). The study was approved by the University of East London Ethics Committee (UREC\_1415\_29, see Appendix I) and all experiments were conducted in accordance with the Declaration of Helsinki. Data of three subjects were discarded because of problems during data acquisitions (2 males, 1 female), leaving a total of fifteen subjects [age mean = 26 ( $\pm$  3), 5 male/10 female, range = 20-31]. One subject (female) was ultimately excluded from group-level analysis due to the very high level of gait-related noise within the neurophysiological data, leaving a total of fourteen subjects [age mean = 26 ( $\pm$  3), 5 male/9 female, range = 2-31].

### **7.2.2 Experimental protocol**

Subjects were first prepared in the laboratory room UH.2.07, University House building (UH), Stratford Campus, University of East London (Figure 7-1). Once ready, they started the experiment by performing three minutes of resting state (i.e. Baseline) standing still with their eyes open in the lab. Subjects were then guided through the UH building outside

to the garden (Figure 7-1): during this period, no signals were recorded and subjects were told to get familiar with the setup and communicate to the experimenter if anything was not properly set. Once outside, subjects were given all the details related to the experiment, specifically 1) the predefined walking path was shown to them (Figure -1), 2) they were told to walk at their preferred natural speed, as it has been shown that it optimizes gait behaviour (Sekine et al., 2013) and 3) they were asked to minimize any artefacts or extreme-movements that could have affected the recordings. Experiments consisted of three conditions during which subjects walked along the predefined path naturally (Single-Task, ST), conversing with the experimenter (Dual-Task1, DT1) or texting with their smartphone (Dual-Task2, DT2). The dual-task conditions were randomized across subjects in order to avoid bias in gait behaviour and recordings, whereas the ST condition was performed always as first in order to have a common baseline before the dual-task and to familiarise the participants with the walking path. The designed dual-task conditions were meant to represent real-life situations and, to standardise them, conversations during DT1 were based on a set of standard questions, whereas in DT2 subjects read and replied to a standard email (Table 7-1). In each condition, subjects walked the predefined path twice covering a total distance of 200 metres. Between-condition resting periods were given to subjects to avoid fatigue and to remind them of the next condition instructions. The experimenter followed the subjects during each condition recording videos of gait behaviour. Experiments were carried out only during dry days free from strong winds and/or rain. During the ST condition, the subject walked freely with arms swinging on either side of the trunk; in both the dual-task conditions the subject walked with the hands in front holding the smartphone, but with the head straight when conversing (i.e. DT1) and bent downwards slightly looking at the smartphone when texting (i.e. DT2). Consequently, each condition is characterised by slightly different whole-body biomechanics. A summary of each single subject experiment is reported in Table 7-2.

### **7.2.3 Recording techniques**

The implemented setup presented in 7 6-2 is fully mobile and allows the recording of physiological and behavioural data during walking (or any other mobile situation). Muscle activity (EMG; mV) was recorded from the right/left Tibialis Anterior and Soleus by two monopolar superficial electrodes per muscle, positioned at a 1.5 cm inter-electrode distance according to the belly-belly montage and following the SENIAM guidelines (Hermens et al., 2000). Brain activity (EEG;  $\mu$ V) was recorded via a high-density 64 channel Waveguard cap (ANT Neuro, Enschede, Netherlands), with impedances kept

below 5 k $\Omega$  for the whole duration of the experiment. EMG and EEG activities were simultaneously and continuously recorded by an EEGoPro amplifier (ANT Neuro, Enschede, Netherlands) at a sampling frequency of 1 kHz and filtered between 0.1 and 500 Hz. During the recording, EEG data were referenced to the FCz channel. The EEG cap was connected to the amplifier via two separate 32-pins serial ports (i.e. 32 channels per port). Surface EMG electrodes were plugged into a bipolar-channel box external to the amplifier and connected to it via a secondary 25-pins serial port. Data were recorded and saved within the same file (thus they were already synchronized) by the EEGoPro software installed on a DELL tablet, connected via USB to the amplifier and carried by the subject within the backpack, together with the amplifier. A Samsung Galaxy S4 mini smartphone was fixed at the subject's lower back with an elastic belt and data from its internal accelerometers and gyroscope were recorded through the AndroSensor app (<http://www.fivasim.com/androsensor.html>) at a frequency of 200 Hz, saved as .csv files at the end of each condition and ultimately downloaded for offline analyses. Smartphone position choice was dictated by literature investigation: lower back position is the currently most preferred and reliable location to observe changes in gait patterns across different conditions and populations (Iosa et al., 2014). Two digital Force Sensing Resistor sensors (FSRs) were employed as contact switches and fixed underneath the subject's heels to detect times of heel strikes. Data were recorded at 1 kHz by a 14 bit analog-to-digital converter (DataLog MWX8, Biometrics Ltd, Newport, UK) fixed at the subject's hip by the elastic belt. These sensors return a digital binary output where the active edge is set 1-to-0, i.e. 0 when the heels make contact with the ground. A digital button (1-to-0 active edge) was also connected to the converter and pressed by the subject for circa 5 seconds at the beginning and at the end of each condition to define time points of start and finish. Signals were recorded on a micro SD card and further downloaded and stored for offline analyses. Elastic bands were also placed around the subject thighs to fix the cables of contact switches and surface EMG electrodes to avoid uncomfortable situations and prevent the subject from falling/stepping on them. To synchronize data from the digital sensors representing important time points (i.e. start, heel strikes, end) with physiological evidences, a common TTL pulse was simultaneously sent to both the DataLog MWX8 converter and the EEGoPro amplifier at the beginning and at the end of the experiment, and then offline used as milestones for realigning the signals' time axes. Moreover, a video of the subject walking during each condition was recorded to monitor the behaviour and keep track of any important events (e.g. external disturbance, big movements, etc).



Figure 7-1: UEL Stratford Campus map and subjects walking path.

Subjects were first prepared in the laboratory (pink star) and then accompanied outside along the black-dashed path. They were then given specific instructions on the path to follow during the experiment (red-dashed path), starting and finishing always in the same position (yellow start).

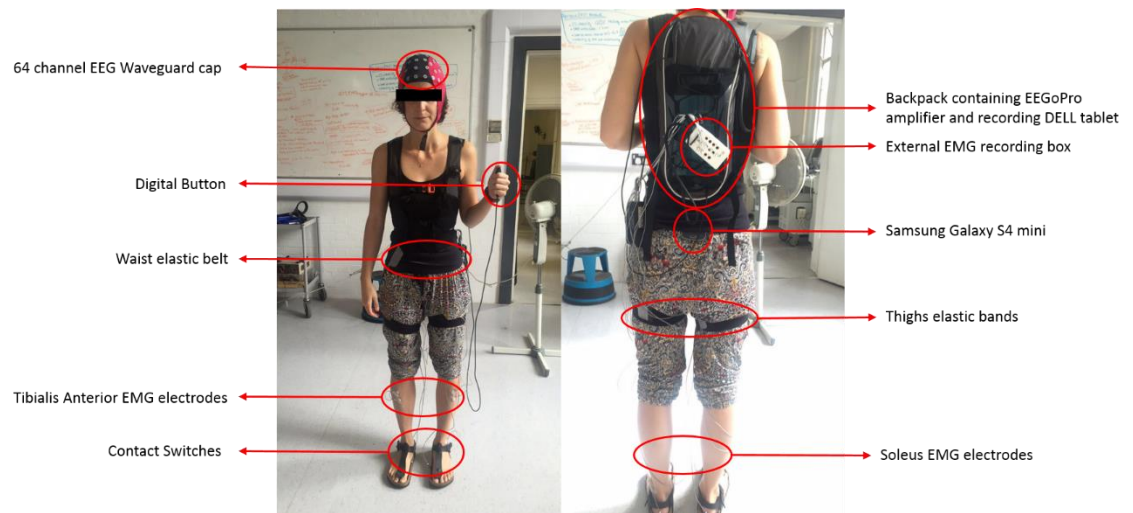


Figure 7-2: Mobile Setup for real-world experiments.

During walking experiments, subjects carried all the setup on themselves. Brain activity was recorded by a 64 channel EEG Waveguard cap connected to the EEGoPro amplifier via 2 serial ports (32 channels connection per port). The amplifier was put into a backpack together with a DELL tablet on which the recording software ran. Surface EMG electrodes were placed on the subject's Tibialis Anterior and Soleus muscles on both legs and plugged into an external box connected to the EEGoPro amplifier via a secondary serial port. Contact Switches were placed underneath the subject's heels and connected to a digital input of the MWX8 DataLog analog-to-digital converter. The converter was fixed at the subject's hips level by an elastic belt. Elastic bands placed around the subject's thighs made sure cables remained fixed and didn't disturb the gait performance. A digital button was also connected to the converter through a secondary digital input and eventually pressed by the subject at specific time points. The Samsung Galaxy S4 mini was firmly placed at the subject's lower back through the elastic belt.

Table 7-1: Dual-task conditions.

Conversations and texts were always based on the same set of questions and email, respectively

<b>Questions for DT1 condition</b>	<ol style="list-style-type: none"> <li>1. How was your last weekend?</li> <li>2. What are you currently doing and where?</li> <li>3. Where do you live?</li> <li>4. Have long have you been in London? Do you like it?</li> <li>5. (How was your summer?)</li> </ol>
<b>Email for DT2 condition</b>	<p>Hi there,</p> <p>How are u?! Hope everything is going well!</p> <p>As you probably remember from our last meeting, it is about time we start thinking about the company's party!</p> <p>Since you volunteered to take over this, I am here reminding you of few things you should think about, specifically:</p> <ul style="list-style-type: none"> <li>- Date and time of the day (previously we have always started in the late afternoon, but I think it's time for a change!);</li> <li>- Location (something suggestive or rooftop?! definitely in case also a Plan B option according to weather!)</li> <li>- Theme of the party: to this everything else should be related as costumes, decorations, finger-food etc;</li> <li>- Invites and who will be in charge of doing them (again, made according to the party theme!);</li> <li>- Last but not least: "price for the best..."</li> </ul> <p>Please do not hesitate to ask for any help or suggestions!</p> <p>Best, S.</p>

Table 7-2: Summary of each single subject experiment.

Out of 18 subjects recruited, 3 were excluded (R) because of technical issues during recordings (i.e. Contact Switches not properly working), and 1 was eventually excluded from the analysis because of major gait artefacts in the EEG data. In DT1, subjects were asked the same questions and only for few subjects one additional question was asked before the end of the predefined path. In DT2, some subjects didn't manage to finish replying to the email reported in Table 7-1 (n.a.), whereas for the others the total number of characters (including blank spaces) in the reply-email is here reported.

Subjects	Questions asked	Email number of characters	Maintained (M)/Rejected (R)
AC	1, 2, 3, 4	472	M
AP	1, 2, 3, 4	N.A.	M
CB	1, 2, 3, 4	N.A.	M
CK	1, 2, 3, 4	204	M
EB	1, 2, 3, 4	N.A.	M
FB	1, 2, 3, 4, 5	535	M
IF	1, 2, 3, 4	371	M
JS	1, 2, 3, 4	N.A.	R – technical issue in recording
KO	1, 2, 3, 4	99	R – big gait artefacts in EEG data
LGV	1, 2, 3, 4, 5	N.A.	M
MP	1, 2, 3, 4	N.A.	M
MT	1, 2, 3, 4	289	R – technical issue in recording
MTT	1, 2, 3, 4	N.A.	M
MW	1, 2, 3, 4	928	R – technical issue in recording
PS	1, 2, 3, 4, 5	400	M
RC	1, 2, 3, 4, 5	31	M
SC	1, 2, 3, 4	336	M
ST	1, 2, 3, 4	184	M



#### **7.2.4 Data analyses**

Offline data analyses were run in MatLab 2015b (The MathWorks, Inc.) and Figure 7-3 describes the analytical pipeline followed for the analyses. First of all, the time of the first TTL pulse was detected in both the digital and the physiological recordings in order to synchronize the data. The binary signal obtained from the contact switches was used as the reference for synchronization: either part of its initial data was removed (i.e. backward shifting), if the DataLog converter started recording before the EEGoPro amplifier, or a series of 1 was added in the beginning (i.e. forward shifting), if the DataLog converter started recording after the EEGoPro amplifier. The amount of data removed/added to the signal was calculated to match times of the first common TTL pulse between the two separate recordings. Secondly, time points of each button press were identified to divide the continuous recordings into conditions: when the binary signal from the button was equal to 0 for a period longer than 4 seconds, for the first, third and fifth presses (i.e. condition start) the last instant of changed polarity (i.e. from 0 to 1) was defined as “Button Press - Start”, whereas for the second, fourth and sixth presses (i.e. condition end), the first instant of changed polarity (i.e. from 1 to 0). Eventually, time points of each heel strike were extracted (i.e. when the binary signal from the contact switches changed polarity (i.e. from 1 to 0, the first moment of change was defined as “Heel Strike”, right- or left-) and related events were created in the physiological data file. From these latencies, measures of gait behaviour, such as Step latency and Stride Duration, were also evaluated for later usage.

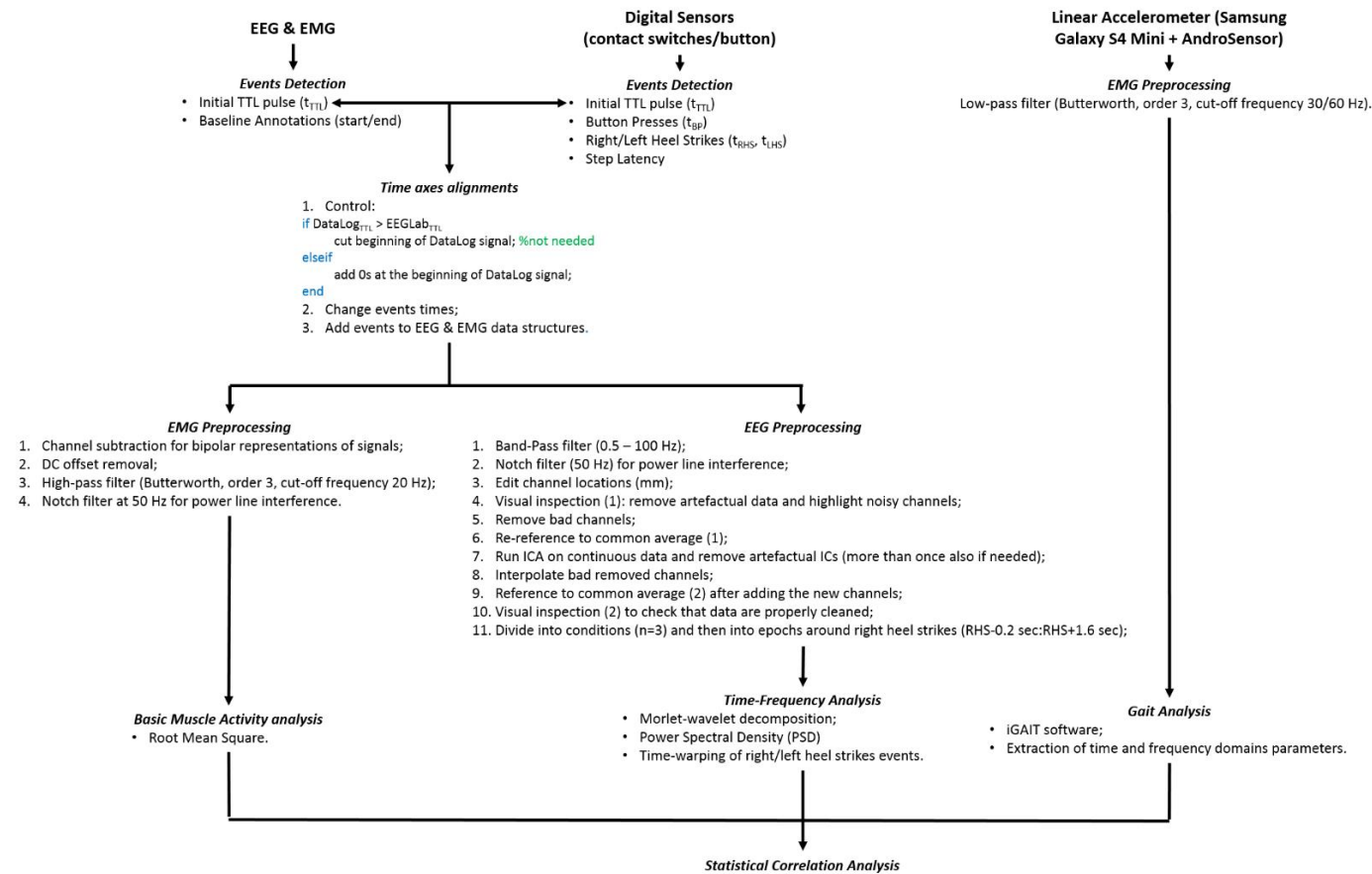


Figure 7-3: Offline analyses analytical pipeline.

The offline analytical pipeline provides means for offline synchronization of the recorded evidences so that time axes of physiological data and digital sensors are first re-aligned thanks to the common TTL pulse, and then synchronized so that times of button presses and heel strikes are added to the physiological evidences. Once synchronized, all data are pre-processed and cleaned before performing any analyses.

## Gait measures

Linear acceleration data recorded in each condition with the smartphone were separately uploaded into the free software iGAIT (MatLab interface) for the analysis of gait pattern (Yang et al., 2012). This toolbox provides a simple user-friendly GUI to display and analyse gait linear acceleration data recorded by different types of accelerometers. Spatio-temporal as well as frequency features of gait were assessed and saved as .txt files. Extracted and further used measures were, for example, Cadence (step/min), Mean Step Length (m), Velocity (m/s), Stride Regularity, Step Regularity and Symmetry in the Vertical and Antero-Posterior directions, acceleration Root Mean Square (RMS) in each movement direction (i.e. Vertical (ver-), Medio-Lateral (ml-), Antero-Posterior (ap-)). Acceleration RMS is a measure of the magnitude of the acceleration in each movement direction and has been previously extensively applied in the evaluation of gait abnormalities in healthy subjects as well as neurological patients (Latt et al., 2009; Iosa et al., 2014; Van Crielinge et al., 2017). Recent findings have also successfully proved that normalized acceleration RMS in the medio-lateral direction is a good marker of gait stability and abnormality regardless of the walking speed (Sekine et al., 2013). To consistently investigate gait stability across our experimental conditions, a measure of normalized RMS (RMS Ratio, RMSR) was employed and calculated according to the equation:

$$RMSR_x = \frac{RMS_x}{\sqrt{RMS_{AP}^2 + RMS_{Ver}^2 + RMS_{ML}^2}}$$

Equation 7-1: RMSR formula.

where x = ver-, ap- and ml- directions of acceleration.  $RMSR_x$  represents the ratio between the RSM in each direction and the overall RMS magnitude.

## EMG pre-processing and basic muscle activity

As reported in paragraph 7.2.3, EMG and EEG data were simultaneously recorded and stored in the same file. In the pre-processing phase the two data types were considered separately: signals recorded from the two monopolar surface EMG electrodes located on the same muscle were first subtracted to obtain a bipolar representation of each muscle activation. Continuous EMG data were first de-trended, high-pass filtered at 20 Hz (Butterworth, order 3, dual-pass fashion to avoid phase-lag) to remove intrinsic low-frequency noise sources (De Luca et al., 2010), and notch filtered (50 Hz, IIR Comb Notching filter as designed in MatLab, order 20) to remove the power-line noise. When performing visual inspection (see next paragraph), EMG data were inspected in parallel

with EEG evidence to remove the same artefactual periods from the two physiological signals. After visual inspection, EMG data were segmented into epochs of 1.8 seconds from -200 ms to 1600 ms around each right heel strike to capture a full gait stride even at the lowest speeds. Segmented data were then rectified and normalized for each muscle maximum activation through all the recording to remove differences across subjects and recordings due to skin conductance and surface electrodes positioning. A low pass filter with cut-off frequency at 6 Hz (Butterworth, order 3, dual-pass fashion to avoid phase-lag) was then applied to compute the linear envelope of each muscle signal and the Root Mean Square (RMS) was eventually calculated epoch-by-epoch for each muscle in each condition and for each subject.

### **EEG pre-processing**

Since EEG data are highly sensitive to movement artefacts as well as to physiological and environmental noises, a meticulous cleansing of the raw recorded signals was performed for each subject. Offline pre-processing of EEG data was carried out using EEGLab toolbox for MatLab (Delorme and Makeig, 2004) following a customised self-developed pipeline adapted to our data from literature. Data were first band-pass filtered between 0.5 Hz and 100 Hz (FIR filter, order automatically set by EEGLab), to minimize slow drifts and remove high-frequency components, and notch filtered at 50 Hz (FIR notch filter, order = 3302), to remove the power line noise. Visual inspection was performed on continuous data: EEG channels affected by major noise sources throughout the whole experiment were identified and temporarily removed from the analyses; prominent artefacts affecting all the recording channels were also removed from the data. Next, data were re-referenced to the common average reference and then decomposed using Independent Component Analysis (ICA) with the extended Infomax algorithm as implemented in EEGLab (Cardoso, 1997; Delorme et al., 2007). Power spectral, spatial and temporal features of each Independent Component (IC) were carefully inspected and those representing typical artefacts (e.g. eye blinks, saccades, neck muscles etc.) were eventually removed from the data. Remaining components were projected back to the scalp channels. Previously removed bad channels were then interpolated (method = 'spherical' as implemented in EEGLab, which uses superfast spherical interpolation, Perrin et al., 1989; Ferree, 2000) and all data then re-referenced again to the common average reference. Continuous data were then segmented into epochs of 1.8 sec duration from -200 ms to 1600 ms around each right heel strikes in order to capture a complete stride (composed by, in order: right, left, right heel strikes) even at the slowest speed. One last visual inspection was ultimately performed to check the quality of the cleaned data

and eventually remove still noisy epochs. Of note, the final number of channels for each subject in each condition, after interpolation, was 63 and not 64. This was due to the default hardware reference within the EEGoPro amplifier (i.e. CPz, changed to FCz in this study as per better contact with the scalp) not listed in the active channels, thus not directly recorded by the system.

### **Time-Frequency analyses**

Time-Frequency (TFr) analysis represents a decomposition of the EEG signal into amplitude and phase information for each frequency within the EEG (so-called “spectral decomposition”) and the characterization of their changes over time with respect to task events. However, according to our experimental design, each condition could be considered as “continuous” since no specific external triggers were applied and the subject performed the same task for the whole duration. Consequently, data were first explored and their quality checked in both the time- and frequency-domain and then to remove the time domain from further statistical analysis. Therefore, the time-frequency spectral correlates of each condition for each subject were first investigated through means of Morlet wavelet decomposition, and then the Power Spectral Density (PSD) in each condition during its whole duration for each subject. Both analyses were run with EEGLab toolbox for MatLab.

### **Morlet-wavelet decomposition**

In order to visualize the responses in the time-frequency domain, for each subject, separately for the three conditions, for each electrode (except for the mastoids), the spectral power changes were measured with respect to the baseline (i.e. resting-state) in each epoch using wavelet decomposition through the EEGLab function *pop\_newtimef* with the following parameters:

- High frequency: 50 Hz;
- Wavelet width at lowest frequency: 3 oscillation cycles;
- Wavelet width at highest frequency: 14.35;
- Hanning window size: 359 ms;
- Time steps: 10 ms.

Single-epoch spectrograms were first computed and time warped to the median step latency (across subjects) using linear interpolation. With this method, time points of heel strikes in each epoch were aligned across epochs. Spectral power changes with respect to the baseline (i.e. resting state) were evaluated through the mean difference between each

single-epoch log-spectrum and the mean Baseline log-spectrum. Significant deviations from Baseline were detected using a non-parametric bootstrap approach (Grandchamp and Delorme, 2011), with the statistical significance level set at  $p < 0.01$ . This method was employed in order to obtain an informative visualization of each subject power spectrum during one full stride in each condition and check the quality of the pre-processed data. Figure 7-3 shows the results of this method for each subject across the three conditions (epochs averaged: ST = 179 ( $\pm$  28), DT1 = 148 ( $\pm$  20), DT2 = 188 ( $\pm$  30)) from two representative electrodes located above the posterior parietal cortices (i.e. P3 and P4) with values expressed in dB. The frequency range considered in the analyses spread from 8.4 Hz to 50 Hz, whereas the time range covered from -0.4 ms to 1399 ms around each right heel strike. Such ranges are the result of the algorithm optimization as implemented in EEGLab. On the left-hand side of each condition section, the real power spectral changes with respect to the baseline are reported; on the right-hand side, a green mask has been applied on those pixels that didn't pass the bootstrap statistical test (i.e. pixels whose value is not significantly different from Baseline). The majority of subjects showed typical gait-related power spectral changes along the time axis and across frequencies with respect to a standing upright condition (i.e. our Baseline, resting state), as previously shown in literature (Seeber et al., 2014; Gwin et al., 2010). Specifically, a sustained  $\alpha$  (8.4 – 12 Hz) and  $\beta$  (15 – 30 Hz) desynchronization (colour coded in blue) is clear in all subjects and is also fairly consistent across conditions. A modulated synchronization (colour coded red) is then visible at higher frequencies, from 30 to 50 Hz, with stronger values mostly in the DT1 condition. The fact that DT1 shows stronger synchronization in high-frequency could be related to the type of task undertaken by the subjects during this condition: talking indeed implies the activation of facial muscles and the alternating opening of the mouth to create speech. Muscle activity could have indeed added to the brain-related sources. Consequently, high-frequency brain oscillations will not be further considered in the analyses as potentially influenced by task-related artefacts during walking while conversing. Of note, one subject (Subject 8) was removed from further analyses after careful inspection of TFr data and identification of ineligible gait-related artefacts (Oliveira et al., 2017).

### **Power Spectral Density (PSD)**

To assess spectral information regardless of the time domain, for each subject, separately for each condition (also for the resting-state) and for each electrode (except for the mastoids), PSD was measured in each epoch through the EEGLab function *spectopo*. This function uses the Welch's overlapped segment averaging estimator as implemented in

MatLab (*pwelch()* MatLab function) to calculate the PSD. A default Hamming window of 400 ms with a 50% overlap (i.e. 200 ms) was adopted and PSD for frequencies from 2 Hz to 50 Hz calculated. Figure 7-4 shows topological representations (i.e. topoplots) of the PSD grand-average (epochs averaged: RS = 96 ( $\pm 7$ ), ST = 179 ( $\pm 28$ ), DT1 = 148 ( $\pm 20$ ), DT2 = 188 ( $\pm 30$ )) across all subjects for the three main frequency bands of interest (FOIs):  $\theta$  (4 - 7 Hz),  $\alpha$  (8 – 12 Hz) and  $\beta$  (15 – 30 Hz) (values expressed in dB). Empty circles in Figure 7-4 represent electrodes location according to the 64-channel cap used during recordings. PSD data format was then adjusted so that it could be handled by FieldTrip toolbox for MatLab (Oostenveld et al., 2010) for further statistical analyses which focused on differences across conditions.

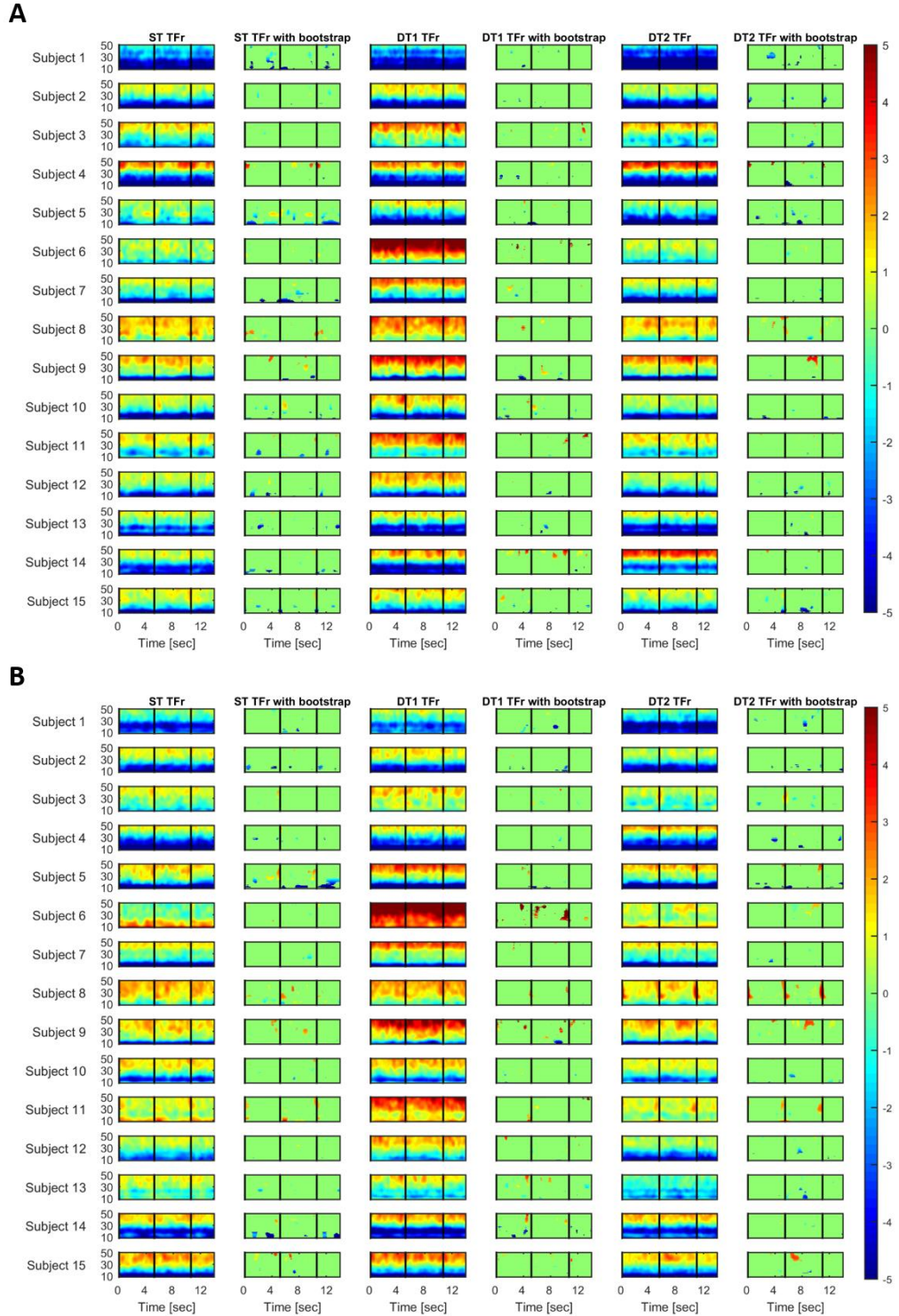


Figure 7-4: Time-Frequency power spectrum for each single subject across conditions from P3 (A) and P4 electrode (B).

A time–frequency image of each subject ERSPs with respect to baseline (i.e resting state) is here reported on the right side of each condition section. A time–frequency image of each subject significant changes with respect to baseline (green mask according to the bootstrap method) is reported on the left side of each condition section. Colour-bar (dB) is constant across plots and reports increase (values  $> 0$ , warm-colour coded) and decrease (values  $< 0$ , cold-colour coded) of power spectrum with respect to the baseline.



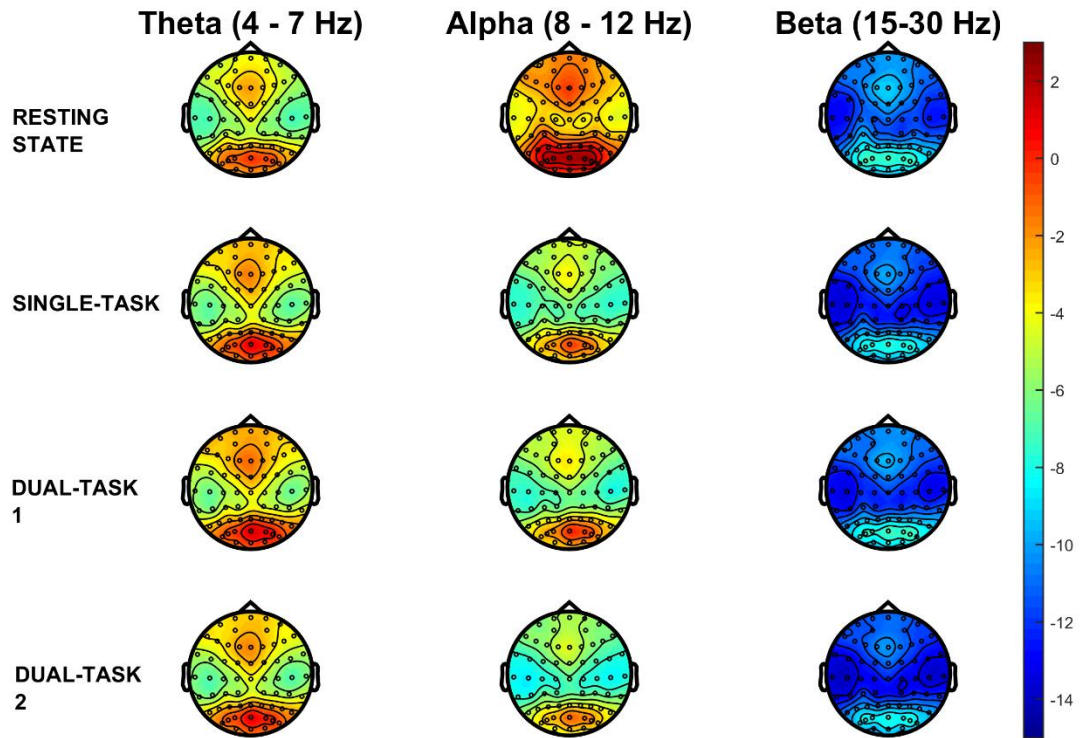


Figure 7-5: Condition specific topoplots of PSD grand-average across all subjects in each FOI.

Average ( $N = 14$ ) condition-by-condition topological representations of PSD show a similar spatial pattern across condition. Colour-bar (dB) is constant across plots and describes high (warm-colour coded) and low (cold-colour coded) intensities of PSD.

### **7.2.5 Statistics**

Statistical analyses were run mostly in SPSS 23 software (IBM). EEG specific analyses were run in MatLab 2015b as per methods implemented in FieldTrip (Maris and Oostenveld, 2007).

#### **Statistical analyses of gait measures**

Gait measures were first assessed separately for each condition and for each subject and ultimately group-level differences between conditions were assessed. Kolmogorov-Smirnoff test for normality was first used to test the distribution of the data. Data were all normally distributed, thus parametric statistical tests were further employed. 1 way repeated measures ANOVA with factor “Condition” (3 conditions) was applied to each gait measure of interest to identify variance differences across conditions. Subsequently, paired samples T-tests with Bonferroni correction for multiple comparisons were run to specifically define differences between conditions. Significance level was set at  $\alpha = 0.05$ , with number of repeated measures = 3 (ST vs DT<sub>i</sub> with  $i = 1, 2$  and DT1 vs. DT2), which meant an adjusted  $\alpha = 0.05/3 = 0.0167$  for multiple comparisons. The choice of Bonferroni correction through all the statistical analyses of this study was dictated by the less-controlled environment: as Bonferroni correction is an extremely robust method, results are less likely to be biased by chance.

#### **Statistical analyses of EMG measures**

EMG RMS measures were averaged across all epochs within each condition (epochs averaged: ST = 179 ( $\pm 28$ ), DT1 = 148 ( $\pm 20$ ), DT2 = 188 ( $\pm 30$ )) for each subject and ultimately group-level differences between conditions were assessed. Kolmogorov-Smirnoff test for normality was first used to test the distribution of the data. Data were all normally distributed, thus parametric statistical tests were further employed. 1 way repeated measures ANOVA with factor “Condition” (3 conditions) was applied to each muscle RMS measure to identify variance differences across conditions. Subsequently, paired samples T-tests with Bonferroni correction for multiple comparisons were run to specifically define differences between conditions. Significance level was set at  $\alpha = 0.05$ , with number of repeated measures = 3 (ST vs DT<sub>i</sub> with  $i = 1, 2$  and DT1 vs. DT2), which meant an adjusted  $\alpha = 0.05/3 = 0.0167$  for multiple comparisons.

#### **Non-parametric cluster-based permutation tests on PSD**

Differences of sensor-level power spectral density across conditions (ST vs DT<sub>i</sub> with  $i = 1, 2$  and DT1 vs. DT2) were assessed through non-parametric cluster-based permutation tests as provided in FieldTrip. This analysis has been extensively used in EEG studies as

it successfully tackles the Multiple Comparisons Problem (MCP) (Maris and Oostenveld, 2007; Negrini et al., 2017). Specifically, a paired sample t-Test was conducted for each electrode and t-values exceeding an “a priori” threshold were clustered based on adjacent neighbouring electrodes. Cluster-level statistics were computed by taking the sum of the t-values within every cluster. The statistical comparisons were done with respect to the maximum values of summed t-values. By means of a permutation test (i.e. randomizing data across conditions and rerunning the statistical test N times, Monte-Carlo approximation) a randomization distribution of the maximum of summed cluster t-values was obtained to evaluate the statistics of the actual data. Clusters in the original dataset were considered to be significant at an alpha level ( $\alpha_{\text{cluster}}$ ) of 1% if less than the 5% of the permutations ( $\alpha_{\text{cluster}} = 0.01$ ,  $\alpha = 0.025$  for 2-tailed tests,  $N = 1500$ ) used to construct the reference distribution yielded a maximum cluster-level statistics larger than the cluster-level value observed in the original data. As three different tests were carried out (ST vs DT<sub>i</sub> with  $i = 1, 2$  and DT1 vs. DT2), further correction for multiple comparison was run with Bonferroni method ( $p = 0.025/3 = 0.0083$  for two-tailed test). Cluster-based permutation tests were run on PSD data for each FOI separately, specifically  $\theta$  (4 - 7 Hz),  $\alpha$  (8 – 12 Hz) and  $\beta$  (15 – 30 Hz). Of note, all the 63 channels were simultaneously entered in the analysis, which resulted in a high number of multiple comparisons. This choice was guided by the exploratory nature of this analyses requiring to reject results given only by chance. Given our a-priori hypothesis, a more restricted number of electrodes could have been included in the analyses, which however would have biased our results. Specifically, this robust analysis should have confirmed the a-priori hypothesis of changes in frontal-parietal areas across conditions, even with the most restrictive parameters.

## 7.3 Results

### 7.3.1 Gait measures

Subjects ( $N = 14$ ) walked along the predefined path of 200 m in an average time of 226 sec ( $\pm 25$  sec) during single-task (ST) walking, 235 sec ( $\pm 28$  sec) when walking while conversing (DT1) and 260 sec ( $\pm 41$  sec) when walking while texting over the smartphone (DT2). Measures of velocity (Figure 7-6) and acceleration RMS/RMSR (Figure 7-7) in each direction are represented by an averaged condition-by-condition trend (thick lines) and standard deviation (whiskers). Condition-by-condition descriptive statistics across the three conditions are reported in Table 7-3. Repeated measures ANOVA values were not significantly different across conditions for measures of Mean Step Length, ml-RMSR, ver-Step Regularity, ver-Stride Regularity and ver-Symmetry ( $F < 3.099$ ,  $p >$

0.05). Paired samples t-Tests with Bonferroni correction for multiple comparisons revealed Velocity as the only measure significantly different (ANOVA  $F = 34.215$ ,  $p = 0.001$ ) in both DT1 ( $t = 4.199$ ,  $p = 0.001$ ) and DT2 ( $t = 6.847$ ,  $p = 0.001$ ) with respect to the ST condition, and between DT1 vs. DT2 ( $t = 4.991$ ,  $p = 0.001$ ). Gait measures of Stride Duration, ver-RMS and ap-RMS, whose ANOVA was significant ( $F > 12.165$ ,  $p < 0.001$ ), only showed statistical differences, according to paired-samples t-Test, between DT2 vs. ST ( $t > (-) 3.503$ ,  $p < 0.004$ ) and DT2 vs. DT1 ( $t > (-) 3.793$ ,  $p < 0.002$ ). Gait measures of Cadence, ml-RMS, ap-Step Regularity and ap-Stride Regularity, whose ANOVA was significant ( $F > 4.559$ ,  $p < 0.043$ ), only showed statistical differences, according to paired-samples t-Test, between DT2 vs. ST ( $t > 2.772$ ,  $p < 0.016$ ). Gait measures of ver-RMSR, ap-RMSR and ml-Stride Regularity, whose ANOVA was significant ( $F > 3.990$ ,  $p < 0.031$ ), only showed statistical differences, according to paired-samples t-Test, between DT2 vs. DT1 ( $t > 3.618$ ,  $p < 0.003$ ).

### **7.3.2 EMG RMS measures**

Figure 7-8 shows EMG profiles averaged across epochs and subjects for each muscle in each condition. A slightly higher activation can be seen in all the lower limb muscles during single-task walking in comparison to the dual-task conditions. The difference is statistically confirmed as reported in Table 7-4, where Repeated Measures ANOVA showed a significant effect of Condition for all the muscles ( $F > 10.498$ ,  $p < 0.005$ ). Paired samples t-Test with Bonferroni correction for multiple comparison showed a consistent decrease of RMS from single-task to dual-task conditions for all muscles ( $p < 0.0167$ ) except for left Tibialis Anterior during DT2. RMS of left Tibialis Anterior was significantly higher during DT2 in comparison to DT1 ( $t = -2.770$ ,  $p = 0.016$ ). This is the only muscle for which the comparison DT2 vs. DT1 passes the adjusted significance value for multiple comparisons.

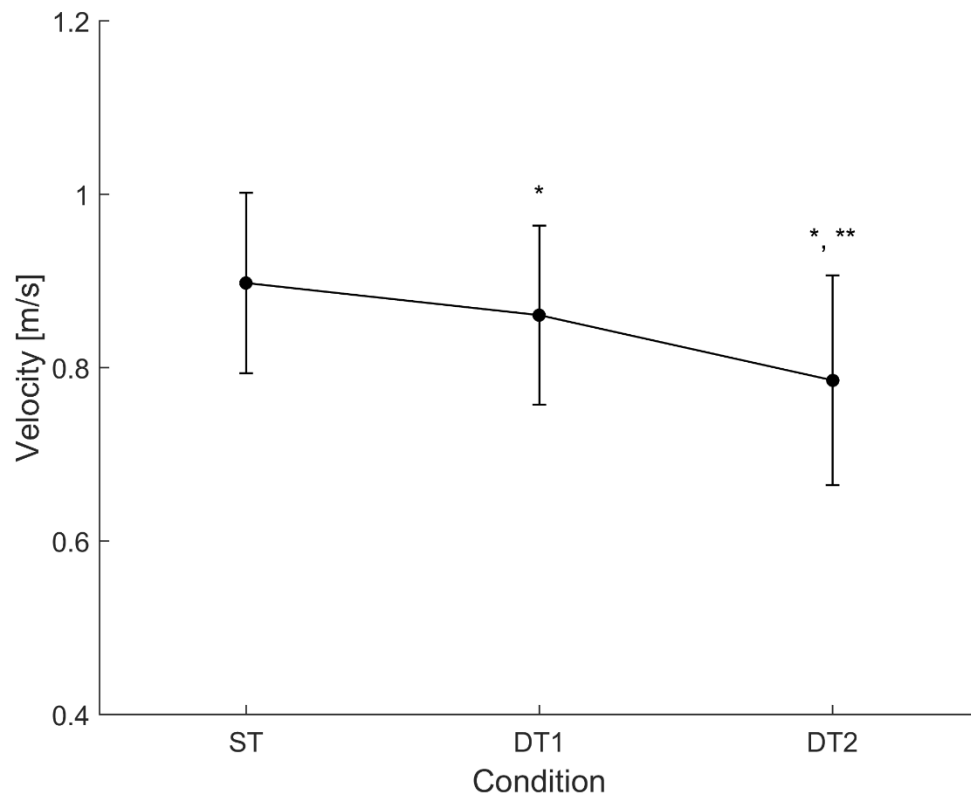


Figure 7-6: Condition-by-condition gait speed.

A condition-by-condition population average ( $N = 14$ ) profile with standard deviation error bars. Average gait velocity decreases in the two dual-task conditions with respect to the single-task condition. Statistically significant paired-samples t-test corrected for multiple comparisons (Bonferroni,  $\alpha = 0.0167$ ) are highlighted with \* (ST vs DT<sub>i</sub> with  $i = 1, 2$ ) and/or \*\* (DT1 vs. DT2). Detailed results are reported in Table 7-3.

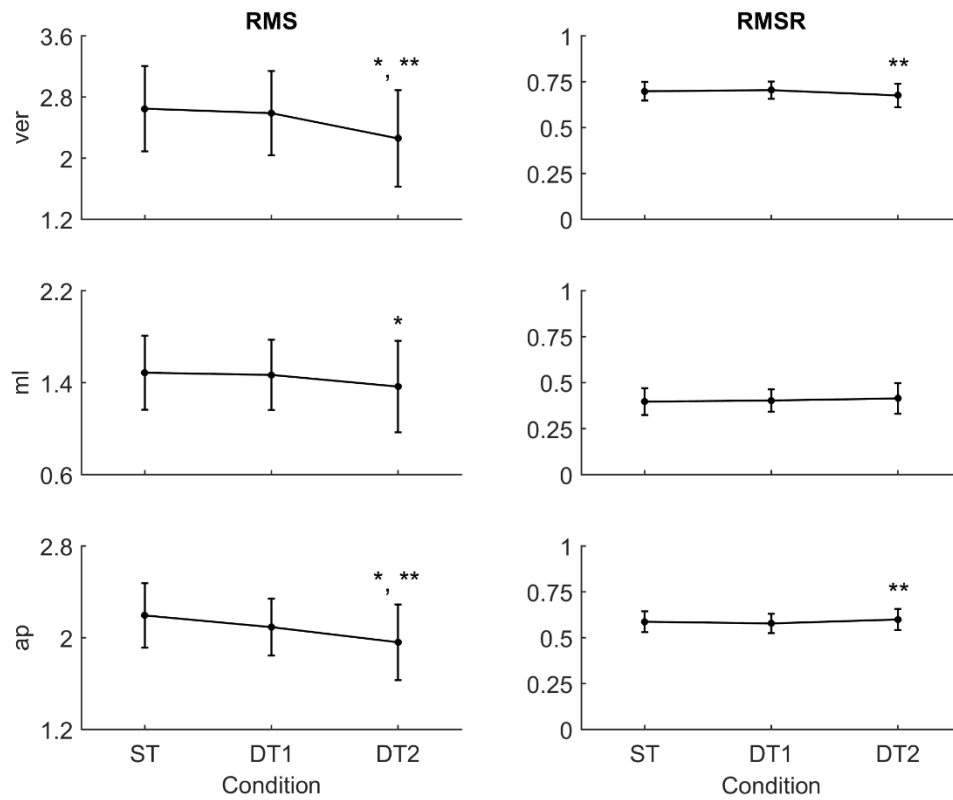


Figure 7-7: Condition-by-condition acceleration RMS and RMSR profiles.

Condition-by-condition population average ( $N = 14$ ) profiles with standard deviation error bars for each movement direction (ver = Vertical, ml = Medio-Lateral, ap = Antero-Posterior). Statistically significant paired-samples t-test corrected for multiple comparisons (Bonferroni,  $\alpha = 0.0167$ ) are highlighted with \* (ST vs DT<sub>i</sub> with  $i = 1, 2$ ) and/or \*\* (DT1 vs. DT2). Detailed results are reported in Table 7-3. Average acceleration RMS decrease in the two dual-task conditions with respect to the single-task condition regardless of movement direction. Average acceleration RMSR decrease in the vertical direction and increase in the medio-lateral and antero-posterior directions decrease in the two dual-task conditions with respect to the single-task condition regardless of movement direction.

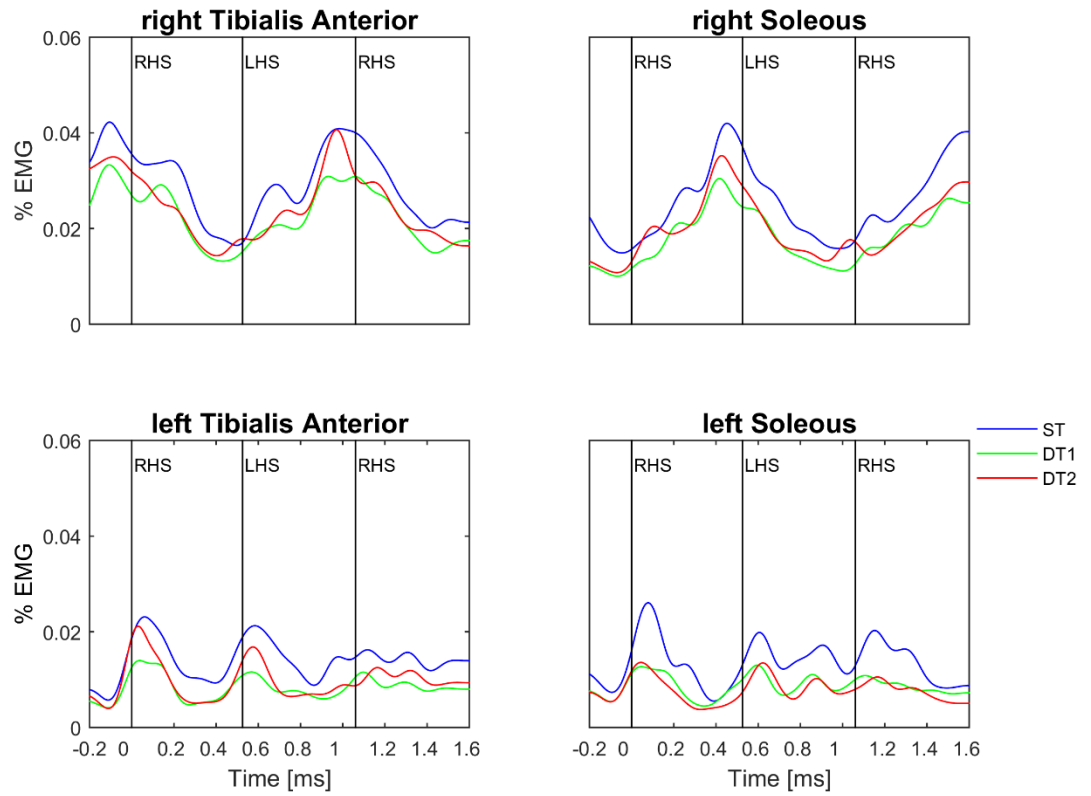


Figure 7-8: Lower limb muscles EMG profiles.

Each muscle EMG activity was averaged first across epochs and then across subjects ( $N = 14$ ). Vertical black lines represent median time of right/left heel strikes across subjects ( $N = 14$ ). Averaged EMG profiles of the three conditions are reported together with different colours (blue = ST, green = DT1, red = DT2).

Table 7-3: Single- and Dual-task conditions gait measures.

Condition-by-condition (n = 3) mean ( $\pm$  std) of the measures of gait of interest for the sample population (N = 14). Repeated measures ANOVA p-values are reported in the sixth column on the right. Statistically significant paired-samples t-test corrected for multiple comparisons (Bonferroni,  $\alpha = 0.0167$ ) are highlighted with \* (ST vs DT<sub>i</sub> with i = 1, 2) and/or \*\* (DT1 vs. DT2).

	Single Task	Dual Task 1	Dual Task 2	Anova F	Anova p
<b>Stride Duration (ms)</b>	1054 ( $\pm$ 87)	1060 ( $\pm$ 79)	1106 ( $\pm$ 107) *, **	12.165	0.001
<b>Cadence (step/min)</b>	107 ( $\pm$ 10)	104 ( $\pm$ 12)	99 ( $\pm$ 16) *	4.559	0.043
<b>Mean Step Length (m)</b>	0.53 ( $\pm$ 0.06)	0.52 ( $\pm$ 0.08)	0.51 ( $\pm$ 0.07)	0.0769	N.S.
<b>Velocity (m/s)</b>	0.90 ( $\pm$ 0.10)	0.86 ( $\pm$ 0.10) *	0.78 ( $\pm$ 0.12) *, **	34.215	0.001
<b>ver-RMS</b>	2.65 ( $\pm$ 0.56)	2.59 ( $\pm$ 0.55)	2.26 ( $\pm$ 0.63) *, **	17.554	0.001
<b>ml-RMS</b>	1.48 ( $\pm$ 0.32)	1.47 ( $\pm$ 0.31)	1.37 ( $\pm$ 0.40) *	7.769	0.008
<b>ap-RMS</b>	2.19 ( $\pm$ 0.28)	2.09 ( $\pm$ 0.25)	0.96 ( $\pm$ 0.33) *, **	16.946	0.001
<b>ver-RMSR</b>	0.70 ( $\pm$ 0.05)	0.70 ( $\pm$ 0.05)	0.67 ( $\pm$ 0.06) **	5.839	0.008
<b>ml-RMSR</b>	0.40 ( $\pm$ 0.07)	0.40 ( $\pm$ 0.06)	0.41 ( $\pm$ 0.08)	1.735	N.S.
<b>ap-RMSR</b>	0.59 ( $\pm$ 0.06)	0.58 ( $\pm$ 0.053)	0.60 ( $\pm$ 0.06) **	7.165	0.003
<b>ver-Step Regularity</b>	0.75 ( $\pm$ 0.09)	0.69 ( $\pm$ 0.19)	0.69 ( $\pm$ 0.13)	2.027	N.S.
<b>ver-Stride Regularity</b>	0.75 ( $\pm$ 0.07)	0.68 ( $\pm$ 0.19)	0.65 ( $\pm$ 0.16)	2.537	N.S.
<b>ver-Symmetry</b>	0.03 ( $\pm$ 0.02)	0.04 ( $\pm$ 0.03)	0.06 ( $\pm$ 0.04)	3.099	N.S.
<b>ap-Step Regularity</b>	0.76 ( $\pm$ 0.09)	0.73 ( $\pm$ 0.11)	0.71 ( $\pm$ 0.09) *	6.642	0.005
<b>ap-Stride Regularity</b>	0.72 ( $\pm$ 0.08)	0.69 ( $\pm$ 0.10)	0.65 ( $\pm$ 0.12) *	7.158	0.009
<b>ap-Symmetry</b>	0.03 ( $\pm$ 0.02)	0.05 ( $\pm$ 0.03)	0.07 ( $\pm$ 0.05)	4.783	0.034
<b>ml-Stride Regularity</b>	0.46 ( $\pm$ 0.20)	0.46 ( $\pm$ 0.13)	0.35 ( $\pm$ 0.16) **	3.990	0.031

Table 7-4: Single- and Dual-task conditions EMG measures.

Condition-by-condition (n = 3) mean ( $\pm$  std) of the measures of RMS for each lower limb muscle for the sample population (N = 14). Repeated measures ANOVA p-values are reported in the sixth column on the right. Statistically significant paired-samples t-test corrected for multiple comparisons (Bonferroni,  $\alpha = 0.0167$ ) are highlighted with \* (ST vs DT<sub>i</sub> with i = 1, 2) and/or \*\* (DT1 vs. DT2).

Muscle RMS [a.u.]	Single Task	Dual Task 1	Dual Task 2	Anova F	Anova p
<b>Right Tibialis Anterior</b>	0.03 ( $\pm$ 0.01)	0.02 ( $\pm$ 0.01) *	0.02 ( $\pm$ 0.01) *	11.005	0.001
<b>Right Soleus</b>	0.023 ( $\pm$ 0.01)	0.02 ( $\pm$ 0.01) *	0.02 ( $\pm$ 0.01) *	10.666	0.004
<b>Left Tibialis Anterior</b>	0.02 ( $\pm$ 0.01)	0.01 ( $\pm$ 0.01) *	0.02 ( $\pm$ 0.01) **	10.872	0.002
<b>Left Soleus</b>	0.02 ( $\pm$ 0.01)	0.01 ( $\pm$ 0.01) *	0.01 ( $\pm$ 0.01) *	10.498	0.004



### 7.3.3 Natural walking vs. resting-state EEG: non-parametric cluster-based tests on PSD

Significant cluster-based permutation tests t-values topological maps are reported in Figure 7-9 for the comparison ST vs. resting state EEG. Specifically, significant differences were found in:

- $\alpha$  (8 - 12 Hz)

Negative Cluster = all electrodes,  $p = 0.001$ ;

- $\beta$  (15 – 30 Hz)

Negative Cluster = {FP2, F3, FZ, F4, FC1, FC2, FC6, C3, CZ, C4, T8, CP5, CP1, CP2, CP6, P3, AF4, AF8, F2, F6, FC3, FCZ, FC4, C1, C2, CP3, CP4, P5, P1, FT8},  $p = 0.002$ .

A positive cluster represents a statistically significant increase of activity in the first term of one comparison with respect to the second term. A negative cluster represents a statistically significant decrease of activity in the first term of one comparison with respect to the second term. From the above it can be said that:

- There is a significant decrease of PSD in the  $\alpha$  band over the whole brain during natural walking in comparison to resting-state standing still, with stronger differences (i.e. deeper blue colour = lower t-values) bilaterally over the sensorimotor cortices;
- There is a significant decrease of PSD in the  $\beta$  band in a wide cluster including frontal-, central- and parietal- bilateral areas when naturally walking with respect to resting-state standing still.
- No significant differences were detected for  $\theta$  PSD.

### 7.3.4 Dual-task vs. single-task walking EEG: non-parametric cluster-based permutation tests on PSD

Significant cluster-based permutation tests t-values topological maps are reported in Figure 7-10 for the comparison DT1 vs. ST and Figure 7-11 for the comparison DT2 vs. DT1. No statistically significant differences were obtained for the comparison Dt2 vs. ST. Specifically, significant differences were found in:

- DT1 vs. ST  $\theta$  (4 - 7 Hz)

Positive cluster 1 = {CP2, CP6, P4, P8, O2, CP4, P2, P6, PO4, PO6, TP8, PO8},  $p = 0.002$ ;

Positive cluster 2 = {T7, F7, FC5, AF7, F5, FT7},  $p = 0.002$ ;

- DT1 vs. ST  $\beta$  (15 – 30 Hz)

Positive Cluster = {P4, P8, O2, P6, PO4, PO6, TP8, PO8},  $p = 0.005$ .

And in:

- DT2 vs DT1  $\beta$  (15 – 30 Hz)

Negative cluster = {FP1, FPZ, FP2, F7, F4, F8, FC5, FC2, FC6, T7, C4, CP2, CP6, PZ, P4, P8, POZ, O2, AF7, AF3, AF4, AF8, F5, F2, F6, FC4, C5, CP4, P2, P6, PO4, PO6, FT7, FT8, PO8},  $p = 0.002$ .

A positive cluster represents a statistically significant increase of activity in the first term of one comparison with respect to the second term. A negative cluster represents a statistically significant decrease of activity in the first term of one comparison with respect to the second term. From the above it can be said that:

- There is a significant increased PSD in the  $\theta$  band in a right-parietal-temporal cluster as well as in a left-frontal-temporal cluster during DT1 with respect to ST;
- There is a significant increase of PSD in the  $\beta$  band in a right-parietal cluster during DT1 in comparison to ST;
- There is a significant decrease of PSD in the  $\beta$  band in a wide frontal- and right-parietal cluster during DT2 with respect to DT1.

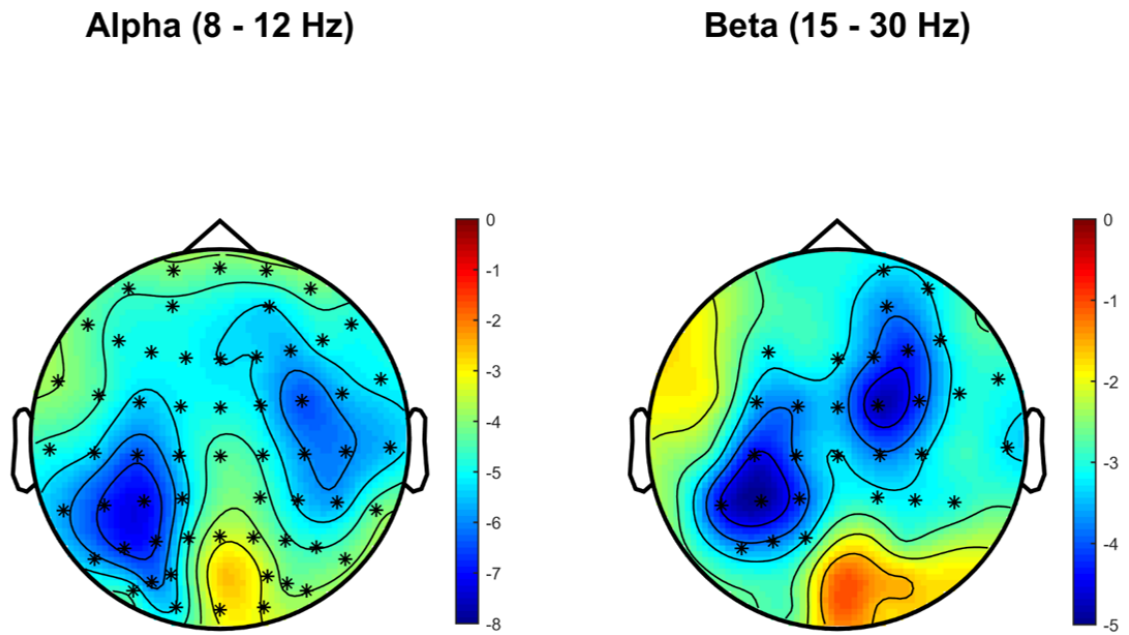


Figure 7-9: Non-parametric cluster-based permutation test comparing PSD in ST and Resting State.

FOI-topological maps are colour-coded according to the permutation tests t-values resulted from the comparison of PSD between ST and Resting-State. Clusters of electrodes whose PSD is significantly different between the two conditions are highlighted (\* for  $p < 0.01$ , x for  $0.01 < p < 0.05$ , Bonferroni corrected  $p < 0.0083$ ). In the  $\alpha$  frequency band, a general decrease of PSD activity is reported over the whole brain. In the  $\beta$  frequency band, a decreased PSD activity is reported in a wide cluster including left-frontal-, bilateral-central- and bilateral parietal areas.

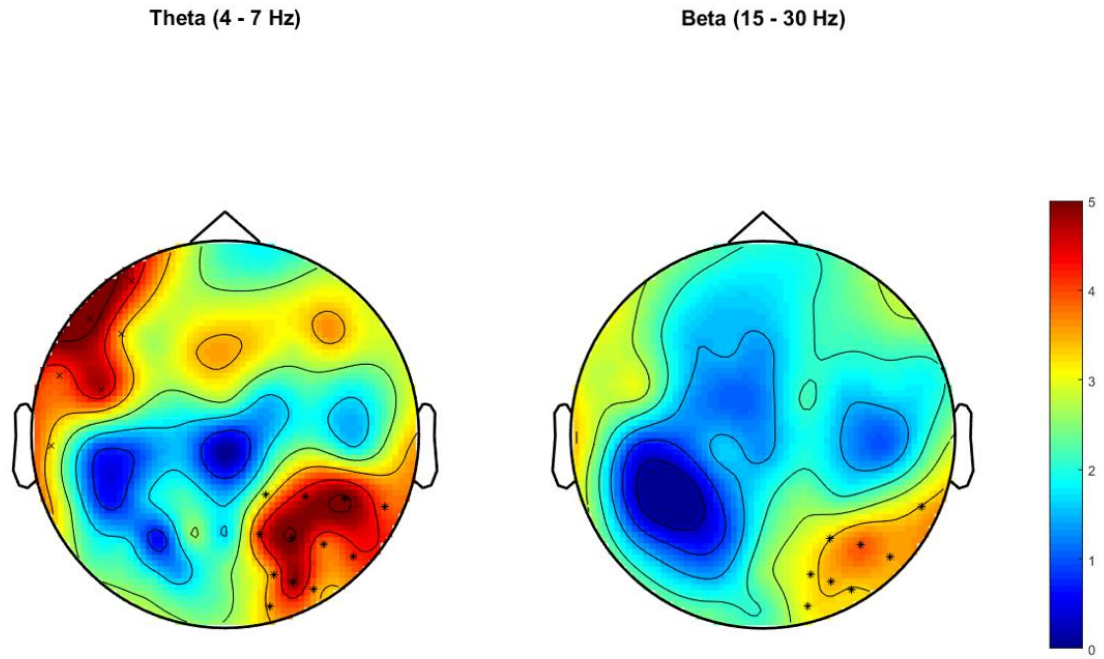


Figure 7-10: Non-parametric cluster-based permutation test comparing PSD in DT1 vs. ST.

FOI-topological maps are colour-coded according to the permutation tests t-values resulted from the comparison of PSD between DT1 and ST. Clusters of electrodes whose PSD is significantly different between the two conditions are highlighted (\* for  $p < 0.01$ , x for  $0.01 < p < 0.05$ , Bonferroni corrected  $p < 0.0083$ ). In the  $\theta$  frequency band, an increased PSD activity is reported in a left frontal and in a right occipital-parietal cluster. In the  $\beta$  frequency band, an increased PSD activity is reported in a right occipital-parietal cluster.

### Beta (15 - 30 Hz)

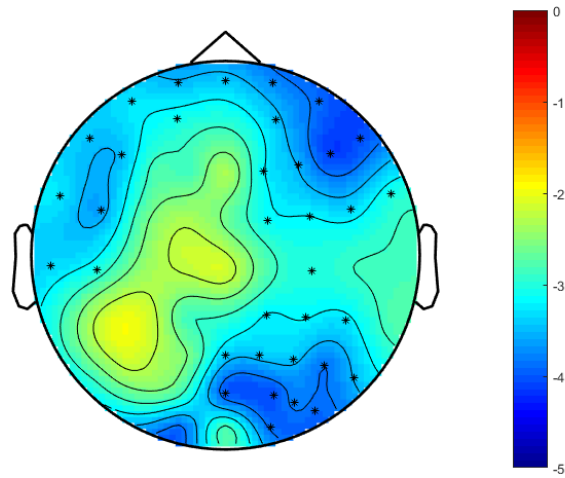


Figure 7-11: Non-parametric cluster-based permutation test comparing PSD in DT2 vs. and DT1.

FOI-topological maps are colour-coded according to the permutation tests t-values resulted from the comparison of PSD between DT2 and DT1. Clusters of electrodes whose PSD is significantly different between the two conditions are highlighted (\* for  $p < 0.01$ , x for  $0.01 < p < 0.05$ , Bonferroni corrected  $p < 0.0083$ ). In the  $\beta$  frequency band, a decreased PSD activity is reported in a wide cluster extending from left-central frontal-temporal regions to right occipital-parietal areas.

## **7.4 Discussions**

### **7.4.1 Novel findings**

The current study provides novel evidence of neural correlates of walking under different conditions in the real world, outside the over-protected laboratory environment. A novel fully-mobile setup was designed and created with the aim for ambulatory daily-life applications and hereby tested with natural walking paradigms embedded into real-life situations. The successful performance of the setup and the customized offline analysis pipeline is validated by the obtained results of gait performance and neurophysiological activity. Specifically, gait performance (as described with measures of velocity, RMSR and regularity) decreased with increasing task demands and challenges in line with previous literature (Menz et al., 2003; Menz et al., 2003). In parallel, brain activations as assessed via electroencephalography showed activation patterns specific to walking (see Figure 7-4), which also find ground truth within the current literature (Bradford et al., 2016; Bulea et al., 2015; Wagner et al., 2016). Despite the major great interest of previous literature on the prefrontal cortex (PFC) during multi-tasking (Al-Yahya et al., 2016; Maidan et al., 2017), it was here demonstrated that also posterior parietal brain regions are involved during different dual-task conditions and that they are specifically recruited by the brain according to attentional and possible energy-optimization strategies (Wahn and König, 2017).

### **7.4.2 Gait and EMG measures**

Even though only healthy young adults with no neurological or muscular history were recruited in the current study, changes of gait pattern and performance were still observed across conditions. Specifically, decreased of gait velocity, regularity and muscular activity was observed during dual-task with respect to single-task walking. Previous studies reported changes in gait pattern when simultaneously talking (Holtzer et al., 2011) or texting (Schabrun et al., 2014; Agostini et al., 2015; Caramia et al., 2017). Both secondary tasks induced a decrease of gait speed, with the latter also impairing gait stability. In line with these studies, our results demonstrated a general decrease of gait velocity in both dual-task conditions in comparison to a natural walking condition, but a more significantly impaired gait behaviour during walking while texting, expressed through various gait measures as reported in Table 7-3. This could be first attributed to the fact that people are more used to walk while talking than they are to walk while texting. Previous studies have investigated the relationship between dual-task demand and gait behaviour with the aim of identifying which elements mostly undermines performance.

Cognitive interferences as mental arithmetic (Springer et al., 2006; Francis et al., 2015) and sensorimotor tasks (Beurskens and Bock, 2013) seem not to affect gait performance as much as motor interferences such as road complexity (Menz et al., 2003; Menz et al., 2003; Lin and Lin, 2016; Maidan et al., 2016) and hand engagement (Beurskens et al., 2016). Secondary tasks that require a higher continuous visual processing have been classified as more likely to impair gait performance (Beurskens and Bock, 2013; Francis et al., 2015). Indeed, a continuous scan of the surrounding environment is crucial when walking on difficult paths. Walking and texting prevent subjects from monitoring the surroundings as their eyes are mostly focused on the phone, thus decreasing the visual scan of the environment and altering the gait performance. This doesn't hold for walking and talking for example, during which subjects could continuously (or periodically, if sometimes looking at the speaker) scan the surrounding environment thus maintaining gait stability and performance. Gait deficits related to lack of constant visual processing are indeed exacerbated in people with reduced executive functions capabilities such as the elderly with a history of falls (Springer et al., 2006). If lack of visual processing skills is the major contributor to gait instability during dual-task walking in health, then other neurological impairments could undermine gait performance per se as a consequence of neural injuries. Elderly (Holterz et al., 2011; Iosa et al., 2014), Parkinson's disease patients (Latt et al., 2009; Maidan et al., 2016) and stroke survivors (Al-Yahya et al., 2016) always demonstrate reduced performance paired with stronger brain activations when task demands increase. Conversely, healthy young adults usually show little to moderate changes in gait behaviour when simultaneously performing secondary tasks, which could be related to their more effective adaptive strategies and mechanisms. This theory was validated during a prioritization study with both healthy young and older adults (Yogev-Silgeman et al., 2010), whereby the behavioural correlates of single-task walking and dual-task walking (i.e. while simultaneously performing a cognitive Verbal Fluency Test) were investigated. When walking while performing the cognitive task without any specific prioritization instruction both young and elderly adults reduced their walking speed with respect to the natural walking speed. When priority was given to the motor task gait speed significantly increased in both groups, although to a less extent for elderly adults. The simultaneous performance of the cognitive task influenced gait variability in older but not in young adults, and this effect did not depend on prioritization instructions. To summarise, walking while carrying out a secondary cognitive task without any specific priority increases gait variability in both young and older adults, whereas task prioritization seems to influence gait variability more in young subjects,

likely due to ageing reduced skills to flexibly allocate different attentional resources to simultaneous tasks.

### **7.4.3 Neurophysiological evidence**

Previous investigations questioned whether dual-tasking significantly alters brain activity, which elements influence these changes the most and which populations are most affected by lack of multi-tasking abilities. fNIRS over the pre-frontal cortex has been widely used for testing these hypotheses. Different groups have found consistent increases in oxygen levels in the pre-frontal cortex of healthy young adults when performing any type of dual-task condition (Holtzer et al., 2011; Al-Yahya et al., 2016; Lin and Lin, 2016) and the increases are greatest in those populations who are more cognitively impaired such as the elderly, stroke patients and Parkinson's disease patients (Holtzer et al., 2011; Al-Yahya et al., 2016; Maidan et al., 2017). These studies confirm the active recruitment of the prefrontal cortex during multi-tasking but were limited by the restricted number of channels that could be recorded (i.e. only pre-frontal cortex, no possibility for whole-brain recordings). Consequently, there is the need for more complete and accurate brain scans during dual-task conditions. Thanks to the recent developments in mobile technologies, it is now possible to record ambulatory electroencephalography of the whole brain with little to moderate (but removable) artefactual components from the external environment. The results presented here are amongst the first of this kind and they confirm previous findings obtained from the protected laboratory environment with virtual reality or treadmill walking with or without gait support (Bradford et al., 2016; Seeber et al., 2014; Wagner et al., 2012; Wagner et al., 2014; Wagner et al., 2016).

### **Natural walking in the real-world**

Single subject brain activities registered over the posterior parietal areas during natural walking (ST) showed sustained  $\alpha$  and  $\beta$  desynchronization through all the gait duration in parallel with a more time-specific higher frequency modulation (Figure 7-4). The careful inspection of the time-frequency representation of each subject neural activity aimed at validating the quality of the data. At the group level (Figure 7-5 and Figure 7-9),  $\alpha$  and  $\beta$  frequency band desynchronization is evidently strong over the two sensori-motor areas, in line with previous EEG (Gwin et al., 2010; Seeber et al., 2014) as well as fNIRS studies (Miyai et al., 2001). As previously suggested in literature (Wagner et al., 2012; Ehinger et al., 2014; Wagner et al., 2014),  $\alpha$  and  $\beta$  desynchronization represent an "active state" of the brain and are likely to be involved in maintenance of the current



motor status that promotes the voluntary movement of walking (Engel and Fries, 2010).  $\alpha$  PSD is lower over the whole brain during natural walking with respect to resting-state recorded standing still, with however higher values over posterior-occipital areas likely to be involved in visual scan and processing of inputs from the environment.

### **Walking while conversing**

Walking while talking to a friend is one of the most common dual-task activities people perform in their daily-life. The neural correlates of such an everyday activity were here compared to those of a natural non-communicative walk. Specifically, a significantly higher  $\theta$  theta activity was observed in a cluster of electrodes located over the left frontal-temporal cortex, which could be associated to an increased activity of the Broca area for the creation of speech. Moreover, a second group of channels located over the right posterior parietal-occipital cortex (see Figure 7-10) showed significantly higher  $\theta$  and  $\beta$  activities. Recent studies reported a major role for the right occipital-parietal cortical region during spatial attention and how it could be affected by age (Learmonth 2017). Intracranial studies on monkeys performing a visual search attention task showed the active involvement of  $\beta$  and the sequence of communication between frontal (first, the sender) and parietal (second, the receiver) regions during top-down attention (Buschman and Miller, 2007). Neurological impairments such as neglect could cause a reduction of frontal-parietal network strength within the  $\theta$  and  $\beta$  frequency bands during conscious visual tasks (Yordanova et al., 2016), validating the hypothesis of their involvement in both spatial attention and visual processing. However, in this work of research, subjects were not performing a simple visual attention task, but a dual-task combining walking along a known predefined path, listening to questions posed by the experimenter and speaking in response to the posed enquiries by recollecting personal memories and experiences (see Table 7-1). A recent fNIRS investigation hypothesised and demonstrated that plural cortical areas (i.e. temporal, premotor and parietal regions) are involved in walking while talking (i.e. Verbal Fluency Task) (Metzeger et al., 2017). Specifically, increased oxygenation levels were observed in areas expanding from the inferior frontal gyrus to the middle temporal gyrus in both hemispheres, thus including both Broca's and other areas. The authors suggested that the augmented cortical activations seemed not to be simply related to language production itself, but more broadly to the engagement of higher executive functions required to perform the two tasks simultaneously, in line with other previous findings (Mirelman et al., 2014).  $\theta$  synchronization of prefrontal and medial-temporal lobe has been previously shown to positively correlate with successful recall of encoded words (Sederberg et al., 2003), with successful decision making

regardless of spatial learning (Guitart-Masip et al., 2013), and with orchestrating item distinction, verbal working memory and long-term memory (Meyer et al., 2015). Moreover, studies on speech detection, understanding and creation demonstrated the active involvement of right temporal  $\theta$  activity (Giraud et al., 2007). A decrease of  $\theta$  coherence between frontal and temporal areas was also reported in studies of schizophrenia and further linked to the misattribution of inner thoughts to the external voice (Ford et al., 2002). It is therefore suggested that, during the DT1 condition, it is likely that a collaboration between the left pre-frontal and the right temporo-parieto-occipital clusters was developed by subjects as a top-down attentional mechanism to simultaneously orientate through space, identify and understand the question/cue (i.e. by the Anterior and Ventro-Lateral PFC), search for (i.e. by the Medio-Temporal Lobe) and verify (i.e. by the Dorso-Lateral PFC) the required memory, and finally use it for conscious thoughts through speech (Simons and Spiers, 2003; Giraud et al., 2007).

### **Walking while texting with a smartphone**

Walking while texting over the phone is becoming more common even in the most complex situations, as crossing a crowded road or stepping on/off the train or bus. As previously mentioned (see paragraph 7.4.2), gait abnormalities and attention alterations arise from such a risky behaviour. Indeed, the healthy young population sample recruited in our study showed a velocity reduction and significant gait impairments (e.g. stride irregularity and changes in acceleration RMS) when walking and texting over the phone. From a neurophysiological perspective, different results were obtained which could be attributed to different roles of each frequency band of interest. When comparing the neural activations during DT2 with the ones obtained during ST and DT1, only the latter comparison led towards strong statistical significance. Previous studies reported a stronger electroencephalographic power activity during speech generation tasks in comparison to reading or listening (Galin et al., 1992), which were not due to artefactual components. Of great interest is the statistically significant decrease, in DT2 with respect to DT1, of  $\beta$  activity in a broad cluster of electrodes spreading from over the left motor/premotor regions, to the bilateral prefrontal and frontal cortex to the right sensorimotor and parietal cortex (see Figure 7-11). Recent fMRI findings reported a systematic decrease of hemodynamic activity during dual-tasks with respect to single-task simulated gait in a broad cortical network including cingulate motor area, supplementary motor area, sensorimotor cortex and superior parietal lobule (Bürki et al., 2017). The authors contextualized the results within the dual-task interference hypothesis, claiming that the neural activation patterns are determined by the amount of resource

overlap between the two simultaneously performed tasks (Nijboer et al., 2014). In the current study, decrease of activity in left motor, premotor and frontal (Broca) areas are likely related to the lack of speech detection and production in this second dual-task condition. Moreover, it has been previously shown that subjects engaged in a secondary highly challenging task generate a stronger  $\beta$  desynchronization over the bilateral posterior parietal cortex (Wagner et al., 2016) as well as over the midline electrodes (Beurskens et al., 2016). As previously mentioned,  $\beta$  desynchronization represent an “active state” of the brain during which sensorimotor integration is promoted to maintain the ongoing voluntary movement (Buneo and Andersen, 2006; Engel and Fries, 2010). More challenging motor or secondary tasks have been shown to induce an even stronger  $\beta$  desynchronization as a basis for stronger sensorimotor integration, performance maintenance and error monitoring (Bradford et al., 2016; Bulea et al., 2015; Sipp et al., 2013). Moreover, the motor areas here were doubling their work, as not only the lower limb were generating a voluntary movement, but also the upper limb (i.e. fingers and hands) were engaged to voluntary type over the phone. Thus, the stronger  $\beta$  desynchronization could also be the results of activating both upper and lower limb as well as monitoring their performance through all the duration of the task. It is here therefore suggested that when walking while texting, subjects require a higher level of sensorimotor integration to monitor their walking behaviour while engaging hands in the secondary task of typing over the phone. This likely resulted in a stronger  $\beta$  desynchronization as a basis for a more “active state” to maintain the current status quo. Moreover, the most challenging dual-task paradigms for both healthy young adults and neurologically impaired populations are those in which visual scanning of the external environment is prevented or altered. All these elements lead to the conclusion that a stronger sensorimotor integration, as expressed in terms of stronger  $\beta$  desynchronization, is needed for maintaining gait stability and spatial navigation as well as performing the secondary cognitive and manual task. Comparisons between natural with multitasking walking then showed changes in bilateral frontal, motor and right posterior parietal areas, but interestingly not in the left PPC, which therefore appears to be constantly active across the three conditions. Bilateral PPC has been attributed a vast number of roles (Buneo and Andersen, 2006), and a link between the ability to spatially navigate through space and goal-directed ambulatory movement planning has been recently proposed (Calton and Taube, 2009). Among the two hemispheres, the right-PPC (together with the PFC) is also the main character of attentional networks (Dosenbach et al., 2007; Corbetta and Schulman, 2002) and visual spatial processing tasks (Yordanova et al., 2016), which

makes it more likely to be modulated across different conditions and frequency bands, as also this study has shown. On the other hand, left-PPC activation does not change across conditions, thus it seems to be constantly involved in online sensori-motor integration and control of voluntary movement (Lenka et al., 2016). Further analysis validating these evidences are reported in chapter 8.

#### **7.4.4 The role of the cortex in gait control**

As previously discussed (see paragraph 2.3.1), human gait control is suggested to be based on a complex hierarchical structure whereby both peripheral (i.e. CPGs) and central regions (i.e. neural cortex, deep brain structures and brainstem) have a role. Previous investigations on paraplegic patients found activations patterns similar to those of natural gait when electrically stimulating the injured spine (Dimitrijevic et al., 1998), suggesting the presence of muscle activators at peripheral level. Moreover, non-invasive brain imaging studies on both neurologically impaired patients (Bartels and Leenders, 2008) and healthy subjects (Jahn et al., 2008) also confirmed the activation of specific neural substrates during real and/or imagined walking. However, given the limited possibility to study humans invasively, the definite role of each of these elements is yet to be properly defined (Takakusaki, 2017). A recent study investigated how human gait is encoded at the level of the leg primary motor cortex invasively by means of ECoG in epileptic patients walking on a treadmill (McCrimmon et al., 2017). The study goal was to determine the role of the primary motor cortex during gait, whether of high-level (i.e. obstacle avoidance, speed determination), of low-level (i.e. muscle activations) or of integrative functions (i.e. integration with sensory drives). A strong  $\gamma$  band synchronization was recorded during walking, modulated along each stride periodically and consistently across different gait speeds. Interestingly, the  $\gamma$  activations observed during natural walking were of a different nature of those observed during single lower limb muscle contractions and did not correlate with lower limb trajectories. The authors suggested that the observed neural synchronization and modulation were a symbol of the high-level functions encoded within the primary motor cortex during walking, which was therefore proposed to control, for example, walking speed and movement duration. These new and outstanding results further validate the proposed theories that high-level functions of human gait control are executed centrally (i.e. by the neural cortex and deep brain structures), whereas low-level functions are administered by the peripheral component of the hierarchy (i.e. by the CPGs) (Takakusaki, 2013; Takakusaki, 2017). Previous whole-head fNIRS investigations suggested that the cortex has a central role in the control of gait, especially after a neural injury when restoring impaired pathways is

required. When investigating the neural correlates of three different gait training paradigms (i.e. stepping walking, treadmill walking and robot-assisted walking), increased sensorimotor, premotor and supplementary motor activities were always detected, with the robot-assisted protocol recruiting a broader and more global network (Kim et al., 2016). In another study, stroke survivors with severe hemiplegia were asked to walk on a treadmill with maximal assistance (BWS) while performing three different types of assisted training: simple BWS walking, BWS walking with assistance from the physiotherapist for the paralyzed leg control (CON), and BWS walking with assistance from the physiotherapist for facilitating pelvis control (FT) (Miyai et al., 2002). The FT intervention induced greater activations in the affected hemisphere than the other two conditions, and prominent effects were observed in the premotor regions of the affected hemisphere as well as in the sensorimotor, supplementary motor and pre-supplementary motor regions of the unaffected hemisphere. The authors suggested that the increased PMC activity could resemble engaged adaptive locomotion control as well as compensation and/or reorganization of cortical networks, whereas the increased pre-SMA activations could be related to novel motor learning and restoration of impaired gait after stroke. In general, these studies speculated that locomotion is mediated by both supra-spinal and spinal structures, and that the observed increased cortical activations in the respective studies hint towards a central control of gait whereby proprioceptive feedback are employed to modulate input to the rhythm generators (i.e. CPGs) and to facilitate symmetric locomotor patterns adapting to the contextual environmental changes (Kim et al., 2016). Our results are in line with these arguments and further validate them: it is likely that the neural cortex detected and managed the increased cognitive demand during the dual-task conditions (especially when walking while texting with the smartphone) and adapted motor performance (i.e. reducing speed) so that the secondary task could be undertaken whilst maintaining safety over the execution. The lower limb muscular evidence reported in the current study further supports this theory: the observed reduction of muscular activities in the two dual-task conditions could likely be the result of the reduced focus of the brain only on gait control (in favour of dual-task performance) and subsequently of the reduced descending motor drives to spinal structures, which in turn activate muscles to a less extent (Artoni et al., 2017). According to this theory, determination of high-level gait features, such as speed and movement duration, would be the result of higher cortical functions integrating primary motor, sensory and pre-frontal areas. In turn, peripheral elements as the CPGs would subsequently receive motor

commands from the centre and simply actuate them by activating lower limb muscles as required, periodically.

#### **7.4.5 Limitations**

The recruited participants were all healthy young adults (i.e. students), with no history of psychiatric, neuromuscular and/or orthopaedic problems, and all with a good level of physical fitness as all mentioned practicing a sport. Therefore, it is unlikely that the level of physical fitness and of neural executive functions caused different motor and cognitive performance. Nevertheless, it was evident that subjects had different levels of experience in walking with the mobile phone, which in turn allowed to have enough variety of skills and performance level within the recruited sample. Moreover, all subjects were right-handed, which could have biased our results (Miyai et al., 2001). Future studies should consider a more complete cohort of subjects and eventually identify differences due to subject-specific handedness neural wiring. The limited number of subjects recruited was dictated mostly by weather limitations as experiments could not be properly carried out during winter time in London. The strong analysis pipeline developed compensated for the limited number of available subjects by maximizing the single-subject physiological content and minimizing external artefacts. Indeed, only one subject out of fifteen in total showed statistically significant artefactual activations across the whole frequency spectrum exactly time-locked at the moment of heel strike, which proves that the pre-processing pipeline built to clean the data from external noise and remove gait-related artefacts is considerably robust. However, further tests are needed to further validate the experimental framework. In terms of study design, during single-task walking subjects were left free to think about anything they wanted, thus it is unknown what they were actually “thinking” when walking. Subject-specific internal/personal factors as well as external distractions (e.g. weather, people passing by, etc) might have influenced the actual performance during the tasks, especially the recorded neural data. This goes far beyond the goal and purpose of the current study, which does not aim to identify real-world activations of the human brain to each single external input and distractions, but instead to observe overall behaviour and gait performance when inserted in a partially-controlled multi-stimuli environment. Mobile Brain/Body Imaging (Gramann et al., 2014; Gramann et al., 2017; Ladouce et al., 2017) is a very novel field of research investigating the human behaviour in its natural environment. The biggest challenge here consists of defining what is potentially measurable and inferable from such studies in comparison to controlled laboratory-based investigations. In addition, the level of attention and engagement subjects gave to each single task and/or to both tasks together was unknown.

The results presented here pave the way for future more specific studies in which attentional levels and their impact on behaviour and performance could be further investigated within the real-world scenario.

## **8 Brain and behaviour: investigating the relationships between brain activations and gait patterns during single- and dual-task walking in the real world**

### **8.1 Introduction**

The recent developments in mobile technologies allow scientists to design and implement experimental frameworks with ambulatory settings, both within and/or outside the laboratory environment. The advantage of such applications relies in testing the subject in an active state of performing natural tasks during which neural and behavioural correlates of the task are investigated in conjunction (Ladouce et al., 2017). Many different types of studies are currently under way investigating the neural correlates of gait intentions in neurological impaired patients (Choi et al., 2016), the neural correlates of different types of artistic performances, from dancing to music playing (Contreras-Vidal et al., 2017), as well as the neural correlates of walking within different city areas, from traffic zone to green parks (Aspinall et al., 2013; Tilley et al., 2017). The most interesting aspect of these novel approaches based on simultaneous recordings is the possibility to correlate brain and behaviour, thus identifying specific bio-markers of an activity or task. In a rehabilitation or assistive perspective, such potentiality could turn out to be essential in determining which brain areas most relate to a specific ambulatory task, how the relationship is built and how supportive technologies could eventually contribute and compensate for any impairments that prevent the proper execution of such activities.

Human walking behaviour has been extensively studied and very recently a novel marker of the quality and variability of this process has been successfully proposed. Acceleration Root Mean Square (RMS) is a measure of the intensity of walk, usually recorded at the level of the pelvis, in any 3D directions of movement, and its normalized values (allowing for comparison across different populations and tasks) has been shown to correlate with age (Iosa et al., 2014) as well as with neurological impairments (Sekine et al., 2013; Sekine et al., 2014). Acceleration RMS in the vertical and antero-posterior direction of walking have been shown to be negatively correlated with age, whereas RMS in the medio-lateral direction decrease with age until a certain point when it sharply increases, probably due to augmented lateral swinging because of reduced cognitive functions resulting in stiff upper body and impaired lower limbs. Neurological impairments also affect walking acceleration, with a systemic decrease of RMS in any directions in Parkinson's disease patients regardless of the risk of falling (Latt et al., 2009), whereas stroke survivors usually show increased medio-lateral and antero-posterior trunk accelerations (Van Crieginge et al., 2017). However, the relationships established with



the measure of acceleration RMS (normalized or not) are so far limited to age and level/type of neurological impairment. No direct relationship between quality of walking and neural activations have been proposed yet to our knowledge.

A preliminary investigation of the potential relationships between neural brain activity, as recorded through means of EEG, and walking accelerations RMS normalized (RMSR) across different conditions and level of secondary task difficulty was here explored. According to the recent literature and our previous results (see Study II, chapter 7, paragraph 7.3.1), potential relationships were expected to establish between acceleration RMSR and neural activity, expressed in terms of EEG spectral power, recorded from electrodes located over the (pre-) frontal cortex (PFC, anterior and dorso-lateral areas) and the bilateral posterior parietal cortices (PPC). The choice of these specific three ROIs was dictated by the current common interest towards the PFC as involved in multitasking, mostly in fNIRS studies (Al-Yahya et al., 2016; Holtzer et al., 2011; Maidan et al., 2016), and the recent evidence of an active engagement of bilateral PPC in secondary motor adaptation during walking (Sipp et al., 2013; Bradford et al., 2016; Wagner et al., 2016). These regions have been also showed to be jointly involved in different attentional (Dosenbach et al., 2007) and executive functions networks (Rosenberg-Katz et al., 2016), thus of major interest for the ambulatory tasks performed in this study. A Regions of Interest (ROIs)-based approach will be followed in this analysis, with the goal of identifying which brain areas most contribute to the quality of walking across different conditions in the real-world.

## **8.2 Materials and methods**

### **8.2.1 Experimental setup and recording techniques**

The raw gait and EEG data were obtained in the experiments described in chapter 7 of Study II. For a detailed description of data collection and primary analysis see chapter 7, paragraphs 7.2.1, 7.2.2 and 7.2.3.

### **8.2.2 Data analyses**

#### **Gait measures**

Gait measures of fourteen subjects were analysed through the iGAIT free toolbox for MatLab (Yang et al., 2012) as fully described in chapter 7, paragraph 7.2.4. Of major interest for this chapter are the measures of acceleration RMS Ratio (RMSR) as calculated through the formula reported in chapter 7, paragraph 7.2.4, section Gait Measures. These measures are indeed representative of the quality and/or abnormality of a person gait (Sekine et al., 2013) and here therefore further used as such in relationship with central

neural activations. Previous studies have shown that gait behaviour and patterns are optimized when walking at the natural speed (Menz et al., 2003; Sekine et al., 2013), thus in this study subjects were specifically asked to walk at their preferred speed. However, it has been demonstrated that velocity influences gait behaviour (as described through measures of acceleration RMS, both normalized and not) both in healthy and neurological populations (Menz et al., 2003; Sekine et al., 2013; Iosa et al., 2014; Van Crieginge et al., 2017). Consequently, velocity will be always included in the analysis of the relationship between neural activity and gait behaviour as it might influence the outcome.

### **EEG pre-processing and ROI-based power spectrum**

EEG data of fourteen subjects were pre-processed through EEGLab open source toolbox for MatLab (Delorme and Makeig, 2004) as fully described in chapter 7, paragraph 7.2.4, sections EEG pre-processing. Power Spectral Density (PSD) content in the frequency domain of each channel, in each frequency for each subject were calculated as detailed in chapter 7, paragraph 7.2.4, section Power Spectral Density (PSD). Here analyses focused only on three Regions of Interest (ROIs), as per hypothesis changes in gait behaviour were expected to be related to changes in brain activities in those areas mostly employed during executive functions, spatial attention and navigation, sensorimotor integration and adaptation during multi-tasking. Previous findings have localized consistent brain activities during both single-task and dual task as well as adaptation in walking (Bradford et al., 2016; Lin and Lin, 2016; Wagner et al., 2016) in (pre-) frontal and bilateral posterior parietal clusters. 3 ROIs were therefore defined and identified the electrodes laying over such areas were identified, specifically:

- **Pre-Frontal/Frontal ROI** = {FP1, FPZ, FP2, AF7, AF3, AF4, AF8}. This ROI covers Brodmann Areas 9, 10 and 46, namely Dorsolateral/Anterior Prefrontal Cortex (see <https://www.trans-cranial.com/>). Together with deeper structures as basal ganglia and hippocampus, the DLPFC plays a role in some of the highest cognitive functions as planning, organization and regulation, whereas the APFC participates in memory functions, specially working memory and memory retrieval;
- **Left/Right-Posterior Parietal ROIs** = {P7, P5, P3, PO3, PO5, PO7}/ {P8, P6, P4, PO4, PO6, PO8}. This two ROIs include bilaterally the Associative Visual Cortex, which carries out some language related functions (e.g. confrontation naming); the Fusiform Gyrus, i.e. the occipital-temporal lobe mainly involved in processing of colours, face and body as well as words and numbers recognition; the Angular Gyrus, involved in high-cognitive functions (sensorimotor integration) as cross modal

association among somatosensory info, auditory and visual information (see <https://www.trans-cranial.com/>).

Figure 8-1 shows the spatial location of the electrodes grouped in the three ROIs according to the 64-channel cap montage used during the recordings. The average PSD across each ROI-specific electrode was calculated for each subject, in each FOI and for each condition separately.

### **Models of gait behaviour vs. EEG PSD activations**

Models of the relationships between brain activity and gait behaviour were run both with SPSS 23 software (IBM). Separate models for single- and each dual-task condition were created with accelerations RMSR in each direction as Dependent Variables (DVs), given their successful previous usage reported in literature (Menz et al., 2003; Sekine et al., 2013). PSD in each specific FOI (x3) and ROI (x3) were used as Independent Variables (IVs, i.e. predictors), for a total of 9 neurophysiological IVs. Additionally, Velocity was also included in the models as an IV given its potential effects on these gait patterns (Sekine et al., 2013). For each DV, three models were generated separately for each experimental condition (i.e. ST, DT1 and DT2). Multiple Regression models were created with the format:

$$RMSR_x = \beta_0 + \beta_1 \cdot Velocity + \beta_{ij} \cdot PSD\_ROI_i\_FOI_j + \varepsilon$$

Equation 8-1: Multiple regression models for RMSR formula.

where  $RMSR_x$  is the acceleration RMSR in the direction x (i.e. vertical, antero-posterior, medio-lateral) during each walking condition separately,  $PSD\_ROI_i\_FOI_j$  is the PSD in the ROI i (i.e. frontal, right-parietal, left-parietal) and in the FOI j ( $\theta$ ,  $\alpha$ ,  $\beta$ ) stepwise entered into the model,  $\beta_n$  are the intercept and coefficient associated to each model predictor, and  $\varepsilon$  is the error. Data were first centred (i.e. the mean score was subtracted from each observation) and scaled (i.e. standard deviation was set equal to 1) in order to reduce the chance of multicollinearity. When working with multiple regression models, all the assumptions were tested and checked before reporting results. Measure of Goodness-of-Fit (B) and p-value associated to each significant predictor will be reported.

## **8.3 Results**

### **8.3.1 Relationship between single-task walking acceleration and neurophysiological activity**

Multiple linear regression did not provide statistically significant models for ml-RMSR and ap-RMSR during single-task walking. However, a regression model was successfully

created for ver-RMSR (R-squared = 0.725,  $p = 0.001$ ) for which all assumptions were met (no multicollinearity, no auto-correlation, no homoscedasticity). Specifically, only the IVs significantly contributing to the prediction of ver-RMSR were entered stepwise into the model. The final model predicts the DV based on Velocity ( $B = 0.355$ ,  $p = 0.001$ ) and left-parietal  $\theta$  PSD ( $B = 0.009$ ,  $p = 0.026$ ), as shown in Figure 8-2. The final model equation can therefore be written as follow:

$$verRMSR = 0.699 + 0.355 \cdot Velocity + 0.009 \cdot left\ Parietal\_ \theta\_ PSD$$

Equation 8-2: Multiple regression model for verRMSR during ST formula.

### 8.3.2 Relationship between dual-task walking acceleration and neurophysiological activity: walking while conversing

Multiple linear regression did not provide statistically significant models for ap-RMSR when walking while conversing. A significant model was created for ml-RMSR (R-squared = 0.745,  $p = 0.003$ ) but assumptions of multicollinearity were not met, thus the model couldn't be considered as reliable. A regression model was successfully created for ver-RMSR (R-squared = 0.727,  $p = 0.001$ ) for which all assumptions were met (no multicollinearity, no auto-correlation, no homoscedasticity). Specifically, only the IVs significantly contributing to the prediction of ver-RMSR were entered stepwise into the model. The final model predicts the DV based on Velocity ( $B = 0.029$ ,  $p = 0.003$ ) and left-parietal  $\alpha$  PSD ( $B = 0.021$ ,  $p = 0.020$ ), as shown in Figure 8-3. The final model equation can therefore be written as follow:

$$verRMSR = 0.704 + 0.029 \cdot Velocity + 0.021 \cdot left\ Parietal\_ \alpha\_ PSD$$

Equation 8-3: Multiple regression model for verRMSR during DT1 formula.

### 8.3.3 Relationship between dual-task walking acceleration and neurophysiological activity: walking while texting with a smartphone

Multiple linear regression did not provide statistically significant models for ver-RMSR and ap-RMSR walking while texting over the phone. However, a regression model was successfully created for ml-RMSR (R-squared = 0.434,  $p = 0.010$ ) for which all assumptions were met (no multicollinearity, no auto-correlation, no homoscedasticity). Specifically, only the IVs significantly contributing to the prediction of ver-RMSR were entered stepwise into the model. The final model predicts the DV based only on left-parietal  $\beta$  PSD ( $B = -0.055$ ,  $p = 0.010$ ), as shown in Figure 8-4. The final model equation can therefore be written as follow:

$$mlRMSR = 0.414 - 0.055 \cdot left\ Parietal\_ \beta\_ PSD$$

Equation 8-4: Multiple regression model for mlRMSR during DT2 formula.

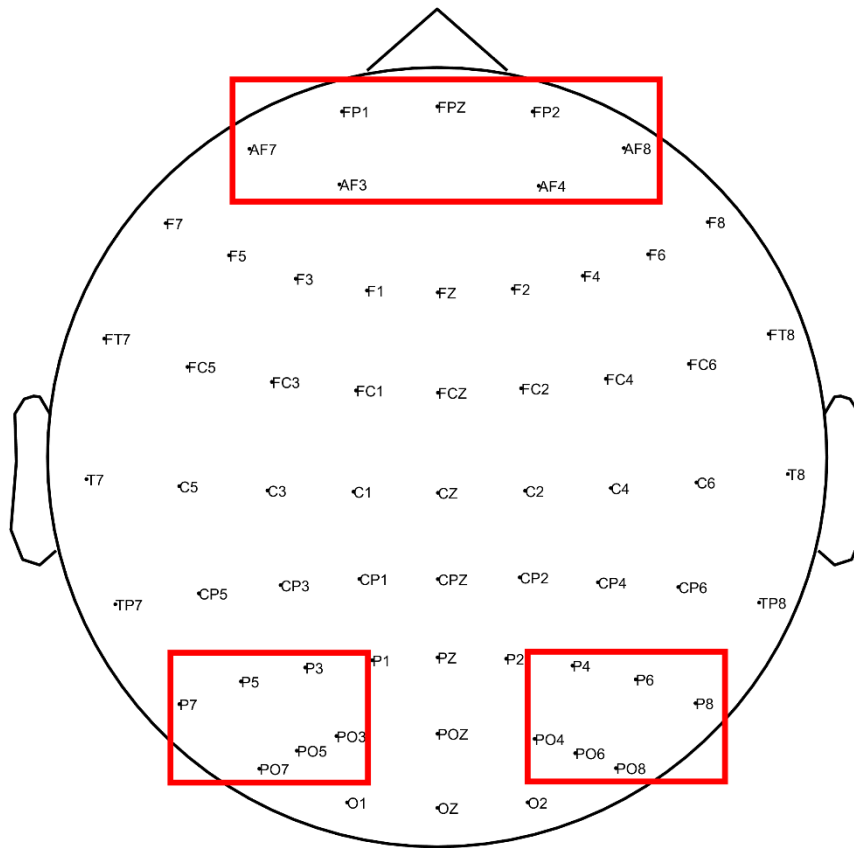


Figure 8-1: ROIs of interest.

The electrodes topological layout of the 64-channel cap used during the recordings is here reported with electrodes names in their right location. Red rectangles highlight the electrodes included into the defined (pre-) frontal and left/right parietal Regions of Interest (ROIs).

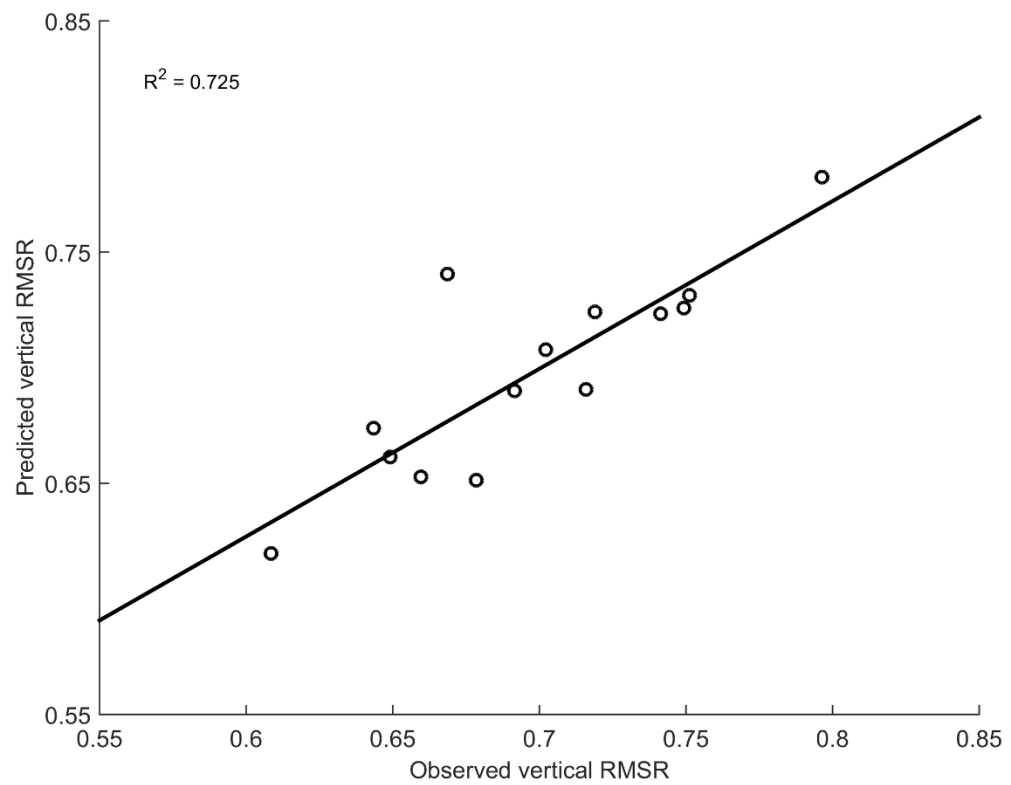


Figure 8-2: Observed vs. Predicted ver-RMSR values according to the multiple regression model during ST.

The model R-squared value associated to the line of fit of the model is printed on the graph.

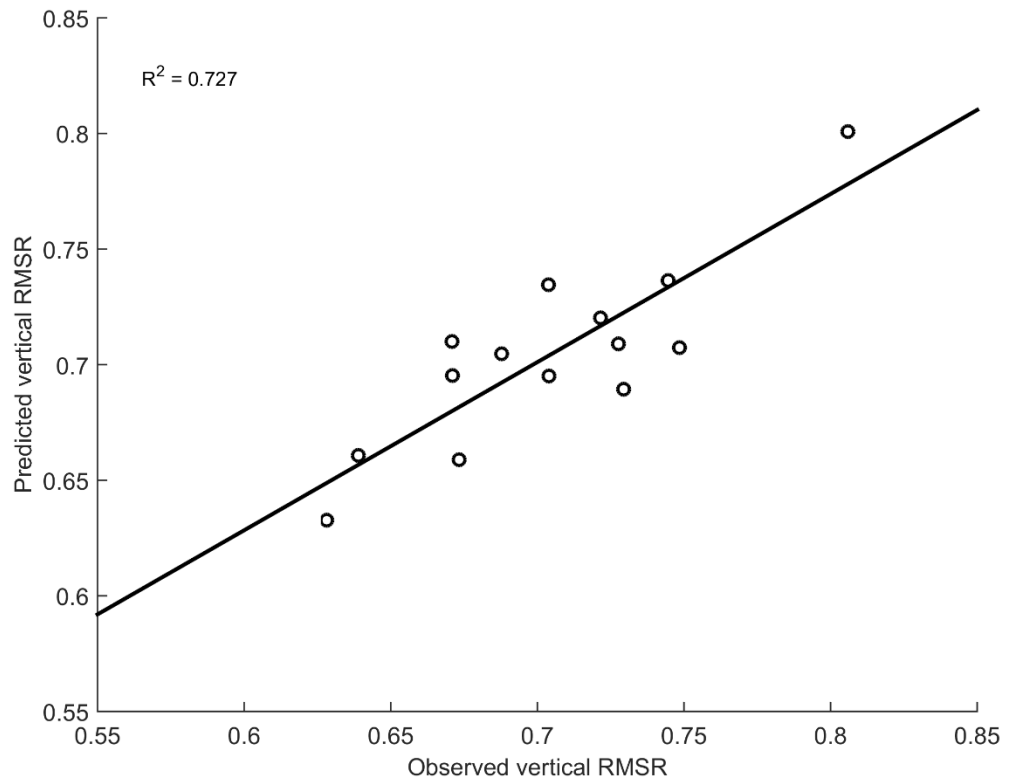


Figure 8-3: Observed vs. Predicted ver-RMSR values according to the multiple regression model during DT1.

The model R-squared value associated to the line of fit of the model is printed on the graph.

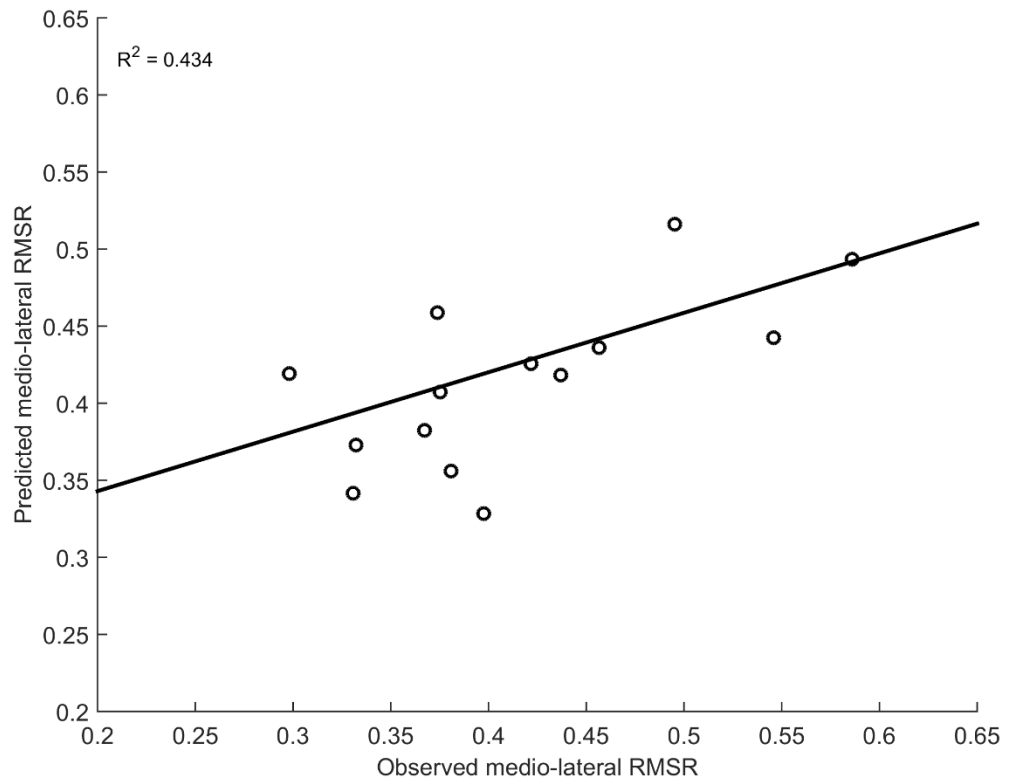


Figure 8-4: Observed vs. Predicted ml-RMSR values according to the multiple regression model during DT2.

The model R-squared value associated to the line of fit of the model is printed on the graph.



## **8.4 Discussions**

### **8.4.1 Novel findings**

The current findings describe a direct linear relationship between gait behaviour and brain activations. Measures of gait variability and abnormality as conveyed via acceleration RMSR were correlated with brain activations as expressed in terms of Power Spectral Density. Single-task walking and walking while conversing were characterised by a direct positive relationship between ver-RMSR, velocity and left parietal PSD in  $\theta$  and  $\alpha$  frequency bands respectively. On the other hand, walking while texting with a smartphone featured a direct negative relationship between ml-RMSR and left parietal PSD in the  $\beta$  frequency band. Despite the change in frequency activity, the left posterior parietal cortex is here suggested to play a role in locomotion control in the real-world regardless of the secondary task simultaneously performed.

### **8.4.2 Gait acceleration RMS as measure of gait stability and behaviour**

Acceleration RMS has been extensively used in studies of gait in both healthy and neurologically impaired populations (Menz et al., 2003; Latt et al., 2009). Previous investigations have shown that, in both healthy young and older adults, acceleration values tend to augment when walking on an insidious surface (i.e. more difficult) at the level of the pelvis (i.e. lower back) (Menz et al., 2002). Concurrent registration of accelerations at the head did not show such changes across surfaces: it can be said that the ultimate goal during walking consists in stabilizing the head (thanks also to the spine that attenuates walking steps vibrations). Therefore, the choice of placing the acceleration recording phone at the lower back level of our subjects was based on previous literature investigations (Kavanagh and Menz, 2008) and aimed to maximize the acceleration variability across subjects (as per physiological and anatomical differences) and across conditions (related to task difficulty). Then, in order to render the gait behaviour expressed through this measure comparable across different types of populations (healthy vs. elderly vs. neurologically impaired), across subjects and across different speeds, normalization procedures have been proposed (Terrier and Reynard, 2015; Iosa et al., 2014). The normalized measure of acceleration RMS Ratio (RMSR) adopted in the current study has been previously shown to successfully correlate with gait variability and abnormality in both healthy adults and neurologically impaired (Sekine et al., 2013; Sekine et al., 2014). Moreover, other measures such as velocity have been shown to change across any type of conditions regardless of presence of gait instability, thus not proper for our aim. Indeed, reduced walking velocity and altered trunk movements are

two of most undertaken compensatory strategies for reduced executive functions capabilities in the elderly (Menz et al., 2003) and in stroke survivors with lower limb impairment (Iosa et al., 2014; Van Crieginge et al., 2017). Consequently, in elderly and neurological populations an increase in upper body acceleration values (as measures at the lower back level), might result from a combination of reduced cognitive capabilities, motor impairment and compensatory strategies. Therefore, measures of normalized acceleration RMSR were here employed to validate this hypothesis by testing healthy young adults in different difficulty-level walking conditions.

#### **8.4.3 Relationship between brain and behaviour**

It was here purposely tested whether (pre-) frontal and bilateral posterior parietal sensor-level spectral activity could relate to gait behaviour as it has been shown that these are the most modulated cortical areas during dual-task walking (Lin and Lin, 2016; Al-Yahya et al., 2016; Wagner et al., 2016; Maidan et al., 2017) and in dual-task laboratory-based experiments (Wahn and König, 2017). Pre-frontal activity (specifically from the rostral prefrontal cortex) was shown to be graded as a function of cognitive demand during dual-task walking whereby more challenging tasks recruited higher oxygenation levels, and subjects that performed better in the secondary cognitive task (i.e. subtracting 7 by a random starting 3-digit number) showed lower oxygenation levels (Mirelman et al., 2014). The authors suggested that these subjects likely required less effort and oxygenation levels than those participants who performed worse and required more pre-frontal activity in order to be able to perform the two tasks simultaneously together. Curiously, in our study left PPC (not the PFC) was related to gait behaviour regardless of the secondary task type undertaken. The left PPC has been extensively studied in laboratory-based experiments both on animals and humans (Calton and Jeffrey, 2009). Currently it is thought to act as the sensorimotor integrator and online rapid updater of movement planning (Fogassi and Luppino, 2005; Buneo and Andersen, 2006, Churchland et al., 2006), integrating spatial information of the surroundings and sensory feedback with motor planning and executive commands (Calton and Jeffrey, 2009). Indeed, the spatial navigation deficits seen after damages of bilateral PPC as the Balint's syndrome (Balint, 1909) or neglect (Yordanova et al., 2016) arise because of the inability to integrate spatial orientation with current/future planning of the voluntary movement needed to accomplish the end goal. If the PPC is in general believed to play such a complicated role, each hemispheric area has been characterized with specific duties: on one hand, the right-PPC, in connection with frontal regions, is also involved in multiple types of attention (Tang et al., 2016; Dosenbach et al., 2007); on the other hand, the left

PPC has been recently shown to play a major role as sensorimotor integrator since Parkinson's disease patients that exhibit Freezing of Gait (FoG) also display reduced connection between left PPC and multiple brain regions such as somatosensory and auditory areas (Lenka et al., 2016). Left PPC is therefore suggested to more consistently work as a sensorimotor integrator during online movement planning and monitoring, whereas right PPC in parallel more actively engages with different attentional networks. This hypothesis is confirmed by our previous results (see chapter 7, paragraph 7.3.4 for a detailed summary) in which no differences across conditions in any frequency band of interest were found within clusters of electrodes located over the left PPC. A recent fMRI investigation of the hemodynamic correlates of simulated walking under single- and dual-task conditions reported a similar relationship between stepping variability and activity within the superior parietal lobule (SPL), principally in the left hemisphere, whereby higher SPL activations were associated to slower stepping speed in older adults (Bürki et al., 2017). SPL is known to be involved in multitasking and task switching performance (Al-Hashimi et al., 2015), and was shown to be sensitive to cognitive-motor dual tasking. Moreover, SPL appeared similarly activated across both single- and dual-task conditions, demonstrating its crucial role in motor coordination and control under both single- and dual-task locomotion, in line with the left PPC activations observed in the current study. Consequently, the left PPC is here suggested to play a primary active role in monitoring and planning the walking movement regardless of any secondary conditions in parallel undertaken. The relationships between this brain region and gait pattern though change across conditions in terms of the gait measure and the frequency bands that successfully correlates.

### **Task-specific relationships between brain activation and gait behaviour**

When walking naturally, a positive linear predictive relationship could be identified between left PPC activity in the  $\theta$  frequency band and ver-RMSR and velocity. Ver-RMS(R) has been shown to depend linearly on gait speed and to represent the quality of gait, with higher values symbolic of a more stable and rapid walk (typical of healthy young adults) and lower values symbolic of reduced flexibility and bent postures (typical of older adults) (Iosa et al., 2014; Menz et al., 2003; Sekine et al., 2013). We confirmed the positive relationship between ver-RMSR and velocity but added a predictive neural component (left PPC). When walking naturally without engaging in any secondary tasks, left PPC has been shown to be active in the  $\theta$  range (4 – 7 Hz) (Caplan et al., 2003; Ekstrom et al., 2005; Chiu et al., 2012) and is believed to be connected to deeper

structures such as the hippocampus actively engaged in the navigation process (Bohbot et al., 2017).

When walking while conversing, a positive predictive relationship could be identified between left PPC activity in the  $\alpha$  frequency band and ver-RMSR and again velocity. As  $\theta$  neural oscillations likely engage in memory retrieval and organization of ‘thoughts’ when subjects are engaged in a conversation (Giraud et al., 2007; Simons and Spiers, 2003), is it likely that higher frequency oscillations (i.e.,  $\alpha$ ) took over the duty of sensorimotor integrator and monitor during walking in the present study. This hypothesis is further supported by recent studies showing involvement of  $\alpha$  (8 – 12 Hz) oscillations in spatial navigation (Chiu et al., 2012; Lin et al., 2015) and sensorimotor integration during walking speed adaptation to an external pace cue (Wagner et al., 2016).

A significant negative predictive relationship was found between left PPC spectral activity in the  $\beta$  frequency band (15 – 30 Hz) and ml-RMSR when walking while texting. ml-RMSR has been recently validated as a marker of gait abnormality and recovery, where abnormally high values of trunk acceleration decrease alongside recovery (Sekine et al., 2013; Sekine et al., 2014). Moreover, stronger  $\beta$  desynchronization is required in arduous conditions in order to maintain the ‘status quo’ and to promote the voluntary action in a more challenging dual-task context (Engel and Fries, 2010; Sipp et al., 2013; Bradford et al., 2016; Wagner et al., 2016). The negative relationship suggests that those subjects showing higher gait variability in the medio-lateral direction required stronger  $\beta$  desynchronization in order to accomplish the simultaneous tasks. This is in line with previous studies that showed that  $\beta$  PSD in the posterior parietal and occipital areas could be used to reliably classify and detect events such as FoG and GIF in Parkinson’s disease patients (Handojoseno et al., 2015; Ly et al., 2016), thus confirming the involvement of this brain region in postural and movement online control via sensorimotor integration. Of note, ml-RMSR did not correlate with velocity in this study as previously reported in the literature (Sekine et al., 2013).

#### **8.4.4 The potential role of the left posterior parietal cortex in gait rehabilitation**

As previously mentioned, non-invasive recordings in humans are still very limited, which in turn constrains the understanding of the role that each element within the gait control hierarchy has. The ground-breaking findings of McCrimmon and colleagues (McCrimmon et al., 2017) open the doors to more solid interpretations of the role of the primary motor cortex during gait, but much future work remains. The current investigation reported preliminary evidence of the relationship between neural activity in

the left posterior parietal cortex and measures of trunk acceleration during gait, hypothesising a role in motor behaviour and performance control for the left PPC. The PPC is believed to promote sensorimotor integration during different types of movements in humans (Buneo and Andersen, 2006), but invasive evidence during gait are still to be reported. Extensive observations on the PPC activity during walking were however presented by animal studies, whereby intra-cortical recordings allowed the monitoring of single neurons activations while cats performed walks with (Beloozerova and Sirota, 2003) and without (Marigold and Drew, 2011) visual guidance. It was postulated that PPC is involved in high-level functions of both visuo-motor integration, for example allowing the detection of obstacles features, as well as of memory and storage, conserving information on the previously processed features to permit gait even in the absence/obstruction of visual guidance. Activity of the superior parietal lobule (prominently in the left hemisphere) was shown to correlate with stepping variability during simulated dual-task walking in older adults whereby higher SPL activations were associated to more variable behaviour, thus suggesting a fundamental role of the parietal structure in locomotion control (Bürki et al., 2017). Our results appear to be in line with the above-mentioned theories: PPC activity positively predicted trunk acceleration during single-task walking and during walking while talking, likely promoting sensorimotor integration between internal and external spatio-temporal features. At the same time, it negatively predicted trunk acceleration when walking while texting over the smartphone, a condition in which subjects had a partially limited vision of the path in front of them, likely promoting both sensorimotor integration and storage of information for the periods of prevented visual guidance. Indeed, those subjects with higher PPC activity showed higher trunk acceleration and better motor performance. These findings and interpretations seem therefore to give even more credit to the theories on the high-level functions performed by the neural cortex during gait control with respect to the peripheral structures (i.e. CPGs), entitled to simply generate rhythmic muscle activations in response to the sensorimotor integrated drives coming from central sources (Takakusaki, 2013; Takakusaki, 2017; McCrimmon et al., 2017). The predictive role of the left PPC could be exploited by novel rehabilitation paradigms. Recent interventions for both balance and gait training reported preliminary positive outcomes when providing intensive biofeedback training. Healthy elderly adults were trained to increase their sensori-motor rhythm (12-15 Hz) and decrease their theta waves (4-7 Hz) (registered from the O1 and O2 occipital electrodes, placed over structures involved in balance control such as occipital lobe, substantia nigra, basal ganglia and cerebellum) while playing video games

on a PC during neurofeedback training sessions ( $n = 15$ , five weeks in total, 30 min each); balance skills were assessed both before and after the training period (Azarpaikan and Torbati, 2017). Balance performance significantly improved after neurofeedback training, which surprisingly facilitated subjects' control mostly on static postural sway. Positive neurofeedback training outcomes were also recently reported with a cohort of stroke survivors performing dual-task walking (Lee et al., 2015). Patients assigned to the neurofeedback group were trained to increase their sensori-motor rhythm (registered from the Cz electrodes located over the paracentral lobule including the lower limb motor areas) while playing video games on a PC; dual-task performance (both motor and cognitive) was tested before and after the training period as patients walked along a predefined path while counting backwards from 100 by steps of 7. Patients trained with the neurofeedback protocol showed both higher cognitive (i.e. less counting backwards errors) and motor (i.e. higher velocity, cadence, foot weight on the ground, stance phase index) performance in comparison to patients located in the control group, which did not receive any specific biofeedback training. In summary, employing neurofeedback training specific to the end goal (e.g. targeting occipital areas for balance training and central regions for gait performance) seems to be a promising tool to promote recovery and a reliable as well as entertaining (as participants always played videogames) way to teach how to self-regulate the neural mechanisms responsible for specific balance and gait performance. Given these preliminary positive findings and considering the potential role of the left PPC in the control of gait, future studies could define a biofeedback training based on the activity of this region (in a first instance likely testing different frequency ranges) in order to teach subjects how to self-modulate the rhythm eventually involved in the control of sensorimotor integration and postural control during gait. Such a protocol would have a strong impact on the rehabilitation of neurological patients such as stroke survivors and PD patients, as it would promote their ability to control posture by engaging appropriate neural mechanisms.

#### **8.4.5 Limitations**

As our healthy population sample was limited, it would be interesting to expand the study including more healthy young adults, as well as healthy older adults or neurological patients, in order to further test the hypothesis of the left PPC consistently involved in monitoring the walking process with different roles according to the task difficulty level expected. Moreover, future studies should determine guidelines to properly classify “good” and “bad” performers, especially in the dual-task conditions, to further disentangle the neurophysiological bases of dual-task walking within the sample

population. Ultimately, the correlation approach undertaken in this study looked for a very simple (linear) relationship between brain and behaviour, with brain spectral activity averaged across electrodes in a ROI-based approach thus to rule out any unwanted effects of multicollinearity. Future studies should employ a higher number of channels/ROIs in order to reliably reconstruct cortical sources from sensor recordings, and eventually use the numerous sensor-level data within a more complicated regression framework (e.g. Partial Least Square Regression, PLSR) able to tackle multicollinearity and describe more complicated relationships between brain and behaviour.

## 9 Final conclusions

Novel insights on the neurophysiological correlates of human motor control (of both upper- and lower-limb) were reported in the current research programme. They shed new light on the different mechanisms involved in motor control of natural movements (such as reaching and walking) in both stable and unstable situations. The findings gathered in these two scenarios further strengthen the theories on the central role of the human brain in the control of both upper- and lower-limb and identify crucial cortical regions that could be target of future rehabilitative practice.

### 9.1 The central role of the human brain in motor control of both upper- and lower-limb

Several studies had already demonstrated that, during reaching, the human brain exerts prime management functions. The primary motor cortex was shown to be responsible for translating high-level sensorimotor information into low-level motor commands through directional tuning (Fabbri et al., 2010; Toxopeus et al., 2011). Most interestingly, not only the primary motor cortex but also other cortical areas such as premotor cortex, parietal cortex, anterior and medial inter-parietal sulcus showed directional tuning effects due to different reaching directions, suggesting that a broader network is potentially involved in the programming of the movement (Fabbri et al., 2010). The findings reported in the current work confirm these theories, specifically through evidence of cortico-muscular coherence whereby changes in the neural-muscular synchronization due to the adaptation process were observed in a global network including supplementary motor, premotor, primary motor and parietal regions. The planning and adaptation of the movement to the external environmental changes is therefore confirmed to be promoted by a broad cortical network, whereby the medial supplementary motor areas seem to play a major role in the modulation of the exerted force.

In contrast, there is still much debate on the function of each of the structures involved in the control of gait, specifically on the role of the brain and of the spinal rhythm generators (CPGs) as well as on their relationship. Animals studies have hinted on the potential high-level control of the brain on the spinal centres (Beloozerova and Sirota, 2003; Lajoie et al., 2010; Marigold and Drew, 2001), but human evidence is still limited due to technical and ethical restrictions. Early suggestions on the central role of the human brain in gait control were reported during treadmill walking with both healthy adults and neurologically impaired patients undertaking different types of gait training (Miyai et al., 2002; Kim et al., 2016). Increased oxygenation levels in a broad cortical network



encompassing sensorimotor, premotor and supplementary motor areas were reported, suggesting that high-level control and adaptation of gait to external environmental changes are mediated by the brain, which in turn modulates inputs to the spinal rhythm generators for the generation of the required lower limb muscles activations. Further validation of this hypothesis has been recently provided by the first intra-cortical investigation with epileptic patients walking on a treadmill (McCrimmon et al., 2017), whereby high-frequency neural oscillations recorded from the primary motor cortex were postulated to encode high-level functions of gait control (for example, determination of gait speed and movement duration). The evidence reported in the current research appear to further validate these theories. As postulated, during dual-task walking the brain recruited both gait control mechanisms as well as secondary-task specific strategies as observed through changes in average spectral power with respect to natural single-task walking. Neural resources previously associated only to gait control were thus eventually divided between gait control and simultaneous secondary task performance, consequently reducing the actual work exerted by the central main motor control mechanisms (Nijboer et al., 2014). Considering the brain as the main actor in the gait control hierarchy, the systematic decrease in muscular activation profiles observed across the monitored lower limb muscles in both dual-task conditions could be interpreted as the result of the reduced gait control due to the simultaneous engagement of secondary mechanisms. Changes in central management were indeed hypothesised to result in less descending motor cortical drives to the spinal rhythm generators. The current work did not provide any evidence of direct cortico-muscular couplings during the real-life ambulatory activities, but very recent findings have reliably demonstrated that cortical activations are directly responsible for locomotion control, and specifically that unidirectional descending drives from the contralateral primary motor cortex exert fine control of leg in the swing phase (Artoni et al., 2017). The relationship between the spectral power within the left posterior parietal cortex and trunk acceleration during walking conditions again suggest that the cortical region appears to be directly involved in the control of gait stability and posture (Pizzamiglio et al., 2018), in line with previous findings (Bürki et al., 2017).

To summarise, the investigations carried out in this research programme support the hypothesis that the human brain is the principal manager of motor control of both upper- and lower-limbs, and that spinal structures are directly depending on its inputs to autonomously trigger the requested muscular activations (Fabbri et al., 2010; Takakusaki et al., 2013; McCrimmon et al., 2017; Takakusaki et al., 2017). As previously reported and here further demonstrated, the brain always recruits a global network including

frontal (anterior and dorsolateral), premotor, supplementary motor, primary motor and posterior parietal regions in order to promote sensorimotor integration and adaptation to the external environment (Shadmehr and Holcomb, 1997; Krebs et al., 1998; Miyai et al., 2002; Kim et al., 2016), and the primary motor cortex is responsible for translating high-level movement programme information into descending low-level motor commands (Toxopeus et al., 2010; McCrimmon et al., 2017). The current findings pave the way for further research required to more strongly validate the proposed theory.

## **9.2 Novel indicators of human motor control of both upper- and lower-limb**

Besides providing further evidence on the central role of the brain in motor control of both upper- and lower-limb, the current research identified plural markers of the analysed motor acts thanks to thorough and diversified analyses.

In the first study, muscles-specific (co-contraction, IMC), brain-specific (ERN) and cortico-muscular (CMC) indicators of adaptation to changes in the external environment during reaching have been identified. All these signatures of the implemented motor process have a high potential for being exploited into different neurorehabilitation practices. Co-contraction and IMC profiles could, for example, be employed as paradigm-specific targets to train neurologically impaired patients to self-modulate abnormal muscular co-activations. As the re-acquisition of range of movement and flexibility after neural injury is accompanied by the development of unnatural muscular patterns (Dipietro et al., 2007; Huang and Krakauer, 2009), providing training paradigms tailored to the specific needs of each patient would surely boost effective recovery. For example, the setup and protocol exploited in the current research could be further employed to train patients through either a clockwise either a counter-clockwise velocity dependent force-field according to which muscles need to be trained most, and both co-contraction and IMC profiles could be employed as measures of the quality of the performed movements (Wright et al., 2014). The two physiological markers could be even exploited as reference for brain-machine interface training, whereby a certain level of co-contraction and/or IMC between a priori defined muscles pairs could trigger robot-mediated movements in line with previous evidence (Ang et al., 2015), thus effectively exploiting the Hebbian principles of intentional motor acts paired with peripheral feedback. Care would be needed to be taken as muscular activations in neurologically impaired patients are frequently variable and unstructured, thus such trainings would likely be an option only for a limited cohort of eligible patients. In contrast, the negative spontaneous neural oscillations (event-related negativity, ERN) detected over the medial frontal cortex (and

likely originating from the anterior cingulate cortex) was hypothesised to be an indicator of the trial-by-trial error processing functions exerted by these brain regions during adaptation and interestingly shown to be independent of the type of the applied external perturbation (Falkenstein et al., 2000; Desowska, Pizzamiglio and Turner, 2018, *under review*). As similar correlates were observed during reaching adaptation to both clockwise and counter-clockwise force-field, it results as a reliable indicator of error processing despite the difference in the performed protocol. Moreover, ageing and neurological injuries were shown to systematically reduce the spontaneous component amplitude (Hogan et al., 2006; Colino et al., 2017). Therefore, ERN could be employed during motor adaptation and learning trainings as a marker of the abilities to detect and predict movement errors and as classifier of the level of impairment in error-based protocols. In contrast to the muscle-specific indicators, ERN would be used to promote comprehensive re-acquisition of high-level adaptive skills. Receiving visual feedback and trying to modulate the level of produced ERN while reaching in an unstable situation on a trial-by-trial basis could indeed promote the re-acquisition or simply the improvement of lost/impaired predictive and adaptive functionalities. Moreover, previous neurofeedback investigations have demonstrated that medial frontal regions, such as SMA and ventral PMC, are better targets than the primary motor cortex during motor control training with motor imagery (Marins et al., 2014; Linden and Turner, 2016), thus strengthening the potentials of the medial-frontal ERN as a valid target for neurorehabilitation practices. Lastly, the current research identified a significant moderate relationship between the level of SMA-ECR cortico-muscular coupling and the amount of force exerted to counteract the external perturbation. ECR is one of the most recruited muscles in the counter-clockwise protocol, and the corresponding neuro-muscular coupling with the supplementary motor area likely influences and regulates the amount of force required to counteract the applied perturbation. Further research is needed to identify stronger relationships between cortico-muscular evidence and behaviour, but these preliminary insights already suggest a potential applicability of CMC in self-training rehabilitative practices. Promising evidence on the employment of cortico-muscular evidence in neurofeedback training has been recently provided by an EEG study in which healthy young adults managed to self-regulate their level of CMC without changing the amount of produced force (von Carlowitz-Ghori et al., 2015). Targeting CMC during motor adaptation could therefore promote the re-storage of impaired neurophysiological mechanisms at the brain and at the spinal level, either jointly either separately according to the training hypotheses.

In the second real-world scenario, a potential predictor of gait stability has been found within the left posterior parietal cortex. Spectral power in the low frequency spectrum ( $\theta$  and  $\alpha$ ) positively correlated with trunk acceleration along the vertical direction when walking naturally (ST) and while conversing (DT) respectively; in contrast, spectral power within the medium frequencies ( $\beta$ ) negatively correlated with trunk acceleration along the medio-lateral direction. Previous investigations have proposed a direct relationship between cortical activations and measures of motor and/or cognitive performance during ambulatory activities, but results are often in contrast. For example, higher oxygenation levels averaged from all optodes located over pre-frontal cortex (thus including anterior, dorsolateral prefrontal cortex and inferior frontal gyrus) positively correlated with the rate of correct alphabet letters recited aloud while walking in both young and healthy elderly adults (Holtzer et al., 2015). These findings suggested that both populations could allocate attentional resources to both the motor and the cognitive task simultaneously to maintain a good performance (Cabeza et al., 2002). The level of executive functions (evaluated through Stroop interference) exhibited when walking was also negatively correlated with the hemodynamic activity registered from the left inferior frontal gyrus in elderly with MCI, proving that those subjects with higher impairments show, as a result, less activations (Doi et al., 2013). On the other hand, in another study, levels of oxygenation detected from the rostral prefrontal cortex (BA 10) negatively correlated with measures of gait variability as well as with rate of corrected subtractions made while walking in a cohort of young adults (Mirelman et al., 2014). In this case, the authors claimed that subjects that performed better in both tasks are those that require less effort and activations, whereas subjects struggling in simultaneously performing the two tasks require more prefrontal activations. In an fMRI study of simulated gait analyses whilst performing a cognitive task (Verbal Fluency Task), activity in the superior parietal lobule (SPL) correlated with measure of gait variability as well as with executive control performance (Bürki et al., 2017). Specifically, subjects that stepped slower activated the SPL area more, and those subjects performing worse in the cognitive task activated the SPL to a larger extent. The evidence of the current work of research are in line with the above-reported findings as the left posterior parietal cortex appears to be directly involved in the control of gait stability. It could be suggested that subjects that were naturally more prone to have good motor control exhibited high spectral activations in the left PPC during natural ambulatory activities; in turn, they exhibited less increased activations in situations requiring high cognitive effort and divided attentional resources, as walking while texting with the smartphone, than subjects struggling in performing more tasks

simultaneously. Interestingly, recent evidence on the relationship between neural and kinematic variability also reported a principal role of the posterior parietal cortex (Haar et al., 2017). This study focused on the inter-trial variability across subjects and upper-limb reaching directions as it has been demonstrated that differences between individuals likely determine the level of exhibited motor capabilities (Braun et al., 2009; Herzfeld and Shadmehr, 2014, Wu et al., 2014). A significant relationship between neural variability of the inter-parietal sulcus significantly correlated with kinematic variability during movements, whereby almost one-quarter of the between-subjects motor differences were explained by subject-specific neural variability in the posterior parietal cortex. It therefore seems that high variability in neural activity in the posterior parietal cortex is predictive of high motor variability during movement of the upper-limb, in line with the findings reported in the current research on the prime role of left PPC in control of locomotion. Therefore, the left PPC could be a valid target for rehabilitation practice to improve gait as well as upper-limb motor control skills and boost recovery after neural injuries. In contrast, the study reported poor variability in the primary motor cortex, in line with previous considerations on M1 not being a good target for specific rehabilitative practices (Linden and Turner, 2016). Recent preliminary investigations of the effects of neurofeedback training of gait control reported positive and promising results: during a period of few weeks participants regularly trained to self-regulated the sensorimotor rhythm recorded from the leg motor area (Lee et al., 2015) and the occipital area (Azarpaikan and Torbati, 2017), after which their gait and balance control abilities significantly improved, respectively. Tailored neurofeedback training could therefore be designed so that activity of the left posterior parietal cortex is targeted, and subjects could learn how to self-control body stability when walking exploiting any mental strategy that better suits them, thus without restricting their potentials.

### **9.3 Future considerations**

This research programme explored the neurophysiological correlates of human motor control through different analyses in order to provide a comprehensive overview of the investigated real-world scenarios, and both positive outcomes and limitations were observed.

In the first study, it was hypothesised that subjects would adapt on a trial-basis so that, by the end of the adaptation condition, movements would not show significant differences with natural reaching (see chapter 1, paragraph 1.2.1). Partially in line with what was expected, subjects did adapt to the external perturbation and significantly reduced the

movement error from early to late adaptation (see figure 4-5) but did not return to a natural motor behaviour by the end of the condition. The designed protocol could therefore be defined as of short-term motor adaptation: this is further supported by the neurophysiological findings whereby no shift from the cortico-striatal to the cortico-cerebellar network were observed from any of the reported correlates. Indeed, measures of ERP, ERSP and source-level CMC revealed a significant activity during adaptation always located over the medial frontal, premotor and supplementary motor areas (see chapter 5, paragraph 5.3, and chapter 6, paragraph 6.3) which are known to be involved in the early stages of adaptation (Shadmehr and Holcomb, 1997; Krebs et al., 1998), but did not report any significant activation of posterior parietal regions towards the end adaptation. The behavioural and neurophysiological results all together confirm the nature of the implemented protocol as of short-term motor adaptation and suggest that longer conditions (i.e. more trials) are needed in order to observe the effects of long-term motor adaptation. However, the designed paradigm allowed the detection of several indicators of early adaptation since all the reported neural correlates confirmed the constant involvement of medial frontal, premotor and supplementary motor areas. Moreover, the amount of force exerted to counteract the external perturbation was significantly predicted by the level of spectral synchronization between SMA and the forearm extensor, confirming the direct involvement of the frontal medial areas in force modulation and control of the motor output. It is therefore not surprising that preliminary investigation on the potentials of neurofeedback training revealed poor self-modulating performance when targeting M1 but good outcomes when controlling PMC and SMA (Linden and Turner, 2016). Our results therefore, in line with previous findings, suggest that the frontal medial and premotor regions 1) play an important role in adaptive control of the upper-limb when changes in the environment are detected and 2) are eligible candidates for future neurorehabilitative practice whereby the level of motor control could be boosted by self-regulation training. Interestingly, also the posterior parietal cortex could be another potential target of novel rehabilitative paradigms as very recently demonstrated to be directly involved in the determination of kinematic variability and in the prediction of individual-specific motor abilities in the control of both the upper- and lower-limb (Haar et al., 2017; Bürki et al., 2017).

In the second scenario it was postulated that motor performance would worsen from single- to dual-task conditions, and that walking while texting with the smartphone would reveal greatest motor impairments due to the lack of constant visual scanning of the surroundings as well as to the high cognitive demand of the secondary task (see chapter

1, paragraph 1.2.2). In line with what was expected, participants showed the highest level of motor impairment as expressed through lower gait speed and higher trunk acceleration when walking while texting with the smartphone with respect to the other two conditions (see figure 7-6 and 7-7). However, the specific reason why these effects were observed could only be hypothesised: indeed, no dual-task costs and/or difficulty level in each condition were assessed. Priority in fact was given to the investigation of the neurophysiological correlates of locomotion control during stable and unstable real-life situations and, given the complexity of the designed secondary task, it was decided not to investigate cognitive performance and its direct effects on motor outcomes. Future studies should therefore aim to evaluate the level of cognitive effort and dual-task difficulty in order to more reliably speculate on the origins of the observed changes in motor performance. Interestingly though, neural correlates of single- and dual-task performance revealed whole-brain and condition-specific changes. The reported whole-brain changes further strengthen recent comments on the nature of latest dual-task investigations, as many studies a priori focus only on the activity of the pre-frontal regions of the human brain, when other cortical areas would likely show related changes (Metzger et al., 2017; Bürki et al., 2017). In contrast with previous studies speculating that only the pre-frontal cortex would show a systematic increase of activity when performing dual-task exercises (Holtzer et al., 2011; Doi et al., 2013; Mirelman et al., 2014; Holtzer et al., 2015; Al-Yahya et al., 2016; Holtzer et al., 2016), the current research reported changes specific to the type of secondary task undertaken involving the pre-frontal regions as well as other cortical areas, in line with previous findings (Nijboer et al., 2014; Lin and Lin, 2016; Metzger et al., 2017; Bürki et al., 2017). Future studies should therefore consider a whole-brain approach in order to obtain a more comprehensive overview of the effects of the requested dual-task on cortical activations instead of making a priori decisions that could prevent the identification of significant contributors to motor and cognitive performance. The whole-brain comprehensive approach followed in the current research allowed the observation of dual-task specific changes in neurophysiological activity and the identification of a potential neural predictor of gait stability within the posterior parietal cortex. In summary, it appears that the posterior parietal region could be a valid target for neurorehabilitation of both the upper- and lower-limb (Bürki et al., 2017; Haar et al., 2017), thus further sustaining the claims that the human brain is directly involved in the control of both motor systems despite the different structures and complexity (Takakusaki et al., 2013; Kim et al., 2016; Artoni et al., 2017; McCrimmon et al., 2017; Takakusaki et al., 2017).

## 9.4 Methodological considerations

This research focused on the investigation of behavioural and neuro-muscular correlates of human motor control in two different real-world contexts: a neuro-rehabilitation scenario and a real-world ambulatory scenario, based on real-life situations in the urban environment. The biggest challenge was developing an experimental framework (composed by study design, setup and analytical pipeline) that could be successfully translated from a lab-based, controlled yet noisy domain, to a real-world, partially-controlled and noisier environment. From a technical point of view, the key elements shared by the two studies are:

- The study design, based on a within-subject format, and the consequent statistical approaches;
- The experimental skeleton, based on the investigation of behavioural, muscular and neural features of human motor control. Instrumental synchronization and time-axes correspondence was crucial for an accurate and correct inspection of human physiological evidence;
- The body of the analytical pipeline developed in MatLab programming environment, based on the same signal processing principles but customizable according to the study specifics.

The implemented robust technical frame allowed the demonstration of novel findings on human motor control of both upper- and lower limb which may contribute to the development of different real-world applications in the field of neuro-rehabilitation and computer science. Indeed, research is currently pushing towards promoting free-living and home-based applications: human physiological evidence obtained in lab-settings is often misleading as subjects and patients strive to do well knowing that they are observed, but their daily-life performance and behaviour can be slightly different (usually worse) when inserted in a less controlled and multiple-stimulated environment (Del Din et al., 2016; Ladouce et al., 2017). The proposed experimental framework successfully explored both behavioural and neuro-muscular correlates of human motor control in two different real-world scenarios, thus it would be a useful and valid working approach for future studies. From a methodological perspective, the most innovative contribution of this research is the developed Mobile Brain/Body Imaging (MoBI) setup, which would be a useful experimental approach to study performance and difficulties in everyday life activities in the neurologically impaired. A potential application of the designed mobile



setup is described in chapter 10, where it was employed within hospital settings for a one-patient test to verify reliability and applicability in real clinical scenarios.

## 10 Future perspectives: a case study

The clinical relevance of this thesis is demonstrated by a case study carried out in collaboration with the Queen's Hospital (Romford, London, UK), where the designed mobile setup was given a chance to be clinically tested during a standard clinical evaluation session of a Parkinson's disease patient.

Parkinson's disease is characterized by a degeneration and death of the dopaminergic nigrostriatal projections to the striatum of the basal ganglia. According to the Rate Model of basal ganglia dysfunction (see Figure 9-1), this causes 1) an enhanced activity of striatal neurons within the indirect basal-ganglia loop as well as 2) an increased activity of the subthalamic nucleus that excessively inhibits the neurons of the thalamus. The result is a net inhibition of the output from the basal ganglia and a subsequent reduced activation of the cortical motor areas (Peterson and Horak, 2016). Typical PD symptoms include hypokinesia (i.e. reduction of voluntary movements), rigidity and elevated muscles tone, as well as limb tremor at 4-6 Hz when at rest (Baehr and Frotscher, 1998). Human locomotion is mediated by different brain areas such as premotor and motor cortex, basal ganglia, cerebellum and brain stem (Takakusaki, 2013), all impaired in PD patients. Therefore, gait of PD patients is characterized by impaired behaviours such as excessive slowness, abnormal step variability and difficult postural control. These dysfunctions are thought to originate from the degeneration of different mechanisms within a PD patient brain (Peterson and Horak, 2016), which is further confirmed by the efficacy of medications and Deep-Brain Stimulation (DBS) not on all of them simultaneously. Moreover, due to the impaired basal ganglia, PD patients show reduced capacity to adapt and learning rate abilities (Krebs et al., 2001), as well as reduced retention skills (Nelson et al., 2017). Attention is another critical aspect for PD patients, mostly for those suffering of Freezing of Gait (FoG) (Tard et al., 2016): the performance of simultaneous tasks, that divides attentional sources, prevent them from being able to adapt to sudden changes in the environment and promote the necessary motor commands (Latt et al., 2009; Nieuwhof et al., 2016). It was indeed recently shown that alterations in the beta frequency band in parietal and occipital areas correlated with the advent of FoG events (Handojoseno 2015) and Gait Initiation Failure (GIF) (Ly et al., 2016). Moreover, controlled lab-based and free-living home-based recordings have shown substantial differences in performance, indeed worsening in real-world situations (Del Din et al., 2016): there is the need for novel technologies able to assess the performance decay of PD patients in their free-living situation which could serve as more reliable evidences for

optimizing therapies. The mobile-setup was therefore utilized within hospital settings to test the ability of a DBS-implanted PD patient to walk naturally during a routine clinical evaluation appointment with the neurosurgeon in charge. The study was the first pilot of our mobile setup in a clinical environment and the goal was 1) to test whether the patient accepted it in terms of weight and encumbrance, and 2) to observe which type of analyses could be actually performed.

The patient (female) suffered of PD for ten years, had a DBS implant (bipolar stimulation, frequency of stimulation 130 Hz) and was on Levodopa medication. When tested, the stimulator was on (DBS ON) as well as the medications (Med ON). The patient was asked to walk along a 9 m hallway within the hospital forth and back for a total of 18 m; the walk was repeated twice and the best trial was chosen for further analysis (see Figure 9-2). Part of the full mobile setup designed for Study II was employed: electrocortical activity was recorded through the 64-channel Waveguard cap connected to the EEGoPro amplifier (ANT Neuro, Enschede, Netherlands). Sampling frequency was set at 1 kHz, activity was recorded with reference set in FCz and all electrodes impedances were kept below 5 k $\Omega$ . The Samsung Galaxy S4 mini smartphone was fixed at the patient's lower back with an elastic belt and data from its internal accelerometers and gyroscope were recorded through the AndroSensor app. Due to not having proper clothing, EMG activity from lower limb muscles and times of heel strikes through contact switches sensors couldn't be recorded. Overall, the patient was comfortable with the wearable instruments and gave positive feedback on the experience.

At the moment, the analyses of EEG data is delayed by the definition of an optimal filter able to remove the major source of noise due to the DBS stimulator. However, the linear acceleration data recorded in the best trial with the smartphone were uploaded into the free software iGAIT (Yang et al., 2012) and all the measures used in Study II were extracted (see Table 9-1). Of major interest were the measure of ver-RMSR and ml-RMSR as previously shown as potential markers of gait stability and abnormalities respectively (see Study II, chapter 8, paragraph 8.4.2). To inspect the patient behaviour with respect to the healthy sample recruited in Study II, a regression between the two RMS ratio variables (Dependent Variables, DVs) and Velocity (Independent Variable) was performed. Figure 9-3 shows the result of the regression analysis: ver-RMSR was positively predicted by Velocity as previously shown ( $R^2 = 0.646$ ,  $p < 0.001$ , all assumptions met) according to the formula:

$$verRMSR = 0.32 + 0.418 * Velocity$$

Equation 10-1: Multiple regression model for verRMSR with PD patient's data when simply walking. whereas ml-RMSR was negatively predicted by Velocity ( $R^2 = 0.294$ ,  $p = 0.037$ ) according to the formula:

$$mlRMSR = 0.721 - 0.359 * Velocity$$

Equation 10-2: Multiple regression model for mlRMSR with PD patient's data when simply walking. Figure 9-3 shows the PD patient behaviour as a red circle. As expected, she walked more slowly than any other healthy subject, showed the lowest ver-RMSR value (symbolic of rigidity) and one of the biggest ml-RMSR values (symbolic of poor postural control in the medio-lateral direction), in line with values previously reported in literature (Del Din et al., 2016). One previous study employed the measure of ml-RMSR to study abnormalities of gait in PD patients on and off medications (Sekine et al., 2014). The validity and reliability of such a measure was here further confirmed.

This case study is the first testimony of the reliability and effectiveness of our mobile setup for the study of clinical populations, in this case of Parkinson's disease patients but definitely extendable to other neurological populations. Future work is needed to improve the mobile setup, in order to make it even more comfortable for patients, as well as the analytical pipeline, in order to be able to remove potential case-specific big source of noise (e.g. DBS stimulator). Moreover, not only could the setup be actively used in clinical practice as a gait-monitoring tool, but could be eventually used to monitor patient behaviour in free-living conditions. This would provide further knowledge on the neurophysiology of clinical populations when inserted in a familiar and natural environment and give the possibility to study specific motor mechanisms in more natural settings: for example, instead of performing robot-mediated reaching movements, patients could be actually reaching towards and grasping a kitchen tool, which would likely highlight similar but different motor control strategies.

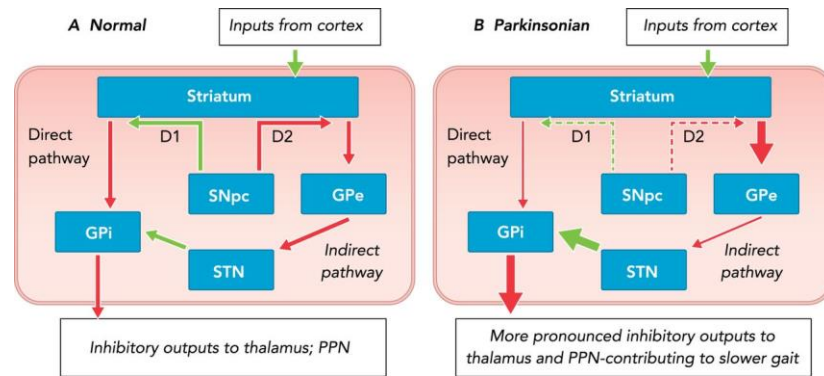


Figure 10-1: The direct and indirect basal ganglia pathways according to the Rate Model.

The diagram on the left represents the basal ganglia connections in healthy subject, whereas the diagram on the right shows the pathological circuits in Parkinsonian patient. Green arrows = excitatory pathways, red arrows = inhibitory pathways. SNpc = Substantia Nigra, GPe = Globus Pallidus External, GPi = Globus Pallidus Internal, STN = Subthalamic Nucleus (adapted from Peterson and Horak, 2016).

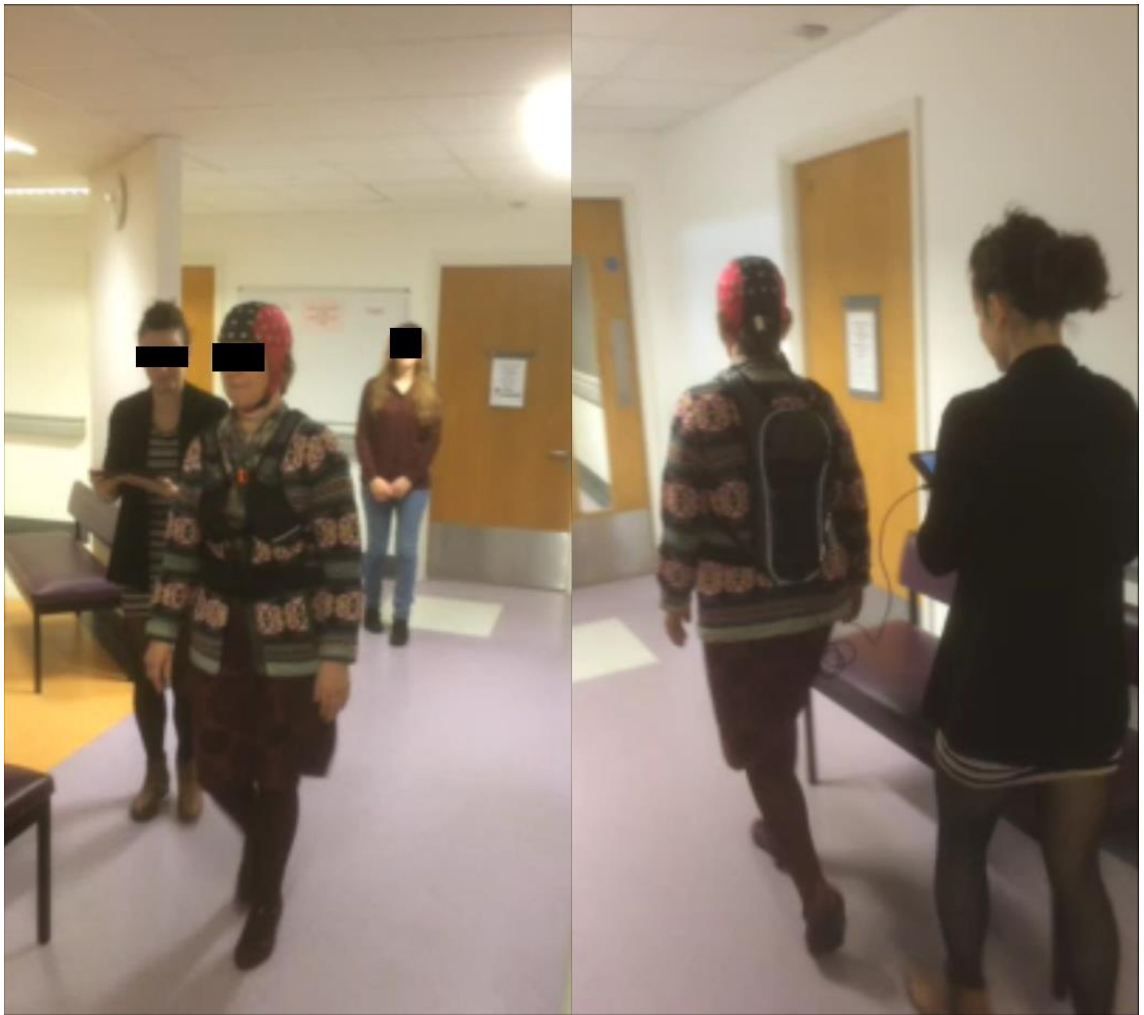


Figure 10-2: Pilot study with one Parkinson's disease patient.

The patient walked along a 9 m hallway forth and back for a total of 18 m distance, starting at the centre of a Start white square (left), turning when at the centre of a second Turn white square (right) and then returning to the starting point. The patient carried all the setup on herself: brain activity was recorded by a 64 channel EEG Waveguard cap connected to the EEGoPro amplifier. The Samsung Galaxy S4 mini was firmly placed at the subject's lower back through the elastic belt.

Table 10-1: Natural walking gait measures of one Parkinson's disease patient.

The table reports all the values of all the gait measures evaluated through iGAIT toolbox from the linear acceleration data recorded at the level of the pelvis of the PD patient

	<b>Natural Walking (18 m distance)</b>
<b>Cadence (step/min)</b>	101.93
<b>Mean Step Length (m)</b>	0.50
<b>Velocity (m/s)</b>	0.71
<b>ver-RMS</b>	1.61
<b>ml-RMS</b>	1.35
<b>ap-RMS</b>	1.82
<b>ver-RMSR</b>	0.58
<b>ml-RMSR</b>	0.49
<b>ap-RMSR</b>	0.65
<b>ver-Step Regularity</b>	0.71
<b>ver-Stride Regularity</b>	0.62
<b>ver-Symmetry</b>	0.09
<b>ap-Step Regularity</b>	0.73
<b>ap-Stride Regularity</b>	0.77
<b>ap-Symmetry</b>	0.04
<b>ml-Stride Regularity</b>	0.14

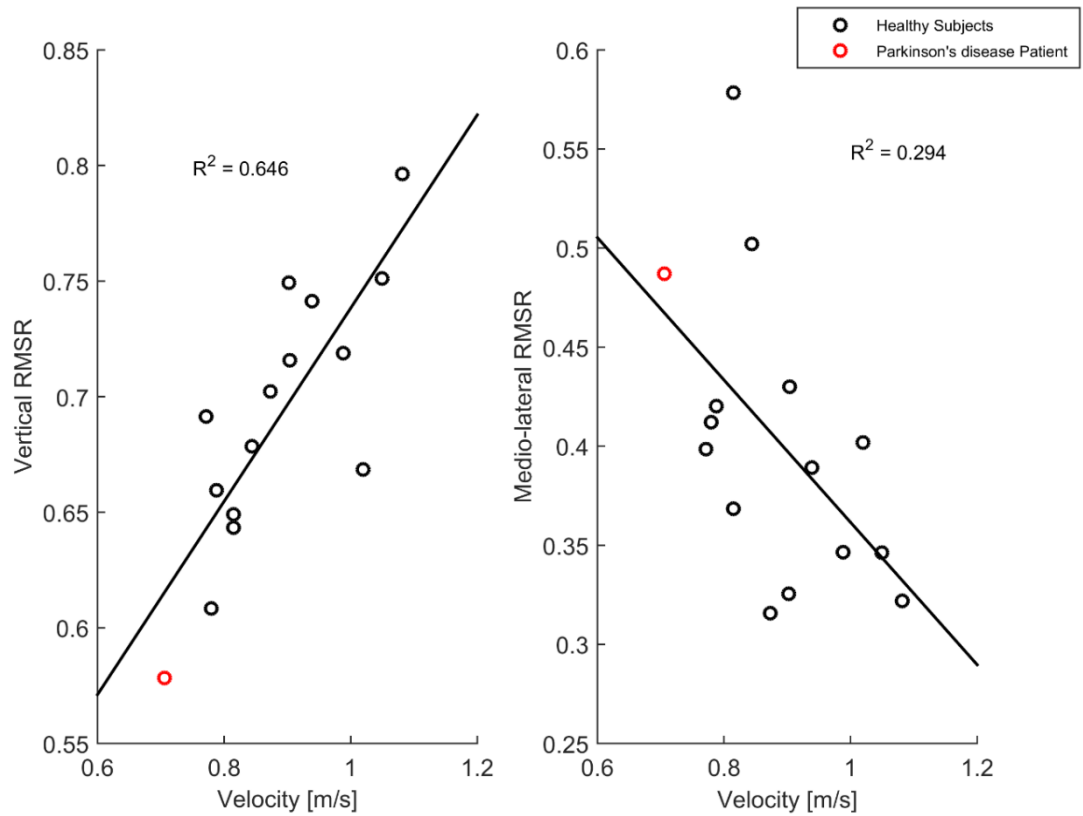


Figure 10-3: Example of one Parkinson's disease patient's natural walking performance with respect to the healthy subjects sample recruited in Study II.

The values of ver-RMSR and ml-RMSR of a DBS implanted Parkinson's disease (PD) patient have been added to the regression models with the independent variable Velocity to observe potential differences between healthy and impaired behaviour. As previously reported, ver-RMSR highly depends on Velocity ( $R^2 = 0.646$ ,  $p = 0.001$ ) and the PD patient (red empty dot) shows the lowest velocity and smallest ver-RMSR values. A significant moderate-to-weak regression was also successfully created for the dependent variable ml-RMSR as predicted by values of Velocity ( $R^2 = 0.294$ ,  $p = 0.037$ ), whereby the PD patient shows one of the higher values of ml-RMSR.



## References

- AGOSTINI, V., FERMO, F. L., MASSAZZA, G. & KNAFLITZ, M. 2015. Does texting while walking really affect gait in young adults? *Journal of Neuroengineering and Rehabilitation*, 12, 86.
- AIRAKSINEN, K., MÄKELÄ, J. P., NURMINEN, J., LUOMA, J., TAULU, S., AHONEN, A. & PEKKONEN, E. 2015. Cortico-muscular coherence in advanced Parkinson's disease with deep brain stimulation. *Clinical Neurophysiology*, 126, 748-755.
- AJEMIAN, R., BULLOCK, D. & GROSSBERG, S. 2001. A model of movement coordinates in the motor cortex: posture-dependent changes in the gain and direction of single cell tuning curves. *Cerebral Cortex*, 11, 1124-1135.
- ALAIS, D., MORRONE, C. & BURR, D. 2006. Separate attentional resources for vision and audition. *Proceedings of the Royal Society of London B: Biological Sciences*, 273, 1339-1345.
- ALLEN, J. L. & NEPTUNE, R. R. 2012. Three-dimensional modular control of human walking. *Journal of Biomechanics*, 45, 2157-2163.
- AL-YAHYA, E., JOHANSEN-BERG, H., KISCHKA, U., ZAREI, M., COCKBURN, J. & DAWES, H. 2016. Prefrontal cortex activation while walking under dual-task conditions in stroke: a multimodal imaging study. *Neurorehabilitation and Neural Repair*, 30, 591-599.
- AMJAD, A., HALLIDAY, D., ROSENBERG, J. & CONWAY, B. 1997. An extended difference of coherence test for comparing and combining several independent coherence estimates: theory and application to the study of motor units and physiological tremor. *Journal of Neuroscience Methods*, 73, 69-79.
- ANDERSEN, R. A., SNYDER, L. H., BRADLEY, D. C. & XING, J. 1997. Multimodal representation of space in the posterior parietal cortex and its use in planning movements. *Annual Review of Neuroscience*, 20, 303-330.
- ANG, K. K., CHUA, K. S. G., PHUA, K. S., WANG, C., CHIN, Z. Y., KUAH, C. W. K., LOW, W. & GUAN, C. 2015. A randomized controlled trial of EEG-based motor imagery brain-computer interface robotic rehabilitation for stroke. *Clinical EEG and Neuroscience*, 46, 310-320.
- ARENZ, A., DREWS, M. S., RICHTER, F. G., AMMER, G. & BORST, A. 2017. The temporal tuning of the *Drosophila* motion detectors is determined by the dynamics of their input elements. *Current Biology*, 27, 929-944.
- ARRIGHI, R., LUNARDI, R. & BURR, D. 2011. Vision and audition do not share attentional resources in sustained tasks. *Frontiers in Psychology*, 2.
- ARTEMIADIS, P. K. & KREBS, H. I. On the control of the MIT-Skywalker. *Engineering in Medicine and Biology Society (EMBC), 2010 Annual International Conference of the IEEE*, 2010. IEEE, 1287-1291.
- ARTONI, F., FANCIULLACCI, C., BERTOLUCCI, F., PANARESE, A., MAKEIG, S., MICERA, S., & CHISARI, C. 2017. Unidirectional brain to muscle connectivity reveals

motor cortex control of leg muscles during stereotyped walking. *NeuroImage*, 159, 403-416.

ASPINALL, P., MAVROS, P., COYNE, R. & ROE, J. 2013. The urban brain: analysing outdoor physical activity with mobile EEG. *Br J Sports Med*, bjsports-2012-091877.

AUER, T., SCHWEIZER, R., & FRAHM, J. 2015. Training efficiency and transfer success in an extended real-time functional MRI neurofeedback training of the somatomotor cortex of healthy subjects. *Frontiers in human neuroscience*, 9, 547.

AWAD, A. J., KELLNER, C. P., MASCITELLI, J. R., BEDERSON, J. B., & MOCCO, J. 2016. No early mobilization after stroke: lessons learned from the AVERT trial. *World Neurosurgery*, 87, 474.

AYAZ, H., SHEWOKIS, P. A., BUNCE, S., IZZETOGLU, K., WILLEMS, B., & ONARAL, B. 2012. Optical brain monitoring for operator training and mental workload assessment. *NeuroImage*, 59(1), 36-47.

AZARPAIKAN, A., & TORBATI, H. T. 2017. Effect of somatosensory and neurofeedback training on balance in older healthy adults: a preliminary investigation. *Aging clinical and experimental research*, 1-9.

BABILONI, C., DEL PERCIO, C., VECCHIO, F., SEBASTIANO, F., DI GENNARO, G., QUARATO, P. P., MORACE, R., PAVONE, L., SORICELLI, A. & NOCE, G. 2016. Alpha, beta and gamma electrocorticographic rhythms in somatosensory, motor, premotor and prefrontal cortical areas differ in movement execution and observation in humans. *Clinical Neurophysiology*, 127, 641-654.

BABILONI, C., VECCHIO, F., BARES, M., BRAZDIL, M., NESTRASIL, I., EUSEBI, F., ROSSINI, P. M. & REKTOR, I. 2008. Functional coupling between anterior prefrontal cortex (BA10) and hand muscle contraction during intentional and imitative motor acts. *NeuroImage*, 39, 1314-1323.

BAEHR, M. & FROTSCHER, M. 1998. *Duus' Topical Diagnosis in Neurology*, 5<sup>th</sup> Edition, Stuttgart. Thieme.

BAKER, S. N. 2007. Oscillatory interactions between sensorimotor cortex and the periphery. *Current Opinion in Neurobiology*, 17, 649-655.

BÁLINT, R. 1909. Seelenlahmungs des' Schauens', optische Ataxie, raumliche Störung der Aufmerksamkeit. *Monatsschr Psychiat Neurol*, 25, 51-81.

BALL, T., DEMANDT, E., MUTSCHLER, I., NEITZEL, E., MEHRING, C., VOGT, K., AERTSEN, A. & SCHULZE-BONHAGE, A. 2008. Movement related activity in the high gamma range of the human EEG. *NeuroImage*, 41, 302-310.

BARTELS, A. L., DE JONG, B. M., GILADI, N., SCHAAFSMA, J. D., MAGUIRE, R. P., VEENMA, L., PRUIM, J., BALASH, Y., YODIM, M. B. & LEENDERS, K. L. 2006. Striatal dopa and glucose metabolism in PD patients with freezing of gait. *Movement Disorders*, 21, 1326-1332.

BARTELS, A. L. & LEENDERS, K. L. 2008. Brain imaging in patients with freezing of gait. *Movement Disorders*, 23.

- BASMAJIAN, J., GOPAL, D. & GHISTA, D. 1985. Electrodiagnostic model for motor unit action potential (MUAP) generation. *American Journal of Physical Medicine*, 64, 279-294.
- BASSETT, D. S., WYMBS, N. F., PORTER, M. A., MUCHA, P. J., CARLSON, J. M. & GRAFTON, S. T. 2011. Dynamic reconfiguration of human brain networks during learning. *Proceedings of the National Academy of Sciences*, 108, 7641-7646.
- BATTAGLIA-MAYER, A., CAMINITI, R., LACQUANITI, F. & ZAGO, M. 2003. Multiple levels of representation of reaching in the parieto-frontal network. *Cerebral Cortex*, 13, 1009-1022.
- BAYRAM, M. B., SIEMIONOW, V. & YUE, G. H. 2015. Weakening of corticomuscular signal coupling during voluntary motor action in aging. *Journals of Gerontology Series A: Biomedical Sciences and Medical Sciences*, 70, 1037-1043.
- BAYS, P. M., FLANAGAN, J. R. & WOLPERT, D. M. 2005. Interference between velocity-dependent and position-dependent force-fields indicates that tasks depending on different kinematic parameters compete for motor working memory. *Experimental Brain Research*, 163, 400-405.
- BELARDINELLI, P., LAER, L., ORTIZ, E., BRAUN, C. & GHARABAGHI, A. 2017. Plasticity of premotor cortico-muscular coherence in severely impaired stroke patients with hand paralysis. *NeuroImage: Clinical*, 14, 726-733.
- BELOOZEROVA, I. N. & SIROTA, M. G. 2003. Integration of motor and visual information in the parietal area 5 during locomotion. *Journal of Neurophysiology*, 90, 961-971.
- BERGER, H. 1931. Über das Elektrenkephalogramm des Menschen. *European Archives of Psychiatry and Clinical Neuroscience*, 94, 16-60.
- BERMAN, B. D., HOROVITZ, S. G., VENKATARAMAN, G., & HALLET, M. 2012. Self-modulation of primary motor cortex activity with motor and motor imagery tasks using real-time fMRI-based neurofeedback. *Neuroimage*, 59(2), 917-925.
- BERNHARDT, J., LANGHORNE, P., LINDLEY, R. I., THRIFT, A. G., ELLERY, F., COLLIER, J., ... & DONNAN, G. 2015. Efficacy and safety of very early mobilisation within 24 h of stroke onset (AVERT): a randomised controlled trial. *Lancet*, 386(9988), 46-55.
- BEURSKENS, R. & BOCK, O. 2013. Does the walking task matter? Influence of different walking conditions on dual-task performances in young and older persons. *Human Movement Science*, 32, 1456-1466.
- BEURSKENS, R., STEINBERG, F., ANTONIEWICZ, F., WOLFF, W. & GRANACHER, U. 2016. Neural correlates of dual-task walking: effects of cognitive versus motor interference in young adults. *Neural Plasticity*, 2016.
- BEYAERT, C., VASA, R. & FRYKBERG, G. E. 2015. Gait post-stroke: Pathophysiology and rehabilitation strategies. *Neurophysiologie Clinique/Clinical Neurophysiology*, 45, 335-355.
- BIRBAUMER, N. & COHEN, L. G. 2007. Brain-computer interfaces: communication and restoration of movement in paralysis. *The Journal of Physiology*, 579, 621-636.

- BIRBAUMER, N., GHANAYIM, N., HINTERBERGER, T., IVERSEN, I., KOTCHOUBEY, B., KÜBLER, A., PERELMOUTER, J., TAUB, E. & FLOR, H. 1999. A spelling device for the paralysed. *Nature*, 398, 297.
- BOHBOT, V. D., COPARA, M. S., GOTMAN, J. & EKSTROM, A. D. 2017. Low-frequency theta oscillations in the human hippocampus during real-world and virtual navigation. *Nature Communications*, 8, 14415.
- BOONSTRA, T. W. 2013. The potential of corticomuscular and intermuscular coherence for research on human motor control. *Frontiers in Human Neuroscience*, 7.
- BOOTHE, D. L., COHEN, A. H. & TROYER, T. W. 2013. Phase locking asymmetries at flexor-extensor transitions during fictive locomotion. *PloSOne*, 8, e64421.
- BOSECKER, C. J. & KREBS, H. I. MIT-skywalker. *Rehabilitation Robotics*, 2009. ICORR 2009. IEEE International Conference on, 2009. IEEE, 542-549.
- BRADFORD, J. C., LUKOS, J. R. & FERRIS, D. P. 2016. Electro cortical activity distinguishes between uphill and level walking in humans. *Journal of Neurophysiology*, 115, 958-966.
- BRÆNDVIK, S. M. & ROELEVELD, K. 2012. The role of co-activation in strength and force modulation in the elbow of children with unilateral cerebral palsy. *Journal of Electromyography and Kinesiology*, 22, 137-144.
- BRASHERS-KRUG, T., SHADMEHR, R. & BIZZI, E. 1996. Consolidation in human motor memory. *Nature*, 382, 252.
- BRAUN, D. A., AERTSEN, A., WOLPERT, D. M., & MEHRING, C. 2009. Motor task variation induces structural learning. *Current Biology*, 19(4), 352-357.
- BRONFENBRENNER, U. 1977. Toward an experimental ecology of human development. *American Psychologist*, 32, 513.
- BROVELLI, A., CHICHARRO, D., BADIÉ, J.-M., WANG, H. & JIRSA, V. 2015. Characterization of cortical networks and corticocortical functional connectivity mediating arbitrary visuomotor mapping. *Journal of Neuroscience*, 35, 12643-12658.
- BROWN, J. S., KNAUFT, E. & ROSENBAUM, G. 1948. The accuracy of positioning reactions as a function of their direction and extent. *The American Journal of Psychology*, 61, 167-182.
- BROWN, P., SALENIUS, S., ROTHWELL, J. C. & HARI, R. 1998. Cortical correlate of the Piper rhythm in humans. *Journal of Neurophysiology*, 80, 2911-2917.
- BRUIJN, S. M., VAN DIEËN, J. H. & DAFFERTSHOFER, A. 2015. Beta activity in the premotor cortex is increased during stabilized as compared to normal walking. *Frontiers in Human Neuroscience*, 9.
- BRUNNSTROM, S. 1970. Movement therapy in hemiplegia. A neurophysiological approach. New York, Harper and Row Publishers, pp 7-33.
- BRUNSWIK, E. 1943. Organismic achievement and environmental probability. *Psychological Review*, 50, 255.

- BUCH, E. R., LIEW, S.-L. & COHEN, L. G. 2017. Plasticity of sensorimotor networks: multiple overlapping mechanisms. *The Neuroscientist*, 23, 185-196.
- BULEA, T. C., KIM, J., DAMIANO, D. L., STANLEY, C. J. & PARK, H.-S. 2015. Prefrontal, posterior parietal and sensorimotor network activity underlying speed control during walking. *Frontiers in Human Neuroscience*, 9, 247.
- BUNEO, C. A. & ANDERSEN, R. A. 2006. The posterior parietal cortex: sensorimotor interface for the planning and online control of visually guided movements. *Neuropsychologia*, 44, 2594-2606.
- BURNFIELD, M. 2010. Gait analysis: normal and pathological function. *Journal of Sports Science and Medicine*, 9, 353.
- BUSCHMAN, T. J. & MILLER, E. K. 2007. Top-down versus bottom-up control of attention in the prefrontal and posterior parietal cortices. *Science*, 315, 1860-1862.
- BUSSE, M. E., WILES, C. M., & VAN DEURSEN, R. W. 2006. Co-activation: its association with weakness and specific neurological pathology. *Journal of Neuroengineering and Rehabilitation*, 3, 26. doi: 10.1186/1743-0003-3-26
- BUTCHER, P. A., IVRY, R., KUO, S.-H., RYDZ, D., KRAKAUER, J. W. & TAYLOR, J. A. 2017. The cerebellum does more than sensory-prediction-error-based learning in sensorimotor adaptation tasks. *BioRxiv*, 139337.
- BÜRKI, C. N., BRIDENBAUGH, S. A., REINHARDT, J., STIPPICH, C., KRESSIG, R. W., & BLATOW, M. 2017. Imaging gait analysis: An fMRI dual task study. *Brain and behavior*, 7(8).
- CABEZA, R. 2002. Hemispheric asymmetry reduction in older adults: the HAROLD model. *Psychology and aging*, 17(1), 85.
- CALTON, J. L. & TAUBE, J. S. 2009. Where am I and how will I get there from here? A role for posterior parietal cortex in the integration of spatial information and route planning. *Neurobiology of Learning and Memory*, 91, 186-196.
- CAPLAN, J. B., MADSEN, J. R., SCHULZE-BONHAGE, A., ASCHENBRENNER-SCHEIBE, R., NEWMAN, E. L. & KAHANA, M. J. 2003. Human  $\theta$  oscillations related to sensorimotor integration and spatial learning. *Journal of Neuroscience*, 23, 4726-4736.
- CARAMIA, C., BERNABUCCI, I., D'ANNA, C., DE MARCHIS, C., & SCHMID, M. 2017. Gait parameters are differently affected by concurrent smartphone-based activities with scaled levels of cognitive effort. *PloS one*, 12(10), e0185825.
- CARDOSO, J.-F. 1997. Infomax and maximum likelihood for blind source separation. *IEEE Signal Processing Letters*, 4, 112-114.
- CARLEN, M. 2017. What constitutes the prefrontal cortex? *Science*, 358(6362), 478-482.
- CAVINESS, J. N., SHILL, H. A., SABBAGH, M. N., EVIDENTE, V. G., HERNANDEZ, J. L. & ADLER, C. H. 2006. Corticomuscular coherence is increased in the small postural tremor of Parkinson's disease. *Movement Disorders*, 21, 492-499.

- CEVALLOS, C., ZARKA, D., HOELLINGER, T., LEROY, A., DAN, B. & CHERON, G. 2015. Oscillations in the human brain during walking execution, imagination and observation. *Neuropsychologia*, 79, 223-232.
- CHAE, J., YANG, G., PARK, B.K., & LABATIA, I. 2002. Muscle weakness and cocontraction in upper limb hemiparesis: relationship to motor impairment and physical disability. *Neurorehabilitation and Neural Repair*, 16(3), 241-248
- CHAPIN, H., BAGARINAO, E., & MACKEY, S. 2012. Real-time fMRI applied to pain management. *Neuroscience letters*, 520(2), 174-181.
- CHEN, G., KING, J. A., BURGESS, N. & O'KEEFE, J. 2013. How vision and movement combine in the hippocampal place code. *Proceedings of the National Academy of Sciences*, 110, 378-383.
- CHERON, G., PETIT, G., CHERON, J., LEROY, A., CEBOLLA, A., CEVALLOS, C., PETIEAU, M., HOELLINGER, T., ZARKA, D. & CLARINVAL, A.-M. 2016. Brain oscillations in sport: toward EEG biomarkers of performance. *Frontiers in Psychology*, 7.
- CHEUNG, V. C., TUROLLA, A., AGOSTINI, M., SILVONI, S., BENNIS, C., KASI, P., ...BIZZI, E. 2012. Muscle synergy patterns as physiological markers of motor cortical damage. *Proc Natl Acad Sci U S A*, 109(36), 14652-14656. doi: 10.1073/pnas.1212056109
- CHEYNE, D., BELLS, S., FERRARI, P., GAETZ, W. & BOSTAN, A. C. 2008. Self-paced movements induce high-frequency gamma oscillations in primary motor cortex. *NeuroImage*, 42, 332-342.
- CHIU, T. C., GRAMANN, K., KO, L. W., DUANN, J. R., JUNG, T. P. & LIN, C. T. 2012. Alpha modulation in parietal and retrosplenial cortex correlates with navigation performance. *Psychophysiology*, 49, 43-55.
- CHOI, J., KANG, H., CHUNG, S. H., KIM, Y., LEE, U. H., LEE, J. M., KIM, S.-J., CHUN, M. H. & KIM, H. Detecting voluntary gait intention of chronic stroke patients towards top-down gait rehabilitation using EEG. *Engineering in Medicine and Biology Society (EMBC), 2016 IEEE 38th Annual International Conference of the, 2016. IEEE*, 1560-1563.
- CHUNG, B. P. H. 2017. Effectiveness of robotic-assisted gait training in stroke rehabilitation: A retrospective matched control study. *Hong Kong Physiotherapy Journal*, 36, 10-16.
- CHURCHLAND, M. M., & ABBOTT, L. F. 2012. Two layers of neural variability. *Nature Neuroscience*, 15(11), 1472.
- CHURCHLAND, M. M., CUNNINGHAM, J. P., KAUFMAN, M. T., FOSTER, J. D., NUYUJUKIAN, P., RYU, S. I. & SHENOY, K. V. 2012. Neural population dynamics during reaching. *Nature*, 487, 51.
- CIRSTEA, M. & LEVIN, M. F. 2000. Compensatory strategies for reaching in stroke. *Brain*, 123, 940-953.
- CLARK, D. J., TING, L. H., ZAJAC, F. E., NEPTUNE, R. R. & KAUTZ, S. A. 2010. Merging of healthy motor modules predicts reduced locomotor performance and muscle coordination complexity post-stroke. *Journal of Neurophysiology*, 103, 844-857.

- COLINO, F. L., HOWSE, H., NORTON, A., TRSKA, R., PLUTA, A., LUEHR, S. J., ... & KRIGOLSON, O. E. 2017. Older adults display diminished error processing and response in a continuous tracking task. *Psychophysiology*, 54(11), 1706-1713.
- COLLINGER, J. L., WODLINGER, B., DOWNEY, J. E., WANG, W., TYLER-KABARA, E. C., WEBER, D. J., MCMORLAND, A. J., VELLISTE, M., BONINGER, M. L. & SCHWARTZ, A. B. 2013. High-performance neuroprosthetic control by an individual with tetraplegia. *The Lancet*, 381, 557-564.
- CONTRERAS-VIDAL, J. L., CRUZ-GARCIA, J. & KOPTEVA, A. Towards a whole body brain-machine interface system for decoding expressive movement intent Challenges and Opportunities. *Brain-Computer Interface (BCI)*, 2017 5th International Winter Conference on, 2017. IEEE, 1-4.
- CONWAY, B., HALLIDAY, D., FARMER, S., SHAHANI, U., MAAS, P., WEIR, A. & ROSENBERG, J. 1995. Synchronization between motor cortex and spinal motoneuronal pool during the performance of a maintained motor task in man. *The Journal of Physiology*, 489, 917-924.
- CORBETTA, M. & SHULMAN, G. L. 2002. Control of goal-directed and stimulus-driven attention in the brain. *Nature Reviews. Neuroscience*, 3, 201.
- COSTA, Á., IÁÑEZ, E., ÚBEDA, A., HORTAL, E., DEL-AMA, A. J., GIL-AGUDO, Á. & AZORÍN, J. M. 2016. Decoding the attentional demands of gait through EEG gamma band features. *PloSOne*, 11, e0154136.
- COURTINE, G., MICERA, S., DIGIOVANNA, J. & DEL R MILLÁN, J. 2013. Brain-machine interface: closer to therapeutic reality? *The Lancet*, 381, 515-517.
- DAL MASO, F., LONGCAMP, M. & AMARANTINI, D. 2012. Training-related decrease in antagonist muscles activation is associated with increased motor cortex activation: evidence of central mechanisms for control of antagonist muscles. *Experimental Brain Research*, 220, 287-295.
- DARAINY, M. & OSTRY, D. J. 2008. Muscle cocontraction following dynamics learning. *Experimental Brain Research*, 190, 153-163.
- DARIAN-SMITH, C., DARIAN-SMITH, I., BURMAN, K. & RATCLIFFE, N. 1993. Ipsilateral cortical projections to areas 3a, 3b, and 4 in the macaque monkey. *Journal of Comparative Neurology*, 335, 200-213.
- DAWSON, J., PIERCE, D., DIXIT, A., KIMBERLEY, T. J., ROBERTSON, M., TARVER, B., HILMI, O., MCLEAN, J., FORBES, K. & KILGARD, M. P. 2016. Safety, feasibility, and efficacy of vagus nerve stimulation paired with upper-limb rehabilitation after ischemic stroke. *Stroke*, 47, 143-150.
- DE LUCA, C. J., GILMORE, L. D., KUZNETSOV, M. & ROY, S. H. 2010. Filtering the surface EMG signal: Movement artifact and baseline noise contamination. *Journal of Biomechanics*, 43, 1573-1579.
- DE XIVRY, J.-J. O., AHMADI-PAJOUH, M. A., HARRAN, M. D., SALIMPOUR, Y. & SHADMEHR, R. 2013. Changes in corticospinal excitability during reach adaptation in force fields. *Journal of Neurophysiology*, 109, 124-136.

- DEBAS, K., CARRIER, J., ORBAN, P., BARAKAT, M., LUNGU, O., VANDEWALLE, G., TAHAR, A. H., BELLEC, P., KARNI, A. & UNGERLEIDER, L. G. 2010. Brain plasticity related to the consolidation of motor sequence learning and motor adaptation. *Proceedings of the National Academy of Sciences*, 107, 17839-17844.
- DEL DIN, S., GODFREY, A., GALNA, B., LORD, S. & ROCHESTER, L. 2016. Free-living gait characteristics in ageing and Parkinson's disease: impact of environment and ambulatory bout length. *Journal of Neuroengineering and Rehabilitation*, 13, 46.
- DELLA-MAGGIORE, V., LANDI, S. M. & VILLALTA, J. I. 2015. Sensorimotor adaptation: multiple forms of plasticity in motor circuits. *The Neuroscientist*, 21, 109-125.
- DELLA-MAGGIORE, V. & MCINTOSH, A. R. 2005. Time course of changes in brain activity and functional connectivity associated with long-term adaptation to a rotational transformation. *Journal of Neurophysiology*, 93, 2254-2262.
- DELLA-MAGGIORE, V., VILLALTA, J. I., KOVACEVIC, N. & MCINTOSH, A. R. 2017. Functional evidence for memory stabilization in sensorimotor adaptation: a 24-h resting-state fMRI study. *Cerebral Cortex*, 27, 1748-1757.
- DELORME, A. & MAKEIG, S. 2004. EEGLAB: an open source toolbox for analysis of single-trial EEG dynamics including independent component analysis. *Journal of Neuroscience Methods*, 134, 9-21.
- DELORME, A., SEJNOWSKI, T. & MAKEIG, S. 2007. Enhanced detection of artifacts in EEG data using higher-order statistics and independent component analysis. *NeuroImage*, 34, 1443-1449.
- DEMANDT, E., MEHRING, C., VOGT, K., SCHULZE-BONHAGE, A., AERTSEN, A. & BALL, T. 2012. Reaching movement onset-and end-related characteristics of EEG spectral power modulations. *Frontiers in Neuroscience*, 6.
- DEROSIÈRE, G., ALEXANDRE, F., BOURDILLON, N., MANDRICK, K., WARD, T. & PERREY, S. 2014. Similar scaling of contralateral and ipsilateral cortical responses during graded unimanual force generation. *NeuroImage*, 85, 471-477.
- DIEDRICHSEN, J. & KORNYSHEVA, K. 2015. Motor skill learning between selection and execution. *Trends in Cognitive Sciences*, 19, 227-233.
- DIMITRIJEVIC, M. R., GERASIMENKO, Y. & PINTER, M. M. 1998. Evidence for a spinal central pattern generator in humans. *Annals of the New York Academy of Sciences*, 860, 360-376.
- DIPIETRO, L., KREBS, H. I., FASOLI, S. E., VOLPE, B. T. & HOGAN, N. 2009. Submovement changes characterize generalization of motor recovery after stroke. *Cortex*, 45, 318-324.
- DIPIETRO, L., KREBS, H. I., FASOLI, S. E., VOLPE, B. T., STEIN, J., BEVER, C. & HOGAN, N. 2007. Changing motor synergies in chronic stroke. *Journal of Neurophysiology*, 98, 757-768.
- DIPIETRO, L., POIZNER, H. & KREBS, H. I. 2014. Spatiotemporal dynamics of online motor correction processing revealed by high-density electroencephalography. *Journal of Cognitive Neuroscience*, 26, 1966-1980.



- DOBKIN, B. H., FIRESTINE, A., WEST, M., SAREMI, K. & WOODS, R. 2004. Ankle dorsiflexion as an fMRI paradigm to assay motor control for walking during rehabilitation. *NeuroImage*, 23, 370-381.
- DOI, T., MAKIZAKO, H., SHIMADA, H., PARK, H., TSUTSUMIMOTO, K., UEMURA, K., & SUZUKI, T. 2013. Brain activation during dual-task walking and executive function among older adults with mild cognitive impairment: a fNIRS study. *Aging clinical and experimental research*, 25(5), 539-544.
- DOSENBACH, N. U., FAIR, D. A., MIEZIN, F. M., COHEN, A. L., WENGER, K. K., DOSENBACH, R. A., FOX, M. D., SNYDER, A. Z., VINCENT, J. L. & RAICHLE, M. E. 2007. Distinct brain networks for adaptive and stable task control in humans. *Proceedings of the National Academy of Sciences*, 104, 11073-11078.
- DOYON, J., BELLEC, P., AMSEL, R., PENHUNE, V., MONCHI, O., CARRIER, J., LEHÉRICY, S. & BENALI, H. 2009. Contributions of the basal ganglia and functionally related brain structures to motor learning. *Behavioural Brain Research*, 199, 61-75.
- DREW, T., PRENTICE, S. & SCHEPENS, B. 2004. Cortical and brainstem control of locomotion. *Progress in Brain Research*, 143, 251-261.
- EHINGER, B. V., FISCHER, P., GERT, A. L., KAUFHOLD, L., WEBER, F., PIPA, G. & KÖNIG, P. 2014. Kinesthetic and vestibular information modulate alpha activity during spatial navigation: a mobile EEG study. *Frontiers in Human Neuroscience*, 8.
- EKSTROM, A. D., CAPLAN, J. B., HO, E., SHATTUCK, K., FRIED, I. & KAHANA, M. J. 2005. Human hippocampal theta activity during virtual navigation. *Hippocampus*, 15, 881-889.
- ENGEL, A. K. & FRIES, P. 2010. Beta-band oscillations—signalling the status quo? *Current Opinion in Neurobiology*, 20, 156-165.
- ESPENHAHN, S., DE BERKER, A. O., VAN WIJK, B. C., ROSSITER, H. E. & WARD, N. S. 2017. Movement-related beta oscillations show high intra-individual reliability. *NeuroImage*, 147, 175-185.
- FABBRI, S., CARAMAZZA, A. & LINGNAU, A. 2010. Tuning curves for movement direction in the human visuomotor system. *Journal of Neuroscience*, 30, 13488-13498.
- FALKENSTEIN, M., HOORMANN, J., CHRIST, S., & HOHNSBEIN, J. 2000. ERP components on reaction errors and their functional significance: a tutorial. *Biological psychology*, 51(2-3), 87-107.
- FANG, Y., DALY, J. J., SUN, J., HVORAT, K., FREDRICKSON, E., PUNDIK, S., SAHGAL, V. & YUE, G. H. 2009. Functional corticomuscular connection during reaching is weakened following stroke. *Clinical Neurophysiology*, 120, 994-1002.
- FARINA, D., NEGRO, F. & JIANG, N. 2013. Identification of common synaptic inputs to motor neurons from the rectified electromyogram. *The Journal of Physiology*, 591, 2403-2418.
- FELDMAN, A. G., LEVIN, M. F., MITNITSKI, A. M. & ARCHAMBAULT, P. 1998. 1998 ISEK Congress Keynote Lecture: Multi-muscle control in human movements. *Journal of Electromyography and Kinesiology*, 8, 383-390.

- FERREE, T. C. 2000. Spline interpolation of the scalp EEG. Secondary TitleEGI.
- FINLEY, M. A., DIPIETRO, L., OHLHOFF, J., WHITALL, J., KREBS, H. I. & BEVER, C. T. 2009. The effect of repeated measurements using an upper extremity robot on healthy adults. *Journal of Applied Biomechanics*, 25, 103-110.
- FINOIA, P., MITCHELL, D. J., HAUKE, O., BESTE, C., PIZZELLA, V. & DUNCAN, J. 2015. Concurrent brain responses to separate auditory and visual targets. *Journal of Neurophysiology*, 114, 1239-1247.
- FOCKE, A., STOCKINGER, C., DIEPOLD, C., TAUBERT, M. & STEIN, T. 2013. The influence of catch trials on the consolidation of motor memory in force field adaptation tasks. *Frontiers in Psychology*, 4.
- FOGASSI, L., & LUPPINO, G. 2005. Motor functions of the parietal lobe. *Current opinion in neurobiology*, 15(6), 626-631.
- FORD, J. M., MATHALON, D. H., WHITFIELD, S., FAUSTMAN, W. O. & ROTH, W. T. 2002. Reduced communication between frontal and temporal lobes during talking in schizophrenia. *Biological Psychiatry*, 51, 485-492.
- FORMAGGIO, E., STORTI, S. F., GALAZZO, I. B., GANDOLFI, M., GERON, C., SMANIA, N., FIASCHI, A. & MANGANOTTI, P. 2015. Time-frequency modulation of ERD and EEG coherence in robot-assisted hand performance. *Brain Topography*, 28, 352-363.
- FORMAGGIO, E., STORTI, S. F., GALAZZO, I. B., GANDOLFI, M., GERON, C., SMANIA, N., SPEZIA, L., WALDNER, A., FIASCHI, A. & MANGANOTTI, P. 2013. Modulation of event-related desynchronization in robot-assisted hand performance: brain oscillatory changes in active, passive and imagined movements. *Journal of Neuroengineering and Rehabilitation*, 10, 24.
- FOURIER, J. 1822. *Theorie analytique de la chaleur*, par M. Fourier, Chez Firmin Didot, père et fils.
- FRANCIS, C. A., FRANZ, J. R., O'CONNOR, S. M. & THELEN, D. G. 2015. Gait variability in healthy old adults is more affected by a visual perturbation than by a cognitive or narrow step placement demand. *Gait & Posture*, 42, 380-385.
- FRANKLIN, D. W., OSU, R., BURDET, E., KAWATO, M. & MILNER, T. E. 2003. Adaptation to stable and unstable dynamics achieved by combined impedance control and inverse dynamics model. *Journal of Neurophysiology*, 90, 3270-3282.
- FRY, A., MULLINGER, K. J., O'NEILL, G. C., BARRATT, E. L., MORRIS, P. G., BAUER, M., FOLLAND, J. P. & BROOKES, M. J. 2016. Modulation of post-movement beta rebound by contraction force and rate of force development. *Human Brain Mapping*, 37, 2493-2511.
- FU, A., XU, R., HE, F., QI, H., ZHANG, L., MING, D., BAI, Y. & ZHANG, Z. Corticomuscular coherence analysis on the static and dynamic tasks of hand movement. *Digital Signal Processing (DSP)*, 2014 19th International Conference on, 2014. IEEE, 715-718.

- FU, Q., FLAMENT, D., COLTZ, J. & EBNER, T. 1995. Temporal encoding of movement kinematics in the discharge of primate primary motor and premotor neurons. *Journal of Neurophysiology*, 73, 836-854.
- FUJIMOTO, H., MIHARA, M., HATTORI, N., HATAKENAKA, M., KAWANO, T., YAGURA, H., MIYAI, I. & MOCHIZUKI, H. 2014. Cortical changes underlying balance recovery in patients with hemiplegic stroke. *NeuroImage*, 85, 547-554.
- GALEA, J. M., MALLIA, E., ROTHWELL, J. & DIEDRICHSEN, J. 2015. The dissociable effects of punishment and reward on motor learning. *Nature Neuroscience*, 18, 597-602.
- GALIN, D., RAZ, J., FEIN, G., JOHNSTONE, J., HERRON, J. & YINGLING, C. 1992. EEG spectra in dyslexic and normal readers during oral and silent reading. *Electroencephalography and Clinical Neurophysiology*, 82, 87-101.
- GANDOLFO, F., LI, C.-S., BENDA, B., SCHIOPPA, C. P. & BIZZI, E. 2000. Cortical correlates of learning in monkeys adapting to a new dynamical environment. *Proceedings of the National Academy of Sciences*, 97, 2259-2263.
- GASTAUT, H. 1970. Clinical and electroencephalographical classification of epileptic seizures. *Epilepsia*, 11, 102-112.
- GENTILI, R. J., BRADBERRY, T. J., OH, H., COSTANZO, M. E., KERICK, S. E., CONTRERAS-VIDAL, J. L. & HATFIELD, B. D. 2015. Evolution of cerebral cortico-cortical communication during visuomotor adaptation to a cognitive-motor executive challenge. *Biological Psychology*, 105, 51-65.
- GEORGOPOULOS, A. P. 1986. On reaching. *Annual Review of Neuroscience*, 9, 147-170.
- GEORGOPOULOS, A. P., CAMINITI, R., KALASKA, J. F. & MASSEY, J. T. 1983. Spatial coding of movement: a hypothesis concerning the coding of movement direction by motor cortical populations. *Experimental Brain Research*, 7, 336.
- GEORGOPOULOS, A. P. & CARPENTER, A. F. 2015. Coding of movements in the motor cortex. *Current Opinion in Neurobiology*, 33, 34-39.
- GEORGOPOULOS, A. P., KALASKA, J. F., CAMINITI, R. & MASSEY, J. T. 1982. On the relations between the direction of two-dimensional arm movements and cell discharge in primate motor cortex. *Journal of Neuroscience*, 2, 1527-1537.
- GEORGOPOULOS, A. P., MERCHANT, H., NASELARIS, T. & AMIRIKIAN, B. 2007. Mapping of the preferred direction in the motor cortex. *Proceedings of the National Academy of Sciences*, 104, 11068-11072.
- GILADI, N. & HAUSDORFF, J. M. 2006. The role of mental function in the pathogenesis of freezing of gait in Parkinson's disease. *Journal of the Neurological Sciences*, 248, 173-176.
- GIRAUD, A.-L., KLEINSCHMIDT, A., POEPEL, D., LUND, T. E., FRACKOWIAK, R. S. & LAUFS, H. 2007. Endogenous cortical rhythms determine cerebral specialization for speech perception and production. *Neuron*, 56, 1127-1134.

- GONZALEZ ANDINO, S. L., MICHEL, C. M., THUT, G., LANDIS, T. & GRAVE DE PERALTA, R. 2005. Prediction of response speed by anticipatory high-frequency (gamma band) oscillations in the human brain. *Human Brain Mapping*, 24, 50-58.
- GOWLAND, C., DEBRUING, H., BASMAJIAN, J.V., PLEWS, N., & BURCEA, I. 1992. Agonist and antagonist activity during voluntary upper limb movement in patients with stroke. *Physical Therapy*, 72(9), 624-633.
- GRAFTON, S. T., FAGG, A. H., WOODS, R. P. & ARBIB, M. A. 1996. Functional anatomy of pointing and grasping in humans. *Cerebral Cortex*, 6, 226-237.
- GRAMANN, K., FAIRCLOUGH, S. H., ZANDER, T. O. & AYAZ, H. 2017. Editorial: Trends in Neuroergonomics. *Frontiers in Human Neuroscience*, 11.
- GRAMANN, K., FERRIS, D. P., GWIN, J. & MAKEIG, S. 2014. Imaging natural cognition in action. *International Journal of Psychophysiology*, 91, 22-29.
- GRANDCHAMP, R. & DELORME, A. 2011. Single-trial normalization for event-related spectral decomposition reduces sensitivity to noisy trials. *Frontiers in Psychology*, 2, 236.
- GREENHAFF, P. L. 2003. Milestones in human physiology: muscle energy metabolism and blood flow during contraction. *The Journal of Physiology*, 551, 397-399.
- GROß, J., KUJALA, J., HÄMÄLÄINEN, M., TIMMERMAN, L., SCHNITZLER, A. & SALMELIN, R. 2001. Dynamic imaging of coherent sources: studying neural interactions in the human brain. *Proceedings of the National Academy of Sciences*, 98, 694-699.
- GROSSE, P., CASSIDY, M. & BROWN, P. 2002. EEG-EMG, MEG-EMG and EMG-EMG frequency analysis: physiological principles and clinical applications. *Clinical Neurophysiology*, 113, 1523-1531.
- GUITART-MASIP, M., BARNES, G. R., HORNER, A., BAUER, M., DOLAN, R. J. & DUZEL, E. 2013. Synchronization of medial temporal lobe and prefrontal rhythms in human decision making. *Journal of Neuroscience*, 33, 442-451.
- GWIN, J. T. & FERRIS, D. P. 2012. Beta-and gamma-range human lower limb corticomuscular coherence. *Frontiers in Human Neuroscience*, 6, 258.
- GWIN, J. T., GRAMANN, K., MAKEIG, S. & FERRIS, D. P. 2011. Electrocortical activity is coupled to gait cycle phase during treadmill walking. *NeuroImage*, 54, 1289-1296.
- HAAR, S., DONCHIN, O., & DINSTEIN, I. 2017. Individual movement variability magnitudes are explained by cortical neural variability. *Journal of Neuroscience*, 37(37), 9076-9085.
- HACMON, R. R., KRASOVSKY, T., LAMONTAGNE, A. & LEVIN, M. F. 2012. Deficits in intersegmental trunk coordination during walking are related to clinical balance and gait function in chronic stroke. *Journal of Neurologic Physical Therapy*, 36, 173-181.
- HALLIDAY, D., ROSENBERG, J., AMJAD, A., BREEZE, P., CONWAY, B. & FARMER, S. 1995. A framework for the analysis of mixed time series/point process

data—theory and application to the study of physiological tremor, single motor unit discharges and electromyograms. *Progress in Biophysics and Molecular Biology*, 64, 237-278.

HAMMOND, M. C., FITTS, S. S., KRAFT, G. H., NUTTER, P. B., TROTTER, M. J., & ROBINSON, L. M. 1988. Co-contraction in the hemiparetic forearm: quantitative EMG evaluation. *Arch Phys Med Rehabil*, 69(5), 348-351

HANDOJOSENO, A. A., GILAT, M., LY, Q. T., CHAMTIE, H., SHINE, J. M., NGUYEN, T. N., TRAN, Y., LEWIS, S. J. & NGUYEN, H. T. An EEG study of turning freeze in Parkinson's disease patients: The alteration of brain dynamic on the motor and visual cortex. *Engineering in Medicine and Biology Society (EMBC), 2015 37th Annual International Conference of the IEEE*, 2015. IEEE, 6618-6621.

HARDWICK, R. M., LESAGE, E., EICKHOFF, C. R., CLOS, M., FOX, P. & EICKHOFF, S. B. 2015. Multimodal connectivity of motor learning-related dorsal premotor cortex. *NeuroImage*, 123, 114-128.

HARDWICK, R. M., ROTTSCHY, C., MIAL, R. C. & EICKHOFF, S. B. 2013. A quantitative meta-analysis and review of motor learning in the human brain. *NeuroImage*, 67, 283-297.

HAROUSH, K., DEOUELL, L. Y. & HOCHSTEIN, S. 2011. Hearing while blinking: Multisensory attentional blink revisited. *Journal of Neuroscience*, 31, 922-927.

HARRIS, F. J. 1978. On the use of windows for harmonic analysis with the discrete Fourier transform. *Proceedings of the IEEE*, 66, 51-83.

HATHOUT, G. M. & BHIDAYASIRI, R. 2005. Midbrain ataxia: an introduction to the mesencephalic locomotor region and the pedunculopontine nucleus. *American Journal of Roentgenology*, 184, 953-956.

HEBB, D. O. 1949. *The organization of behavior: A neuropsychological approach*, John Wiley & Sons, New York.

HELM, E. E. & REISMAN, D. S. 2015. The split-belt walking paradigm: exploring motor learning and spatiotemporal asymmetry poststroke. *Physical medicine and rehabilitation clinics of North America*, 26, 703-713.

HEMING, E. A., LILLICRAP, T. P., OMRANI, M., HERTER, T. M., PRUSZYNSKI, J. A. & SCOTT, S. H. 2016. Primary motor cortex neurons classified in a postural task predict muscle activation patterns in a reaching task. *Journal of Neurophysiology*, 115, 2021-2032.

HERMENS, H. J., FRERIKS, B., DISSELHORST-KLUG, C. & RAU, G. 2000. Development of recommendations for SEMG sensors and sensor placement procedures. *Journal of Electromyography and Kinesiology*, 10, 361-374.

HERNANDEZ, M. E., HOLTZER, R., CHAPARRO, G., JEAN, K., BALTO, J. M., SANDROFF, B. M., IZZETOGLU, M. & MOTL, R. W. 2016. Brain activation changes during locomotion in middle-aged to older adults with multiple sclerosis. *Journal of the Neurological Sciences*, 370, 277-283.

HERZFELD, D. J., & SHADMEHR, R. 2014. Motor variability is not noise, but grist for the learning mill. *Nature Neuroscience*, 17(2), 149.

- HOGAN A. M., VARGHA-KHADEM, F., SAUNDERS, D. E., KIRKHAM, F. J., & BALDEWEG, T. 2006. Impact of frontal white matter lesions on performance monitoring: ERP evidence for cortical disconnection. *Brain*, 129(8), 2177-2188.
- HOLLERBACH, J. M. & FLASH, T. 1982. Dynamic interactions between limb segments during planar arm movement. *Biological Cybernetics*, 44, 67-77.
- HOLMES, G. 1918. Disturbances of visual orientation. *The British journal of ophthalmology*, 2, 449.
- HOLTZER, R., MAHONEY, J. R., IZZETOGLU, M., IZZETOGLU, K., ONARAL, B. & VERGHESE, J. 2011. fNIRS study of walking and walking while talking in young and old individuals. *The Journals of Gerontology Series A: Biological Sciences and Medical Sciences*, glr068.
- HOLTZER, R., MAHONEY, J. R., IZZETOGLU, M., WANG, C., ENGLAND, S. & VERGHESE, J. 2015. Online fronto-cortical control of simple and attention-demanding locomotion in humans. *NeuroImage*, 112, 152-159.
- HOLTZER, R., VERGHESE, J., ALLALI, G., IZZETOGLU, M., WANG, C. & MAHONEY, J. R. 2016. Neurological gait abnormalities moderate the functional brain signature of the posture first hypothesis. *Brain Topography*, 29, 334-343.
- HOPKINS, P. M. 2006. Skeletal muscle physiology. *Continuing Education in Anaesthesia, Critical Care & Pain*, 6, 1-6.
- HOSHI, E. & TANJI, J. 2004. Area-selective neuronal activity in the dorsolateral prefrontal cortex for information retrieval and action planning. *Journal of Neurophysiology*, 91, 2707-2722.
- HOUWELING, S., VAN DIJK, B. W., BEEK, P. J. & DAFFERTSHOFER, A. 2010. Cortico-spinal synchronization reflects changes in performance when learning a complex bimanual task. *NeuroImage*, 49, 3269-3275.
- HUANG, C., TANG, C., FEIGIN, A., LESSER, M., MA, Y., POURFAR, M., DHAWAN, V. & EIDELBERG, D. 2007. Changes in network activity with the progression of Parkinson's disease. *Brain*, 130, 1834-1846.
- HUANG, H. J. & AHMED, A. A. 2014. Older adults learn less, but still reduce metabolic cost, during motor adaptation. *Journal of Neurophysiology*, 111, 135-144.
- HUANG, V. S. & KRAKAUER, J. W. 2009. Robotic neurorehabilitation: a computational motor learning perspective. *Journal of Neuroengineering and Rehabilitation*, 6, 5.
- HUBERDEAU, D. M., HAITH, A. M. & KRAKAUER, J. W. 2015. Formation of a long-term memory for visuomotor adaptation following only a few trials of practice. *Journal of Neurophysiology*, 114, 969-977.
- HUI, M., ZHANG, H., GE, R., YAO, L., & LONG, Z. 2014. Modulation of functional network with real-time fMRI feedback training of right premotor cortex activity. *Neuropsychologia*, 62, 111-123.

- HULTMAN, E. & SJÖHOLM, H. 1983. Energy metabolism and contraction force of human skeletal muscle in situ during electrical stimulation. *The Journal of Physiology*, 345, 525-532.
- HUNTER, T., SACCO, P., NITSCHKE, M. A. & TURNER, D. L. 2009. Modulation of internal model formation during force field-induced motor learning by anodal transcranial direct current stimulation of primary motor cortex. *The Journal of Physiology*, 587, 2949-2961.
- HYVÄRINEN, A. & OJA, E. One-unit learning rules for independent component analysis. *Advances in neural information processing systems*, 1997. 480-486.
- IKEDA, T., MATSUSHITA, A., SAOTOME, K., HASEGAWA, Y., MATSUMURA, A. & SANKAI, Y. 2016. Muscle activity during gait-like motion provided by MRI compatible lower-extremity motion simulator. *Advanced Robotics*, 30, 459-475.
- INOUE, M., UCHIMURA, M. & KITAZAWA, S. 2016. Error signals in motor cortices drive adaptation in reaching. *Neuron*, 90, 1114-1126.
- IOSA, M., FUSCO, A., MORONE, G. & PAOLUCCI, S. 2014. Development and decline of upright gait stability. *Frontiers in Ageing Neuroscience*, 10.3389.
- JAHN, K., DEUTSCHLÄNDER, A., STEPHAN, T., KALLA, R., WIESMANN, M., STRUPP, M. & BRANDT, T. 2008. Imaging human supraspinal locomotor centers in brainstem and cerebellum. *Neuroimage*, 39, 786-792.
- JASPER, H. 1958. Progress and problems in brain research. *Journal of the Mount Sinai Hospital, New York*, 25, 244-253.
- JATOI, M. A., KAMEL, N., MALIK, A. S., FAYE, I. & BEGUM, T. 2014. A survey of methods used for source localization using EEG signals. *Biomedical Signal Processing and Control*, 11, 42-52.
- JEZERNIK, S., COLOMBO, G., KELLER, T., FRUEH, H. & MORARI, M. 2003. Robotic orthosis lokomat: A rehabilitation and research tool. *Neuromodulation: Technology at the neural interface*, 6, 108-115.
- JUNGNIKKEL, E. & GRAMANN, K. 2016. Mobile brain/body imaging (MoBI) of physical interaction with dynamically moving objects. *Frontiers in Human Neuroscience*, 10.
- JURKIEWICZ, M. T., GAETZ, W. C., BOSTAN, A. C. & CHEYNE, D. 2006. Post-movement beta rebound is generated in motor cortex: evidence from neuromagnetic recordings. *NeuroImage*, 32, 1281-1289.
- KAMP, D., KRAUSE, V., BUTZ, M., SCHNITZLER, A. & POLLOK, B. 2013. Changes of cortico-muscular coherence: an early marker of healthy aging? *Age*, 35, 49-58.
- KAMPER, D. & RYMER, W. 2001. Impairment of voluntary control of finger motion following stroke: role of inappropriate muscle coactivation. *Muscle & Nerve*, 24, 673-681.
- KÄTHNER, I., HALDER, S., HINTERMÜLLER, C., ESPINOSA, A., GUGER, C., MIRALLES, F., VARGIU, E., DAUWALDER, S., RAFAEL-PALOU, X. & SOLÀ, M. 2017. A multifunctional brain-computer interface intended for home use: An evaluation

with healthy participants and potential end users with dry and gel-based electrodes. *Frontiers in Neuroscience*, 11.

KAVANAGH, J. J. & MENZ, H. B. 2008. Accelerometry: a technique for quantifying movement patterns during walking. *Gait & Posture*, 28, 1-15.

KHANNA, P. & CARMENA, J. M. 2017. Beta band oscillations in motor cortex reflect neural population signals that delay movement onset. *eLife*, 6.

KILNER, J., BAKER, S., SALENIUS, S., JOUSMÄKI, V., HARI, R. & LEMON, R. 1999. Task-dependent modulation of 15-30 Hz coherence between rectified EMGs from human hand and forearm muscles. *The Journal of Physiology*, 516, 559-570.

KILNER, J. M., BAKER, S. N., SALENIUS, S., HARI, R. & LEMON, R. N. 2000. Human cortical muscle coherence is directly related to specific motor parameters. *The Journal of Neuroscience*, 20, 8838-8845.

KIM, H. Y., YANG, S. P., PARK, G. L., KIM, E. J., & YOU, J. S. H. 2016. Best facilitated cortical activation during different stepping, treadmill, and robot-assisted walking training paradigms and speeds: a functional near-infrared spectroscopy neuroimaging study. *NeuroRehabilitation*, 38(2), 171-178.

KIRSHBLUM, S. C., BURNS, S. P., BIERING-SORENSEN, F., DONOVAN, W., GRAVES, D. E., JHA, A., ... & SCHMIDT-READ, M. 2011. International standards for neurological classification of spinal cord injury (revised 2011). *The journal of spinal cord medicine*, 34(6), 535-546.

KLEM, G. H., LÜDERS, H. O., JASPER, H. & ELGER, C. 1999. The ten-twenty electrode system of the International Federation. *Electroencephalogr Clin Neurophysiol*, 52, 3-6.

KNAEPEN, K., MIERAU, A., SWINNEN, E., TELLEZ, H. F., MICHELSEN, M., KERCKHOFS, E., LEFEBER, D. & MEEUSEN, R. 2015. Human-robot interaction: does robotic guidance force affect gait-related brain dynamics during robot-assisted treadmill walking? *PloSOne*, 10, e0140626.

KNAEPEN, K., MIERAU, A., TELLEZ, H. F., LEFEBER, D. & MEEUSEN, R. 2015. Temporal and spatial organization of gait-related electrocortical potentials. *Neuroscience Letters*, 599, 75-80.

KNIKOU, M. 2013. Functional reorganization of soleus H-reflex modulation during stepping after robotic-assisted step training in people with complete and incomplete spinal cord injury. *Experimental Brain Research*, 228, 279-296.

KOENRAADT, K. L., DUYSSENS, J., RIJKEN, H., VAN NES, I. J. & KEIJSERS, N. L. 2014. Preserved foot motor cortex in patients with complete spinal cord injury: a functional near-infrared spectroscopic study. *Neurorehabilitation and Neural Repair*, 28, 179-187.

KRAKAUER, J. W. & MAZZONI, P. 2011. Human sensorimotor learning: adaptation, skill, and beyond. *Current Opinion in Neurobiology*, 21, 636-644.



- KRANCZIOCH, C., ATHANASSIOU, S., SHEN, S., GAO, G. & STERR, A. 2008. Short-term learning of a visually guided power-grip task is associated with dynamic changes in EEG oscillatory activity. *Clinical Neurophysiology*, 119, 1419-1430.
- KREBS, H., HOGAN, N., HENING, W., ADAMOVICH, S. & POIZNER, H. 2001. Procedural motor learning in Parkinson's disease. *Experimental Brain Research*, 141, 425-437.
- KREBS, H. I., BRASHERS-KRUG, T., RAUCH, S. L., SAVAGE, C. R., HOGAN, N., RUBIN, R. H., FISCHMAN, A. J. & ALPERT, N. M. 1998. Robot-aided functional imaging: Application to a motor learning study. *Human Brain Mapping*, 6, 59-72.
- KREBS, H. I., PALAZZOLO, J. J., DIPIETRO, L., FERRARO, M., KROL, J., RANNEKLEIV, K., VOLPE, B. T. & HOGAN, N. 2003. Rehabilitation robotics: Performance-based progressive robot-assisted therapy. *Autonomous Robots*, 15, 7-20.
- KRISTEVA, R., PATINO, L. & OMLOR, W. 2007. Beta-range cortical motor spectral power and corticomuscular coherence as a mechanism for effective corticospinal interaction during steady-state motor output. *NeuroImage*, 36, 785-792.
- KRISTEVA-FEIGE, R., FRITSCH, C., TIMMER, J. & LÜCKING, C.-H. 2002. Effects of attention and precision of exerted force on beta range EEG-EMG synchronization during a maintained motor contraction task. *Clinical Neurophysiology*, 113, 124-131.
- KWAKKEL, G. 2006. Impact of intensity of practice after stroke: issues for consideration. *Disability and Rehabilitation*, 28, 823-830.
- LABRIFFE, M., ANNWEILER, C., AMIROVA, L. E., GAUQUELIN-KOCH, G., TER MINASSIAN, A., LEIBER, L.-M., BEAUCHET, O., CUSTAUD, M.-A. & DINOMAS, M. 2017. Brain activity during mental imagery of gait versus gait-like plantar stimulation: a novel combined functional MRI paradigm to better understand cerebral gait control. *Frontiers in Human Neuroscience*, 11.
- LADOUCE, S., DONALDSON, D. I., DUDCHENKO, P. A. & IETSWAART, M. 2016. Understanding Minds in Real-World Environments: Toward a Mobile Cognition Approach. *Frontiers in Human Neuroscience*, 10.
- LAGE, G. M., UGRINOWITSCH, H., APOLINÁRIO-SOUZA, T., VIEIRA, M. M., ALBUQUERQUE, M. R. & BENDA, R. N. 2015. Repetition and variation in motor practice: A review of neural correlates. *Neuroscience & Biobehavioral Reviews*, 57, 132-141.
- LAJOIE, K., ANDUJAR, J.-E., PEARSON, K. & DREW, T. 2010. Neurons in area 5 of the posterior parietal cortex in the cat contribute to interlimb coordination during visually guided locomotion: a role in working memory. *Journal of Neurophysiology*, 103, 2234-2254.
- LAKHANI, B., BORICH, M. R., JACKSON, J. N., WADDEN, K. P., PETERS, S., VILLAMAYOR, A., MACKAY, A. L., VAVASOUR, I. M., RAUSCHER, A. & BOYD, L. A. 2016. Motor skill acquisition promotes human brain myelin plasticity. *Neural Plasticity*, 2016.
- LANGHORNE, P., BERNHARDT, J. & KWAKKEL, G. 2011. Stroke rehabilitation. *The Lancet*, 377, 1693-1702.

- LARSEN, A., MCILHAGGA, W., BAERT, J. & BUNDESEN, C. 2003. Seeing or hearing? Perceptual independence, modality confusions, and crossmodal congruity effects with focused and divided attention. *Perception & Psychophysics*, 65, 568-574.
- LATT, M. D., MENZ, H. B., FUNG, V. S. & LORD, S. R. 2009. Acceleration patterns of the head and pelvis during gait in older people with Parkinson's disease: a comparison of fallers and nonfallers. *The Journals of Gerontology Series A: Biological Sciences and Medical Sciences*, glp009.
- LEARMONTH, G., BENWELL, C. S., THUT, G. & HARVEY, M. 2017. Age-related reduction of hemispheric lateralisation for spatial attention: An EEG study. *NeuroImage*, 153, 139-151.
- LEE, M.-S., KIM, H.-S. & LYOO, C.-H. 2005. "Off" gait freezing and temporal discrimination threshold in patients with Parkinson disease. *Neurology*, 64, 670-674.
- LEE, Y. S., BAE, S. H., LEE, S. H., & KIM, K. Y. 2015. Neurofeedback training improves the dual-task performance ability in stroke patients. *The Tohoku journal of experimental medicine*, 236(1), 81-88.
- LEEB, R., SAGHA, H. & CHAVARRIAGA, R. Multimodal fusion of muscle and brain signals for a hybrid-BCI. *Engineering in Medicine and Biology Society (EMBC), 2010 Annual International Conference of the IEEE*, 2010. IEEE, 4343-4346.
- LEFEBVRE, S., DRICOT, L., GRADKOWSKI, W., LALOUX, P. & VANDERMEEREN, Y. 2012. Brain activations underlying different patterns of performance improvement during early motor skill learning. *NeuroImage*, 62, 290-299.
- LEMON, R. N. 2008. Descending pathways in motor control. *Annual Review Neuroscience*, 31, 195-218.
- LENKA, A., NADUTHOTA, R. M., JHA, M., PANDA, R., PRAJAPATI, A., JHUNJHUNWALA, K., SAINI, J., YADAV, R., BHARATH, R. D. & PAL, P. K. 2016. Freezing of gait in Parkinson's disease is associated with altered functional brain connectivity. *Parkinsonism & Related Disorders*, 24, 100-106.
- LEWEK, M. D., BRADLEY, C. E., WUTZKE, C. J. & ZINDER, S. M. 2014. The relationship between spatiotemporal gait asymmetry and balance in individuals with chronic stroke. *Journal of Applied Biomechanics*, 30, 31-36.
- LI, K. Z., LINDENBERGER, U., FREUND, A. M. & BALTES, P. B. 2001. Walking while memorizing: Age-related differences in compensatory behavior. *Psychological Science*, 12, 230-237.
- LIN, C.-T., CHIU, T.-C. & GRAMANN, K. 2015. EEG correlates of spatial orientation in the human retrosplenial complex. *NeuroImage*, 120, 123-132.
- LIN, M.-I. B. & LIN, K.-H. 2016. Walking while performing working memory tasks changes the prefrontal cortex hemodynamic activations and gait kinematics. *Frontiers in Behavioral Neuroscience*, 10.
- LINDEN, D. E., & TURNER, D. L. 2016. Real-time functional magnetic resonance imaging neurofeedback in motor neurorehabilitation. *Current opinion in neurology*, 29(4), 412.

- LO, A. C., GUARINO, P. D., RICHARDS, L. G., HASELKORN, J. K., WITTENBERG, G. F., FEDERMAN, D. G., RINGER, R. J., WAGNER, T. H., KREBS, H. I. & VOLPE, B. T. 2010. Robot-assisted therapy for long-term upper-limb impairment after stroke. *New England Journal of Medicine*, 362, 1772-1783.
- LOHSE, K., WADDEN, K., BOYD, L. & HODGES, N. 2014. Motor skill acquisition across short and long time scales: a meta-analysis of neuroimaging data. *Neuropsychologia*, 59, 130-141.
- LONINI, L., DIPIETRO, L., ZOLLO, L., GUGLIEMELLI, E. & KREBS, H. I. 2009. An internal model for acquisition and retention of motor learning during arm reaching. *Neural Computation*, 21, 2009-2027.
- LUCK, S. J. 2014. An introduction to the event-related potential technique. Boston, MIT press.
- LY, Q. T., HANDOJOSENO, A. A., GILAT, M., NGUYEN, N., CHAI, R., TRAN, Y., LEWIS, S. J. & NGUYEN, H. T. Detection of Gait Initiation Failure in Parkinson's disease patients using EEG signals. *Engineering in Medicine and Biology Society (EMBC), 2016 IEEE 38th Annual International Conference of the*, 2016. IEEE, 1599-1602.
- MAHAN, M. Y. & GEORGOPOULOS, A. P. 2013. Motor directional tuning across brain areas: directional resonance and the role of inhibition for directional accuracy. *Frontiers in Neural Circuits*, 7.
- MAIDAN, I., BERNAD-ELAZARI, H., GILADI, N., HAUSDORFF, J. M. & MIRELMAN, A. 2017. When is Higher Level Cognitive Control Needed for Locomotor Tasks Among Patients with Parkinson's Disease? *Brain Topography*, 1-8.
- MAIDAN, I., NIEUWHOF, F., BERNAD-ELAZARI, H., REELICK, M. F., BLOEM, B. R., GILADI, N., DEUTSCH, J. E., HAUSDORFF, J. M., CLAASSEN, J. A. & MIRELMAN, A. 2016. The role of the frontal lobe in complex walking among patients with Parkinson's disease and healthy older adults: an fNIRS study. *Neurorehabilitation and Neural Repair*, 30, 963-971.
- MAKEIG, S. 1993. Auditory event-related dynamics of the EEG spectrum and effects of exposure to tones. *Electroencephalography and Clinical Neurophysiology*, 86, 283-293.
- MANGANOTTI, P., GERLOFF, C., TORO, C., KATSUTA, H., SADATO, N., ZHUANG, P. A., LEOCANI, L. & HALLETT, M. 1998. Task-related coherence and task-related spectral power changes during sequential finger movements. *Electroencephalography and Clinical Neurophysiology/Electromyography and Motor Control*, 109, 50-62.
- MARIGOLD, D. S. & DREW, T. 2011. Contribution of cells in the posterior parietal cortex to the planning of visually guided locomotion in the cat: effects of temporary visual interruption. *Journal of Neurophysiology*, 105, 2457-2470.
- MARIS, E. & OOSTENVELD, R. 2007. Nonparametric statistical testing of EEG-and MEG-data. *Journal of Neuroscience Methods*, 164, 177-190.
- MARINS, T. F., RODRIGUES, E. C., ENGEL, A., HOEFLE, S., BASILIO, R., LENT, R., ... & TOVAR-MOLL, F. 2015. Enhancing motor network activity using real-time

- functional MRI neurofeedback of left premotor cortex. *Frontiers in Behavioral Neuroscience*, 9, 341.
- MARSDEN, J., WERHAHN, K., ASHBY, P., ROTHWELL, J., NOACHTAR, S. & BROWN, P. 2000. Organization of cortical activities related to movement in humans. *Journal of Neuroscience*, 20, 2307-2314.
- MASDEU, J. C., ALAMPUR, U., CAVALIERE, R. & TAVOULAREAS, G. 1994. Astasia and gait failure with damage of the pontomesencephalic locomotor region. *Annals of Neurology*, 35, 619-621.
- MAZZOLENI, S., PUZZOLANTE, L., ZOLLO, L., DARIO, P. & POSTERARO, F. 2014. Mechanisms of motor recovery in chronic and subacute stroke patients following a robot-aided training. *IEEE Transactions on Haptics*, 7, 175-180.
- MCCLELLAND, V. M., CVETKOVIC, Z. & MILLS, K. R. 2012. Rectification of the EMG is an unnecessary and inappropriate step in the calculation of corticomuscular coherence. *Journal of Neuroscience Methods*, 205, 190-201.
- MCCRIMMON, C. M., WANG, P. T., HEYDARI, P., NGUYEN, A., SHAW, S. J., GONG, H., ... & DO, A. H. 2017. Electro corticographic encoding of human gait in the leg primary motor cortex. *Cerebral Cortex*, 1-11.
- MCDOWELL, K., JEKA, J. J., SCHÖNER, G. & HATFIELD, B. D. 2002. Behavioral and electrocortical evidence of an interaction between probability and task metrics in movement preparation. *Experimental Brain Research*, 144, 303-313.
- MEHRKANOON, S., BREAKSPEAR, M. & BOONSTRA, T. W. 2014. The reorganization of corticomuscular coherence during a transition between sensorimotor states. *NeuroImage*, 100, 692-702.
- MENDEZ-BALBUENA, I., HUETHE, F., SCHULTE-MÖNTING, J., LEONHART, R., MANJARREZ, E. & KRISTEVA, R. 2011. Corticomuscular coherence reflects interindividual differences in the state of the corticomuscular network during low-level static and dynamic forces. *Cerebral Cortex*, 22, 628-638.
- MENZ, H. B., LORD, S. R. & FITZPATRICK, R. C. 2003. Acceleration patterns of the head and pelvis when walking on level and irregular surfaces. *Gait & Posture*, 18, 35-46.
- MENZ, H. B., LORD, S. R. & FITZPATRICK, R. C. 2003. Age-related differences in walking stability. *Age and Ageing*, 32, 137-142.
- MEYER, L., GRIGUTSCH, M., SCHMUCK, N., GASTON, P. & FRIEDERICI, A. D. 2015. Frontal-posterior theta oscillations reflect memory retrieval during sentence comprehension. *Cortex*, 71, 205-218.
- METZGER, F. G., EHLIS, A. C., HAEUSSINGER, F. B., SCHNEEWEISS, P., HUDAK, J., FALLGATTER, A. J., & SCHNEIDER, S. 2017. Functional brain imaging of walking while talking—An fNIRS study. *Neuroscience*, 343, 85-93.
- MIDDLETON, F. A. & STRICK, P. L. 2000. Basal ganglia and cerebellar loops: motor and cognitive circuits. *Brain Research Reviews*, 31, 236-250.
- MILLÁN, J. D. R., GALÁN, F., VANHOODYDONCK, D., LEW, E., PHILIPS, J. & NUTTIN, M. Asynchronous non-invasive brain-actuated control of an intelligent

wheelchair. Engineering in Medicine and Biology Society, 2009. EMBC 2009. Annual International Conference of the IEEE, 2009. IEEE, 3361-3364.

MILLÁN, J. D. R., RUPP, R., MÜLLER-PUTZ, G. R., MURRAY-SMITH, R., GIUGLIEMMA, C., TANGERMANN, M., VIDAURRE, C., CINCOTTI, F., KÜBLER, A. & LEEB, R. 2010. Combining brain-computer interfaces and assistive technologies: state-of-the-art and challenges. *Frontiers in Neuroscience*, 4.

MILNER, T. E. & FRANKLIN, D. W. 2005. Impedance control and internal model use during the initial stage of adaptation to novel dynamics in humans. *The Journal of Physiology*, 567, 651-664.

MIMA, T. & HALLETT, M. 1999. Corticomuscular coherence: a review. *Journal of Clinical Neurophysiology*, 16, 501.

MIMA, T., MATSUOKA, T. & HALLETT, M. 2000. Functional coupling of human right and left cortical motor areas demonstrated with partial coherence analysis. *Neuroscience Letters*, 287, 93-96.

MIMA, T., SIMPKINS, N., OLUWATIMILEHIN, T. & HALLETT, M. 1999. Force level modulates human cortical oscillatory activities. *Neuroscience Letters*, 275, 77-80.

MIRELMAN, A., MAIDAN, I., BERNAD-ELAZARI, H., NIEUWHOF, F., REELICK, M., GILADI, N., & HAUSDORFF, J. M. 2014. Increased frontal brain activation during walking while dual tasking: an fNIRS study in healthy young adults. *Journal of Neuroengineering and Rehabilitation*, 11(1), 85.

MIYAY, I., TANABE, H. C., SASE, I., EDA, H., ODA, I., KONISHI, I., ... & KUBOTA, K. 2001. Cortical mapping of gait in humans: a near-infrared spectroscopic topography study. *Neuroimage*, 14(5), 1186-1192.

MIYAY, I., YAGURA, H., ODA, I., KONISHI, I., EDA, H., SUZUKI, T., & KUBOTA, K. 2002. Premotor cortex is involved in restoration of gait in stroke. *Annals of neurology*, 52(2), 188-194.

MOISELLO, C., BLANCO, D., LIN, J., PANDAY, P., KELLY, S. P., QUARTARONE, A., DI ROCCO, A., CIRELLI, C., TONONI, G. & GHILARDI, M. F. 2015. Practice changes beta power at rest and its modulation during movement in healthy subjects but not in patients with Parkinson's disease. *Brain and Behavior*, 5.

MORI, F., NAKAJIMA, K., TACHIBANA, A., NAMBU, A. & MORI, S. 2003. Cortical mechanisms for the control of bipedal locomotion in Japanese monkeys: II. Local inactivation of the supplementary motor area (SMA). *Neuroscience Research*, 46, S157.

MORONE, G., BRAGONI, M., IOSA, M., DE ANGELIS, D., VETURIERO, V., COIRO, P., ... & PAOLUCCI, S. 2011. Who may benefit from robotic-assisted gait training? A randomized clinical trial in patients with subacute stroke. *Neurorehabilitation and Neural Repair*, 25(7), 636-644.

MORTON, S. M. & BASTIAN, A. J. 2006. Cerebellar contributions to locomotor adaptations during splitbelt treadmill walking. *Journal of Neuroscience*, 26, 9107-9116.

MOTTOLESE, C., RICHARD, N., HARQUEL, S., SZATHMARI, A., SIRIGU, A. & DESMURGET, M. 2013. Mapping motor representations in the human cerebellum. *Brain*, 136, 330-342.

- MOUNTCASTLE, V. B., LYNCH, J., GEORGOPOULOS, A., SAKATA, H. & ACUNA, C. 1975. Posterior parietal association cortex of the monkey: command functions for operations within extrapersonal space. *Journal of Neurophysiology*, 38, 871-908.
- MURTHY, V. N. & FETZ, E. E. 1992. Coherent 25-to 35-Hz oscillations in the sensorimotor cortex of awake behaving monkeys. *Proceedings of the National Academy of Sciences*, 89, 5670-5674.
- MUSICCO, M., EMBERTI, L., NAPPI, G., CALTAGIRONE, C., & ITALIAN MULTICENTER STUDY ON OUTCOMES OF REHABILITATION OF NEUROLOGICAL PATIENTS. 2003. Early and long-term outcome of rehabilitation in stroke patients: the role of patient characteristics, time of initiation, and duration of interventions. *Archives of Physical Medicine and Rehabilitation*, 84(4), 551-558.
- MUTHURAMAN, M., GALKA, A., DEUSCHL, G., HEUTE, U. & RAETHJEN, J. 2010. Dynamical correlation of non-stationary signals in time domain—A comparative study. *Biomedical Signal Processing and Control*, 5, 205-213.
- NAKAJIMA, K., MORI, F., TACHIBANA, A., NAMBU, A. & MORI, S. 2003. Cortical mechanisms for the control of bipedal locomotion in Japanese monkeys: I. Local inactivation of the primary motor cortex (M1). *Neuroscience Research*, 46, S156.
- NAKAMURA, H., KURODA, T., WAKITA, M., KUSUNOKI, M., KATO, A., MIKAMI, A., SAKATA, H. & ITOH, K. 2001. From three-dimensional space vision to prehensile hand movements: the lateral intraparietal area links the area V3A and the anterior intraparietal area in macaques. *Journal of Neuroscience*, 21, 8174-8187.
- NAM, K. Y., KIM, H. J., KWON, B. S., PARK, J.-W., LEE, H. J. & YOO, A. 2017. Robot-assisted gait training (Lokomat) improves walking function and activity in people with spinal cord injury: a systematic review. *Journal of Neuroengineering and Rehabilitation*, 14, 24.
- NARANJO, J., BROVELLI, A., LONGO, R., BUDAI, R., KRISTEVA, R. & BATTAGLINI, P. 2007. EEG dynamics of the frontoparietal network during reaching preparation in humans. *NeuroImage*, 34, 1673-1682.
- NAS, K., YAZMALAR, L., ŞAH, V., AYDIN, A., & ÖNES, K. 2015. Rehabilitation of spinal cord injuries. *World journal of orthopedics*, 6(1), 8.
- NEGRINI, M., BRKIĆ, D., PIZZAMIGLIO, S., PREMOLI, I. & RIVOLTA, D. 2017. Neurophysiological correlates of featural and spacing processing for face and non-face stimuli. *Frontiers in Psychology*, 8.
- NELSON, A. B., MOISELLO, C., LIN, J., PANDAY, P., RICCI, S., CANESSA, A., DI ROCCO, A., QUARTARONE, A., FRAZZITTA, G. & ISAIAS, I. U. 2017. Beta oscillatory changes and retention of motor skills during practice in healthy subjects and in patients with Parkinson's disease. *Frontiers in Human Neuroscience*, 11.
- NEPTUNE, R. R., CLARK, D. J. & KAUTZ, S. A. 2009. Modular control of human walking: a simulation study. *Journal of Biomechanics*, 42, 1282-1287.
- NIEUWHOF, F., BLOEM, B. R., REELICK, M. F., AARTS, E., MAIDAN, I., MIRELMAN, A., HAUSDORFF, J. M., TONI, I. & HELMICH, R. C. 2017. Impaired

- dual tasking in Parkinson's disease is associated with reduced focusing of cortico-striatal activity. *Brain*, 140, 1384-1398.
- NIJBOER, M., BORST, J., VAN RIJN, H., & TAATGEN, N. 2014. Single-task fMRI overlap predicts concurrent multitasking interference. *NeuroImage*, 100, 60-74.
- NORDIN, N., XIE, S. Q. & WÜNSCHE, B. 2014. Assessment of movement quality in robot-assisted upper limb rehabilitation after stroke: a review. *Journal of Neuroengineering and Rehabilitation*, 11, 137.
- OLIVEIRA, A. S., SCHLINK, B., HAIRSTON, W. D., KÖNIG, P. & FERRIS, D. P. 2017. A channel rejection method for attenuating motion-related artefacts in EEG recordings during walking. *Frontiers in Neuroscience*, 11, 225.
- OMLOR, W., PATINO, L., HEPP-REYMOND, M.-C. & KRISTEVA, R. 2007. Gamma-range corticomuscular coherence during dynamic force output. *NeuroImage*, 34, 1191-1198.
- OOSTENVELD, R., FRIES, P., MARIS, E. & SCHOFFELEN, J.-M. 2010. FieldTrip: open source software for advanced analysis of MEG, EEG, and invasive electrophysiological data. *Computational Intelligence and Neuroscience*, 2011.
- OSU, R., BURDET, E., FRANKLIN, D. W., MILNER, T. E. & KAWATO, M. 2003. Different mechanisms involved in adaptation to stable and unstable dynamics. *Journal of Neurophysiology*, 90, 3255-3269.
- OTTENBACHER, K. J. & JANNELL, S. 1993. The results of clinical trials in stroke rehabilitation research. *Archives of Neurology*, 50, 37-44.
- OVERDUIN, S. A., RICHARDSON, A. G. & BIZZI, E. 2009. Cortical processing during dynamic motor adaptation. *Progress in Motor Control*. Springer.
- OWEISS, K. G. & BADRELDIN, I. S. 2015. Neuroplasticity subserving the operation of brain-machine interfaces. *Neurobiology of Disease*, 83, 161-171.
- PARK, H., KIM, J. S., PAEK, S. H., JEON, B. S., LEE, J. Y. & CHUNG, C. K. 2009. Cortico-muscular coherence increases with tremor improvement after deep brain stimulation in Parkinson's disease. *Neuroreport*, 20, 1444-1449.
- PARK, J. L., FAIRWEATHER, M. M. & DONALDSON, D. I. 2015. Making the case for mobile cognition: EEG and sports performance. *Neuroscience & Biobehavioral Reviews*, 52, 117-130.
- PATTON, J. L. & MUSSA-IVALDI, F. A. 2004. Robot-assisted adaptive training: custom force fields for teaching movement patterns. *IEEE Transactions on Biomedical Engineering*, 51, 636-646.
- PATTON, J. L., STOYKOV, M. E., KOVIC, M. & MUSSA-IVALDI, F. A. 2006. Evaluation of robotic training forces that either enhance or reduce error in chronic hemiparetic stroke survivors. *Experimental Brain Research*, 168, 368-383.
- PEARSON, K. G. 2004. Generating the walking gait: role of sensory feedback. *Progress in Brain Research*, 143, 123-129.

- PEREZ, M. A., LUNDBYE-JENSEN, J. & NIELSEN, J. B. 2006. Changes in corticospinal drive to spinal motoneurons following visuo-motor skill learning in humans. *The Journal of Physiology*, 573, 843-855.
- PERRIN, F., PERNIER, J., BERTRAND, O. & ECHALLIER, J. 1989. Spherical splines for scalp potential and current density mapping. *Electroencephalography and Clinical Neurophysiology*, 72, 184-187.
- PETERSEN, T. H., WILLERSLEV-OLSEN, M., CONWAY, B. A. & NIELSEN, J. B. 2012. The motor cortex drives the muscles during walking in human subjects. *The Journal of Physiology*, 590, 2443-2452.
- PETERSON, D. & HORAK, F. 2016. Neural control of walking in people with Parkinsonism. *Physiology*, 31, 95-107.
- PFURTSCHELLER, G. 2001. Functional brain imaging based on ERD/ERS. *Vision Research*, 41, 1257-1260.
- PFURTSCHELLER, G. & DA SILVA, F. L. 1999. Event-related EEG/MEG synchronization and desynchronization: basic principles. *Clinical Neurophysiology*, 110, 1842-1857.
- PHELPS, M. E., MAZZIOTTA, J. & SCHELBERT, H. 1988. Positron emission tomography, Los Alamos National Laboratory.
- PIZZAMIGLIO, S., DE LILLO, M., NAEEM, U., ABDALLA, H. & TURNER, D. 2017. High-frequency intermuscular coherence between arm muscles during robot-mediated motor adaptation. *Frontiers in Physiology*. 7: 668. doi: 10.3389/fphys.
- PIZZAMIGLIO, S., DESOWSKA, A., SHOJAII, P., TAGA, M. & TURNER, D. L. 2017. Muscle co-contraction patterns in robot-mediated force field learning to guide specific muscle group training. *NeuroRehabilitation*, 1-13.
- PLAHA, P. & GILL, S. S. 2005. Bilateral deep brain stimulation of the pedunculopontine nucleus for Parkinson's disease. *Neuroreport*, 16, 1883-1887.
- PLUMMER, P., APPLE, S., DOWD, C. & KEITH, E. 2015. Texting and walking: Effect of environmental setting and task prioritization on dual-task interference in healthy young adults. *Gait & Posture*, 41, 46-51.
- POLLOK, B., LATZ, D., KRAUSE, V., BUTZ, M. & SCHNITZLER, A. 2014. Changes of motor-cortical oscillations associated with motor learning. *Neuroscience*, 275, 47-53.
- POOL, E.-M., REHME, A. K., FINK, G. R., EICKHOFF, S. B. & GREFKES, C. 2013. Network dynamics engaged in the modulation of motor behavior in healthy subjects. *NeuroImage*, 82, 68-76.
- PRESACCO, A., GOODMAN, R., FORRESTER, L. & CONTRERAS-VIDAL, J. L. 2011. Neural decoding of treadmill walking from non-invasive electroencephalographic signals. *Journal of Neurophysiology*, 106, 1875-1887.
- PRUSZYNSKI, J. A. & SCOTT, S. H. 2012. Optimal feedback control and the long-latency stretch response. *Experimental Brain Research*, 218, 341-359.



- QUATTROCCHI, G., GREENWOOD, R., ROTHWELL, J. C., GALEA, J. M. & BESTMANN, S. 2017. Reward and punishment enhance motor adaptation in stroke. *J Neurol Neurosurg Psychiatry*, jnnp-2016-314728.
- RAMÍREZ, R. R. 2008. Source localization. *Scholarpedia*, 3, 1733.
- RAMOS-MURGUIALDAY, A., BROETZ, D., REA, M., LÄER, L., YILMAZ, Ö., BRASIL, F. L., LIBERATI, G., CURADO, M. R., GARCIA-COSSIO, E. & VYZIOTIS, A. 2013. Brain-machine interface in chronic stroke rehabilitation: a controlled study. *Annals of Neurology*, 74, 100-108.
- REINKENSMEYER, D. J., BURDET, E., CASADIO, M., KRAKAUER, J. W., KWAKKEL, G., LANG, C. E., SWINNEN, S. P., WARD, N. S. & SCHWEIGHOFER, N. 2016. Computational neurorehabilitation: modeling plasticity and learning to predict recovery. *Journal of Neuroengineering and Rehabilitation*, 13, 42.
- REISMAN, D. S., MCLEAN, H., KELLER, J., DANKS, K. A. & BASTIAN, A. J. 2013. Repeated split-belt treadmill training improves poststroke step length asymmetry. *Neurorehabilitation and Neural Repair*, 27, 460-468.
- REYES, A., LAINE, C. M., KUTCH, J. J. & VALERO-CUEVAS, F. J. 2017. Beta Band Corticomuscular drive reflects muscle coordination strategies. *Frontiers in Computational Neuroscience*, 11.
- RIDDING, M. C. & ROTHWELL, J. C. 2007. Is there a future for therapeutic use of transcranial magnetic stimulation? *Nature Reviews. Neuroscience*, 8, 559.
- RIDDLE, C. N. & BAKER, S. N. 2005. Manipulation of peripheral neural feedback loops alters human corticomuscular coherence. *The Journal of Physiology*, 566, 625-639.
- RIENER, R. 2007. Robot-aided rehabilitation of neural function in the upper extremities. *Operative Neuromodulation*, 465-471.
- ROSENBERG, J., AMJAD, A., BREEZE, P., BRILLINGER, D. & HALLIDAY, D. 1989. The Fourier approach to the identification of functional coupling between neuronal spike trains. *Progress in Biophysics and Molecular Biology*, 53, 1-31.
- ROSENBERG-KATZ, K., MAIDAN, I., JACOB, Y., GILADI, N., MIRELMAN, A. & HAUSDORFF, J. M. 2016. Alterations in conflict monitoring are related to functional connectivity in Parkinson's disease. *Cortex*, 82, 277-286.
- ROSSIGNOL, S., DUBUC, R. & GOSSARD, J.-P. 2006. Dynamic sensorimotor interactions in locomotion. *Physiological Reviews*, 86, 89-154.
- ROSSITER, H. E., BOUDRIAS, M.-H. & WARD, N. S. 2014. Do movement-related beta oscillations change after stroke? *Journal of Neurophysiology*, 112, 2053-2058.
- ROSSITER, H. E., EAVES, C., DAVIS, E., BOUDRIAS, M.-H., PARK, C.-H., FARMER, S., BARNES, G., LITVAK, V. & WARD, N. S. 2013. Changes in the location of cortico-muscular coherence following stroke. *NeuroImage: Clinical*, 2, 50-55.
- ROUTSON, R. L., CLARK, D. J., BOWDEN, M. G., KAUTZ, S. A. & NEPTUNE, R. R. 2013. The influence of locomotor rehabilitation on module quality and post-stroke hemiparetic walking performance. *Gait & Posture*, 38, 511-517.

- SAFRI, N. M., MURAYAMA, N., HAYASHIDA, Y. & IGASAKI, T. 2007. Effects of concurrent visual tasks on cortico-muscular synchronization in humans. *Brain Research*, 1155, 81-92.
- SAFRI, N. M., MURAYAMA, N., IGASAKI, T. & HAYASHIDA, Y. 2006. Effects of visual stimulation on cortico-spinal coherence during isometric hand contraction in humans. *International Journal of Psychophysiology*, 61, 288-293.
- SALE, P., INFARINATO, F., DEL PERCIO, C., LIZIO, R., BABILONI, C., FOTI, C. & FRANCESCHINI, M. 2015. Electroencephalographic markers of robot-aided therapy in stroke patients for the evaluation of upper limb rehabilitation. *International Journal of Rehabilitation Research*, 38, 294-305.
- SCHABOWSKY, C. N., HIDLER, J. M. & LUM, P. S. 2007. Greater reliance on impedance control in the nondominant arm compared with the dominant arm when adapting to a novel dynamic environment. *Experimental Brain Research*, 182, 567-577.
- SCHABRUN, S. M., VAN DEN HOORN, W., MOORCROFT, A., GREENLAND, C. & HODGES, P. W. 2014. Texting and walking: strategies for postural control and implications for safety. *PLoSOne*, 9, e84312.
- SCHEIDT, R. A. & STOECKMANN, T. 2007. Reach adaptation and final position control amid environmental uncertainty after stroke. *Journal of Neurophysiology*, 97, 2824-2836.
- SCHOFFELEN, J.-M., OOSTENVELD, R. & FRIES, P. 2005. Neuronal coherence as a mechanism of effective corticospinal interaction. *Science*, 308, 111-113.
- SCHWARTZ, A. B., KETTNER, R. E. & GEORGOPOULOS, A. P. 1988. Primate motor cortex and free arm movements to visual targets in three-dimensional space. I. Relations between single cell discharge and direction of movement. *Journal of Neuroscience*, 8, 2913-2927.
- SCHWARTZ, A. B. & MORAN, D. W. 1999. Motor cortical activity during drawing movements: population representation during lemniscate tracing. *Journal of Neurophysiology*, 82, 2705-2718.
- SCHWARTZ, I. & MEINER, Z. 2015. Robotic-assisted gait training in neurological patients: who may benefit? *Annals of Biomedical Engineering*, 43, 1260-1269.
- SCHWEBEL, D. C., STAVRINOS, D., BYINGTON, K. W., DAVIS, T., O'NEAL, E. E. & DE JONG, D. 2012. Distraction and pedestrian safety: how talking on the phone, texting, and listening to music impact crossing the street. *Accident Analysis & Prevention*, 45, 266-271.
- SCOTT, S. H., CLUFF, T., LOWREY, C. R. & TAKEI, T. 2015. Feedback control during voluntary motor actions. *Current Opinion in Neurobiology*, 33, 85-94.
- SEDERBERG, P. B., KAHANA, M. J., HOWARD, M. W., DONNER, E. J. & MADSEN, J. R. 2003. Theta and gamma oscillations during encoding predict subsequent recall. *Journal of Neuroscience*, 23, 10809-10814.
- SEEBER, M., SCHERER, R., WAGNER, J., SOLIS ESCALANTE, T. & MÜLLER-PUTZ, G. R. 2014. EEG beta suppression and low gamma modulation are different elements of human upright walking. *Frontiers in Human Neuroscience*, 8, 2014.

- SEEBER, M., SCHERER, R., WAGNER, J., SOLIS-ESCALANTE, T. & MÜLLER-PUTZ, G. R. 2015. High and low gamma EEG oscillations in central sensorimotor areas are conversely modulated during the human gait cycle. *NeuroImage*, 112, 318-326.
- SEKINE, M., TAMURA, T., YOSHIDA, M., SUDA, Y., KIMURA, Y., MIYOSHI, H., KIJIMA, Y., HIGASHI, Y. & FUJIMOTO, T. 2013. A gait abnormality measure based on root mean square of trunk acceleration. *Journal of Neuroengineering and Rehabilitation*, 10, 118.
- SEKINE, M., TAMURA, T., YOSHIDA, M., UCHIYAMA, T. & CENTER, C. Application of root mean square ratio of trunk acceleration for evaluation of Parkinson's disease. BSN 2014, Zurich.
- SEMRAU, J. A., HERTER, T. M., SCOTT, S. H. & DUKELOW, S. P. 2015. Examining differences in patterns of sensory and motor recovery after stroke with robotics. *Stroke*, 46, 3459-3469.
- SERGIO, L. E. & KALASKA, J. F. 2003. Systematic changes in motor cortex cell activity with arm posture during directional isometric force generation. *Journal of Neurophysiology*, 89, 212-228.
- SHADMEHR, R. & HOLCOMB, H. H. 1997. Neural correlates of motor memory consolidation. *Science*, 277, 821-825.
- SHADMEHR, R. & MUSSA-IVALDI, F. A. 1994. Adaptive representation of dynamics during learning of a motor task. *Journal of Neuroscience*, 14, 3208-3224.
- SHADMEHR, R. & WISE, S. P. 2005. The computational neurobiology of reaching and pointing: a foundation for motor learning. Cambridge, MIT press.
- SHINER, C. T., TANG, H., JOHNSON, B. W. & MCNULTY, P. A. 2015. Cortical beta oscillations and motor thresholds differ across the spectrum of post-stroke motor impairment, a preliminary MEG and TMS study. *Brain Research*, 1629, 26-37.
- SIMMONS, L., SHARMA, N., BARON, J.-C. & POMEROY, V. M. 2008. Motor imagery to enhance recovery after subcortical stroke: who might benefit, daily dose, and potential effects. *Neurorehabilitation and Neural Repair*, 22, 458-467.
- SIMONS, J. S. & SPIERS, H. J. 2003. Prefrontal and medial temporal lobe interactions in long-term memory. *Nature Reviews Neuroscience*, 4, 637-648.
- SIPP, A. R., GWIN, J. T., MAKEIG, S. & FERRIS, D. P. 2013. Loss of balance during balance beam walking elicits a multifocal theta band electrocortical response. *Journal of Neurophysiology*, 110, 2050-2060.
- SIRTORI, V., CORBETTA, D., MOJA, L. & GATTI, R. 2009. Constraint-induced movement therapy for upper extremities in stroke patients. *Cochrane Database Syst Rev*, 4.
- SLEPIAN, D. 1978. Prolate spheroidal wave functions, Fourier analysis, and uncertainty—V: The discrete case. *Bell Labs Technical Journal*, 57, 1371-1430.
- SMITH, M. A., GHAZIZADEH, A. & SHADMEHR, R. 2006. Interacting adaptive processes with different timescales underlie short-term motor learning. *PLoS Biology*, 4, e179.

- SMITH, M. A. & SHADMEHR, R. 2005. Intact ability to learn internal models of arm dynamics in Huntington's disease but not cerebellar degeneration. *Journal of Neurophysiology*, 93, 2809-2821.
- SOEKADAR, S. R., BIRBAUMER, N., SLUTZKY, M. W. & COHEN, L. G. 2015. Brain-machine interfaces in neurorehabilitation of stroke. *Neurobiology of Disease*, 83, 172-179.
- SOTO-FARACO, S., SPENCE, C., FAIRBANK, K., KINGSTONE, A., HILLSTROM, A. P. & SHAPIRO, K. 2002. A crossmodal attentional blink between vision and touch. *Psychonomic Bulletin & Review*, 9, 731-738.
- SPRINGER, S., GILADI, N., PERETZ, C., YOGEV, G., SIMON, E. S. & HAUSDORFF, J. M. 2006. Dual-tasking effects on gait variability: The role of aging, falls, and executive function. *Movement Disorders*, 21, 950-957.
- STEFANI, A., LOZANO, A. M., PEPPE, A., STANZIONE, P., GALATI, S., TROPEPI, D., PIERANTOZZI, M., BRUSA, L., SCARNATI, E. & MAZZONE, P. 2007. Bilateral deep brain stimulation of the pedunculo pontine and subthalamic nuclei in severe Parkinson's disease. *Brain*, 130, 1596-1607.
- STEINMETZ, M. A. 1998. Contributions of posterior parietal cortex to cognitive functions in primates. *Psychobiology*, 26, 109-118.
- STEVENSON, A. J., MRACHACZ-KERSTING, N., VAN ASSELDONK, E., TURNER, D. L. & SPAICH, E. G. 2015. Spinal plasticity in robot-mediated therapy for the lower limbs. *Journal of Neuroengineering and Rehabilitation*, 12, 81.
- STORTI, S. F., FORMAGGIO, E., MANGANOTTI, P. & MENEGAZ, G. 2015. Brain network connectivity and topological analysis during voluntary arm movements. *Clinical EEG and Neuroscience*, 1550059415598905.
- STUDER, B., KOENEKE, S., BLUM, J. & JÄNCKE, L. 2010. The effects of practice distribution upon the regional oscillatory activity in visuomotor learning. *Behavioral and Brain Functions*, 6, 8.
- SUSKO, T., SWAMINATHAN, K. & KREBS, H. I. 2016. MIT-skywalker: A novel gait neurorehabilitation robot for stroke and cerebral palsy. *IEEE Transactions on Neural Systems and Rehabilitation Engineering*, 24, 1089-1099.
- TAGGART, J. V. & PODOLSKY, R. J. 1961. Muscle physiology and contraction theories. *Circulation*, 24, 399-409.
- TAKAKUSAKI, K. 2013. Neurophysiology of gait: from the spinal cord to the frontal lobe. *Movement Disorders*, 28, 1483-1491.
- TAKAKUSAKI, K. 2017. Functional neuroanatomy for posture and gait control. *Journal of movement disorders*, 10(1), 1.
- TAKAKUSAKI, K., KOHYAMA, J. & MATSUYAMA, K. 2003. Medullary reticulospinal tract mediating a generalized motor inhibition in cats: III. Functional organization of spinal interneurons in the lower lumbar segments. *Neuroscience*, 121, 731-746.

- TAKEI, T. & SEKI, K. 2008. Spinomuscular coherence in monkeys performing a precision grip task. *Journal of Neurophysiology*, 99, 2012-2020.
- TAN, H., WADE, C. & BROWN, P. 2016. Post-movement beta activity in sensorimotor cortex indexes confidence in the estimations from internal models. *Journal of Neuroscience*, 36, 1516-1528.
- TAN, H., ZAVALA, B., POGOSYAN, A., ASHKAN, K., ZRINZO, L., FOLTYNIE, T., LIMOUSIN, P. & BROWN, P. 2014. Human subthalamic nucleus in movement error detection and its evaluation during visuomotor adaptation. *Journal of Neuroscience*, 34, 16744-16754.
- TANG, X., WU, J. & SHEN, Y. 2016. The interactions of multisensory integration with endogenous and exogenous attention. *Neuroscience & Biobehavioral Reviews*, 61, 208-224.
- TARD, C., DUJARDIN, K., BOURRIEZ, J.-L., MOLAEI-ARDEKANI, B., DERAMBURE, P., DEFEBVRE, L. & DELVAL, A. 2016. Attention modulation during motor preparation in Parkinsonian freezers: A time–frequency EEG study. *Clinical Neurophysiology*, 127, 3506-3515.
- TERRIER, P. & REYNARD, F. 2015. Effect of age on the variability and stability of gait: a cross-sectional treadmill study in healthy individuals between 20 and 69 years of age. *Gait & Posture*, 41, 170-174.
- THACH, W. 2007. On the mechanism of cerebellar contributions to cognition. *The Cerebellum*, 6, 163-167.
- THIBAUT, A., SIMIS, M., BATTISTELLA, L. R., FANIULLACCI, C., BERTOLUCCI, F., HUERTA-GUTIERREZ, R., ... & FREGNI, F. 2017. Using brain oscillations and corticospinal excitability to understand and predict post-stroke motor function. *Frontiers in Neurology*, 8, 187.
- THOROUGHMAN, K. A. & SHADMEHR, R. 1999. Electromyographic correlates of learning an internal model of reaching movements. *The Journal of Neuroscience*, 19, 8573-8588.
- TILLEY, S., NEALE, C., PATUANO, A. & CINDERBY, S. 2017. Older people's experiences of mobility and mod in an urban environment: a mixed methods approach using electroencephalography (EEG) and interviews. *International journal of environmental research and public health*, 14, 151.
- TORRECILLOS, F., ALAYRANGUES, J., KILAVIK, B. E. & MALFAIT, N. 2015. Distinct modulations in sensorimotor postmovement and foreperiod  $\beta$ -band activities related to error salience processing and sensorimotor adaptation. *Journal of Neuroscience*, 35, 12753-12765.
- TORRENCE, C. & COMPO, G. P. 1998. A practical guide to wavelet analysis. *Bulletin of the American Meteorological society*, 79, 61-78.
- TOXOPEUS, C. M., DE JONG, B. M., VALSAN, G., CONWAY, B. A., LEENDERS, K. L. & MAURITS, N. M. 2011. Direction of movement is encoded in the human primary motor cortex. *PLoSOne*, 6, e27838.

- TREWARTHA, K. M., GARCIA, A., WOLPERT, D. M. & FLANAGAN, J. R. 2014. Fast but fleeting: adaptive motor learning processes associated with aging and cognitive decline. *Journal of neuroscience*, 34, 13411-13421.
- TRUCCOLO, W., FRIEHS, G. M., DONOGHUE, J. P. & HOCHBERG, L. R. 2008. Primary motor cortex tuning to intended movement kinematics in humans with tetraplegia. *Journal of Neuroscience*, 28, 1163-1178.
- TSU, A. P., BURISH, M. J., GODLOVE, J. & GANGULY, K. 2015. Cortical neuroprosthetics from a clinical perspective. *Neurobiology of disease*, 83, 154-160.
- TUCKER, M. R., OLIVIER, J., PAGEL, A., BLEULER, H., BOURI, M., LAMBERCY, O., DEL R MILLÁN, J., RIENER, R., VALLERY, H. & GASSERT, R. 2015. Control strategies for active lower extremity prosthetics and orthotics: a review. *Journal of Neuroengineering and Rehabilitation*, 12, 1.
- TURESKY, T. K., TURKELTAUB, P. E. & EDEN, G. F. 2016. An activation likelihood estimation meta-analysis study of simple motor movements in older and young adults. *Frontiers in Aging Neuroscience*, 8.
- TURNER, D. L., RAMOS-MURGUIALDAY, A., BIRBAUMER, N., HOFFMANN, U. & LUFT, A. 2013. Neurophysiology of robot-mediated training and therapy: a perspective for future use in clinical populations. *Frontiers in Neurology*, 4.
- ÚBEDA, A., AZORÍN, J. M., CHAVARRIAGA, R. & MILLÁN, J. D. R. 2017. Classification of upper limb center-out reaching tasks by means of EEG-based continuous decoding techniques. *Journal of Neuroengineering and Rehabilitation*, 14, 9.
- UEMURA, Y., KAJIWARA, Y. & SHIMAKAWA, H. Estimating Distracted Pedestrian from Deviated Walking Considering Consumption of Working Memory. *Computational Science and Computational Intelligence (CSCI), 2016 International Conference on*, 2016. IEEE, 1164-1167.
- VALLBO, A. & WESSBERG, J. 1993. Organization of motor output in slow finger movements in man. *The Journal of Physiology*, 469, 673-691.
- VAN CRIEKINGE, T., SAEYS, W., HALLEMANS, A., VELGHE, S., VISKENS, P.-J., VEREECK, L., DE HERTOOGH, W. & TRUIJEN, S. 2017. Trunk biomechanics during hemiplegic gait after stroke: A systematic review. *Gait & Posture*, 54, 133-143.
- VAN MEULEN, F. B., KLAASSEN, B., HELD, J., REENALDA, J., BUURKE, J. H., VAN BEIJNUM, B.-J. F., LUFT, A. & VELTINK, P. H. 2015. Objective Evaluation of the Quality of Movement in Daily Life after Stroke. *Frontiers in Bioengineering and Biotechnology*, 3.
- VAN MEULEN, F. B., REENALDA, J., BUURKE, J. H. & VELTINK, P. H. 2015. Assessment of daily-life reaching performance after stroke. *Annals of Biomedical Engineering*, 43, 478-486.
- VAN WIJK, B., BEEK, P. & DAFFERTSHOFER, A. 2012. Differential modulations of ipsilateral and contralateral beta (de) synchronization during unimanual force production. *European Journal of Neuroscience*, 36, 2088-2097.

- VILLALTA, J. I., LANDI, S. M., FLÓ, A. & DELLA-MAGGIORE, V. 2013. Extinction interferes with the retrieval of visuomotor memories through a mechanism involving the sensorimotor cortex. *Cerebral Cortex*, 25, 1535-1543.
- VÖLKER, M., FIEDERER, L. D., BERBERICH, S., HAMMER, J., BEHNCKE, J., KRŠEK, P., ... & HELIAS, M. (2018). The dynamics of error processing in the human brain as reflected by high-gamma activity in noninvasive and intracranial EEG. *NeuroImage (in publication)*.
- VON CARLOWITZ-GHORI, K., BAYRAKTAROGLU, Z., HOHLEFELD, F. U., LOSCH, F., CURIO, G. & NIKULIN, V. V. 2014. Corticomuscular coherence in acute and chronic stroke. *Clinical Neurophysiology*, 125, 1182-1191.
- VON CARLOWITZ-GHORI, K., BAYRAKTAROGLU, Z., WATERSTRAAT, G., CURIO, G., & NIKULIN, V. V. 2015. Voluntary control of corticomuscular coherence through neurofeedback: a proof-of-principle study in healthy subjects. *Neuroscience*, 290, 243-254.
- VON HOFSTEN, C. 1979. DEVELOPMENT OF VISUALLY IPECTE REACHING: THE APPROACH PHASE1. *Journal of Human Movement Studies*, 5, 160-178.
- WAGNER, J., MAKEIG, S., GOLLA, M., NEUPER, C. & MÜLLER-PUTZ, G. 2016. Distinct  $\beta$  Band Oscillatory Networks Subserving Motor and Cognitive Control during Gait Adaptation. *The Journal of Neuroscience*, 36, 2212-2226.
- WAGNER, J., SOLIS-ESCALANTE, T., GRIESHOFFER, P., NEUPER, C., MÜLLER-PUTZ, G. & SCHERER, R. 2012. Level of participation in robotic-assisted treadmill walking modulates midline sensorimotor EEG rhythms in able-bodied subjects. *NeuroImage*, 63, 1203-1211.
- WAGNER, J., SOLIS-ESCALANTE, T., SCHERER, R., NEUPER, C. & MÜLLER-PUTZ, G. 2014. It's how you get there: walking down a virtual alley activates premotor and parietal areas. *Frontiers in Human Neuroscience*, 8.
- WAHN, B. & KÖNIG, P. 2017. Is Attentional Resource Allocation Across Sensory Modalities Task-Dependent? *Advances in Cognitive Psychology*, 13, 83.
- WALDERT, S., PREISSEL, H., DEMANDT, E., BRAUN, C., BIRBAUMER, N., AERTSEN, A. & MEHRING, C. 2008. Hand movement direction decoded from MEG and EEG. *Journal of Neuroscience*, 28, 1000-1008.
- WEI, K. & KÖRDING, K. 2010. Uncertainty of feedback and state estimation determines the speed of motor adaptation. *Frontiers in Computational Neuroscience*, 4, 11.
- WELCH, P. 1967. The use of fast Fourier transform for the estimation of power spectra: a method based on time averaging over short, modified periodograms. *IEEE Transactions on Audio and Electroacoustics*, 15, 70-73.
- WISE, S. & SHADMEHR, R. 2002. *Motor control*. Elsevier Science.
- WITHAM, C. L., WANG, M. & BAKER, S. 2010. Corticomuscular coherence between motor cortex, somatosensory areas and forearm muscles in the monkey. *Frontiers in Systems Neuroscience*, 4, 38.

- WITT, S. T., LAIRD, A. R. & MEYERAND, M. E. 2008. Functional neuroimaging correlates of finger-tapping task variations: an ALE meta-analysis. *NeuroImage*, 42, 343-356.
- WITTE, M., PATINO, L., ANDRYKIEWICZ, A., HEPP-REYMOND, M. C. & KRISTEVA, R. 2007. Modulation of human corticomuscular beta-range coherence with low-level static forces. *European Journal of Neuroscience*, 26, 3564-3570.
- WRIGHT, Z. A., RYMER, W. Z., & SLUTZKY, M. W. 2014. Reducing abnormal muscle coactivation after stroke using amyoelectric computer interface: A pilot study. *Neurorehabilitation and Neural Repair*, 28(5), 443-451. doi: 10.1177/1545968313517751
- WU, H. G., MIYAMOTO, Y. R., CASTRO, L. N. G., ÖLVECZKY, B. P., & SMITH, M. A. 2014. Temporal structure of motor variability is dynamically regulated and predicts motor learning ability. *Nature Neuroscience*, 17(2), 312.
- XU, T., YU, X., OU, S., LIU, X., YUAN, J., & CHEN, Y. 2017. Efficacy and safety of very early mobilization in patients with acute stroke: a systematic review and meta-analysis. *Scientific Reports*, 7(1), 6550.
- YANG, M., ZHENG, H., WANG, H., MCCLEAN, S. & NEWELL, D. 2012. iGAIT: An interactive accelerometer-based gait analysis system. *Computer methods and programs in biomedicine*, 108, 715-723.
- YEO, S.-H., WOLPERT, D. M. & FRANKLIN, D. W. 2015. Coordinate representations for interference reduction in motor learning. *PloSOne*, 10, e0129388.
- YOGEV-SELIGMANN, G., ROTEM-GALILI, Y., MIRELMAN, A., DICKSTEIN, R., GILADI, N., & HAUSDORFF, J. M. 2010. How does explicit prioritization alter walking during dual-task performance? Effects of age and sex on gait speed and variability. *Physical therapy*, 90(2), 177-186.
- YOO, S. S., LEE, J. H., O'LEARY, H., PANYCH, L. P., & JOLESZ, F. A. 2008. Neurofeedback fMRI-mediated learning and consolidation of regional brain activation during motor imagery. *International journal of imaging systems and technology*, 18(1), 69-78.
- YORDANOVA, J., KOLEV, V., VERLEGER, R., HEIDE, W., GRUMBT, M. & SCHÜRMANN, M. 2017. Synchronization of fronto-parietal beta and theta networks as a signature of visual awareness in neglect. *NeuroImage*, 146, 341-354.
- YOSHIDA, T., MASANI, K., ZABJEK, K., CHEN, R. & POPOVIC, M. R. 2017. Dynamic increase in corticomuscular coherence during bilateral, cyclical ankle movements. *Frontiers in Human Neuroscience*, 11.
- YOUSSEFZADEH, V., ZANOTTO, D., WONG-LIN, K., AGRAWAL, S. K. & PRASAD, G. 2016. Directed functional connectivity in fronto-centroparietal circuit correlates with motor adaptation in gait training. *IEEE Transactions on Neural Systems and Rehabilitation Engineering*, 24, 1265-1275.
- ZICH, C., DEBENER, S., SCHWEINITZ, C., STERR, A., MEEKES, J. & KRANCZIOCH, C. 2017. High-intensity chronic stroke motor imagery neurofeedback training at home: three case reports. *Clinical EEG and Neuroscience*, 1550059417717398.



ZOLLO, L., ROSSINI, L., BRAVI, M., MAGRONE, G., STERZI, S. & GUGLIELMELLI, E. 2011. Quantitative evaluation of upper-limb motor control in robot-aided rehabilitation. *Medical & Biological Engineering & Computing*, 49, 1131.

ZOTEV, V., PHILLIPS, R., YUAN, H., MISAKI, M., & BODURKA, J. 2014. Self-regulation of human brain activity using simultaneous real-time fMRI and EEG neurofeedback. *NeuroImage*, 85, 985-995.

## Appendix I Ethical Approval

16 December 2014

Dear Sara,

<b>Project Title:</b>	<b>NEUROMOTION: Mobilizing non-invasive neuroimaging for assisting the neurologically impaired to navigate the real world.</b>
<b>Researcher(s):</b>	<b>Sara Pizzamiglio</b>
<b>Principal Investigator:</b>	<b>Professor Hassan Abdalla</b>
<b>Reference Number:</b>	<b>UREC_1415_29</b>

I am writing to confirm the outcome of your application to the University Research Ethics Committee (UREC), which was considered at the meeting on **Wednesday 12<sup>th</sup> November 2014**.

The decision made by members of the Committee is **Approved**. The Committee's response is based on the protocol described in the application form and supporting documentation. Your study has received ethical approval from the date of this letter.

Should any significant adverse events or considerable changes occur in connection with this research project that may consequently alter relevant ethical considerations, this must be reported immediately to UREC. Subsequent to such changes an Ethical Amendment Form should be completed and submitted to UREC.

### Approved Research Site

I am pleased to confirm that the approval of the proposed research applies to the following research site.

<b>Research Site</b>	<b>Principal Investigator / Local Collaborator</b>
University of East London	Professor Hassan Abdalla

### Approved Documents

The final list of documents reviewed and approved by the Committee is as follows:

<b>Document</b>	<b>Version</b>	<b>Date</b>
UREC Application Form	1.0	24 October 2014
Participant Information Sheet	2.0	16 December 2014
Consent Form	1.0	24 October 2014

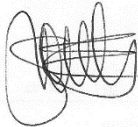
Confidential Volunteer Medical Exclusion Questionnaire	1.0	24 October 2014
--	-----	-----------------

Approval is given on the understanding that the [UEL Code of Good Practice in Research](#) is adhered to.

Please note, it is your responsibility to retain this letter for your records.

With the Committee's best wishes for the success of this project.

Yours sincerely,



Catherine Fieulleateau  
Research Integrity and Ethics Manager  
University Research Ethics Committee (UREC)  
Email: [researchethics@uel.ac.uk](mailto:researchethics@uel.ac.uk)

## Appendix II Confidential volunteer medical questionnaire



### CONFIDENTIAL VOLUNTEER MEDICAL EXCLUSION QUESTIONNAIRE

Programme Title: NEUROMOTION: Mobilizing non-invasive neuroimaging for assisting the neurologically impaired to navigate the real world.

Subject Number:

Age:

Gender:

Date:

Please give details to help us in assessing your possible participation in the project.  
Please answer the following questions:

Do you have Current Medication:

.....

Do you use Drugs or Alcohol:

.....

Have you had Surgery or Chronic Illnesses:

.....

Do you have a History of Head or Spinal Injury (e.g concussion, car crash whiplash):

.....

Do you have any Neurological Disorders (e.g. stroke, spinal cord injury, colour blindness, dyslexia, Parkinson's or Alzheimer's disease, epilepsy/seizures, family history of these):

.....

Do you have a Psychiatric History (e.g. schizophrenia, bipolar disorder, depression, obsessive compulsive disorders, panic disorder, Family History of these):

.....

Do you have a CardioRespiratory Disease (asthma, angina, high blood pressure, respiratory distress):

.....

Do you have a Musculoskeletal Condition: (bone fracture, muscle tear, ligament):

.....

Do you have Metal Implantable Devices outside of mouth (e.g. pacemakers, intracranial plates, skeletal pins, vascular clips):

.....

If you are a woman are you pregnant or experiencing altered menstrual cycles?

.....

Handedness: Upper Body – Writing Hand

Lower Body – Kicking Foot

.....

## Appendix III Written volunteer consent form



### INFORMATION SHEET

We invite you to participate in an investigation. In order to help you to understand what the investigation is about, we are providing you with the following information. Please be sure you understand it before you formally agree to participate. Please ask any questions you have about the information that follows. We will explain and provide any further information you require.

#### **THE TITLE OF THE PROPOSED INVESTIGATION:**

**NEUROMOTION: Mobilizing non-invasive neuroimaging for assisting the neurologically impaired to navigate the real world.**

#### **WHY YOU ARE CHOSEN AS A POSSIBLE PARTICIPANT:**

*As a subject you have confirmed that you are not excluded on physical or mental health grounds and that you are able to undertake exercise such as arm reaching, bicycling and walking (see **CONFIDENTIAL VOLUNTEER MEDICAL EXCLUSION QUESTIONNAIRE**)*

#### **THE GOAL OF THE PROPOSED INVESTIGATION:**

We wish to measure how your reflexes and voluntary brain control over movement may interact.

#### **THE METHODS WHICH WILL BE EMPLOYED IN THE INVESTIGATION TO ACHIEVE THESE GOALS:**

- We will use purpose built exercising machines or treadmills upon which you will exercise.
- We can use video analysis and non-invasive measures of muscle and brain activity to show us how you control and co-ordinate your muscles during exercise.
- We will use several types of sensory cues to activate reflexes (such as tendon/muscle vibration or electrical nerve stimulation). Vibration or electrical stimulation of nerves or muscles can help measure the strength of reflexes during exercise.
- We can test the amount of voluntary control you have over the way in which you are exercising by using transcranial magnetic stimulation (TMS), which test the strength of neural signals from the cerebral cortex of the brain using painless magnetic pulses, which activate nerve cells.
- We can assess the cortical connectivity patterns that are generated inside your brain during movement (reaching/cycling/walking) by using electroencephalography (EEG), which detects the signals generated by your brain non-invasively through scalp electrodes.

#### **WHAT DOES PARTICIPATION IN THE INVESTIGATION PRACTICALLY INVOLVE FOR YOU?**

- Involvement will require you to attend the research laboratories a number of times in order to become familiar with routine measurements and equipment. Each visit will be approximately 3 hours long.
- To undertake mild to moderate exercise (we may wish to ascertain your maximal exercise performance on a separate occasion).

- To exercise whilst we measure reflex and voluntary muscle control using the methods described.
- To abstain from caffeine and alcohol for 12 hours before testing (unless we explicitly state otherwise) and refrain from heavy exercise for 24 hours before testing.

**SPECIFIC BENEFITS ACCRUED FROM THE STUDIES TO YOU:**

There are no direct health benefits to you from the testing, but you will have a better knowledge of how your nervous system controls complex movement and if tested, knowledge of your aerobic fitness.

**POTENTIAL DISCOMFORTS AND HAZARDS OF THE INVESTIGATION:**

- The tests may lead to some muscular fatigue following assessment of aerobic fitness. You will be asked to indicate strenuous activity or unexpected levels of fatigue between sessions and maximal aerobic fitness tests will be symptom limited at your instruction.
- Exercise with reflex and voluntary control measurements will have minimal discomfort or hazard.
- Tests of reflexes and TMS are non-invasive procedures with minimal risks associated with them.
- TMS is associated with a 'click' sound, the loudness of which we can lessen with you wearing earplugs if necessary.

**WHO YOU CAN CONTACT IF YOU ARE WORRIED ABOUT ANY FACTORS INVOLVED IN THE STUDIES:**

The studies will take part in the School of Health, Sport and Biosciences at UEL Stratford Campus.

You are free to seek advice or further description of methods from the principle investigator or the named investigator:

- Sara Pizzamiglio (0747 8295468; Email: [u1433999@uel.ac.uk](mailto:u1433999@uel.ac.uk))
  - Prof Hassan Abdalla (0208 223 2963 Email: [h.s.abdalla@uel.ac.uk](mailto:h.s.abdalla@uel.ac.uk)).
- In addition, you are welcome to contact the Dean of School of Health, Sport and Bioscience for independent advice on the project goals and methods:

Prof Neville Punchard (020 8223 4477; Email: [n.punchard@uel.ac.uk](mailto:n.punchard@uel.ac.uk)).

If you have any concerns about the conduct of the investigator, researcher(s) or any other aspect of this research project, you can contact:

[researchethics@uel.ac.uk](mailto:researchethics@uel.ac.uk).

**CONFIDENTIALITY:**

Your files and data held about you will be stored (and anonymously coded) in secure cabinets under a number rather than your name. You will not be individually identifiable in accordance with the Data Protection Act.

Confidentiality of information provided is subject to legal limitations.

The data generated in the course of the research will be retained in accordance with the University's Data Protection Policy.

**THE UNIVERSITY OF EAST LONDON UNIVERSITY RESEARCH ETHICS**

**COMMITTEE (UREC) HAS APPROVED THE STUDY.**

**THE UNIVERSITY OF EAST LONDON IS THE SPONSOR OF THE STUDY.**

**YOU ARE FREE NOT TO PARTICIPATE AND MAY WITHDRAW FROM THE STUDY AT ANY TIME AND WITHDRAW ANY UNPROCESSED DATA PREVIOUSLY SUPPLIED. THIS WILL NOT JEOPARDISE YOUR COURSE OF STUDY, IF YOU ARE A STUDENT VOLUNTEER.**



**Consent to Participate in an Experimental Research Programme Involving Human Participants.**

**Project Title: NEUROMOTION: Mobilizing non-invasive neuroimaging for assisting the neurologically impaired to navigate the real world.**

**Principle Investigator: Professor Hassan Abdalla**

I have read the information leaflet relating to the above programme of research in which I have been asked to participate and have been given a copy to keep. The nature and purposes of the research have been explained to me, and I have had the opportunity to discuss the details and ask questions about this information. I understand what is being proposed and the procedures in which I will be involved have been explained to me.

I understand that my involvement in this study, and particular data from this research, will remain strictly confidential. Only the researchers involved in the study will have access to the data. It has been explained to me what will happen once the experimental programme has been completed.

I hereby freely and fully consent to participate in the study which has been fully explained to me and for the information obtained to be used in relevant research publications.

Having given this consent I understand that I have the right to withdraw from the study at any time without disadvantage to myself and without being obliged to give any reason.

Participant's Name (BLOCK CAPITALS)  
.....

Participant's Signature  
.....

Investigator's Name (BLOCK CAPITALS)  
.....

Investigator's Signature  
.....

Date: .....

## **Appendix VI Peer-reviewed publications**

### **Published papers**

- PIZZAMIGLIO, S., DE LILLO, M., NAEEM, U., ABDALLA, H. & TURNER, D.L. 2017. High-frequency intermuscular coherence between arm muscles during robot-mediated motor adaptation. *Frontiers in Physiology*. 7: 668. doi: 10.3389/fphys.
- PIZZAMIGLIO, S., DESOWSKA, A., SHOJAII, P., TAGA, M. & TURNER, D. L. 2017. Muscle co-contraction patterns in robot-mediated force field learning to guide specific muscle group training. *NeuroRehabilitation*, 1-13.
- PIZZAMIGLIO, S., NAEEM, U., ABDALLA, H. & TURNER, D.L. 2017 Neural correlates of single- and dual-task walking in the real world. *Frontiers in Human Neuroscience*, 11, 460.
- PIZZAMIGLIO, S., NAEEM, U., ABDALLA, H. & TURNER, D.L. 2018 Neural predictors of gait stability when walking freely in the real world. *Journal of Neuroengineering and Rehabilitation*, 15(1), 11.
- PIZZAMIGLIO, S., NAEEM, U., UR REHMAN, S., SHARIF, M.S., ABDALLA, H. & TURNER, D.L. 2017 A multimodal approach to measure the levels of distraction of pedestrians using mobile sensing. *The 8<sup>th</sup> International Conference on Emerging Ubiquitous Systems and Pervasive Networks (EUSPN 2017)*, Lund (Sweden) 18<sup>th</sup>-20<sup>th</sup> September 2017.

### **Conference abstracts and proceedings**

- PIZZAMIGLIO, S., ABDALLA, H. & TURNER, D.L. Neural correlates of human single- and dual-task natural walking in the urban environment. 1<sup>st</sup> Biannual Neuroadaptive Technology Conference (NAT'17), Berlin (Germany) 19<sup>th</sup>-21<sup>st</sup> July 2017;
- PIZZAMIGLIO, S. & TURNER, D.L. Neural correlates of adaptation to novel force-field: an exploratory ERP study. *School and Symposium on Advanced Neurorehabilitation (SSNR2016)*, Baiona (Spain) 6<sup>th</sup>-10<sup>th</sup> June 2016;
- PIZZAMIGLIO, S., NAEEM, U., ABDALLA, H. & TURNER, D.L. Upper-limb muscle determinants of adaptation to robot-mediated force-field perturbations. *The Society for Research in Rehabilitation (SRR) Summer Meeting*, Newcastle upon Tyne (UK) 9<sup>th</sup> June 2015.

### **Under review:**



- FAIMAN, I., PIZZAMIGLIO, S. & TURNER, D.L. Functional role of resting-state dynamics during motor adaptation: performance prediction and memory (under review in NeuroImage).

#### **In preparation**

- PIZZAMIGLIO, S., BELARDINELLI, P., ZIEMANN, U. & TURNER, D.L. Cortico-muscular correlates of motor adaptation to a robot-mediated force-field;
- DESOWSKA, A.\*, PIZZAMIGLIO, S.\*, & TURNER, D.L. Electrophysiological evidence for predictive model formation during robot-mediated motor adaptation of the upper limb.